20831 -FR

NASA CR 86124

RESEARCH IN ELECTRICALLY SUPPORTED VACUUM GYROSCOPE

VOLUME III-ESVG SUSPENSION RESEARCH

November 1968

Prepared Under Contract NAS-12-542

HONEYWELL INC.
Systems & Research Division
Minneapolis, Minnesota
for

NATIONAL AERONAUTICS AND SPACE ADMINISTRATION

NASA CR

RESEARCH IN ELECTRICALLY SUPPORTED VACUUM GYROSCOPE

Volume III - ESVG Suspension Research

Prepared by K. W. Exworthy

November 1968

Prepared Under Contract NAS-12-542

Honeywell Inc.
Systems and Research Division
Minneapolis, Minnesota

for

National Aeronautics and Space Administration

CONTENTS

CONTENTS - Concluded

ILLUSTRATIONS

ILLUSTRATIONS - Continued

ILLUSTRATIONS - Concluded

TABLES

SECTION I
INTRODUCTION

As can be inferred from its name, the Electrically Supported Vacuum Gyroscope (ESVG) employs electric fields for supporting the rotor, thereby removing mechanical linkages, used in conventional gyros, which impose limitations on gyro usefulness. An important component of the gyro is the set of electronics which generate and control these electrical fields. The ESVG suspension system is a position-sensing, force-producing servo which keeps the gyro rotor as close as possible to a reference position called "case center". The purpose of this study is to delineate the inherent limitations of this servo and to block out a circuit which will meet the dual requirements of high G capability and reduced power input while operating in a low G environment.

This study is reported in three parts. The first part considers the factors which affect the dynamic range of the servo system. Factors such as electric gradient limits, wave form, rotor material density,and rotor wall thickness are used to describe the maximum acceleration limits of the gyro. The loop equations are derived to show the dependencies of dynamic behavior on bandwidth and bias levels. The section concludes with a general discussion of the type system best suited for maximum acceleration environments.

System power requirements are considered in the second part. Bias losses and power minimizing techniques are discussed, and the power losses associated with different waveform outputs are compared. To meet the conflicting requirements of high G capability and low power consumption at low G, a transformer-coupled suspension system is proposed for design. It became obvious during this study that a dual-level power supply is needed to provide maximum efficiency (least loss) during low G operation.

The design of the suspension servo output circuits is described in the third part. The modulating amplifiers, oscillator, power driver output stage, and switched power source were breadboarded and individually tested to verify the calculations detailed in the previous sections. These square wave circuits were then connected together and operated as a complete half-channel.

The results of the testing indicate that with present devices a low G subsystem with the required characteristics can be built with a power input on the order of 240 mW. With acceleration at maximum rated capability, the indicated power consumed by the high G circuits is 20.5 watts with voltage bias at one-fourth maximum output and 27 watts with bias at one-half maximum output.

SECTION II
DYNAMIC RANGE STUDY

INHERENT FACTORS AND BOUNDS

Force Equations

The rotor of the Electrically Supported Vacuum Gyroscope (ESVG) is a free-spinning sphere suspended in a spherical housing. The rotor is centered in the housing with forces produced by an electric suspension system. These suspension forces are developed by a voltage gradient across the gap between the rotor and metallic electrodes which form part of the inner surface of the housing. The electrodes are usually arranged to form an orthogonal set of force axes. Such an arrangement "decouples" the rebalance forces and simplifies suspension circuit design. The equations for electric force as a function of electrode shape, size, and gap are developed in the following paragraphs. Several assumptions made as part of the derivation are: 1) the electrodes and rotor are perfectly spherical; 2) the electric field is uniform over the electrode surface; and 3) perturbations of the electrode and rotor surfaces produce gyro torques, but do not alter the force equations to a significant degree. The notion of uniform gradients is supported because the rotor-electrode gap is, by over an order of magnitude, the smallest spacing which exists in the structure. The direct result of the analysis is a set of integrals which relate capacitance of the electrodes to existing geometry. These capacitance integrals are evaluated for two sets of limits. The first set is the maximum-area case in which the housing is split into six surfaces which are the projections of an inscribed cube. The second case considers circular electrodes which produce a small, uniform cross-axis coupling coefficient.

Separate evaluations are made for voltage-fed and current-fed systems. The basic difference is that current-fed systems develop a gradient directly and, to first order, no change in force occurs with rotor displacements. Voltage-fed systems utilize a source of which output level is not a direct function of displacement. This produces gradient changes and, in the balanced axis case (bias voltage), results in destabilizing forces. Hybrid systems can be developed, and these are described in the last part of this section.

Hexahedral electrodes, force equations. -- The force equations are generally developed by considering the change of energy produced by "virtual" translations in the direction of interest. Energy is stored in the electrode capacitance and is a squared function of the electrode voltage. It is assumed that the rotor is at ground potential and all voltages are measured with respect to ground.

The electric force produced by the charged set of electrodes on the enclosed rotor may then be described by the equation

$$\vec{F} = - \vec{\nabla} W \qquad (1)$$

where

$\vec{F}$ = force developed

W = stored energy

If the structure is isolated and each electrode has some potential, V_i, relative to the rotor, the stored energy may be described as (Ref. 1)

$$W = \frac{1}{2}\left[\sum_{i=1}^{6} C_i V_i^2 + \sum_{i=1}^{6}\sum_{j=1}^{6} (-1)^n C_{ij} V_i V_j\right] \quad \begin{matrix} n = 0 \text{ for } i = j \\ n = 1 \text{ for } i \neq j \end{matrix} \qquad (2)$$

In (2) the total electrode capacitance has been split into two parts. The C_i's are rotor-electrode capacitances, and C_{ij}'s are electrode capacitances to all other parts of the system. This equation is in a form which may be substituted directly into Equation (1) and then used to find the force produced in a given direction.

To simplify the process, the total force vector may be broken into coordinate components such that

$$F_x = -\frac{\partial W}{\partial x}$$

$$F_y = -\frac{\partial W}{\partial y} \qquad (3)$$

$$F_z = -\frac{\partial W}{\partial z}$$

---

[1] Smythe, William R.: Static and Dynamic Electricity, McGraw-Hill, 1950, p. 39.

For the circular or hexahedral structures, symmetry exists that makes these directional derivatives essentially similar. One will be used as an illustration; the other two may be found by substitution of appropriate variables.

$$\frac{\partial W}{\partial z} = \frac{1}{2}\left[\sum_{i=1}^{6} V_i^2 \frac{\partial C_i}{\partial z} + \sum_{i=1}^{6}\sum_{j=1}^{6} (-1)^n V_i V_j \frac{\partial C_{ij}}{\partial z}\right] \quad \begin{array}{l} n = 0 \text{ for } i = j \\ n = 1 \text{ for } i \neq j \end{array} \qquad (4)$$

It is assumed that V_i is not a function of capacitance.

The evaluation of this expression requires knowledge of the variation of capacitance with rotor displacement along the x-axis. Consider first the C_{ij}'s. The only significant parts are interelectrode capacitances that are formed primarily by adjacent electrode edges. The electrode face is "shielded" by the rotor (which makes up C_i) since the rotor-to-electrode gap is typically 1/50 of the interelectrode gap (Volume II, Figure 4). Thus, the change of the C_{ij}'s with change of rotor position is very small and may be neglected. Laboratory tests indicate that the error introduced by neglecting these effects is $1:10^5$ or less.

To evaluate the change in C_i with displacement, the general expression for the electrode capacitance must be derived for the two structures of interest. The capacitance expression may be determined by summing the capacitance elements over the rotor-electrode surface. The ratio of area of the element to the gap between the surface elements determines the element of capacitance contributed by the surface elements. The gap length at a particular elemental area is determined by the rotor position within the housing as shown in Figure 1.

The sides of the triangle, $\vec{\ell}$, $\overrightarrow{(r + d)}$, and $\vec{r}_o$, can be related as follows:

$$(r + d)^2 = \ell^2 + r_o^2 - 2\ell\, r_o \cos A \qquad (5)$$

The case radius, r_o, may be used to define the nominal (centered) gap,

$$r_o = r + d_o \qquad (6)$$

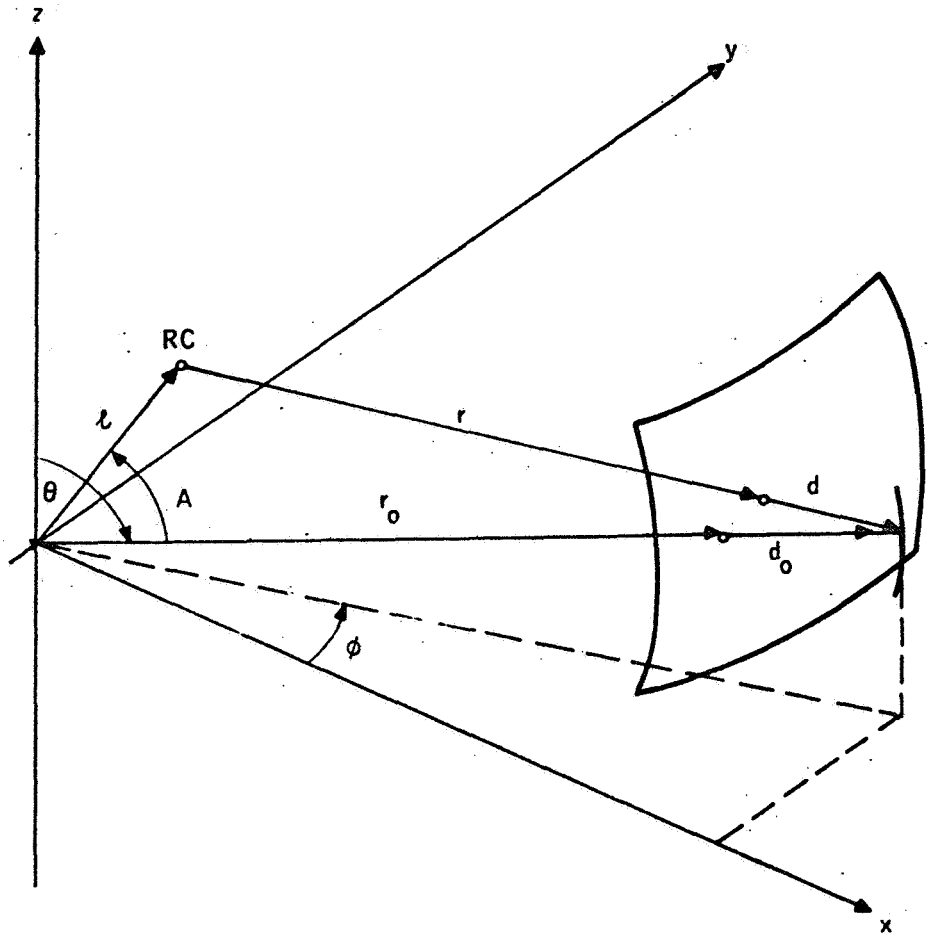

RC = ROTOR CENTROID POSITION
A = TRUE ANGLE BETWEEN $\vec{\ell}$ AND $\vec{r}_o$
ϕ = LONGITUDE ANGLE OF r_o
θ = CO-LATITUDE ANGLE OF r_o
r_o = CASE RADIUS
ℓ = LINE BETWEEN CASE AND ROTOR CENTER
r = ROTOR RADIUS
d = ACTUAL GAP AT r_o, θ, ϕ

Figure 1. Determination of Gap Length

that is used to clear (5) of r_o:

$$r^2 + 2\,rd + d^2 = \ell^2 + r^2 + 2rd_o + d_o{}^2 - 2\ell\,(r + d_o)\cos A \tag{7}$$

This may be reduced by realizing that $|\ell| < |d| \cong |d_o|$, and d_o is three orders of magnitude smaller than r. Collecting and removing second-order terms results in

$$d \cong d_o - \ell \cos A \tag{8}$$

The function $\ell \cos A$ may be evaluated in terms of the spherical angles ϕ and θ by considering substitution of the rectangular coordinates of the vectors $r_o\,(x_2 y_2 z_2)$ and $\ell(x_1 y_1 z_1)$. Particularly,

$$\ell^2 = x_1{}^2 + y_1{}^2 + z_1{}^2$$

$$r_o{}^2 = x_2{}^2 + y_2{}^2 + z_2{}^2$$

$$(r+d)^2 = (x_2 - x_1)^2 + (y_2 - y_1^2) + (z_2 - z_1{}^2)$$

Substitution and rearrangement of the terms gives

$$\ell \cos A = \frac{x_1 x_2 + y_1 y_2 + z_1 z_2}{r_o} \tag{9}$$

In terms of the spherical angle,

$$\begin{aligned} x_2 &= r_o \sin\theta \cos\phi \\ y_2 &= r_o \sin\theta \sin\phi \\ z_2 &= r_o \cos\theta \end{aligned} \tag{10}$$

and x_1, y_1, z_1 are the rectangular coordinates of the rotor center relative to the case center. Substitution of (9) and (10) in (8) yields

$$d = d_o - x_1 \sin\theta \cos\phi - y_1 \sin\theta \sin\phi - z_1 \cos\theta$$

The other factor in the elemental capacitance expression is the area dA for the spherical section. A rectangular area is used. In terms of ϕ, θ, and r, $dA = r^2 \sin\theta \, d\theta \, d\phi$. Each electrode capacitance may be evaluated by using an integral of the form

$$C_i = \int_{S_i} \frac{\epsilon_o r^2 \sin\theta \, d\theta \, d\phi}{d_o - x_i \sin\theta \cos\phi - y_i \sin\theta \sin\phi - z_i \cos\theta} \qquad (11)$$

The integration may be carried out by expanding function into a series.

Bounds on the usable range of x_1, y_1, z_1 may be determined for several cases by considering the usual suspension system characteristics. During rotor lift, $z_1 = d_o$. For static or slowly varying input, x_1, y_1, z_1 are in the range of three orders of magnitude less than d_o. The displacement may become quite large if vibratory accelerations in the midband frequency range (50 - 250 cps) are applied. The amplitude of rotor displacement in this range must be limited so that the gyro drift be small. Also, in a tuned output driver, the capacitance variation must be limited to control the amount of power that must be supplied. These limitations must be designed into the circuit after considering the vibration spectrum that is specified. Maximum value for x_1, y_1, z_1 must usually be 15 percent of the nominal gap. Rotor lift is a special case which can be treated separately.

With maximum values in this range, second-order terms should be retained, but third-order terms may be neglected.

Expanding the integral (11) and retaining first- and second-order terms gives

$$C_i = \frac{\epsilon_o r^2}{d_o} \int_{S_i} \left[\sin\theta + \frac{x_1}{d_o} \sin^2\theta \cos\phi + \frac{y_1}{d_o} \sin^2\theta \sin\phi \right.$$

$$+\frac{z_1}{d_o}\sin\theta\cos\theta+\frac{x_1^2}{d_o^2}\sin^3\theta\cos^2\phi+\frac{y_1^2}{d_o^2}\sin^3\theta\sin^2\phi$$

$$+\frac{z_1^2}{d_o^2}\sin\theta\cos^2\theta+2\frac{x_1y_1}{d_o^2}\sin^3\theta\cos\phi\sin\phi \qquad (12)$$

$$+2\frac{x_1z_1}{d_o^2}\sin^2\theta\cos\theta\cos\phi+2\frac{y_1z_1}{d_o^2}\sin^2\theta\cos\theta\sin\phi\Bigg]d\theta\,d\phi$$

The limits of integration depend on the electrode shape. Hexahedral electrode boundaries are defined by projecting the edges of a cube onto a circumscribed sphere. As explained in detail in Volume II, Section III of this report, the region of integration can be reduced to a segment of the positive z axis electrode by using the symmetry properties of the configuration. After integrating over this region, all of the integrals are subsequently determined by means of simple coordinate transformations from the force axis coordinates.

Let the six electrode capacitances be denoted as follows:

$C_{x+} = C_1$ $\qquad$ $C_{y-} = C_4$

$C_{x-} = C_2$ $\qquad$ $C_{z+} = C_5$

$C_{y+} = C_3$ $\qquad$ $C_{z-} = C_6$

Then the capacitance equation for the positive z electrode is

$$C_5 = \frac{2\pi r_o^2 \epsilon_o}{3 d_o}\left[1+\frac{3\sqrt{2}}{\pi}\frac{z_1}{d_o}\tan^{-1}\frac{1}{\sqrt{2}}\right.$$

$$+ \frac{x_1^2 + y_1^2}{d_o^2} \left(\frac{1 - \frac{\sqrt{3}}{\pi}}{3} \right) + \frac{z_1^2}{d_o^2} \left(\frac{1 + \frac{2\sqrt{3}}{\pi}}{3} \right) \tag{13}$$

$$= C_o \left[1 + \frac{0.83\, z_1}{d_o} + 0.113 \left(\frac{x_1^2 + y_1^2}{d_o^2} \right) + \frac{0.70\, z_1^2}{d_o^2} \right]$$

The expression is normalized in terms of C_o which is 1/6 of the entire centered rotor capacitance. Other expressions are similar and may be derived simply by interchanging variables and signing the linear terms properly. To second-order accuracy, the capacitance equations for the hexahedral electrodes are

$$C_1 = C_o \left[1 + \frac{0.83\, x_1}{d_o} + 0.113 \frac{y_1^2 + z_1^2}{d_o^2} + \frac{0.70\, x_1^2}{d_o^2} \right]$$

$$C_2 = C_o \left[1 - \frac{0.83\, x_1}{d_o} + 0.113 \frac{y_1^2 + z_1^2}{d_o^2} + \frac{0.70\, x_1^2}{d_o^2} \right]$$

$$C_3 = C_o \left[1 + \frac{0.83\, y_1}{d_o} + 0.113 \frac{x_1^2 + z_1^2}{d_o^2} + \frac{0.70\, y_1^2}{d_o^2} \right] \tag{14}$$

$$C_4 = C_o \left[1 - \frac{0.83\, y_1}{d_o} + 0.113 \frac{x_1^2 + z_1^2}{d_o^2} + \frac{0.70\, y_1^2}{d_o^2} \right]$$

$$C_5 = C_o \left[1 + \frac{0.83\, z_1}{d_o} + 0.113 \frac{x_1^2 + y_1^2}{d_o^2} + \frac{0.70\, z_1^2}{d_o^2} \right]$$

$$C_6 = C_o \left[1 - \frac{0.83\, z_1}{d_o} + 0.113 \frac{x_1^2 + y_1^2}{d_o^2} + \frac{0.70\, z_1^2}{d_o^2} \right]$$

Hexahedral electrodes, voltage-fed system. -- The electric force equations can now be derived by substituting the capacitance equations (14) into the potential energy equation (2) (after dropping the interelectrode potential terms) and applying the gradient operator (1). To take into consideration the fact that electrode voltages are controlled (and not charge), the sign of (1) must be changed. For a more complete explanation, refer to Smythe[2]. Therefore,

$$F_z = -\frac{\partial W}{\partial z} = -\frac{1}{2} \sum_{i=1}^{6} V_i^2 \frac{\partial C_i}{\partial z}$$

$$= -\frac{1}{2} \left[V_1^2 \frac{\partial C_1}{\partial z} + V_2^2 \frac{\partial C_2}{\partial z} + V_3^2 \frac{\partial C_3}{\partial z} + V_4^2 \frac{\partial C_4}{\partial z} \right. \quad (15)$$

$$\left. + V_5^2 \frac{\partial C_5}{\partial z} + V_6^2 \frac{\partial C_6}{\partial z} \right]$$

Substituting for the partial derivatives gives

$$F_z = \frac{1}{2} \left\{ \frac{2 C_o V_1^2 z_1}{d_o^2} (0.113) + \frac{2 C_o V_2^2 z_1}{d_o^2} (0.113) \right.$$

$$\left. + \frac{2 C_o V_3^2 z_1}{d_o^2} (0.113) + \frac{2 C_o V_4^2 z_1}{d_o^2} (0.113) \right.$$

---

[2] Ibid., pp. 39-40

$$+ C_o \quad V_5^2 \left[\frac{0.83}{d_o} + \frac{2 z_1 (0.70)}{d_o^2} \right]$$

$$+ C_o \quad V_6^2 \left[\frac{-0.83}{d_o} + \frac{2 z_1 (0.70)}{d_o^2} \right] \tag{16}$$

$$= \frac{0.113 z_1 C_o}{d_o^2} (V_1^2 + V_2^2 + V_3^2 + V_4^2)$$

$$+ \frac{0.70 z_1 C_o}{d_o^2} (V_5^2 + V_6^2) + \frac{0.83 C_o}{2 d_o} (V_5^2 - V_6^2)$$

This expression may be normalized with respect to the force produced by a single electrode at bias voltage level (V_o) on a centered rotor ($z_1 = 0$).

$$F_o = \frac{0.83 C_o}{2 d_o} \quad V_o^2 \tag{17}$$

$$C_o = \frac{2 d_o F_o}{0.83 V_o^2}$$

$$F_z = \frac{0.226 F_o z_1}{0.83 V_o^2 d_o} (V_1^2 + V_2^2 + V_3^2 + V_4^2)$$

$$+ \frac{1.40 F_o z_1}{0.83 V_o^2 d_o} (V_5^2 + V_6^2) + \frac{F_o}{V_o^2} (V_5^2 - V_6^2)$$

$$F_z = F_o \left[\left(\frac{V_5^2 - V_6^2}{V_o^2} \right) + 1.666 \frac{z_1}{d_o} \left(\frac{V_5^2 + V_6^2}{V_o^2} \right) \right. \tag{18a}$$

$$\left. + 0.272 \frac{z_1}{d_o} \left(\frac{V_1^2 + V_2^2 + V_3^2 + V_4^2}{V_o^2} \right) \right]$$

To derive the x and y components of force, the potential energy function, W, is differentiated with respect to x and y, respectively. Since the problem is identical to that for F_z and since the electrodes are symmetric, the equations can be written by submitting x or y, for z, while permuting the V_i's.

$$F_x = F_o \left[\frac{V_1^2 - V_2^2}{V_o^2} + 1.666 \frac{x_1}{d_o} \left(\frac{V_1^2 + V_2^2}{V_o^2} \right) \right. \tag{18b}$$

$$\left. + \frac{0.272\, x_1}{d_o} \left(\frac{V_3^2 + V_4^2 + V_5^2 + V_6^2}{V_o^2} \right) \right]$$

$$F_y = F_o \left[\frac{V_3^2 - V_4^2}{V_o^2} + 1.666 \frac{y_1}{d_o} \left(\frac{V_3^2 + V_4^2}{V_o^2} \right) \right. \tag{18c}$$

$$\left. + \frac{0.272\, y_1}{d_o} \left(\frac{V_1^2 + V_2^2 + V_5^2 + V_6^2}{V_o^2} \right) \right]$$

Hexahedral electrodes, current-fed system. -- The z axis force may also be expressed in terms of electrode currents. Although voltage source control is rather easy to describe from the energy relationships, current source control is not. This type of control is realized by use of high-impedance, a-c output circuits which force the current at the electrode terminal to be a constant (not a function of rotor position). Leakage currents modify the actual electrode currents and modify the form of the equations which are formed. A current-driven system affords certain advantages in torque reduction and, in some systems, current constraints are more practical to implement than voltage constraints. Equation (4) may be evaluated for the case where the V_i's are a function of rotor position.

$$\frac{\partial W}{\partial z} = \frac{1}{2}\left[\sum_{i=1}^{6}\left(V_i^2\ \frac{\partial C_i}{\partial z} + 2\ C_i\ V_i\ \frac{\partial V_i}{\partial z}\right) + \sum_{i=1}^{6}\sum_{j=1}^{6}(-1)^n\ \frac{\partial}{\partial z}\left(V_i\ V_j\ C_{ij}\right)\right] \tag{19}$$

$$n = 0 \text{ for } i = j$$

$$n = 1 \text{ for } i \neq j$$

This summation is difficult to evaluate without making some assumptions about the various capacitances which exist at the device output. The second part breaks down into several terms which may be evaluated separately. They are of the form

$$V_i^2\ C_g + V_i^2\ C_{ij} - 2\ V_i\ V_j\ C_{ij} \ldots$$

where i represents the electrode of interest and j is any (and all) others, $C_g + C_{ij}$ makes up C_{ii} from Equation (4), and C_g is the capacitance to ground. Differentiating this expression in the axis of interest results in terms of the form

$$2\ V_i\ C_g\ \frac{\partial\ V_i}{\partial z} + V_i^2\ \frac{\partial C_g}{\partial z} + 2\ V_i\ C_{ij}\ \frac{\partial V_i}{\partial z} + V_i^2\ \frac{\partial C_{ij}}{\partial z}$$

$$- 2\ V_i\ V_j\ \frac{\partial C_{ij}}{\partial z} - 2\ V_i\ C_{ij}\ \frac{\partial V_j}{\partial z} - 2\ V_j\ C_{ij}\ \frac{\partial V_i}{\partial z}$$

Now, by definition $\frac{\partial C_g}{\partial z} = 0$; also, $\frac{\partial C_{ij}}{\partial z}$ and $\frac{\partial V_j}{\partial z}$ represent such relatively small quantities that they may be neglected. All other derivatives in the summation likewise may be ignored. Three terms remain:

$$2\ V_i\ (C_g + C_{ij})\ \frac{\partial V_i}{\partial z} - 2\ V_j\ C_{ij}\ \frac{\partial V_i}{\partial z}$$

Since current-fed systems are usually three-phase, the sum of the V_j terms is a vector in the i axis and thus may be added directly. Thus, the total term sums to

$$\sum_i \sum_j 2\ V_i\ [C_g + C_{ij}\ (1 - K)]\ \frac{\partial V_i}{\partial z}$$

where K is a nonphased term depending on the relative magnitudes of the cross-axis voltages. The value of K is very nearly (-8) for most systems. Thus, the summation over j reduces the terms to

$$\sum_i 2\ V_i\ (C_g + 9\ C_{ik})\ \frac{\partial V_i}{\partial z}$$

where C_{ik} is a single interelectrode capacitance. Now V_i is the voltage developed across this composite stray capacitance by the impressed current.

$$V_i = \frac{I_i}{j\omega\ (C_i + C_g + 8\ C_{ik})} = \frac{I_i}{j\omega\ (C_i + C_s)} \qquad (20)$$

Now the expression for force in the z axis may be evaluated.

$$\frac{\partial W}{\partial z} = -\frac{1}{2} \sum_{i=1}^{6} \left\{ \frac{I_i^2}{\omega^2\ (C_i + C_s)^2} + \frac{2\ C_i\ I_i}{\omega\ (C_i + C_s} \cdot \frac{(-1)\ I_i}{\omega(C_i + C_s)} \right.$$

$$\left. + \frac{2\ I_i\ C_s}{\omega\ (C_i + C_s)} \cdot \frac{(-1)\ I_i}{(C_i + C_s)^2} \right\} \frac{\partial\ C_i}{\partial z}$$

$$\frac{\partial W}{\partial z} = -\frac{1}{2}\sum_{i=1}^{6}\left[\frac{I_i^2}{\omega^2 (C_i+C_s)^2} - \frac{2 I_i}{\omega^2 (C_i+C_s)^2}\left(\frac{C_i}{C_i+C_s} + \frac{C_s}{C_i+C_s}\right)\right]\frac{\partial C_i}{\partial z} \qquad (21)$$

$$= -\frac{1}{2\omega^2}\sum_{i=1}^{6}\frac{I_i^2}{(C_i+C_s)^2}\frac{\partial C_i}{\partial z}$$

Note that (in contrast to the voltage-fed system) the derivations must be evaluated and then divided by $(C_i + C_s)^2$. As a result, only the value of the bias force (F_o) and the self-axis term is changed. These terms are found by letting $C_s = \beta C_o$ and evaluating in terms of β, the stray to "centered" electrode capacitance ratio. This implies that the stray capacitance is equal in all channels (which is not exactly true, but is a reasonable approximation). Expansion of (21) into its component terms and application of (1) results in the expression:

$$F_z = \frac{1}{2\omega^2}\left[\frac{I_1^2}{(C_1+C_s)^2}\frac{\partial C_1}{\partial z} + \frac{I_2^2}{(C_2+C_s)^2}\frac{\partial C_2}{\partial z} + \frac{I_3^2}{(C_3+C_s)^2}\frac{\partial C_3}{\partial z}\right.$$

$$\left. + \frac{I_4^2}{(C_4+C_s)}\frac{\partial C_4}{\partial z} + \frac{I_5^2}{(C_5+C_s)^2}\frac{\partial C_5}{\partial z} + \frac{I_6^2}{(C_6+C_s)^2}\frac{\partial C_6}{\partial z}\right]$$

$$= \frac{C_o}{2\omega^2}\left[\frac{I_1^2 \dfrac{2 z_1 (0.113)}{d_o^2}}{\left(1+2\beta \dfrac{1.66 x_1}{d_o}\right) C_o^2} + \frac{I_2^2 \dfrac{2 z_1 (0.113)}{d_o^2}}{\left(1+2\beta - \dfrac{1.66 x_1}{d_o}\right) C_o^2}\right.$$

$$\left. + \frac{I_3^2 \dfrac{2 z_1 (0.113)}{d_o^2}}{\left(1+2\beta + \dfrac{1.66 y_1}{d_o}\right) C_o^2} + \frac{I_4^2 \dfrac{2 z_1 (0.113)}{d_o^2}}{\left(1+2\beta - \dfrac{1.66 y_1}{d_o}\right) C_o^2}\right.$$

$$+\frac{I_5^2\left(\frac{0.83}{d_o}+\frac{2\,z_1\,(0.70)}{d_o^2}\right)}{\left(1+2\beta+\frac{1.66\,z_1}{d_o}\right)C_o^2}+\frac{I_6^2\left(-\frac{0.83}{d_o}+\frac{2\,z_1\,(0.70)}{d_o^2}\right)}{\left(1+2\beta-\frac{1.66\,z_1}{d_o}\right)C_o^2}\Bigg]$$

(22)

$$=\frac{C_o}{2\omega^2(1+2\beta)C_o^2}\Bigg[\frac{2\,z_1\,(0.113)}{d_o^2}\left(I_1^2+I_2^2+I_3^2+I_4^2\right)$$

$$+\left(I_5^2-I_6^2\right)\frac{0.83}{d_o}-\left(I_5^2+I_6^2\right)\frac{z_1}{d_o^2}\left([1+2\beta]\,0.843-0.83\right)0.83\Bigg]$$

Define

$$F_o=\frac{I_o^2\,(0.83)}{2\,\omega^2\,C_o\,d_o\,(1+2\beta)}$$

This is the z force per electrode with only bias current applied. Normalized in this way, the z axis force component reduces to

$$F_z=F_o\Bigg[\frac{I_5^2-I_6^2}{I_o^2}-\frac{(0.013+1.686\beta)\,Z_1}{d_o}\left(\frac{I_5^2+I_6^2}{I_o^2}\right)$$

(23a)

$$+\frac{0.272\,z_1}{d_o}\left(\frac{I_1^2+I_2^2+I_3^2+I_4^2}{I_o^2}\right)\Bigg]$$

The corresponding x and y components of the force equation are

$$F_x = F_o\left[\frac{I_1^2 - I_2^2}{I_o^2} - \frac{(0.013+1.686\beta)Y_1}{d_o}\left(\frac{I_1^2 + I_2^2}{I_o^2}\right)\right. \qquad (23b)$$
$$\left. + \frac{0.272\, x_1}{d_o}\left(\frac{I_3^2 + I_4^2 + I_5^2 + I_6^2}{I_o^2}\right)\right]$$

$$F_y = F_o\left[\frac{I_3^2 - I_4^2}{I_o^2} - \frac{(0.013 + 1.686\beta)\, Y_1}{d_o}\left(\frac{I_3^2 + I_4^2}{I_o^2}\right)\right. \qquad (23c)$$
$$\left. + \frac{0.272\, y_1}{d_o}\left(\frac{I_1^2 + I_2^2 + I_5^2 + I_6^2}{I_o^2}\right)\right]$$

Circular electrodes, force equations. -- The same elemental area and gap expressions may be used to evaluate capacitance expressions for the circular electrodes. Figure 2 is an illustration of this type electrode. The boundaries are simpler, being a full circle in ϕ and from 0 to θ_o in θ. Since reduced area electrodes produce smaller cross-coupling coefficients, which results in lower electric drift torques, θ_o is left as a parameter. The maximum value of θ is 45°, the angle at which each electrode is tangent to its neighbors. The largest size of circular electrodes which can be mounted orthogonally in one hemisphere corresponds to $\theta_o \cong 35°$.

The capacitance integral is the same as Equation (12), with the limits altered to describe the circular electrode structure. The capacitance expression for the +z electrode which results from this integration is

$$C_5 = \frac{\varepsilon_o r_o^2 \quad 2\pi (1-\cos\theta_o)}{d_o} \quad \left\{ 1 + \frac{z_1}{2d_o} \quad \frac{\sin^2\theta_o}{(1-\cos\theta_o)} \right.$$

$$+ \frac{z_1^2}{3 d_o^2} \quad \frac{(1 - \cos^3\theta_o)}{(1 - \cos\theta_o)} \quad + \frac{1}{6} \quad \left[\frac{2 - \cos\theta_o (\sin^2\theta_o + 2)}{1 - \cos\theta_o} \right] \qquad (24)$$

$$\left. \frac{x_1^2 + y_1^2}{d_o^2} \right\}$$

This form of the expression is quite unwieldy and may be simplified by normalizing as before and by using constants (K_i's) to represent the functions of θ_o which appear.

$$C_5 = C_o \left[1 + K_1 \frac{z_1}{d_o} + K_2 \frac{z_1^2}{d_o^2} + K_3 \frac{x_1^2 + y_1^2}{d_o^2} \right]$$

where

$$C_o = \frac{\varepsilon_o r_o^2 \cdot 2\pi (1 - \cos\theta_o)}{d_o}$$

$$K_1 = \frac{\sin^2\theta_o}{2 (1 - \cos\theta_o)} \qquad (25)$$

$$K_2 = \frac{(1 - \cos^3\theta)}{3 (1 - \cos\theta_o)}$$

$$K_3 = \frac{\left[2 - \cos\theta_o (\sin^2\theta_o + 2)\right]}{6 (1 - \cos\theta_o)}$$

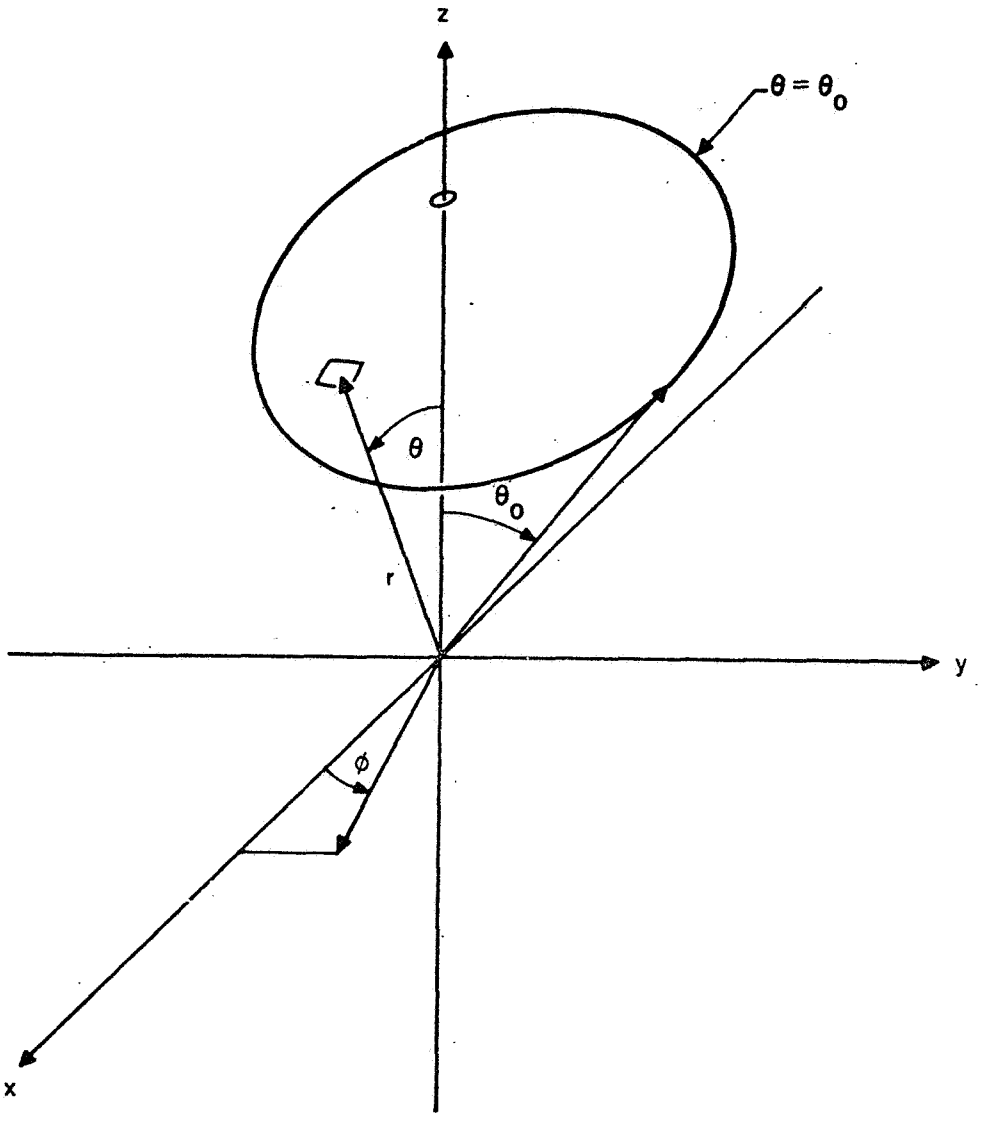

θ = COLATITUDE
θ_0 = ELECTRODE BOUNDARY
ϕ = LONGITUDE
r = NOMINAL RADIUS

Figure 2. Circular Electrode

$$F_z = C_o \left[\frac{K_1}{2d_o} \left(V_5^2 - V_6^2 \right) + \frac{K_3 z_1}{d_o^2} \left(V_1^2 + V_2^2 + V_3^2 + V_4^2 \right) \right. \tag{27}$$

$$\left. + \frac{K_2 z_1}{d_o^2} \left(V_5^2 + V_6^2 \right) \right]$$

Normalizing as before with the equation

$$F_o = \frac{C_o V_o^2 K_1}{2 d_o} \tag{28}$$

the final equation is

$$F_z = F_o \left[\frac{V_5^2 - V_6^2}{V_o^2} + \left(\frac{V_5^2 + V_6^2}{V_o^2} \right) \frac{2 K_2 z_1}{K_1 d_o} \right. \tag{29a}$$

$$\left. + \left(\frac{V_1^2 + V_2^2 + V_3^2 + V_4^2}{V_o^2} \right) \frac{2 K_3 z_1}{K_1 d_o} \right]$$

Similarly, the other force components can be derived

$$F_x = F_o \left[\frac{V_1^2 - V_2^2}{V_o^2} + \left(\frac{V_1^2 + V_2^2}{V_o^2} \right) \frac{2 K_2 x_1}{K_1 d_o} \right. \tag{29b}$$

$$\left. + \left(\frac{V_3^2 + V_4^2 + V_5^2 + V_6^2}{V_o^2} \right) \frac{2 K_3 x_1}{K_1 d_o} \right]$$

The other capacitance equations are obtained by permuting the displacement variables, paying attention to the sign of the linear terms. Equations (26) comprise the complete set.

$$C_1 = C_o \left(1 + K_1 \frac{x_1}{d_o} + K_2 \frac{x_1^2}{d_o^2} + K_3 \frac{\left(y_1^2 + z_1^2\right)}{d_o^2} \right)$$

$$C_2 = C_o \left(1 - K_1 \frac{x_1}{d_o} + K_2 \frac{x_1^2}{d_o^2} + K_3 \frac{\left(y_1^2 + z_1^2\right)}{d_o^2} \right)$$

$$C_3 = C_o \left(1 + K_1 \frac{y_1}{d_o} + K_2 \frac{y_1^2}{d_o^2} + K_3 \frac{\left(x_1^2 + z_1^2\right)}{d_o^2} \right)$$

$$C_4 = C_o \left(1 - K_1 \frac{y_1}{d_o} + K_2 \frac{y_1^2}{d_o^2} + K_3 \frac{\left(x_1^2 + z_1^2\right)}{d_o^2} \right) \qquad (26)$$

$$C_5 = C_o \left(1 + K_1 \frac{z_1}{d_o} + K_2 \frac{z_1^2}{d_o^2} + K_3 \frac{x_1^2 + y_1^2}{d_o^2} \right)$$

$$C_6 = C_o \left(1 - K_1 \frac{z_1}{d_o} + K_2 \frac{z_1^2}{d_o^2} + K_3 \frac{x_1^2 + y_1^2}{d_o^2} \right)$$

Circular electrodes, voltage-fed system. -- Following the same procedure as that used for hexahedral electrodes, the force equations are derived for a voltage-fed system.

The z axis force component is

$$F_y = F_o \left[\frac{V_3^2 - V_4^2}{V_o^2} + \left(\frac{V_3^2 + V_4^2}{V_o^2} \right) \frac{2 K_2 y_1}{K_1 d_o} \right. \qquad (29c)$$

$$\left. + \left(\frac{V_1^2 + V_2^2 + V_5^2 + V_6^2}{V_o^2} \right) \frac{2 K_3 y_1}{K_1 d_o} \right]$$

Circular electrodes, current-fed system. -- For the current-fed system, (21) is used again. Substituting (26) into (21) and performing the differentiation leads to the equation for F_z

$$F_z = \frac{C_o}{2\omega^2} \left[\frac{2 K_3 z_1}{d_o^2} \frac{\left(I_1^2 + I_2^2 + I_3^2 + I_4^2 \right)}{C_o^2 (1 + 2\beta)} \right.$$

$$\left. + \frac{I_5^2 \left(\frac{K_1}{d_o} + \frac{2 K_2 z_1}{d_o^2} \right)}{C_o^2 \left(1 + 2\beta + \frac{2 K_1 z_1}{d_o} \right)} + \frac{I_6^2 \left(- \frac{K_1}{d_o} + \frac{2 K_2 z_1}{d_o^2} \right)}{C_o^2 \left(1 + 2\beta - \frac{2 K_1 z_1}{d_o} \right)} \right] \qquad (30)$$

$$= \frac{C_o}{(1 + 2\beta) 2\omega^2} \left[\frac{2 K_3 z_1}{d_o^2} \frac{\left(\sum_1^4 I_i^2 \right)}{C_o^2} + \frac{\left(I_5^2 - I_6^2 \right)}{C_o^2} \frac{K_1}{d_o} \right.$$

$$\left. + \frac{\left(I_5^2 + I_6^2 \right)}{C_o^2} \left([1 + 2\beta] K_2 - K_1^2 \right) \frac{2 z_1}{d_o^2} \right]$$

This equation is normalized in terms of the centered force F_o

$$F_o = \frac{I_o^2 K_1}{2 \omega^2 C_o d_o (1+2\beta)} \tag{31}$$

The final result for F_z is

$$F_z = F_o \left[\frac{I_5^2 - I_6^2}{I_o^2} + \frac{2 z_1}{d_o} \left(\frac{(1+2\beta)K_2}{K_1} - K_1 \right) \left(\frac{I_5^2 + I_6^2}{I_o^2} \right) \right. \tag{32a}$$

$$\left. + \frac{2 K_3 z_1}{K_1 d_o} \left(\frac{I_1^2 + I_2^2 + I_3^2 + I_4^2}{I_o^2} \right) \right]$$

The x and y force components are

$$F_x = F_o \left[\frac{I_1^2 - I_2^2}{I_o^2} + \frac{2 x_1}{d_o} \left(\frac{(1+2\beta) K_2}{K_1} - K_1 \right) \left(\frac{I_1^2 + I_2^2}{I_o^2} \right) \right.$$

$$\left. + \frac{2 K_3 x_1}{K_1 d_o} \left(\frac{I_3^2 + I_4^2 + I_5^2 + I_6^2}{I_o^2} \right) \right] \tag{32b}$$

$$F_y = F_o \left[\frac{I_3^2 - I_4^2}{I_o^2} + \frac{2 x_1}{d_o} \left(\frac{(1+2\beta) K_2}{K_1} - K_1 \right) \left(\frac{I_3^2 + I_4^2}{I_o^2} \right) \right. \tag{32c}$$

$$\left. + \frac{2 K_3 x_1}{K_1 d_o} \left(\frac{I_1^2 + I_2^2 + I_5^2 + I_6^2}{I_o^2} \right) \right]$$

The numerical evaluation of the circular electrode constants may best be handled by means of a graphical plot of the constants as a function of θ_o. Since ratios of the constants appear in the force equations, the graphs would be more useful if the same ratios were plotted. The first graph is that of the constant K_1 which is the ratio of projected area to spherical area of the electrode.

$$K_1 = \frac{1}{4}\left(\frac{1 - \cos 2\theta_o}{1 - \cos \theta_o}\right) \tag{33}$$

This graph is shown in Figure 3.

The next constant is the ratio

$$\frac{2K_2}{K_1} = \frac{4(1 - \cos^3 \theta_o)}{3 \sin^2 \theta_o} = \frac{4}{3} \cdot \frac{2 - \cos \theta_o - \cos \theta_o \cos 2\theta_o}{1 - \cos^2 \theta_o} \tag{34}$$

This ratio is the self-axis coupling factor and is a measurement of the force perturbation caused by translation in the direction of force. This ratio is plotted in Figure 4.

The final constant is the ratio

$$\frac{2K_3}{K_1} = \frac{2}{3} \cdot \frac{4 - 5 \cos \theta_o + \cos \theta_o \cos 2\theta_o}{1 - \cos^2 \theta_o} \tag{35}$$

that is the cross-coupling factor. Rotor translation along one force axis causes the center of force to shift in the direction of translation as a result of the "wrapping" effect of the spherical geometry. This constant is shown in Figure 5.

The large, "self-axis" coefficient which appears as a destabilizing term in the voltage equations may be reduced by feedback through the suspension servo which is a direct (uncompensated) function of rotor displacement. Using Equation (29b) with

$$V_1 = V_o - K_o \frac{x_1}{d_o} \quad \text{and} \quad V_2 = V_o + \frac{K_o x_1}{d_o}$$

gives

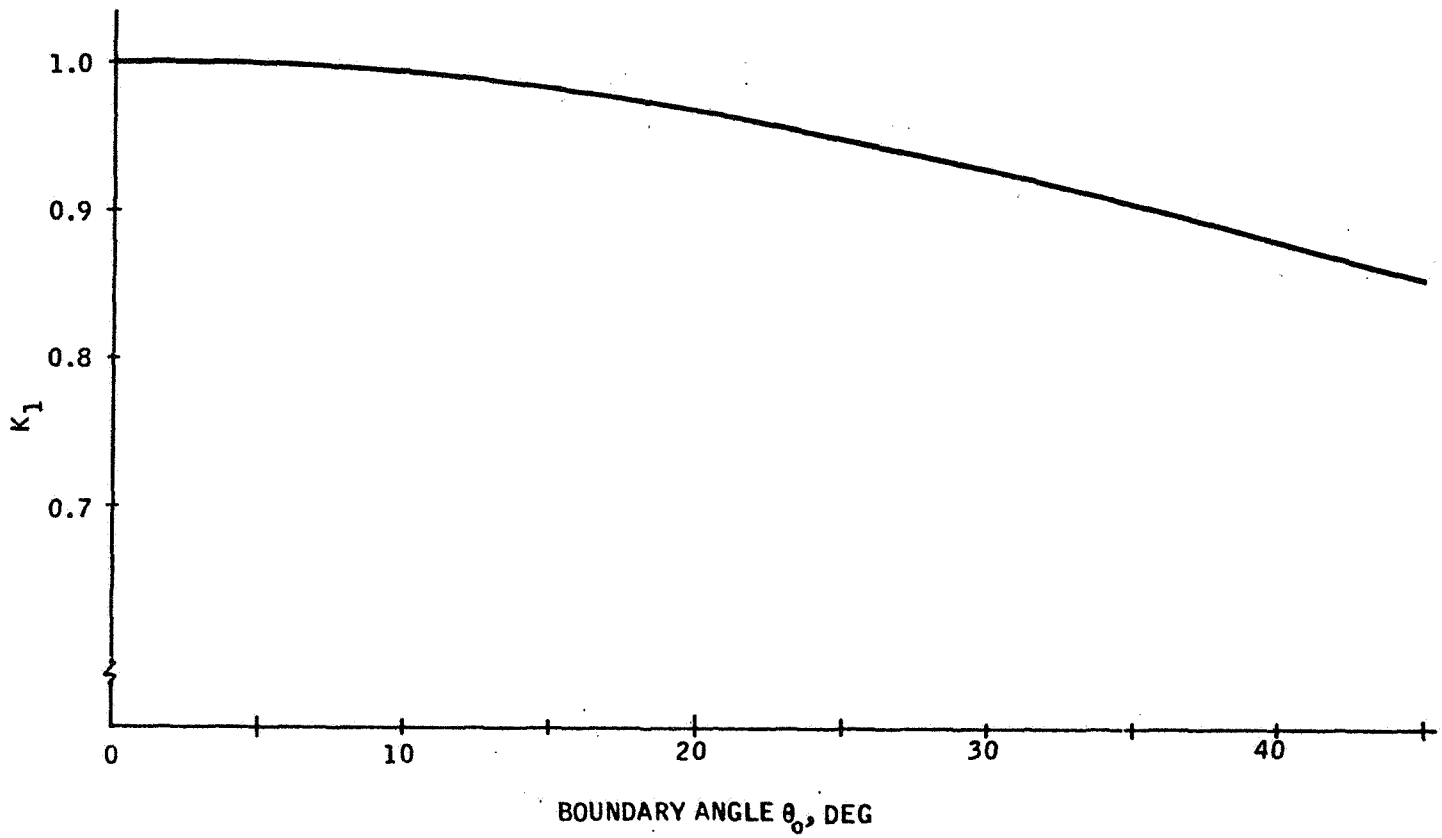

Figure 3. Electrode Area Ratio, K_1 versus Boundary Angle

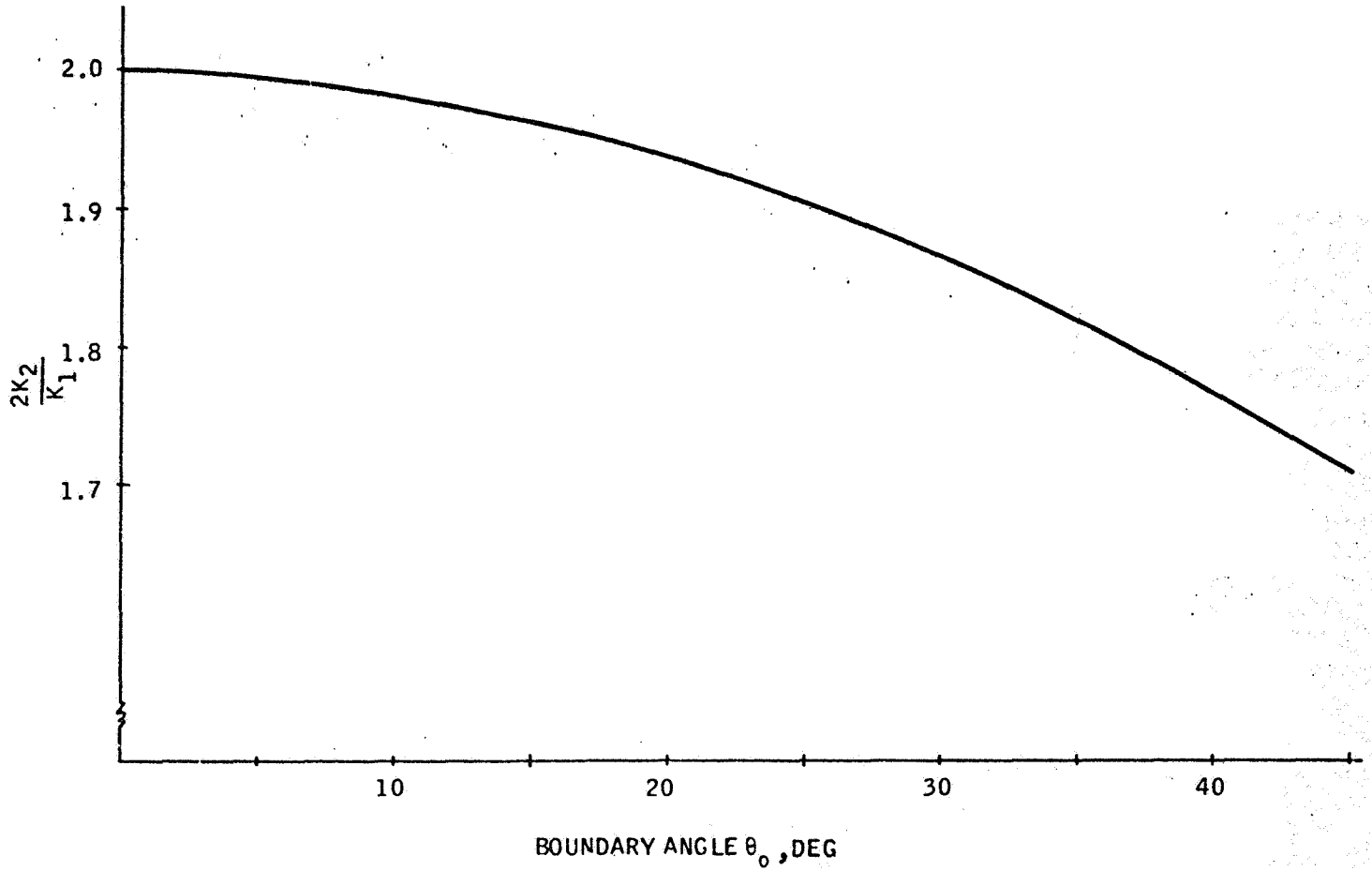

Figure 4. Self-Axis Coupling $\frac{2K_2}{K_1}$ versus Boundary Angle

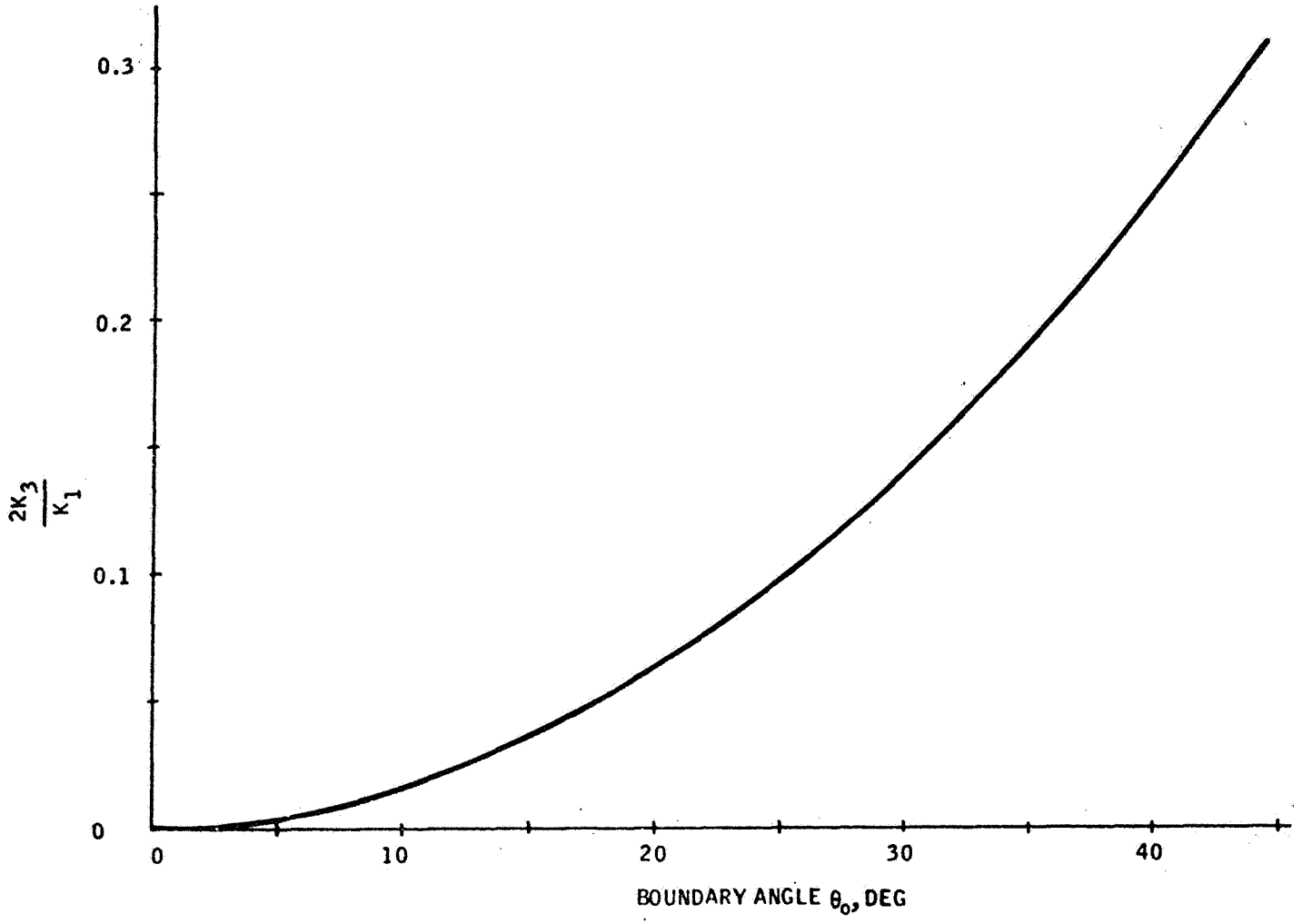

Figure 5. Cross-Axis Coupling Ratio $\frac{2K_3}{K_1}$ versus Boundary Angle

$$F_x = F_o \left[- \frac{4 K_o V_o x_1}{V_o^2 d_o} + \frac{2 V_o^2 + 2 \left(\frac{K_o x_1}{d_o} \right)^2}{V_o^2} \frac{2 K_2 x_1}{d_o d_o} + \ldots \right] \quad (36)$$

For the case where displacement is relatively small ($<0.1\ d_o$), the equation may be solved simply for K_o:

$$K_o = \frac{V_o K_2}{K_1}$$

A feedback path with this gain will produce a system which has near-zero, self-axis force change with rotor displacement.

High G Limitations

There are natural limits to the force capability of the gyro suspension system. These limits are functions of the material and processes used in the gyro manufacture and of the suspension system output waveform. The basic force equations are used to derive these limits in terms of gyro physical parameters.

Equation derivation. -- From Equation (18), it can be deduced that the minimum force condition occurs when the direction of input is along one of the major axes. Since there is no way, in general, to specify direction of input to the instrument, this case will be used to derive the limit equations. It can also be seen that maximum self-axis force can be exerted when one electrode along a given axis is at zero voltage. The voltage relationships for hexahedral electrodes are used, and it is assumed that feedback is employed to change output directly with displacement. This assumption makes the force equations for the voltage-fed and current-fed systems identical.

The suspension servo is usually designed to operate with some bias voltage on the electrodes. This accomplishes small signal linearization and helps to maintain constant servo loop gain. To this bias voltage (V_o of Equation 17) is added a control voltage which balances the forces acting on the gyro rotor and which is a function of rotor displacement. The addition of bias also allows simplification of mechanical structure. For the three-phase, current-fed system, electrode current balance among all three channels can be arranged with only six electrodes. This balance allows the gyro rotor to remain at "virtual" ground potential. To provide maximum effort, this type system must be biased at one-half output. Other systems use 12 electrodes, and each half-axis is balanced.

To obtain the maximum force condition along the positive z axis, the control voltages in the x and y axes are zero; maximum voltage is applied to one z axis electrode and no voltage on the other. The force causes the rotor to be displaced from center along the z axis; this displacement produces a side axis coupling force from the electrode bias voltage into that axis. The worst case for this coupling occurs when V_o is one-half the maximum, centered voltage. Assuming that V_o is one-half the maximum and the displacement is 10 percent of the gap, the maximum force condition along the z axis is obtained by appropriate substitutions into Equation (18a).

$$(F_z)_{max} \quad F_o = \frac{\left(2\,V_o + \frac{1.66\,V_o\,z_1}{d_o}\right)^2}{V_o^2} - \frac{1.66\,(2\,V_o)^2}{V_o^2}\,\frac{z_1}{d_o} \tag{37}$$

$$- \frac{0.272\,z_1}{d_o}\left[\frac{V_o^2 + V_o^2 + V_o^2 + V_o^2}{V_o^2}\right] = 4\,F_o\,(0.973)$$

Equation (17) is evaluated to find F_o.

$$F_o = \frac{0.83\,\epsilon_o\,A}{2}\left(\frac{V_o}{d_o}\right)^2$$

Substituting into Equation (37) yields

$$(F_z)_{max} = \frac{0.807}{2}\left(\frac{2\,V_o}{d_o}\right)^2 \epsilon_o\,A = \frac{0.807}{2}\left(\frac{V_m}{d_o}\right)^2 \epsilon_o\,A \tag{38}$$

$$(\text{for } V_o = 1/2\,V_m)$$

It is not necessary to adhere to the ratio of V_o to V_m used in this illustration. If V_o is reduced, the side-axis bias coupling is reduced, and the numeric constant given in Equation (38) increases slightly.

These equations have been derived without taking into account any time variation of V. Equations in the next section describe the force-producing content of V_m when a time varying waveform is considered. A term (α) must be included in Equation (38) to account for this fact. The area A for the hexahedral structure is 1/6 the spherical area, less about 13 percent (1-1/2 inch size) for interelectrode gaps and auxiliary ports.

$$A = \frac{\pi D^2}{1.13} \cdot \frac{1}{6}$$

Hence,

$$F_{z\,max} = 0.0595\,\pi\,\epsilon_o\,D^2\left(\frac{V_m}{d}\right)^2\alpha \tag{39}$$

The maximum G capability may be determined by consideration of the rotor mass.

$$F_{z\,max} = M\,A\,G \tag{40}$$

where A is the earth's gravitational constant and G is the ratio of applied acceleration to the earth's gravitation. The rotor mass may be simply expressed if it is considered to be a thin-shelled sphere:

$$M = \pi\,D^2\,T\,\delta\,(2.54)^3 \times 10^{-3}\ k_g \tag{41}$$

where T is average thickness in inches, δ is the material density, and D is the rotor diameter in inches. Equation (41) is substituted into Equation (40) which is, in turn, equated to (39). The result is an expression for G in terms of gyro parameters.

$$G = \frac{0.0595\,(10^{-3})}{(9.81)\,(2.54^3 \times 10^{-3})\,36\pi}\left(\frac{V_m}{d}\right)^2\frac{\alpha\,D^2}{D^2\,T\,\delta}$$

$$= 3.28 \times 10^{-12}\left(\frac{V_m}{d}\right)^2\frac{\alpha}{T\,\delta} \tag{42}$$

This equation is derived for voltage output systems; but since current output systems are ultimately voltage limited and compensation has been made for displacement, the form of the equation is the same for either system.

A similar equation may be derived for circular electrodes. The same procedure is followed by substituting V_m into Equation (27) (with the self-axis term again removed) and solving for maximum z axis force.

$$(F_z)_{max} = \frac{C_o}{2}\left[V_m^2 \frac{K_1}{d_o} + V_m^2\, 2K_3 \frac{z_1}{d_o^2}\right]$$

$$= \frac{\epsilon_o r^2 \pi (1 - \cos\theta_o)}{d_o^2} V_m^2 \left[K_1 + \frac{2K_3 z_1}{d_o}\right]$$

Again a maximum displacement of 10 percent of the gap is assumed. Substituting for K_1 and K_2 yields

$$(F_z)_{max} = \frac{\epsilon_o D^2 \pi}{4}\left(\frac{V_m}{d_o}\right)^2 \left[\frac{\sin^2\theta_o}{2} - \frac{0.1}{3}\left[2 - \cos\theta_o(\sin^2\theta_o + 2)\right]\right] \tag{43}$$

Again using Equations (40) and (41), the maximum attainable acceleration is

$$G = 13.7 \times 10^{-12}\left(\frac{V_m}{d_o}\right)^2 \left[\frac{\sin^2\theta_o}{2} - \frac{0.1}{3}\left[2 - \cos\theta_o(\sin^2\theta_o + 2)\right]\right]\frac{\alpha}{T\delta} \tag{44}$$

An example is calculated by evaluating (44) for $\theta_o = 35°$. The maximum G level attainable is

$$G = 1.85 \times 10^{-12}\left(\frac{V_m}{d_o}\right)^2 \frac{\alpha}{T\delta} \tag{45}$$

Attainable acceleration levels for various gradients and waveforms are considered later.

Equations (42) and (45) show that maximum G capability is a function of average rotor thickness, material, waveform, and obtainable gradient. The force dependency on waveform is considered in the next section.

Material. -- The material used has two direct impacts on attainable G level. The most direct is through density. Since the rotor must also be stiff and conductive (from gyro and suspension considerations), a light metal is indicated. Fortunately, one of the lightest metals, beryllium, has the desired properties. The density of beryllium is 1.8 gm/cc; it has a high modulus (40×10^6 $in.^2/lb$) and a high precision elastic limit, which means it is stable while undergoing stress cycling. The second consideration is gradient attainable with the metallic rotor as one electrode. Although beryllium is not as good as some materials in this respect, it is used because of its advantages in the other areas. Various techniques are available to improve breakdown gradient.

Gradient. -- The maximum obtainable voltage gradient is not easy to define. It depends on surface finish, gap, electrode configuration, and material. Gap is determined by several factors; chief among them is the relative electrode and gyro rotor tolerances as a percentage of the gap. The bandwidth of the suspension output circuits depends on the output step-up ratio in some direct fashion. This limits the maximum voltage that may be produced and, hence, for the usual environments, sets the gap upper limit at about six mils. Lower limit is in the one- to two-mil range for present gyro tolerance parameters. There is no significant change in the maximum gradient that may be sustained over this range of gap (one to six mils). Experience and testing have shown that several regions of operation exist. At gradients lower than about 500 volts per mil, there is very little charge transfer from electrodes to rotor, and for most applications no effects are noticeable. Between 500 and 750 volts per mil, the amount of charge transfer depends on previous history, initial surface finish, and materials. Normal ESVG processing includes surface finishes of such quality that charge buildup is limited to low values. Between 750 and 1000 volts per mil, significant charge buildup occurs, but it is limited to values which the suspension can withstand. 1000 volts per mil is the usually accepted upper limit for gyro operation. Above 1000 volts per mil and up to about 1450 volts per mil, large currents flow due to electron emission between electrodes and rotor. These currents are of sufficient magnitude that surface marking of the rotor can occur. Since the readout senses a pattern marked on the rotor, the current marking will degrade readout in some areas and compromise gyro/system performance. Above 1450 volts per mil, the gradient can cause arcing and eventual suspension failure.

These numbers are all approximate and may be changed by use of new materials or finishing techniques. At present, the beryllium rotor and electroless nickel electrodes have proved to be the best overall material combination.

Wall thickness. -- Since the maximum gradients and material density are fairly closely fixed, the necessary acceleration capability may be used to put an upper bound on thickness. A lower bound can be found by considering strength necessary to withstand machining and grinding, tolerances which may be held during manufacture and mass desired. At present, most rotors have average wall thicknesses of 30 to 60 mils. Two uniform wall rotors with thicknesses of 20 mils have been built for accelerometer applications. A probable lower limit on thickness for shaped rotors with a preferred spin axis is in the 15- to 20-mil range using present manufacturing techniques.

Waveform. -- The desired waveform of the electrode signal is one for which maximum force efficiency (which is equal to the mean square value of the signal) is obtained. A d-c signal has maximum efficiency; however, d-c suspension systems have been found to fail to maintain rotor support when a significant transfer of charge occurs between the rotor and an electrode. Suspension systems with a time-varying output recover more quickly when charge is transferred and are, therefore, more reliable. Consequently, all suspension systems use some type of alternating waveform. The calculation of acceleration and force capability for realizable ESVG suspensions must then take into account the reduction of efficiency that results from alternating waveforms.

Waveform Force Equivalents

The force equations derived in the previous section express instantaneous force value as a function of voltage and/or current applied to the electrode structure. For the case of direct voltage drive, the voltage equations may be applied directly. The time average of this force must be determined to find the actual acceleration capability of the instrument. The force averages (which shall be called effective force) are next derived for two usable waveforms, the sloped square wave and the sine wave. Both waveforms have been employed on earlier ESVG suspensions.

The force waveform is proportional to the square of voltage or current, depending on the system used. For expediency, only the voltage waveform shall be treated:

$$F \propto V^2 \tag{46}$$

If a sine wave is applied,

$$V = V_m \sin \omega t$$

$$F \propto V_m \sin^2 \omega t = V_m^2 \, (1/2 - 1/2 \cos^2 \omega t)$$

The time average of this waveform is

$$F \propto \frac{V_m^2}{2} = \left(V_{rms}\right)^2 \tag{47}$$

Note that with this waveform, the ratio of peak voltage to the effective or force producing voltage is $\sqrt{2}$:1.

If a square wave voltage is applied, the force equation (46) can still be used; the normally sloping sides (rise and fall times) modify the force expression. Rise and fall times are produced by circuit bandwidth limitations. The effective force produced by this type waveform is derived below. A picture of the waveform is shown in Figure 6.

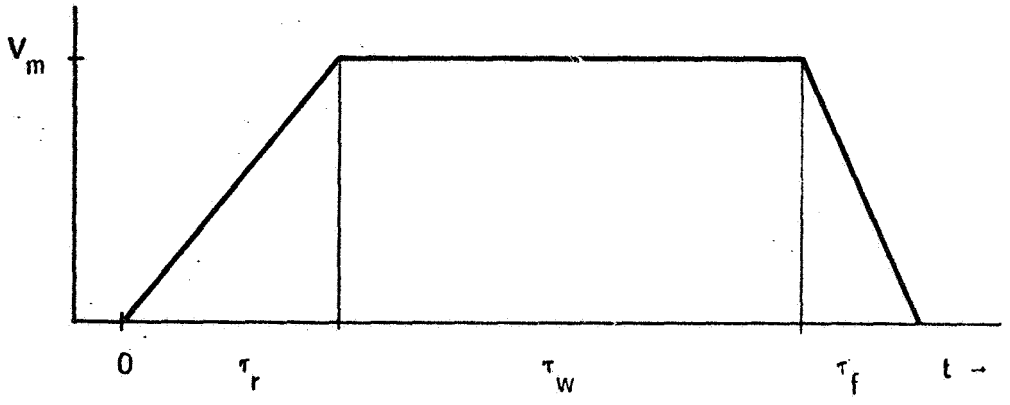

Figure 6. "Square" Waveform

The contribution of each segment is computed separately, and the effective force is evaluated by averaging over the pulse period.

The voltage with time can be expressed by three functions:

1) $V\Big]_0^{\tau_r} = V_m \frac{t}{\tau_r}$

2) $V\Big]_{\tau_r}^{\tau_r + \tau_\omega} = V_m$

$$3)\quad V\Big]_{\tau_r+\tau_\omega}^{\tau_r+\tau_\omega+\tau_f} = V_m\left(1 - \frac{t-(\tau_r+\tau_\omega)}{\tau_f}\right)$$

Over the rising segment

$$F_1 \alpha V_m^2 \frac{t^2}{\tau_r^2}$$

$$\overline{F_1} \alpha V_m^2 \frac{1}{\tau_r}\int_0^{\tau_r}\frac{t^2}{\tau_r^2}\,dt = \frac{V_m^2}{\tau_r^3}\cdot\frac{t^3}{3}\Big]_0^{\tau_r} = \frac{V_m^2}{3} \tag{48}$$

Over the steady segment

$$\overline{F_2} \alpha V_m^2 \tag{49}$$

Over the falling segment

$$F_3 \alpha V_m^2 \left(1 - \frac{t-(\tau_r+\tau_\omega)}{\tau_f}\right)^2,$$

$$\overline{F_3} \alpha \frac{V_m^2}{\tau_f}\int_{\tau_r+\tau_\omega}^{\tau_r+\tau_\omega+\tau_f}\left(\frac{\tau_f+\tau_r+\tau_\omega-t}{\tau_f}\right)\,dt \tag{50}$$

$$= \frac{V_m^2}{\tau_f^3} \cdot \frac{\tau_f^3}{3}$$

$$= \frac{V_m^2}{3}$$

The effective force is

$$F_{net} = \frac{\tau_r F_1 + \tau_\omega F_2 + \tau_f F_3}{\tau_r + \tau_\omega + \tau_f} \tag{51}$$

Thus, the force dependence may be evaluated in terms of a proportionality:

$$F_{net} \alpha V_m^2 \left(\frac{\frac{\tau_r}{3} + \tau_\omega + \frac{\tau_f}{3}}{\tau_r + \tau_\omega + \tau_f} \right) \tag{52}$$

An example of the comparative force available from this type of waveform can be made using (realizable) rise and fall time of five percent of the total half-period. If T is the period,

$$\tau_r = \tau_f = 0.05 \ (\tau_r + \tau_\omega + \tau_f) = 0.05 \ T$$

$$F_{net} \alpha V_m^2 \left(\frac{\frac{0.05T}{3} + 0.9T + \frac{0.05T}{3}}{T} \right) \tag{53}$$

$$F_{net} \alpha 0.93 \ V_m^2$$

Thus, the (modified) square wave is a rather efficient force producer, extracting 93 percent of the maximum available force at the peak voltage specified, for a five-percent risetime ratio.

A more general equation may be derived if the rise and fall times are expressed as a percentage of the total half-cycle time. Let this "risetime ratio" be represented by β:

$$\beta = \frac{\tau_r}{T}$$

Substituting this expression into Equation (52) yields

$$F_{net} \propto V_m^2 \left(\frac{\frac{\beta T}{3} + (1 - 2\beta)\, T + \frac{\beta T}{3}}{T} \right) \tag{54}$$

$$\therefore \quad F_{net} \propto V_m^2 \, (1 - 4/3\, \beta)$$

A plot of this force fraction or efficiency factor is shown in Figure 7.

Figures 8 and 9 are plots of the maximum G capability with all of these factors taken into account.

Loop Equation -- General

Block diagram and derivation. -- The suspension system may be described fairly simply. It is a servo (feedback) control loop which measures the position of an object (the rotor), processes this information, and produces from it a force which keeps the object as close as possible to a fixed reference position. Stability of the system may be determined by considering the transfer function of the fixed elements and the force-producing members.

The loop described above is shown in Figure 10.

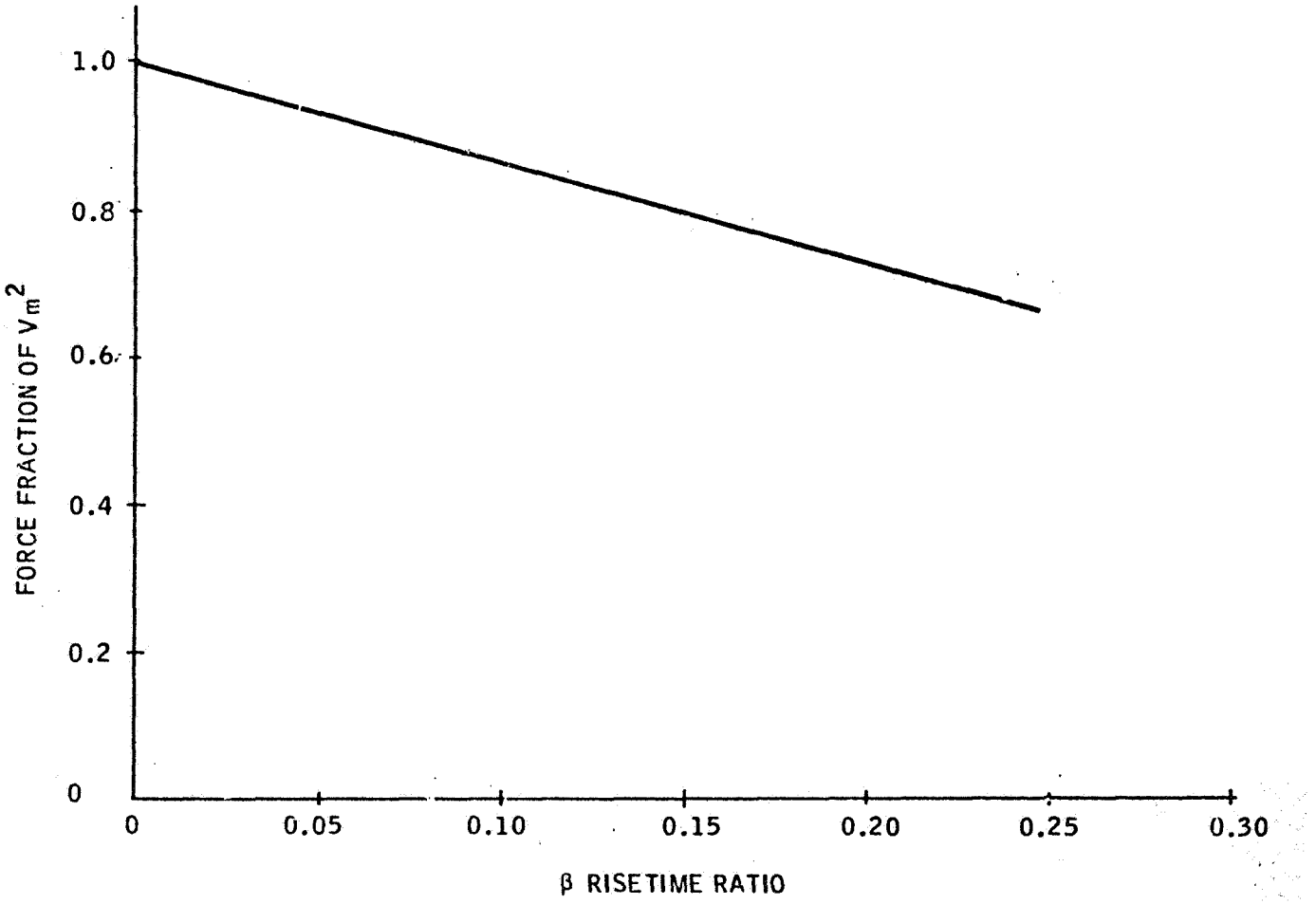

Figure 7. Effect of Rise Time on Effective Force

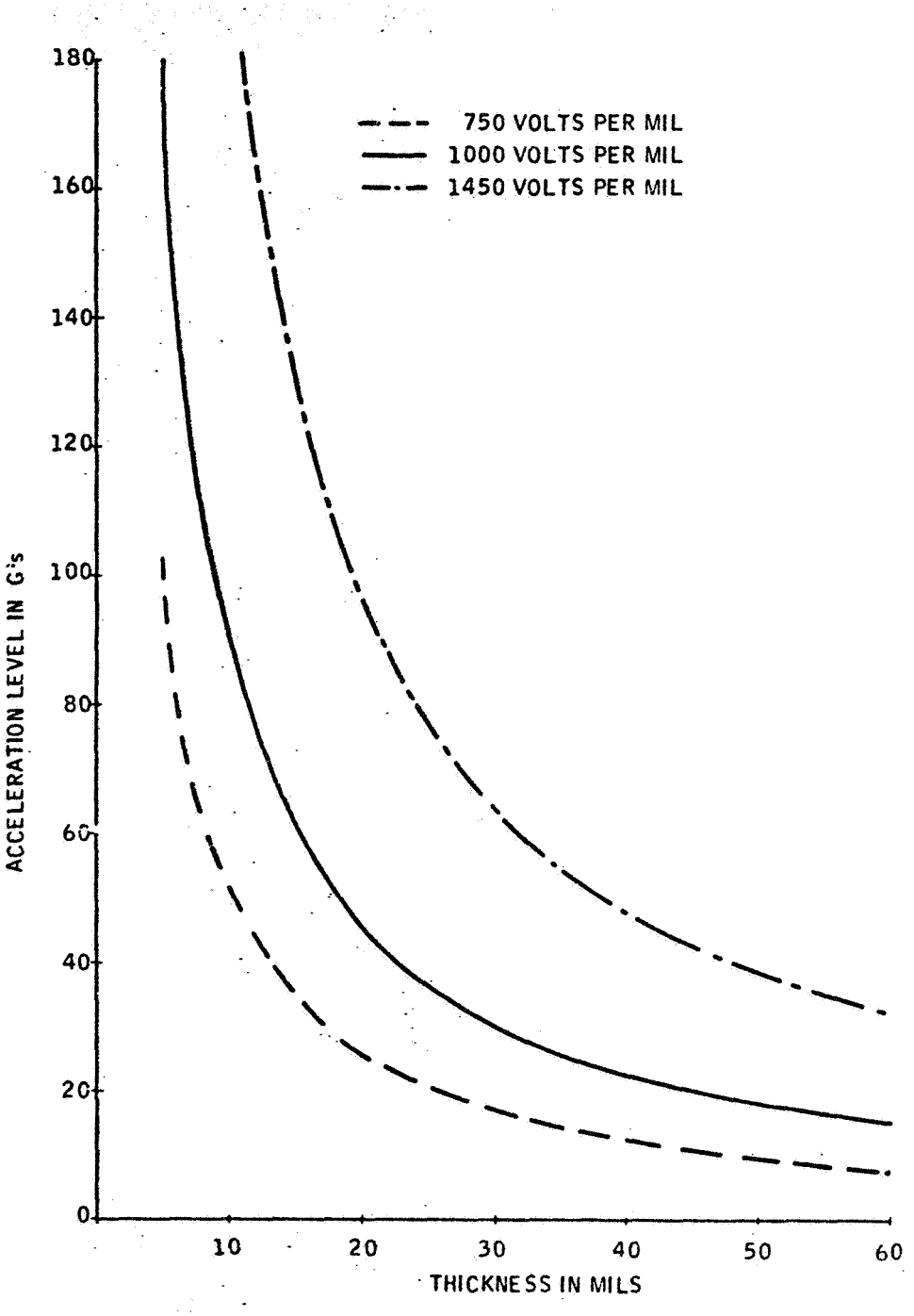

Figure 8. ESVG Acceleration Capability for Sine Wave Output

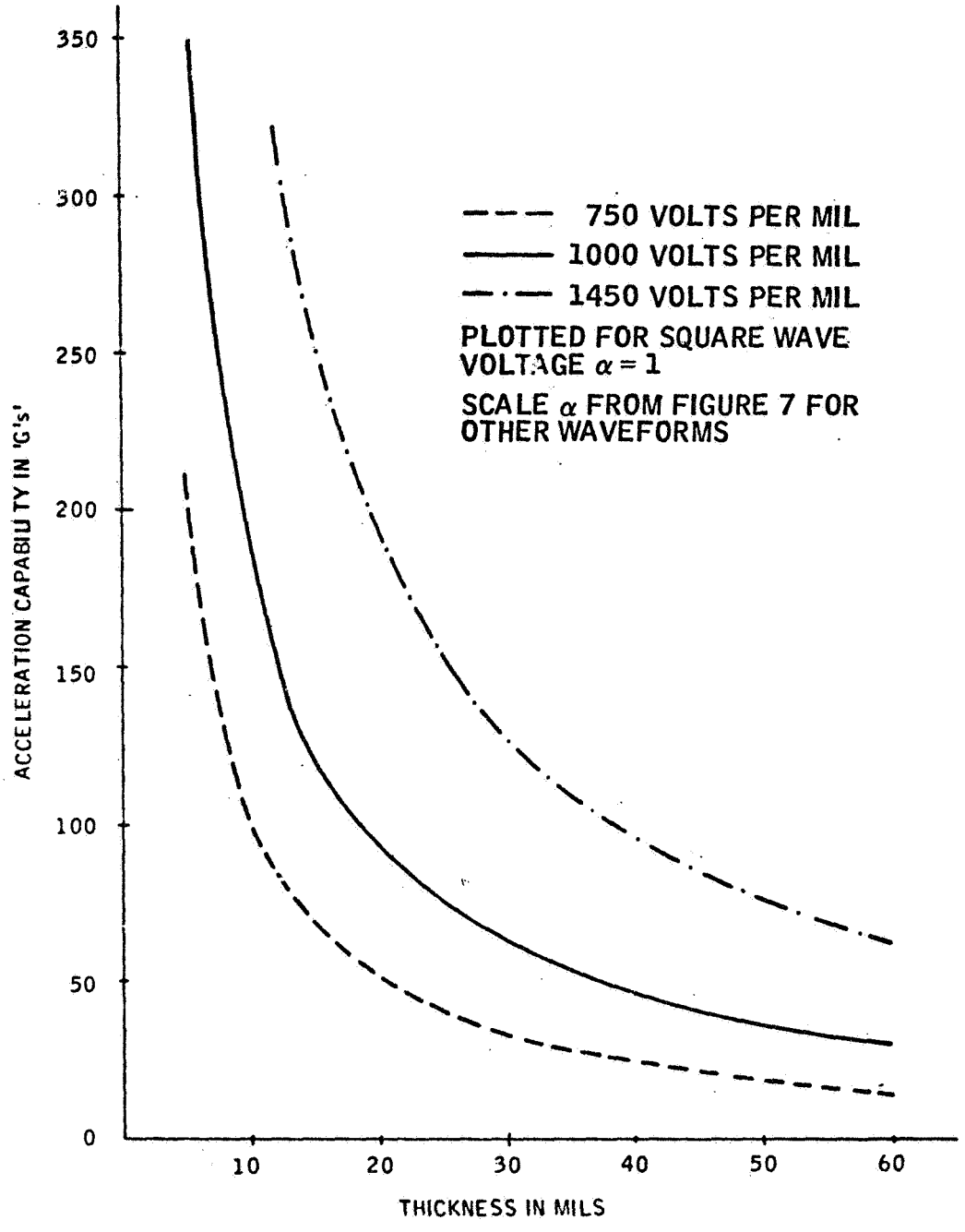

Figure 9. ESVG Acceleration Capability for Square Wave Output

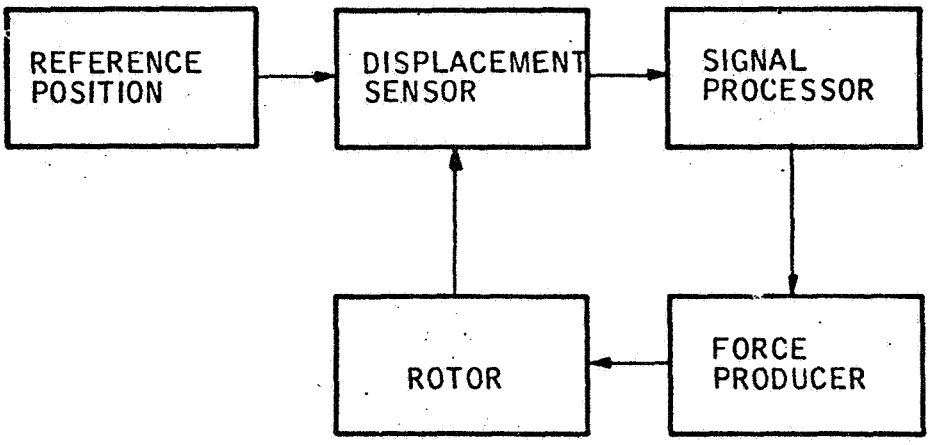

Figure 10. General Diagram of Gyro and Suspension Loop

This diagram is extremely general, and delineation of the device's function will characterize the subassemblies more specifically. The gyro rotor is a spinning body which must be free to rotate about all three body axes. To retain stable gyroscopic properties, its spin axis should be stabilized within the body and its rotation about the spin axis must be relatively drag-free so that the spin speed can be maintained without application of power or disturbing the inertial reference. These requirements are best met by an assembly with the following characteristics:

- Spherical geometry
- Preferred axis internally produced
- Suspension and centering forces produced by electric fields
- Sphere housed in an evacuated chamber
- "No contact" position sensing

The spherical rotor has complete translational freedom within its support bearing as well as complete angular freedom of rotation. It is supported in an evacuated chamber that offers no viscous restraints. Thus, its transfer function in this loop is simply the force-to-distance transformation which is a double integration with respect to time.

The frequency domain transform of this double integration is

$$X(s) = \frac{F(s)}{Ms^2} \tag{55}$$

where X(s) and F(s) are the frequency domain transforms of displacement and force, respectively, and M is the rotor mass. If the (transformed) dynamics of the rest of the loop are represented by K G(s) in dimensions of force per unit displacement, the specific suspension loop may be shown as in Figure 11.

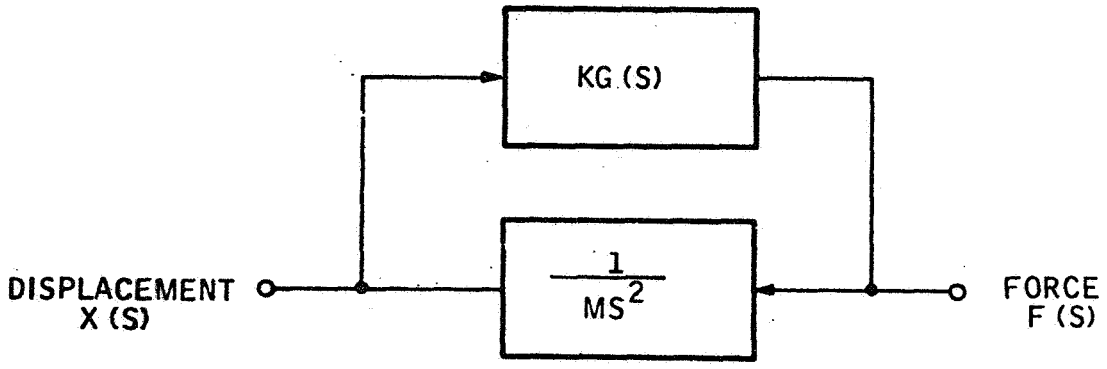

Figure 11. Specific Suspension Diagram

Its characteristic equation is

$$\frac{X(s)}{F(s)} = \frac{\frac{1}{Ms^2}}{1 + \frac{K\,G(s)}{Ms^2}} = \frac{1}{Ms^2 + K\,G(s)} \qquad (56)$$

If G(s) is unity, a force disturbance will produce a continuous translational oscillation of the rotor at a frequency ω, defined in (57).

$$\omega = \sqrt{\frac{K}{M}} \qquad (57)$$

If G(s) contains only a "rolloff" or has "lag" response, then (56) reduces to

$$\frac{X(s)}{F(s)} = \frac{\tau s + 1}{M\tau s^3 + Ms^2 + K} \quad \text{for } G(s) = \frac{1}{\tau s + 1} \tag{58}$$

which is unstable due to the lack of a first-order term. Stability may be supplied by deriving rate feedback electronically with a lead-lag filter. With such a filter, G(s) becomes

$$G(s) = \frac{\tau_1 s + 1}{\tau_2 s + 1} \qquad \tau_1 > \tau_2 \tag{59}$$

The characteristic equation then becomes

$$\frac{X(s)}{F(s)} = \frac{\tau_2 s + 1}{M\tau_2 s^3 + Ms^2 + K\tau_1 s + K} \tag{60}$$

A stable system will now occur when M, K, τ_1, and τ_2 have the proper relationships with each other.

Static stiffness. -- For certain applications, an important part of the specification is the average centroid displacement in the static operating environment. This displacement is one of the determinants of electric torque drifts and occurs when there is acceleration input to the gyro rotor. Displacement due to static inputs may be determined directly from Equation (56) and the final value theorem:

$$\Big[X(t)\Big]_{t \to \infty} = \Big[S\,X(s)\Big]_{S \to 0} \tag{61}$$

The transform of static acceleration input is A/S, where A is the value of the acceleration. Substituting (56) into (61) with the acceleration results in the limit expressed in (62).

$$X(t)\Big]_{t \to \infty} = S\,X(s)\Big]_{S \to 0} = \frac{S \cdot M \cdot A}{S\left[Ms^2 + K\,G(s)\right]} \quad S \to 0$$

$$X(t)\Big]_{t \to \infty} = \frac{M \cdot A}{KG(0)} \tag{62}$$

where $G(0)$ is the d-c transfer gain of the compensating networks.

Bandwidth Limits. -- In all realizable systems, the bandwidth of $G(s)$ is limited, usually by many factors such as

- Sensing circuit frequency
- Sensing circuit bandwidth
- Amplifier rolloff
- Loop filter rolloff
- Transformer bandwidth
- Carrier frequency

Such limits define the maximum gain level which may be achieved. From (56), $KG(s)/Ms^2$ is the expression for the loop gain. The criterion for stability of the system is that the loop gain expression exhibits less than 180° phase at the point where gain is unity. If the gain is too high, the phase accumulated by the bandwidth limiting factors will produce greater than 180° phase at unity gain, and the system will be unstable. To a certain extent, phase lag may be canceled by electronic lead networks; however, these enhance noise in the loop and their use is limited. For the ESVG, the usual limit with present design is in the range of 1 Kc.

Range of Stability. -- Equation (56) may be interpreted to have a fixed-loop transfer function, but variable gain. This condition is usual in real systems. At some frequency, the phase will be -180° due to the influence of compensating (lead) networks and bandwidth limiting lags. If gain is increased, the loop will eventually exhibit a net gain of unity and oscillation will occur. At this point the upper limit of gain is reached. Usually, systems require lag-lead compensation at low frequency to provide the static stiffness necessary. This compensation produces greater than 180° phase shift at low frequencies, which is, in part, canceled by the lead-lag

networks which are placed at intermediate frequencies. If the gain is decreased to the point where phase is 180° at unity loop gain, instability again occurs, which defines the lower limit of gain. Changing gain over this range changes loop damping factor, static stiffness, and dynamic response to acceleration inputs.

SUSPENSION LOOP DETAILS

Form of Output Transfer Function

The suspension output circuit's basic function is to boost the voltage (and power) level of the rebalance signal to provide the necessary gradients in the gyro assembly. For maximum effort these gradients are of the order of 1000 volts per mil, which means output voltage in the 2000-to 4000-volt range for most applications.

Voltage/current versus force - zero bias. -- The magnitude of force produced by output voltage or current is described in Equations (18), (23), (29), and (32) for hexahedral and circular electrodes. Only the first term may be used if displacement compensation is added to the voltage-fed systems and if stray capacitance is small in current-fed systems. Cross coupling may be compensated by applying a correction factor to the maximum force for the maximum displacement designed into the system and, thus, need not be considered.

The simplest case is one in which the output voltage is a direct function of displacement. Since negative (or repelling) forces cannot be developed, only one electrode can be "on" at a time. For this case, Equation (18a) reduces to

$$F_z = \frac{F_o}{V_o^2} V_5^2 \tag{63}$$

$$= \frac{F_o}{V_o^2} (G z)^2$$

where G is the electronic portion of loop gain up to the suspension output (see Equation 56). The ratio of F_o to V_o^2 is a constant as determined from Equations (17) and (28). A plot of force versus displacement has the form shown in Figure 12.

Gain of the force/displacement function is given by the slope of (63), which is

$$\frac{d F_z}{dx} = \frac{F_o}{V_o^2} 2 G^2 z \tag{64}$$

Thus, the gain is a direct function of displacement. From the general discussion of the loop equation, it is evident that the system can exhibit both high-gain and low-gain instability depending on displacement. These regions are also shown in Figure 12.

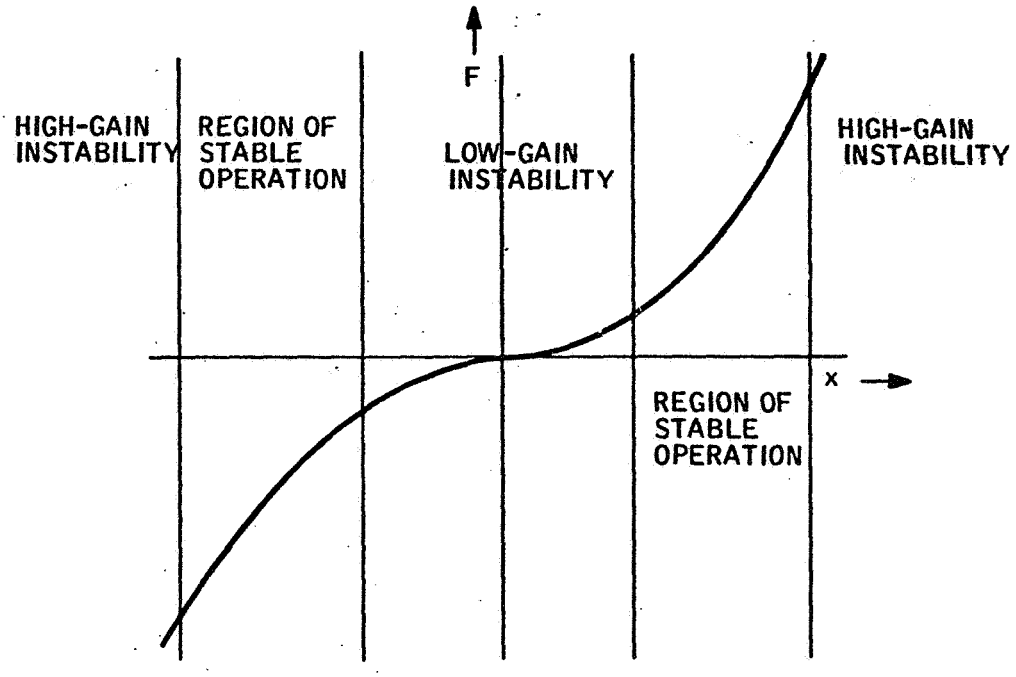

Figure 12. Force versus Displacement - Zero Bias

Although a suspension servo can be operated in a "steady G" environment with a control of this type, generally the loop is linearized, at least for low G levels, by a bias voltage.

Nonlinear networks can also change the effective transfer function to one which is more desirable in terms of gain stability. For example, if a square-root function were used, the gain would be constant. The electronic gain needed may be compared for the two cases

$$\text{Gain}_1 = \frac{F_o}{V_o^2} \; 2 G_1^2 \; z \quad (\text{for } V = G_1 z)$$

$$\text{Gain}_2 = \frac{F_o}{V_o^2} \; G_2 \quad (\text{for } V = \sqrt{G_2 z}) \tag{65}$$

If it is assumed that equal gain is needed at maximum output (thus placing maximum output into the region of stable operation) as well as at other output levels, then G_2 must equal $2\,G_1^2$. This means that a very high electronic gain must be realized. This fact limits the usefulness of such a scheme.

Voltage/current versus force - nonzero bias. -- A biased system differs from the zero-bias system in that the displacement to output voltage transfer function is electrically offset as shown in Figure 13. Since the net force in an axis is the difference of these two curves, there is a linear region of operation. Mathematically, Equation (18a) may be used to illustrate this.

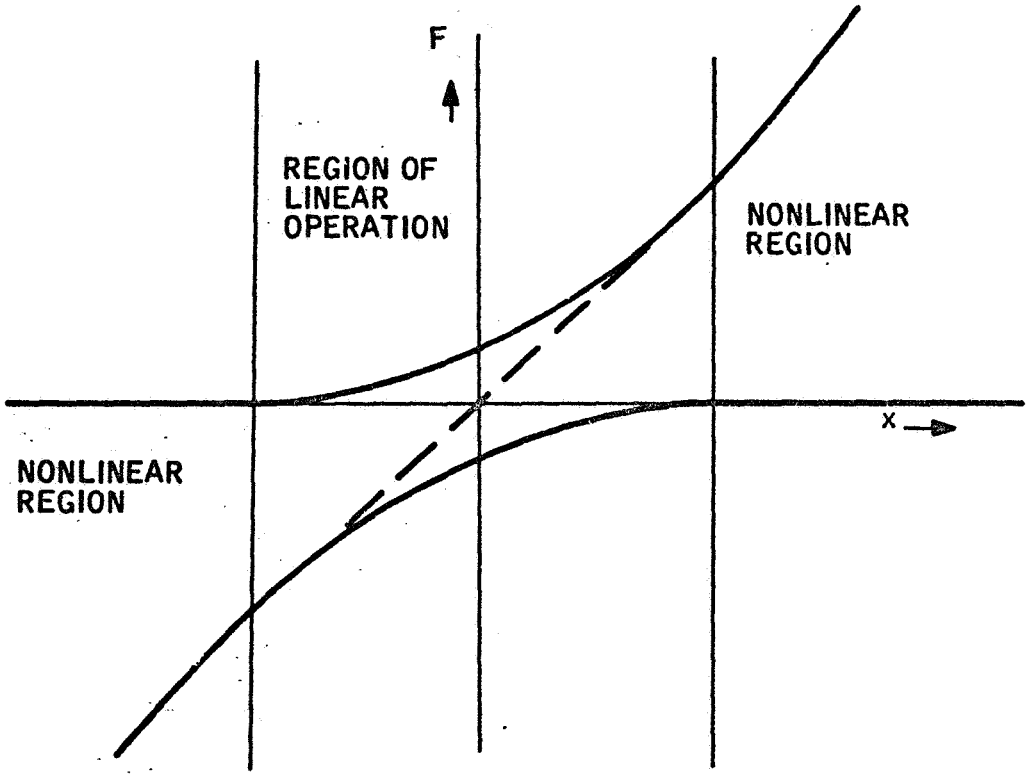

Figure 13. Force versus Displacement - Nonzero Bias

In the linear region, $V_c \equiv G\,z \leq V_o$, where $0 < r \leq 1$ and V_m is the maximum voltage.

$$F_z = \frac{F_o}{V_o^2}\,(V_5^2 - V_6^2) \qquad V_5 = V_o - G\,z \qquad V_6 = V_o + G\,z$$

$$F_z = \frac{F_o}{V_o^2} \left([V_o - G z]^2 - [V_o + G z]^2 \right)$$

$$= \frac{F_o}{V_o^2} [-4 V_o G z]$$

$$F_d = - \frac{F_o}{V_o^2} (4 V_o) \cdot G \cdot z \qquad (66)$$

Let $V_o = r V_m$, where $0 < r \leq 1/2$ and V_m is the maximum voltage. Then,

$$F_z = - \frac{F_o}{V_o^2} (4 \cdot r \cdot V_m \cdot G \cdot z) \qquad (67)$$

$$F_{max} = - K_o 4 r^2 V_m^2$$

$$= - K_o V_m^2 \qquad (68)$$

$$\text{at } r = 1/2$$

The gain provided is found by differentiating Equation (68).

$$\frac{dF}{dz} = - \frac{F_o}{V_o^2} \cdot 4 r V_m G \qquad (69)$$

$$\text{Maximum gain} = - \frac{F_o}{V_o^2} \cdot 2 V_m G \qquad (r = 1/2 V_M)$$

Many of the same concepts may be applied to the nonlinear region where $V_c = G z \geq V_o = r V_m$. Considering only "positive" displacements,

$$V_5 = 0, \; V_6 = V_o + G z$$

$$F_z = \frac{F_o}{V_o^2} (- V_6^2)$$

$$= - \frac{F_o}{V_o^2} [V_o^2 + 2 V_o G z + (G z)^2] \qquad (70)$$

Thus, the applied force depends on the linear region bias and on the added (nonlinear) terms containing G z.

Substituting $V_o = r V_m$,

$$F_z = -\frac{F_o}{V_o^2}\left[r^2 V_m^2 + 2 r V_m G z + (G z)^2\right] \tag{71}$$

$$= -\frac{F_o}{V_o^2} \cdot 4 r V_m G z \left[\frac{1}{2} + \frac{r V_m}{4 G z} + \frac{G z}{4 r V_m}\right]$$

The minimum force in this mode is at $G z = V_o = r V_m$.

$$F_{z\,min} = -\frac{F_o}{V_o^2} \cdot 4 r^2 V_m^2 \left[\frac{1}{2} + \frac{1}{4} + \frac{1}{4}\right] \tag{72}$$

$$= -\frac{F_o}{V_o^2} \cdot 4 \cdot r^2 V_m^2$$

The maximum force occurs when the sum of V_o and $G z$ equals V_m; i.e., when $G z = (1 - r) V_m$:

$$F_{max} = -\frac{F_o}{V_o^2}\left[r^2 V_m^2 + 2 r V_m^2 (1 - r) + (1 - r)^2 V_m^2\right]$$

$$= -\frac{F_o}{V_o^2} V_m^2 \left[r^2 + 2r - 2r^2 + 1 - 2r + r^2\right]$$

$$= -\frac{F_o}{V_o^2} V_m^2 \tag{73}$$

Thus, maximum force is invariant (as we knew it must be).

The gain of the nonlinear system is

$$\text{Gain} = -\frac{d F_z}{d_z} = -\frac{F_o}{V_o^2}\left[2 r V_m G + 2 G z \cdot G\right] \tag{74}$$

$$= -\frac{F_o}{V_o^2}\, 2 G \left[r V_m + G z\right] .$$

Minimum gain occurs at $G z = r V_m$

$$\text{Minimum Gain} = \frac{F_o}{V_o^2}\, 4 V_m G \tag{75}$$

Maximum Gain occurs at $G z = (1 - r) V_m$

$$\text{Maximum Gain} = \frac{F_o}{V_o^2}\, 2 G V_m \tag{76}$$

This is the same gain that the linear system has with $r = 0.5$. Since there is no reason to increase V_o to greater than one-half V_m, and the maximum gain never exceeds the gain at $V_o = 1/2\, V_m$, compensation for the gain given by Equation (75) will produce a system that is always "High-Gain" stable. Whatever the bias or excursion, it will never go into high-frequency instability.

The normalized force and gain are plotted in Figures 14 and 15 against the control voltage (G z).

Range controlling factors. -- The range of bias settings is restricted by constraints imposed by a real system. The upper limit for full output is the gradient which the instrument can withstand. In the case of a three-phase, a-c, six-electrode device designed for maximum G output, the bias can only be one-half V_m. If the device is designed for less than maximum G capability, the bias may be set lower than one-half V_m. In this case, the forcing electrode is driven to maximum gradient, but its opposite also carries voltage which reduces the effectiveness of the forcing electrode. This type of system has the advantage, however, of being linear (constant gain) for all displacements.

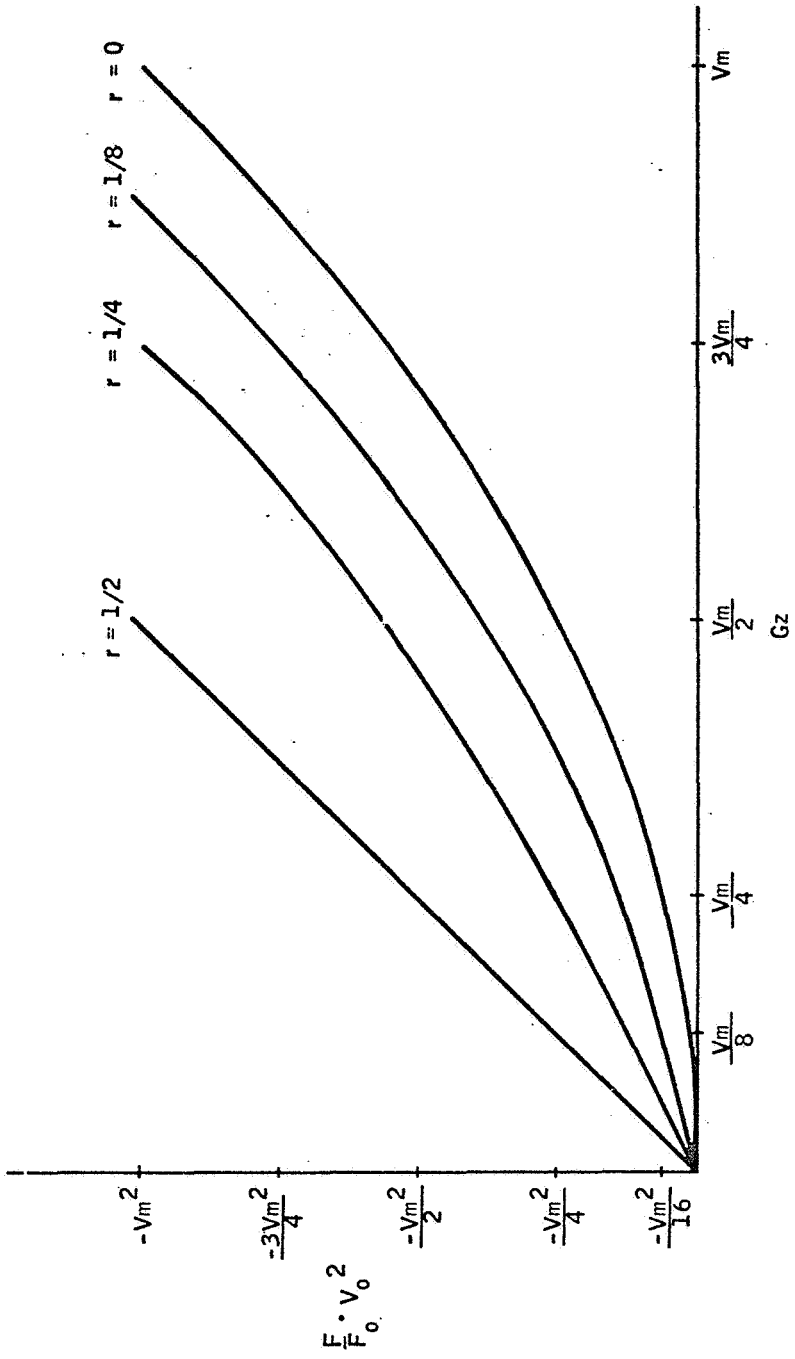

Figure 14. Normalized Force versus Control Voltage

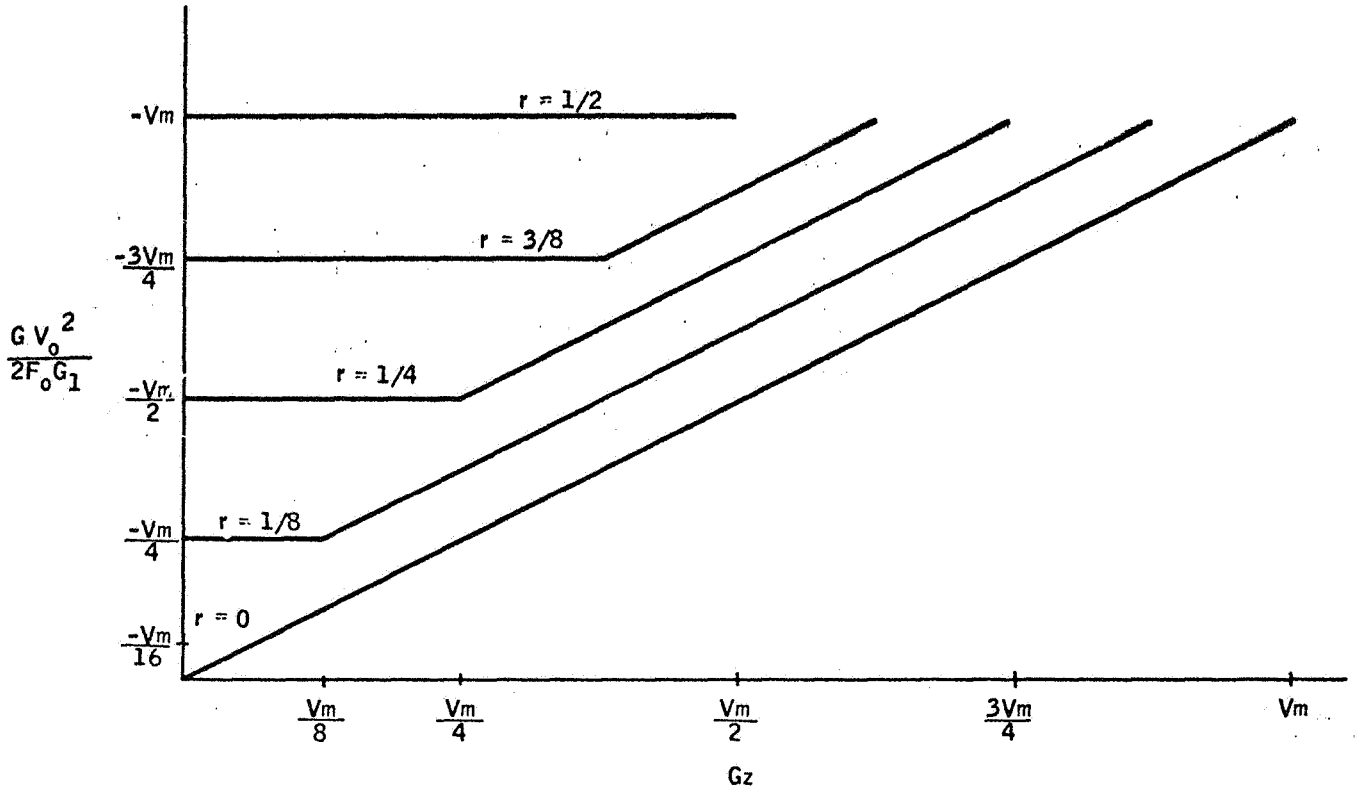

Figure 15. Normalized Gain versus Control Voltage

A single-phase, 12-electrode instrument accomplishes current (or voltage) balance in each half channel. Bias can be set at any level (theoretically). A low bias voltage reduces average power input, average force, and average torque. This is desirable, but difficult to achieve. Referring to Figure 15 and Equation (69), it is evident that gain changes with displacement for output levels above V_o. From the discussion on high- and low-gain instability, it becomes obvious that if bias level is reduced with maximum gain determined by bandwidth, low-gain instability will eventually result. Thus, the range is ultimately determined by the gain margins of the suspension servo.

A technique which can alleviate the problem is to use a nonlinear network to keep gain a constant with output [a square-root device such as that described in Equation (65)]. With a mixed system of this type, the very high gain of the square-root system is reduced to a more manageable level depending on bias chosen. However, setup is more difficult since the nonlinear network must start operating at a particular level for each system, and its accuracy is a function of stability of subassembly components in the system.

Bandwidth Limiting Factors

Each of the various component subassemblies which make up the ESVG suspension system has an effective bandwidth associated with its transfer function. This limits information transfer and the speed with which the gyro and suspension can react to external inputs. Certain filters must also be added to the loop to limit any tendency toward electronic regeneration (as opposed to ordinary servo instability). The sum of these separate effects is a definite limitation on medium-frequency loop gain (affecting static stiffness).

Output circuits. -- The several types of output circuits have different bandwidth limiting mechanisms. Square wave, current-fed sine wave and series-tuned sine wave systems are considered.

A square wave output amplifier drives the electrodes through a switching-type output circuit and transformer. There may also be a series resistor to limit current and provide isolation if the electrodes are used for sensing rotor position. The transformer operates between widely different voltage levels and, thus, has a high turns ratio. It is bandwidth limited by its internal parameters such as leakage inductance, stray capacitance, and magnetizing inductance. The square wave can be modulated during the period of one cycle by a modulation amplifier. This means that the upper-frequency limitation appears when information begins to be lost due to the rise time of the output voltage waveform.

The output of the square wave system is rise-time limited by two factors. The first factor is the current-driving capability of the transistors; the second factor is the filter formed by the output transistor/resistor/capacitor network. These factors produce the waveform of which effective force was calculated [Equation (54)]. Although the filtering and current-driven effects are usually interrelated, they can be considered separately; separate consideration leads to a conservative result.

Under conditions of maximum acceleration with full voltage being produced, the output transistors will necessarily be operating at least near a current-limited condition. Such a limitation is usually designed into the circuit to limit transistor secondary breakdown tendencies and to provide a reasonably linear load for the output switching source. During this type of operation, the collector impedance is high and the transistor output current is determined by its input current and gain. Assuming that current flows at a constant rate during the rise-time interval, we have

$$I = \frac{2 V C}{t} \tag{77}$$

where V = output voltage, C = the rotor-electrode capacitance, and t is the risetime. Substituting for (hexahedral electrode) capacitance yields

$$I = \left(\frac{V}{d}\right) \frac{\epsilon_o \pi D^2}{3.39t} \tag{78}$$

the ratio V/d is the gradient and is related to G capability and rotor thickness. The risetime is inversely proportional to equivalent output circuit bandwidth. Making these substitutions gives

$$I \propto \sqrt{T G} \quad D^2 \quad (B_\omega) \tag{79}$$

Inversion of this proportion makes it evident that bandwidth is a function of output transistor current capability. A typical example would be a 150 pF electrode driven to 2000 volts peak with a bandwidth of 10 kc.

$$I = \frac{4000 \times 150 \times 10^{-12}}{35 \times 10^{-6}} = 0.017 \text{ amp}$$

If this current is supplied by transformers with a 100:1 turns ratio (a reasonable value, since primary voltage is usually approximately 20 V), the primary current is 1.7 amp during the charging interval.

Resistance may be added to the output leads to isolate the switching circuits from the sensing circuits to reduce the effects of open and short circuit conditions at the output transformer. The stray capacitance to electrode capacitance ratio is usually about 10:1 and should be isolated to the 5000:1 range. At the normal impedance levels encountered, a resistor in the 100-kΩ range must be used. A resistor of this magnitude limits the bandwidth to 5 to 10 kc.

The current amplifier type sine wave output uses feedback to broadband the (usually) parallel tuned output stage. Current flowing out of the output (tuned) transformer is passed through a "feedback capacitor". The voltage drop across this capacitor is compared to the voltage at the input of the differential operational amplifier. Since a capacitor is used as the feedback

element and there is a capacitive load, no phase shift occurs and the load current is a faithful reproduction of the input voltage. Bandwidth at low levels is determined by the loop gain and at high levels by the rate at which the output transistors can pump energy into the tuned circuit. This is a limitation very similar to that in the square wave case just considered, and it results in a bandwidth of the same order.

The series tuned output uses voltage drive into a series L-C circuit. If the circuit is tuned slightly off resonance, a passive resonant suspension system results with rebalance voltage being produced proportional to gyro rotor displacement and circuit Q. If the circuit is driven linearly, it will be tuned to resonance and the input varied to provide rebalance voltage. Either way, the bandwidth is limited primarily by the series-tuned circuit. Wider bandwidth may be gained (again) only at the expense of a higher carrier frequency and more power dissipation. The equivalent low-pass filter cutoff is given by

$$f_{co} = \frac{f_o}{2Q} \tag{80}$$

where f_o is carrier frequency and Q is quality factor of the output circuits.

Carrier frequency. -- The square wave cycling frequency affects bandwidth mostly in the area of output transformer response. A transformer built for a particular carrier frequency has dimensions compatible with that frequency and the power required. The upper frequency limit is determined by leakage inductance, stray capacitance, and winding resistance. For small transformers of this type, the upper frequency limit is about 25 times carrier frequency.

Sine wave systems include a modulator to multiply the displacement voltage by a carrier frequency oscillator signal. This device has an inherent information transfer rate of one-half the carrier frequency.

Loop filtering. -- Several filters are necessary in either type of system. The displacement sensor includes harmonic filtering and an amplifier, both of which are relatively wideband compared to other components. The displacement sensor bridge excitation is usually of sufficiently high frequency that no significant limitations are produced. The signal amplifiers which follow the displacement demodulation contain the loop noise filters in the square wave system and harmonic filters in the sine systems. A chart delineating these areas for each system is given in Table I. The displacement sensor frequency is assumed to be two megacycles.

Electronic regeneration. -- The suspension loop has high electronic gain and a direct path from output to input via the displacement-sensing circuit. The forward gain is simply that voltage ratio between output and input which will result in loop stability with the required bandwidth and stiffness. The entire gain is usually of the order of 50 to 100 volts per microinch with a bridge gain of 100 μV/μ inch. This means that the electronic gain must be of the order of 5×10^5. Carrier outputs at high power levels must be

TABLE I. -- BANDWIDTH LIMITS

	Sine Current	Active Series Sine	Passive Series Sine	Square Wave
Harmonic Filter	Approx. fc	Approx. fc	1/2 fc	1 Mc
Sensor Amplifier	1 Mc	1 Mc	N/A*	1 Mc
Sensor Demod	1 Mc	1 Mc	N/A	1 Mc
Compensation Amp	10 kc	10 kc	N/A	10 kc
Carrier Modulation	1/2 fc	1/2 fc	1/2 fc	None
Output Filter	10 kc	10 kc	N/A	5-20 kc
Output Circuit	100 kc	fo/2Q	fo/2Q	5-20 kc
Regeneration Lag	N/A	N/A	Depends on Loop Gain	N/A

* N/A -- Not Applicable

removed from the sensing system. Filters are used which ordinarily produce harmonics of the carrier due to nonlinear response, voltage coefficient, and variable inductance with signal level. These nonlinear effects usually provide a feedthrough coefficient of the order of 10^{-6}. Thus, to ensure electronics stability, additional harmonic filters must be added to the loop.

A second effect, which is not actually regeneration but affects operation, is noise voltage conducted from the output circuits. This interference voltage is generally greater than resistance noise at the input and raises the threshold of the position-sensing demodulator. It does not affect bandwidth directly, but does limit electronic gain.

The passive sine system (or any others in which operation depends on active processing of carrier-generated displacement signals) has an additional inherent lag produced by the feedback of output signals. The cutoff frequency depends on loop gain, Q, and carrier frequency.

Loop Compensation and Dynamics

The suspension-system dynamic response depends on the power capability of the driving circuits, the attainable bandwidth of the fixed elements, and the level of electronic feedback which can be maintained. In this section the general loop equations are expanded into a form which is amenable to graphical treatment, and the determining factors are displayed. Graphical solution is made for the dynamic response and an isolator design. Network range and tradeoff factors are also discussed.

Equation for Dynamic Response

Equation (56) describes the response of the rotor to external acceleration inputs. In Equation (81) the relationship expressed [Equation (56)] is changed into a form which is easier to graph.

$$X(s) = \frac{A_e(s)}{S^2} \cdot \frac{1}{1 + \frac{K_o G_1 \cdot 4 V_b}{Ms^2}} \tag{81}$$

$$= \frac{A_e(s)}{S^2} \cdot \frac{1}{\frac{K_o G_1 \cdot 4 V_b}{Ms^2}} \cdot \frac{\frac{K_o G_1 \cdot 4 V_b}{Ms^2}}{1 + \frac{K_o G_1 4 V_b}{Ms^2}}$$

To plot this on a Bode-type diagram, we take

$$20 \log X(\omega) = 20 \log \frac{A(\omega)}{\omega^2} - 20 \log (\text{loop Gain}) + 20 \log (\text{closed-loop transfer}) \tag{82}$$

$A(\omega)$ may be split into two parts. The first part scales the problem to one "G" and is a straight function of frequency squared. The second part is usually frequency variable [we will let this function be called $G(\omega)$]. $G(\omega)$ is the (usually) specified level of vibratory excitation relative to one G.

Isolator and loop design -- An example of the operations needed to design a system meeting a $G(\omega)$ specification is given. It will follow these steps:

1) Assume a $G(\omega)$ to be specified which must be handled by the system

2) Make a graphical determination of the loop gain needed to meet the specification by a hypothetical suspension system

3) Make a graphical solution for the transfer response characteristic of the hypothetical suspension system

4) Compare the response of a realizable suspension system with the hypothetical suspension and with the specification, and discuss deficiencies

5) Propose an isolator design which will allow the whole system to meet the vibration specification.

Figure 16 depicts the assumed $G(\omega)$. The values shown in Figure 16 are arbitrary, but are chosen to provide regions of force-limited operation, displacement-limited operation, and to point out the necessity of system isolators for some applications.

The system gain needed may be determined graphically from Equation (82) as shown in Figure 17. The specification level permissible is 200-μ in. dynamic and 2 μ in. static error. Working first on the dynamic error, the G scaling line is plotted. This has the value $386/\omega^2$ inches and for this graph is scaled to 0 at 1 μ in. This is shown as the $X(\omega)$ for the one g line on the graph. To this is added the relative G (specified) levels plotted in Figure 16. This results in the $X(\omega)$ for $G(\omega)$ line on the graph. The 200-μ in. excursion limit plots as a straight horizontal line at the 20 log $X(\omega)$ = 46 level. From Equation (82) it can be seen that the loop gain needed is the difference between the displacement specification and the $G(\omega)$ line. (For these frequencies, the closed-loop transfer response is unity).

The loop gain needed is replotted in Figure 18. The next part of the example involves development of a stable loop gain function which will meet the specification. Development of this function usually involves these considerations:

- O dB crossover must be at a rate of $1/\omega$
- Sufficient gain margin must exist

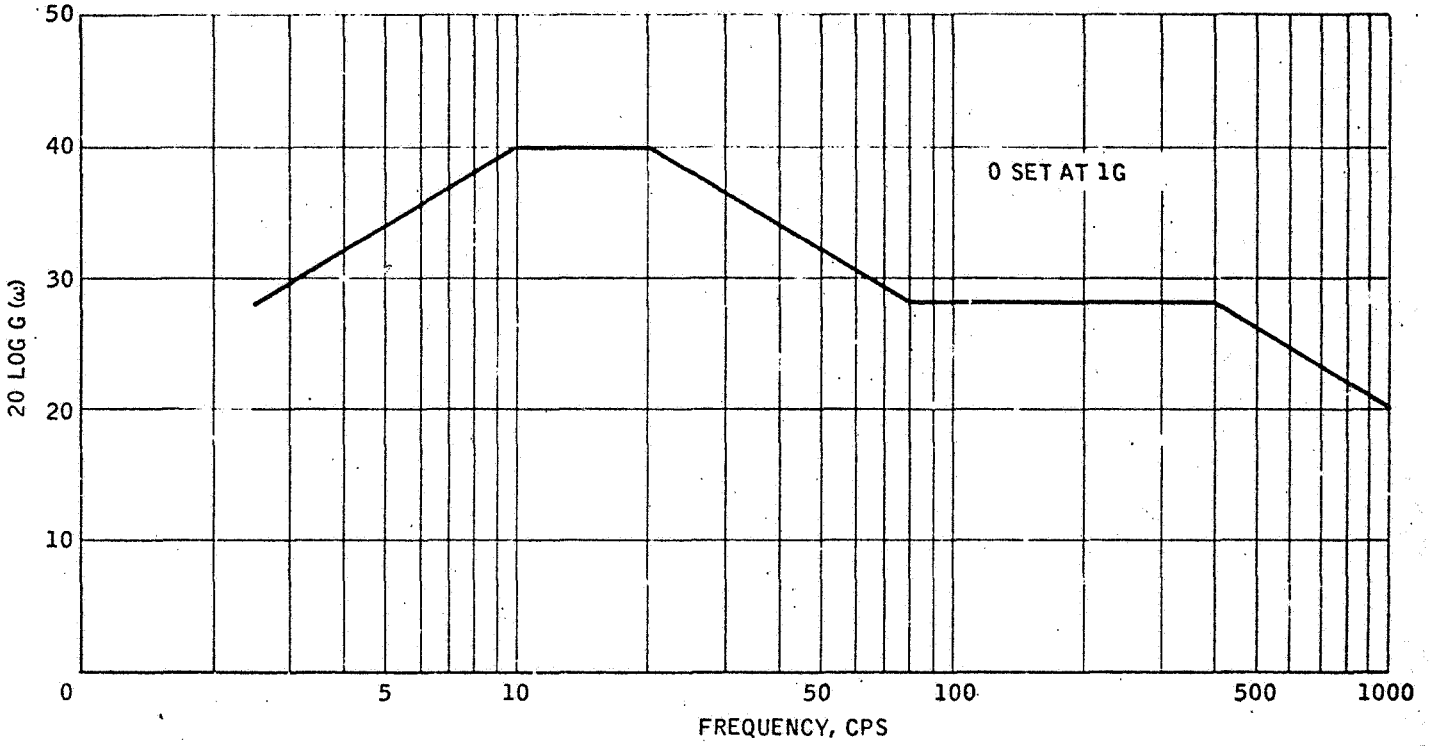

Figure 16. 20 Log G(ω) versus Frequency

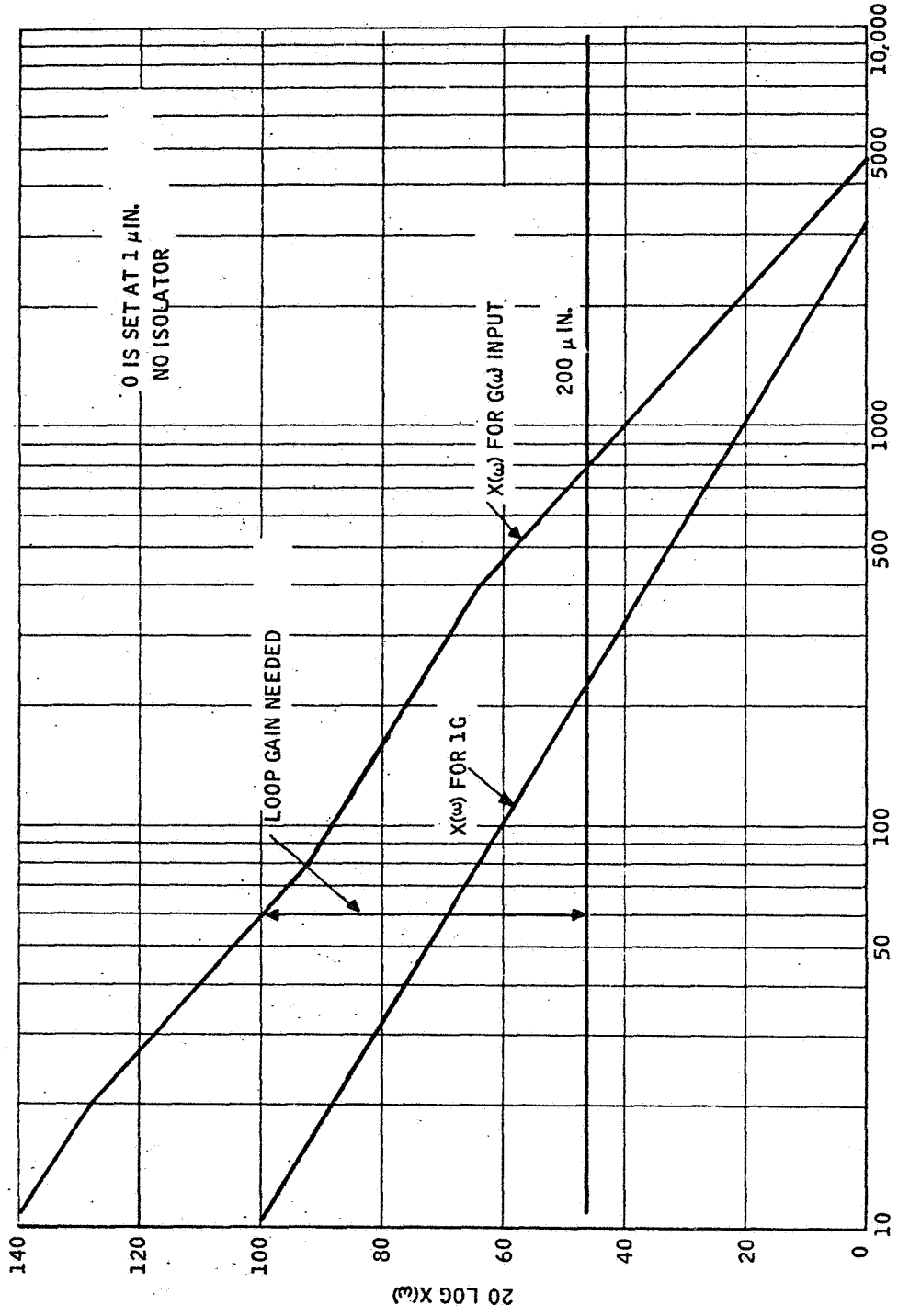

Figure 17. 20 Log X(ω) versus Frequency

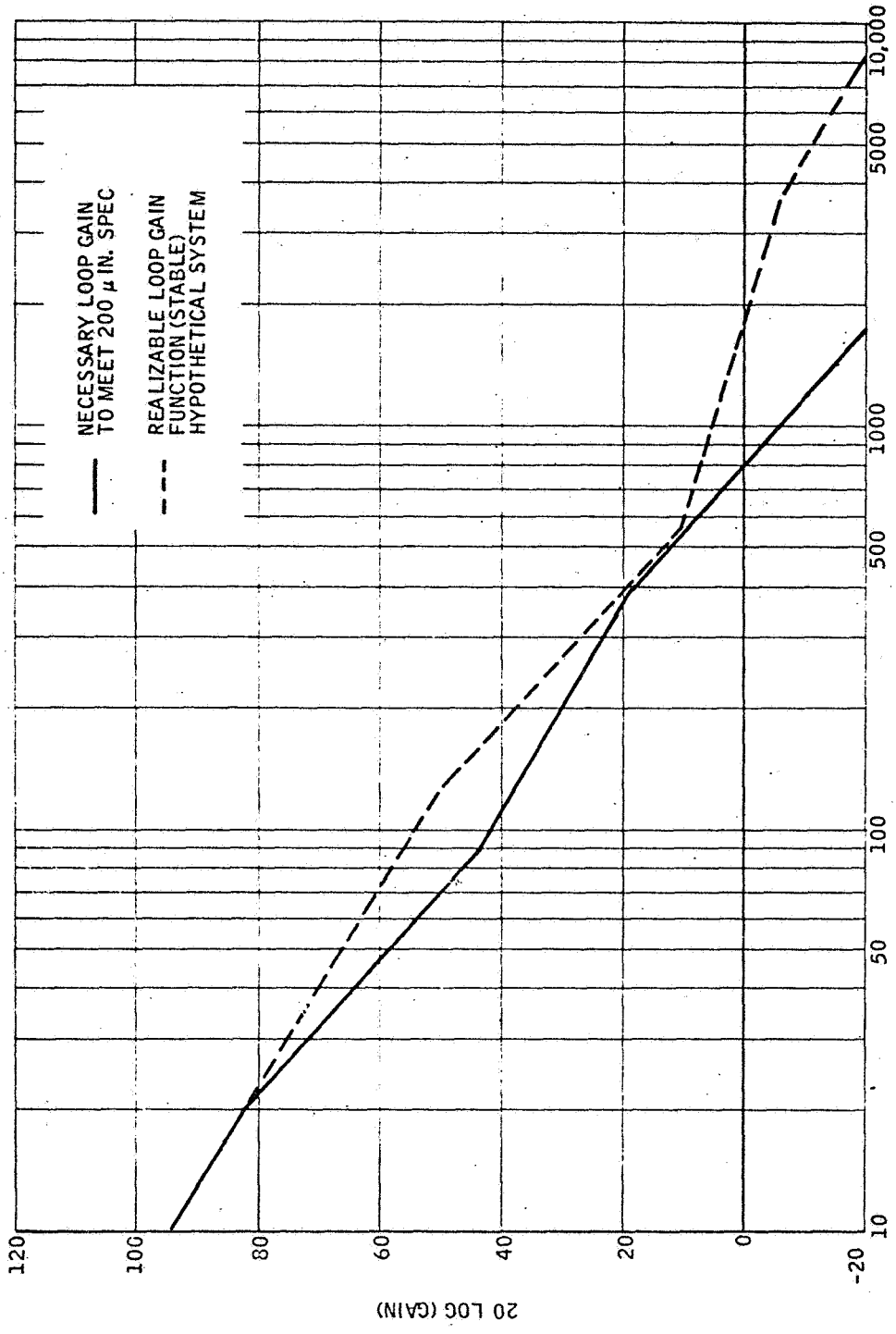

Figure 18. Loop Gain versus Frequency

- Transfer functions which are difficult to mechanize are usually avoided
- It is desirable to achieve the lowest-possible crossover frequency

The hypothetical system of Figure 18 was formed by consideration of the above factors. The system has these parameters:

- Crossover frequency, 1800 cps
- Gain margin, 10 dB (3.16:1)
- Probable bandwidth, 2800 cps
- Transfer function may be synthesized with an R-C Bridged Tee Filter

This system bandwidth is unreasonably large; too much power would be used in the output circuits for most applications. Also, it would be quite hard to realize this bandwidth in the sensing and amplifying circuits.

A more realistic approach would be to describe a usable system and find what isolation would be needed from the environment. Such a system description has been one of the objects of this study. The proposed system has about 1-kc bandwidth. Applying the (above) design considerations results in a transfer function similar to that shown in Figure 19. By depressing the zero for the suspension transfer function to the 200 -μ in. displacement level, the amount of isolation necessary can be read directly from the graph (shaded area). The effect of reduced gain is also shown. Everywhere in the shaded area, the servo is operating in a displacement limited condition. Directly above that area (10 to 18 cps) the servo is force limited. Figure 19 shows that, for the 1-kc servo to meet the (assumed) specification, an isolator which should have the following characteristics must be interposed:

- Rolloff at 13 cps
- Down 12 dB at 26 cps

This describes a second-order isolator with a damping factor greater than 0.6. Since the amount of isolation needed decreases with frequency, some mechanical resonances may be tolerated if Q's are not high. Static gain is met by simply allowing $G(\omega)$ to remain constant to 0 frequency.

It is instructive to carry out the analysis for a "standard" $G(\omega)$. The one selected is that given in MIL-S-167, the shipboard vibration specification. This specification states:

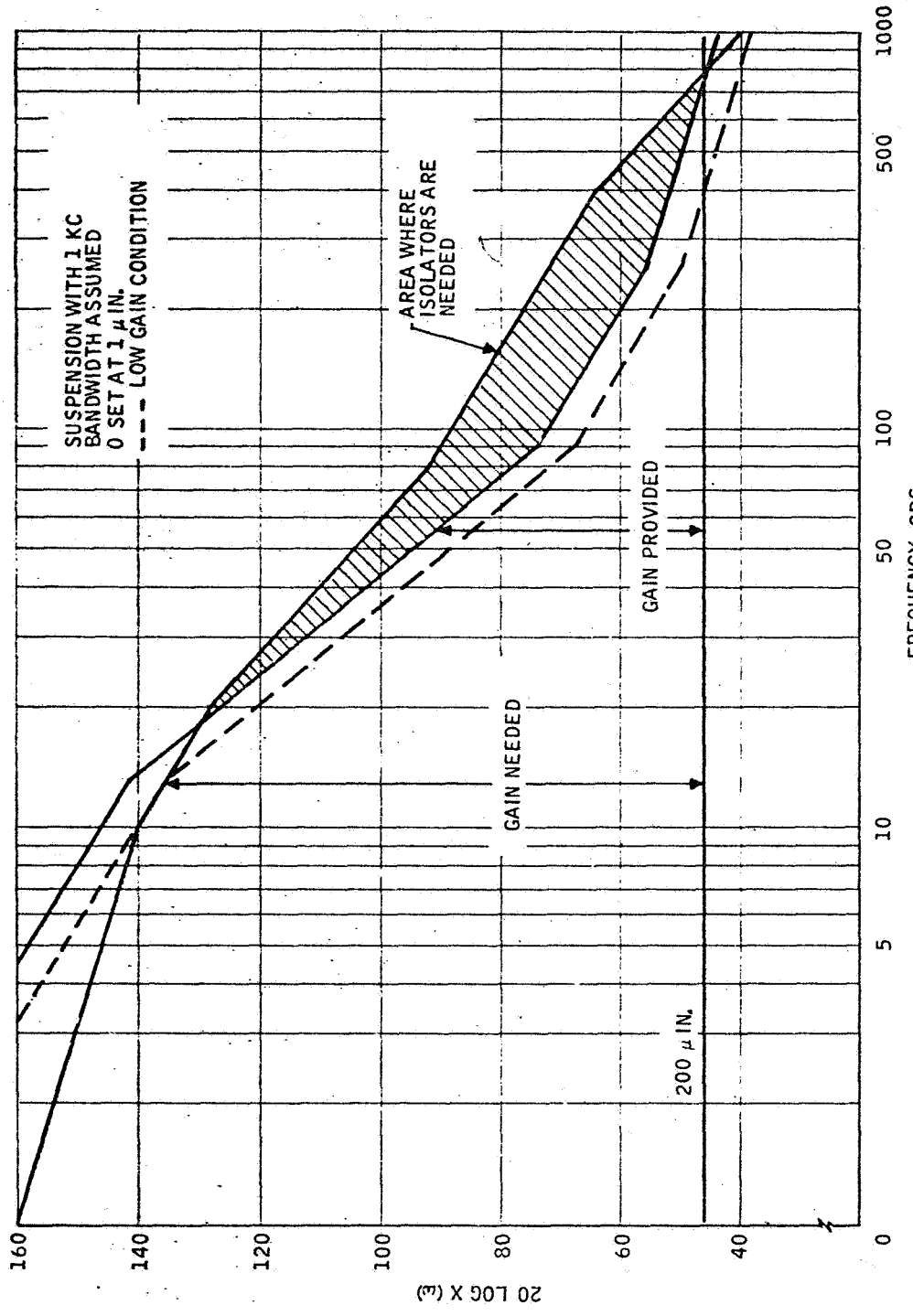

Figure 19. 20 Log X(ω) versus Frequency

5 - 15 cps	0.03-inch peak
15 - 25 cps	0.02-inch peak
25 - 33 cps	0.01-inch peak

These are shown in Figure 20, where the displacement specifications translate into three horizontal lines. If we again assume a 2-μ in. static, 200-μ in. dynamic specification, loop gain (dynamic) needed can be plotted as in Figure 21. Loop gain to meet the static specification may be found from a modification of Equation (81).

$$Xt\Big]_{t\to\infty} = SX(s)\Big]_{s\to\infty} = S\cdot\frac{A}{S}\cdot\left[\frac{1}{\frac{S^2+K_oG_1\,4\,V_b}{M}}\right]_{S\to o} \tag{83}$$

$$= \frac{A}{\text{Gain at zero frequency}}$$

$$A = 386 \text{ in./sec for one G}$$

$$Xt = 2\times10^{-6} \text{ in.}$$

$$\therefore \text{Gain at zero frequency} = 1.93\times10^{8}$$

$$= 10^{8.27}$$

If G_1 is at its zero frequency value at $\omega = 1$, then the gain at zero frequency equals the loop gain at $\omega = 1$. For cases where this is not true, appropriate adjustments may be made. Plotted on our scale, this is a line of slope $1/\omega^2$ passing through the $20 \log 10^{8.27} = 165.4$ point at $\omega = 1$ ($f = 0.159$). The point is actually plotted at $f = 3.18$ cps, 113.4 in Figure 21.

As shown in Figure 21, the specification is met by a system with crossover at 400 cps and bandwidth of about 550 cps. Simple lag-lead and lead-lag networks are used for stabilization.

It should be obvious at this point that the loop gain versus frequency characteristic of the suspension system is very flexible and depends on the specifications which must be met. It also is very probable that isolators will be needed if the device is operated in a severe vibration environment. Isolators should be used with a system for which the specified $G(\omega)$ makes necessary a bandwidth greater than 1 kc.

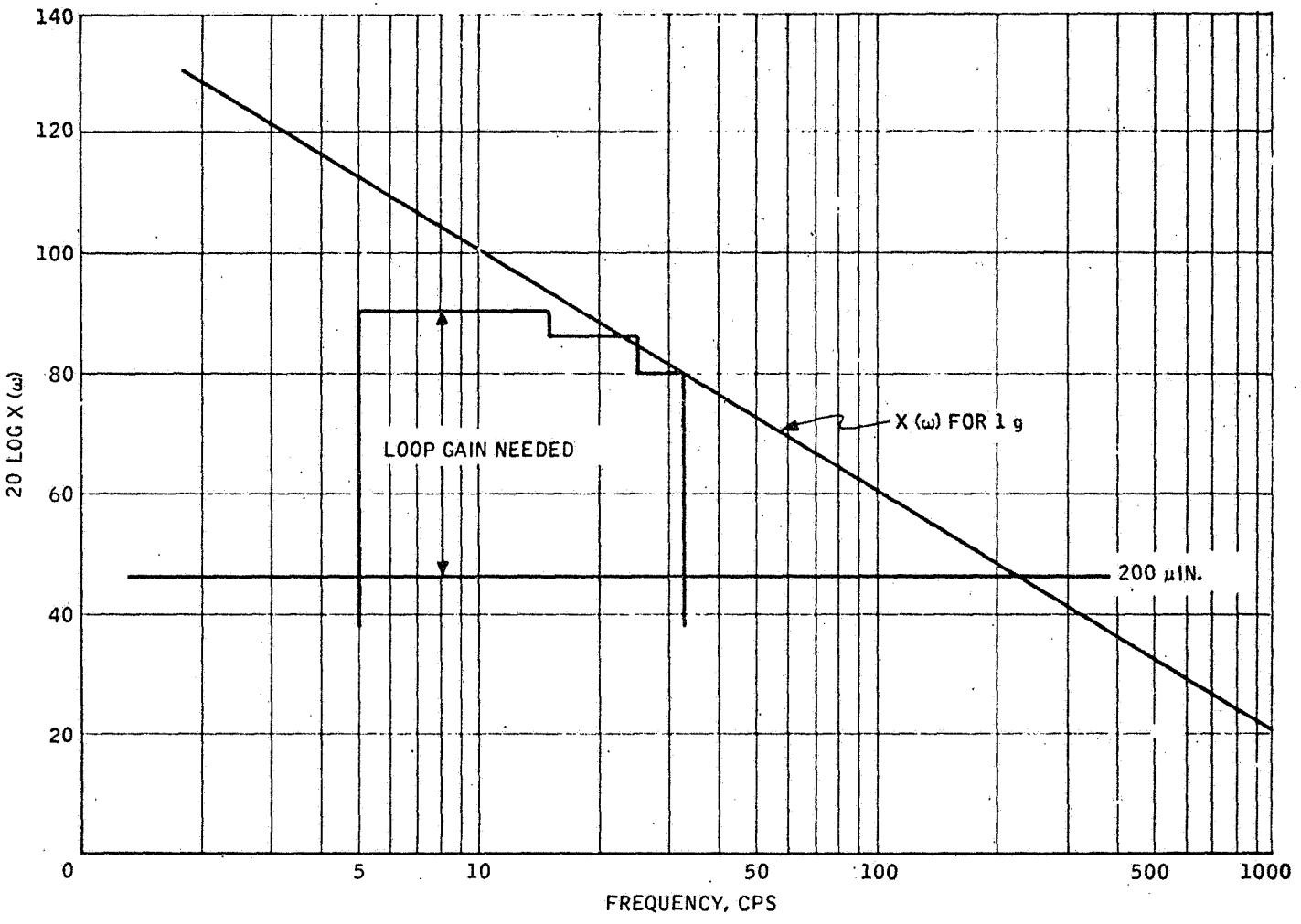

Figure 20. X(ω) for MIL-S-167 Vibration Specifications

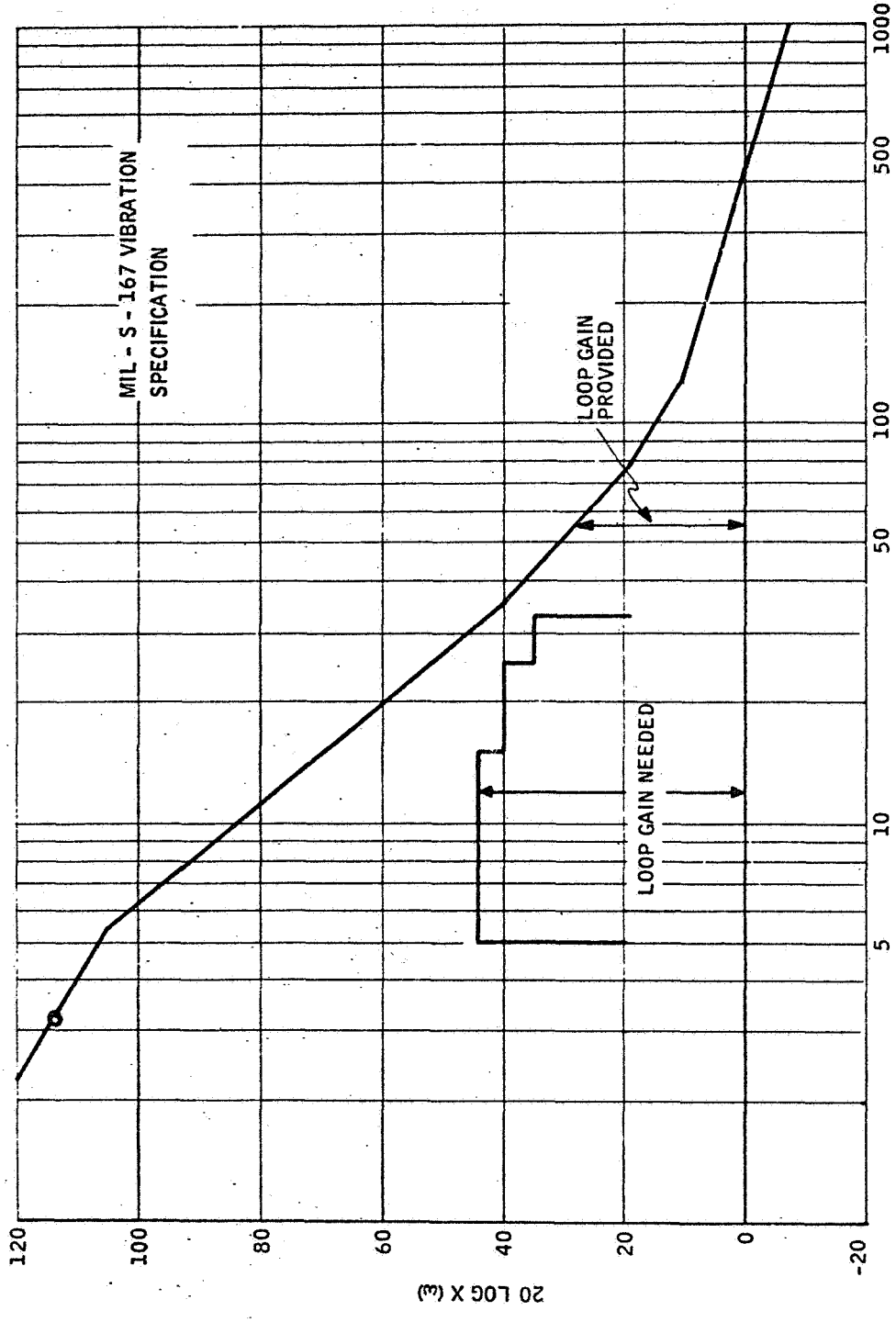

Figure 21. Loop Gain versus Frequency

Other conditions also enter the design. For example, the bias may be lower than half maximum output; a large phase margin (good damping) or large gain margin (allowing for component or bias shift) may be desired.

For the purposes of this study, we propose the following specifications for the high G loop.

- 1-kc bandwidth
- Effective 3000-cps loop cutoff
- 20-dB gain margin (lower)
- Damping factor equivalent, 0.4 Mp = 1.3
- Static displacement, 2μ in. at 1 G

Figure 22 shows the Bode plot of this loop, and Figure 23 shows the gain-phase plot. Closed-loop responses are taken from the gain-phase plot and shown in Figure 24.

As an aid in possible isolator design, the loop gain provided [G (ω) which can be met] is shown in Figure 13 for the 200-μ in. dynamic excursion allowed.

Low G loop response -- The low G loop response is determined in exactly the same fashion as the high G. Since the object of the low G loop is to use a minimum amount of power in an orbital environment, it is reasonable to specify performance at orbital levels of acceleration input. The specifications which were decided upon are

- 0.01 G maximum static input, 2-μ in. displacement
- Dynamic displacement 2μ in. with device at 10 feet from axis of body revolving at 1 rpm
- Dynamic input with superimposed static input of 0.003 G to produce <5-μ in. displacement at -15 dB from normal loop gain.

The transfer response of a system which will meet these specifications is shown in Figure 25.

Networks -- The type of networks which are finally specified depend somewhat on the system used. For instance, a squarewave system which can be one-fourth voltage biased may need a nonlinear element to absorb the loop-gain variation . A dual-range system such as is proposed in this study needs networks either of a very large dynamic range or switched networks. Switching the compensation brings up some interesting problems in stability, but may be necessary.

The range of stabilizing networks may be found by considering the change in natural crossover frequencies produced by range changes of the instrument. The loop equation is of the form given in Equation (81) and repeated here:

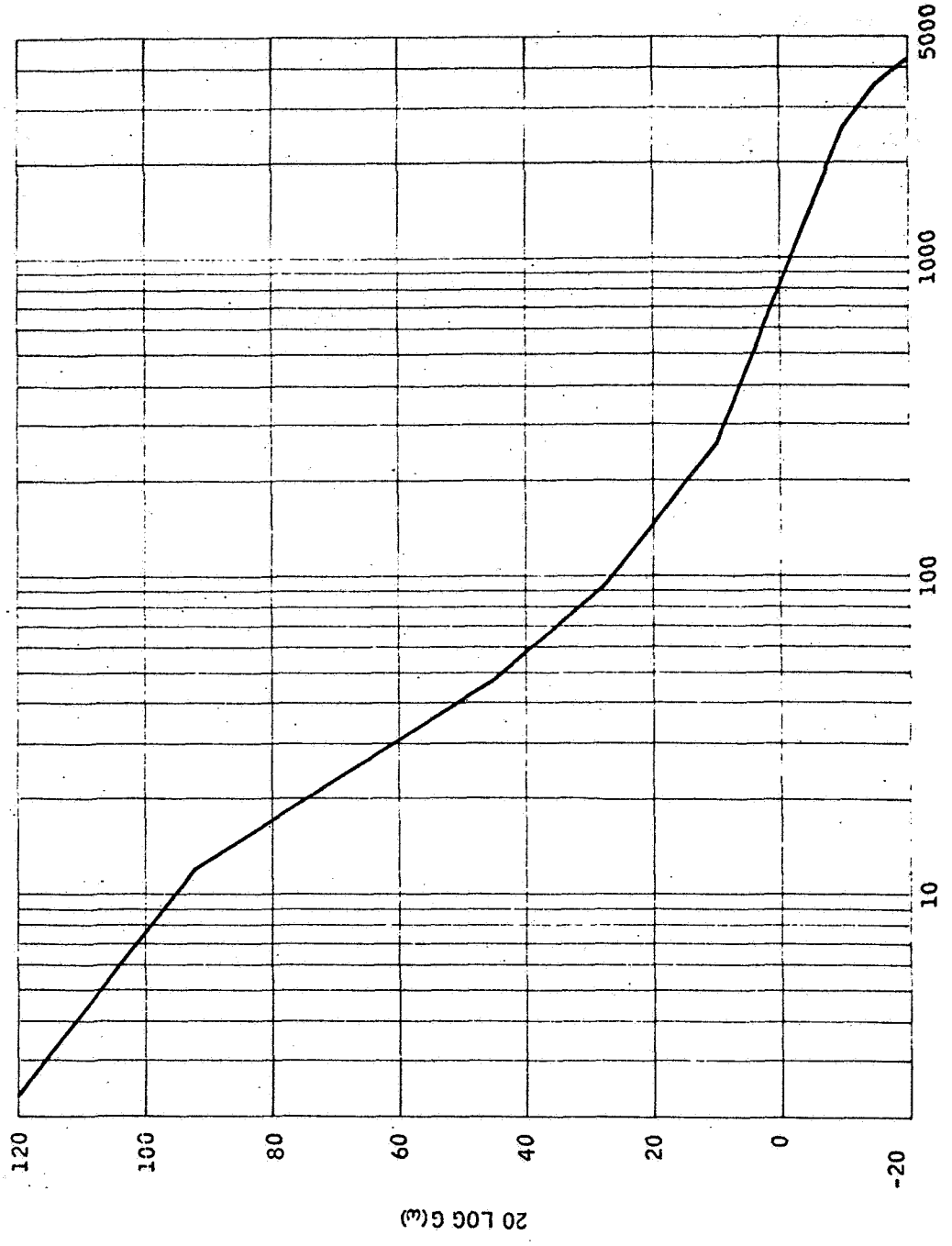

Figure 22. 20 Log G(ω) versus Frequency - High G Loop

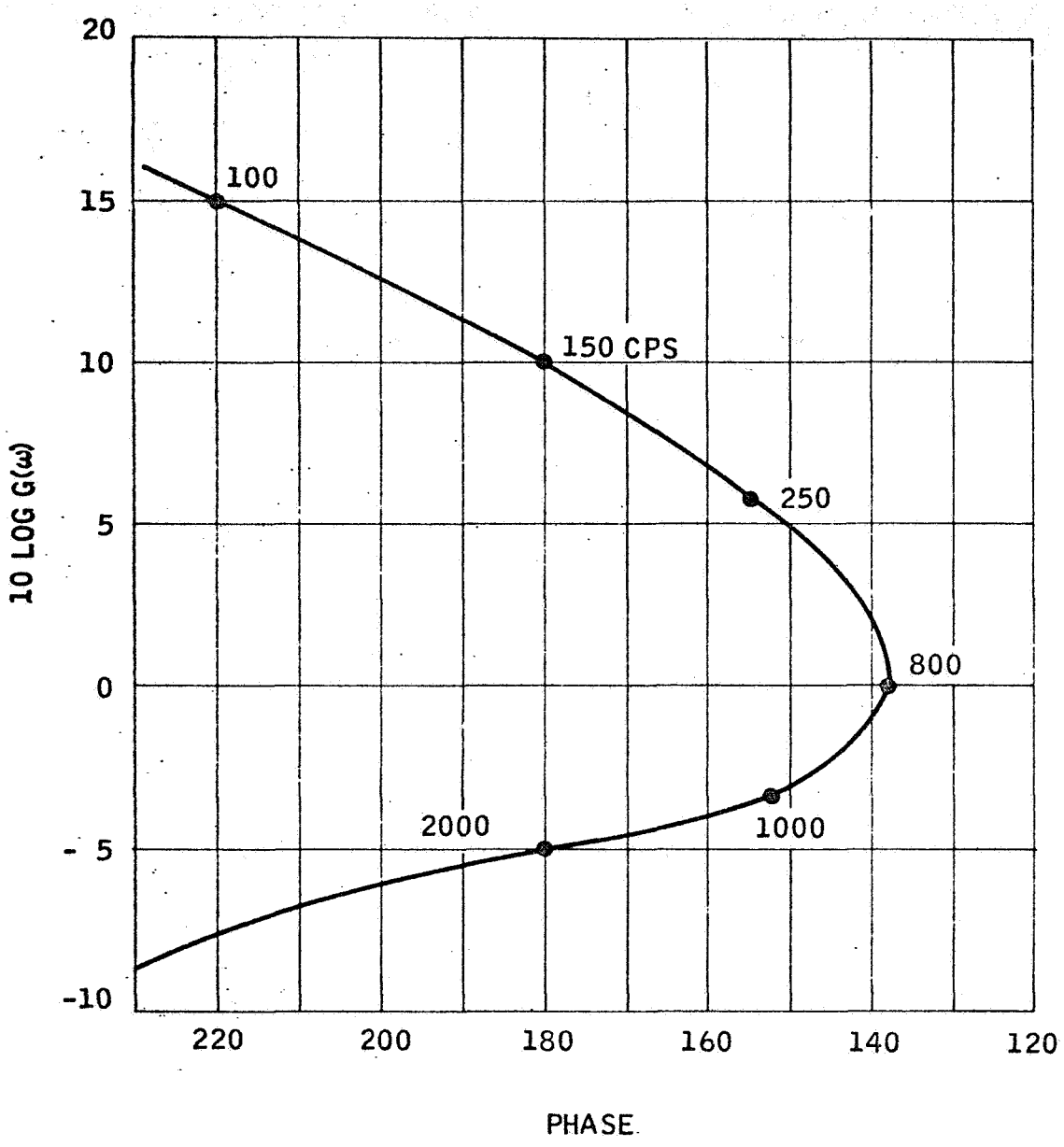

Figure 23. Gain-Phase Plot - High G Loop

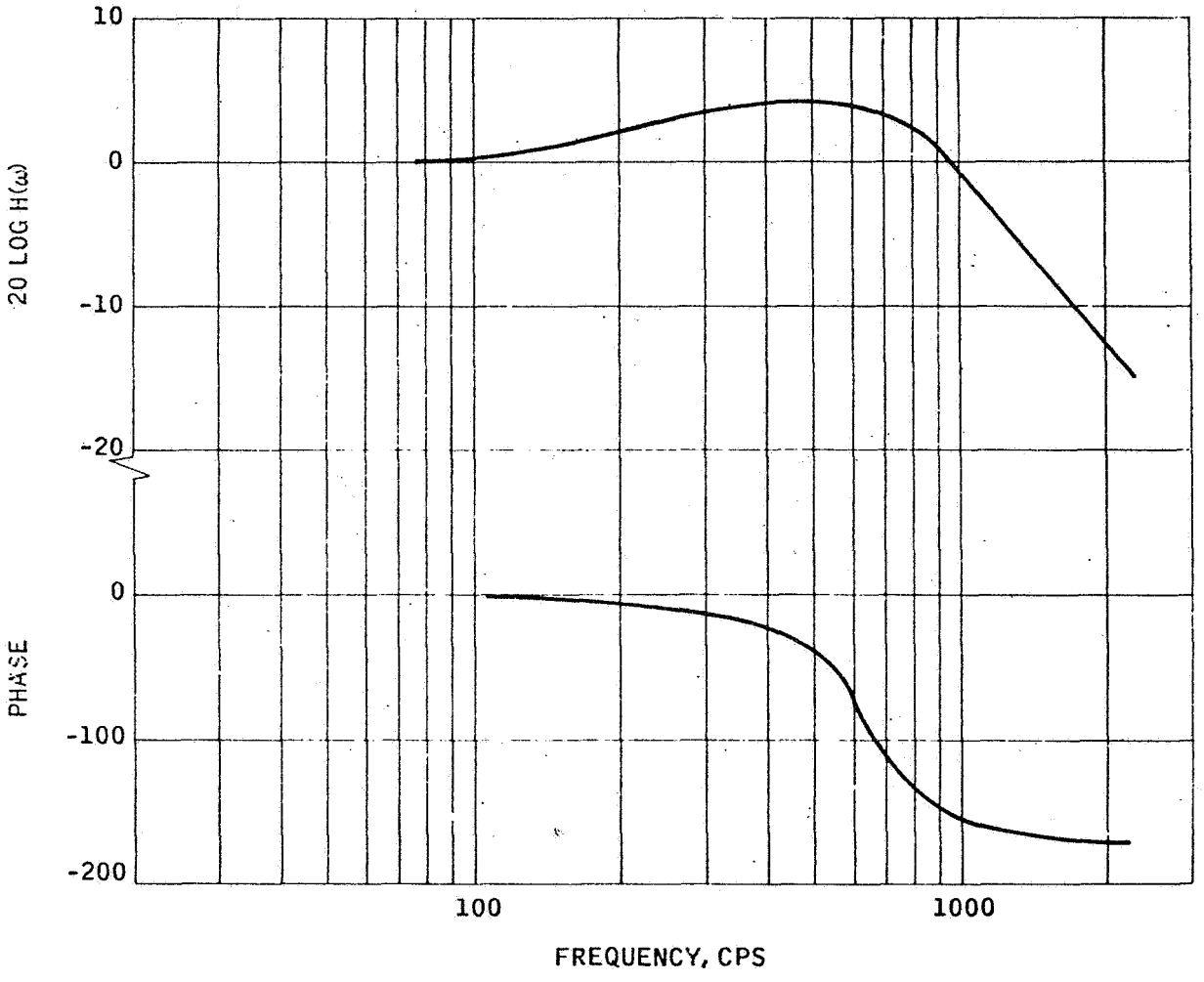

Figure 24. Closed Loop Response - High G Loop

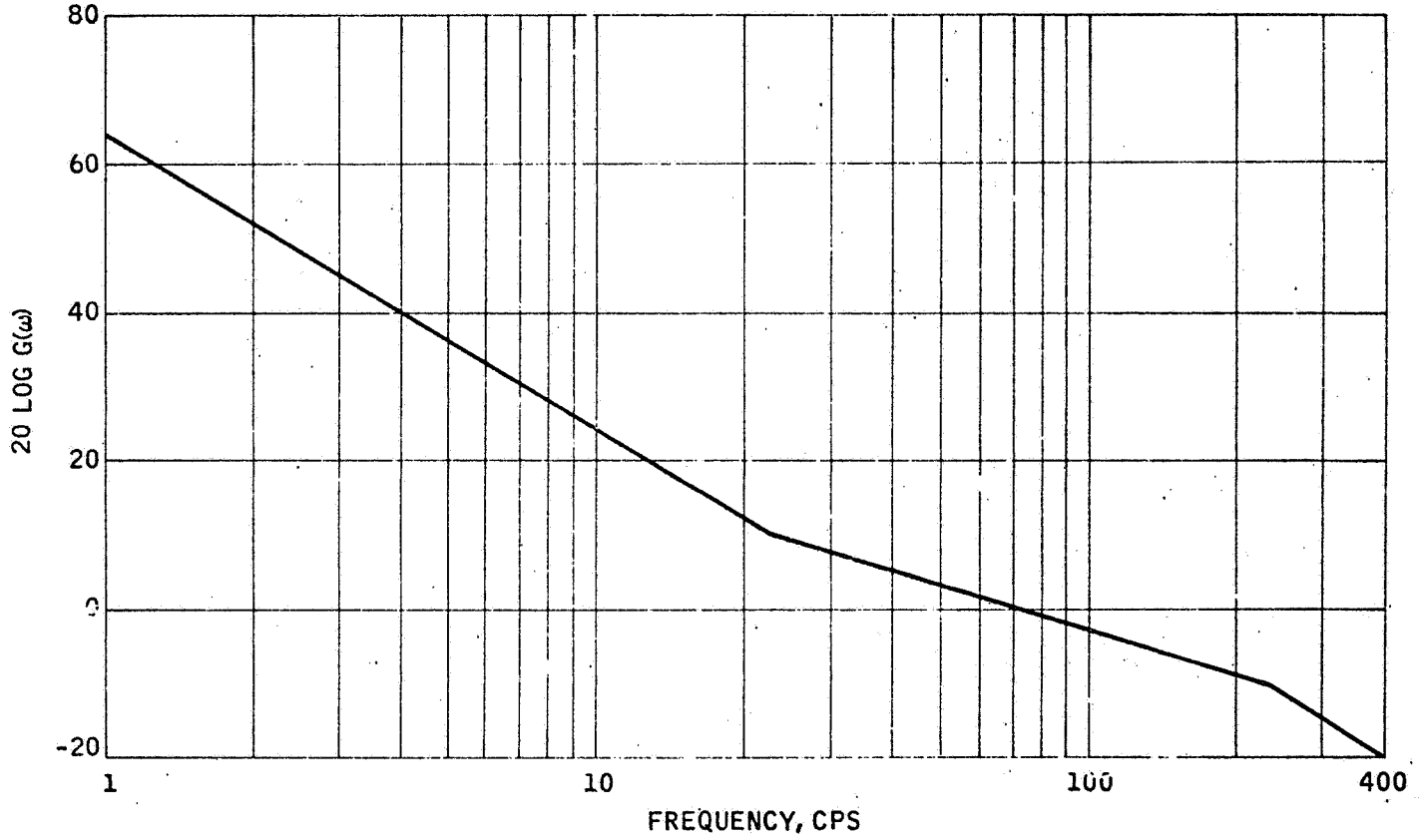

Figure 25. 20 Log G(ω) versus Frequency - Low G Loop

$$\frac{X}{a}(s) = \frac{1/S^2}{1 + \frac{G_1 V_o G(s)}{MS^2}}$$

X = rotor displacement

a = input acceleration

G_1 = electronic gain (volts per μ in.)

M = rotor mass

V_o = bias voltage

G(s) = network impulse response

The real frequency where gain is unity may be found by setting

$$\frac{G_1 V_o G(\omega)}{M} = -(j\omega)^2$$

and solving for ω. Let the frequency be ω_c;

$$\omega_c = \sqrt{\frac{G_1 V_o G(\omega)}{M}}$$

From the force equation,

$$Fm = K_o \cdot 4 \cdot V_o^2$$

where K_o is the constant of proportionality. Thus,

$$\omega_c = \sqrt{\frac{G_1 \cdot G(\omega)}{M}} \cdot \sqrt{\frac{F_m}{4 K_o}}$$

From these equations it is observed that

- If only maximum force is scaled, the crossover frequency is proportional to the fourth root of maximum force
- G_1 can be adjusted inversely to V_o to keep ω_c constant
- $G(\omega)$ can change to keep the crossover point stable even if it changes in frequency

If we make the reasonable assumption that the point of maximum phase lead of $G(\omega)$ follows ω_c, then for the four order of magnitude change in F_m, one order of magnitude change occurs in ω_c. Since this loop is conditionally stable, the 10:1 shift plus the necessary safety margins require the use of a switched network.

The design of switched networks is greatly facilitated if there is some correlation between the networks used to stabilize the high G and low G loops. This means attempting to use the same breakpoints in the compensation design.

Figure 26 is a Bode plot of the two loops with adjustments made in the previous (Figures 25 and 22) breakpoints to allow use of the same networks in both loops.

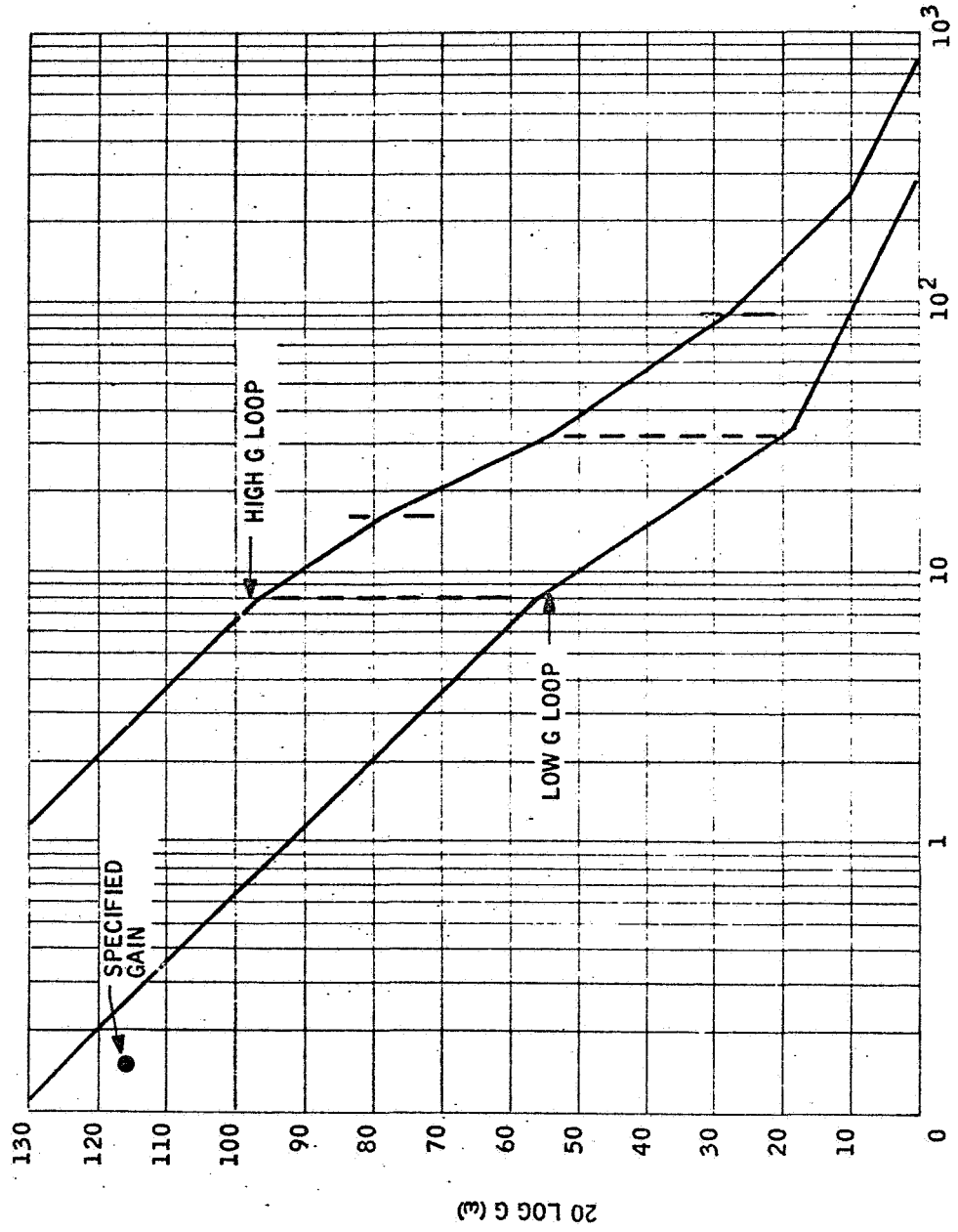

Figure 26. Modified Transfer Function for High G and Low G Loops with Common Breakpoints

GENERAL CONSIDERATIONS IN THE CHOICE OF SUSPENSION FOR MAXIMUM RANGE

The ESVG suspension system which will be used in a given application can be any of several types which are distinguished by the output waveforms. They range from a low-frequency square wave, through a medium-frequency sine wave, to various types of pulsed or switched systems. Up to this point, no specific choices have been made.

In an application where high-acceleration capability is demanded, as well as good drift performance in a low-level acceleration environment, the suspension must have two modes of operation. In the high G region, the important factors are sufficient G capability, power consumption, and incorporation of voltage constraints. In the low G region the important factor is power consumption. In this study it is convenient to specify the division point between the two acceleration regions. They are defined by the mission requirements to be

Low G: 0 to 0.01 G

High G: 0.01 G to maximum capability

An important part of the system will be the method of coupling and switching between the two modes of operation.

In the high-acceleration region, suspension output voltages will tend to be high. High voltages eliminate the possibility of switching at the electrodes or of driving them directly. For this reason, only the transformer output low-frequency square wave and high-frequency sine wave systems can be considered for the high G system.

Two limitations apply to either type of system. The first is a physical limitation placed on the acceleration capability by realizable rotor thickness, rotor material, and maximum electric fields; this limitation has been defined. The second type is that imposed by support electronics and certain scaling relationships which for most ESVG applications should be included. These are not easily defined in a general sense. To facilitate a comparison between the sine and square wave systems, specific gyro parameters (rotor-electrode gap, rotor thickness and size) must be selected and a system of each type compared.

Physical Limitations

The most-sensitive scaling variable is the actual operating gap between electrode and rotor in the gyro. A second major variable is rotor diameter. Several factors which influence the choice of these parameters are

- Gyro fabrication tolerances
- Thermal environments

- Rotor structural stability
- Output circuit bandwidth
- Insulation requirements
- Power considerations

Generally, the torque from fabrication error is proportional to the ratio of the error to rotor electrode gap. Therefore, a larger gap is more desirable from this standpoint. A gyro with a gap of less than one mil is likely to exhibit intolerable drift levels from error torque.

Usually, the rotor and electrode housing have different thermal expansion coefficients. The magnitude of this difference, plus consideration of the thermal environments to which the gyro will be subjected whether operating or nonoperating, establishes a minimum value that the ratio of gap to diameter can assume. With presently used materials in moderately extreme thermal changes ($\Delta T \leq 200°F$), this ratio should not be less than 0.0005.

Angular momentum depends on rotor material density, stress limits (which determine maximum rotor speed for a given size), shell thickness, and rotor size. To provide high G capability, the shell thickness is minimized. To avoid intolerably high drift as a result of low momentum, the rotor diameter should not be too small. A minimum size limit is considered to be one inch.

Another important factor is the structural integrity and shape stability of the rotor. This factor is a function of the ratio of shell thickness to rotor size, with greater stability present if this ratio is increased. To maintain reasonable stability in a high G capable application, the rotor diameter should not exceed three inches.

Generally, potentials over 4000 volts are difficult to produce. Transformer output leakage reactance increases to the point where it is a bandwidth-limiting factor in square wave systems. The small capacitance of assemblies over a four-mil gap makes tuning of sine wave systems difficult. The tuning reactors become large and tend toward self reasonance, requiring carrier frequencies to be reduced; this in turn limits bandwidth.

As noted in a previous section, the power that is required depends on the gap and the square of the rotor diameter. Although a definite limit does not exist, the power begins to become large for resonant systems of three-inch diameter and gaps of the order of three mils. Switched systems suffer from the same problem; however, both may be reduced by lowering the cycling or carrier frequency. Gaps over six mils require output potentials exceeding 6000 volts, causing insulation problems in miniature gyro assemblies.

The size and gap regions where these factors become dominant problems are sketched in Figure 27 for the maximum performance gyro. A reasonably good parametric compromise of all these factors is a 1.5-inch diameter and a two-

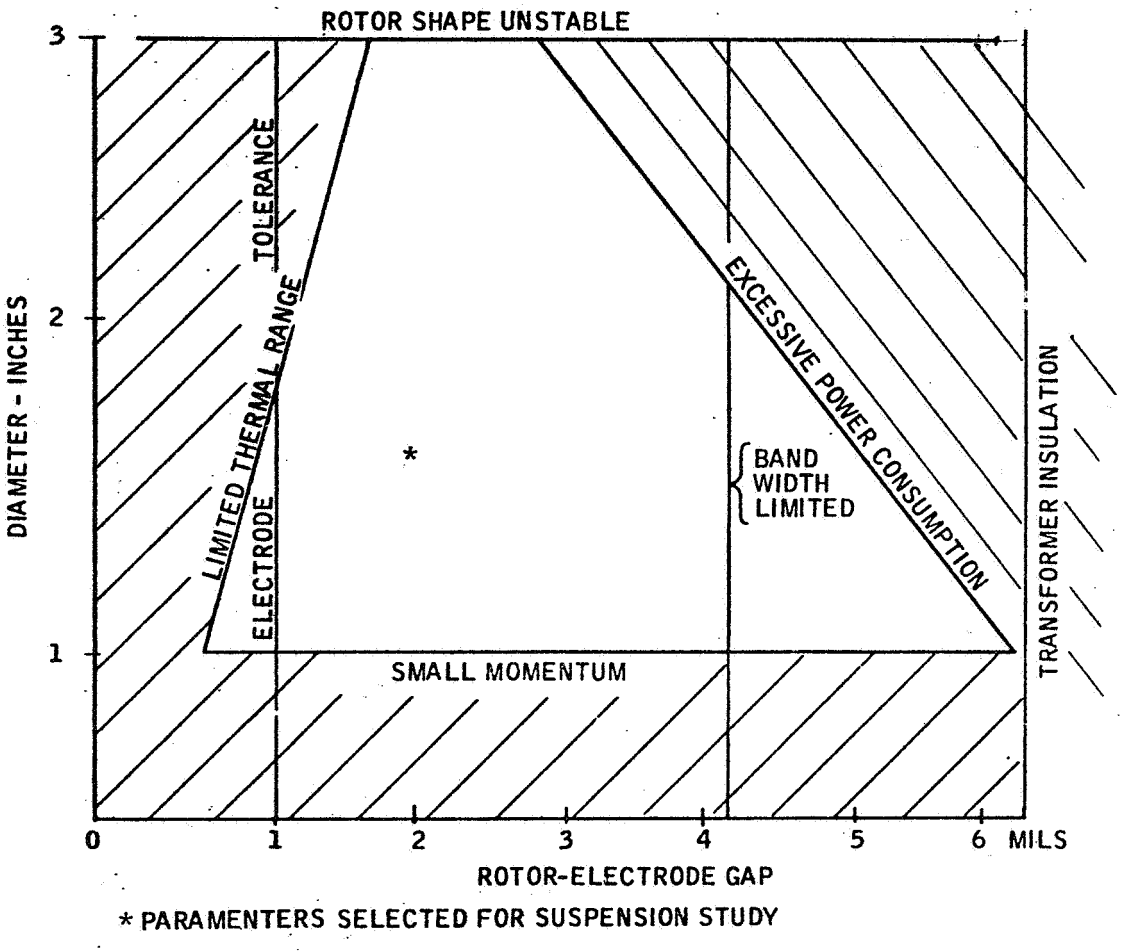

Figure 27. Parameter Choice for Maximum Capability

mil rotor-electrode gap. It will be assumed that the maximum gradient is 1000 volts/mil and the output voltage is linear for rotor displacements up to 15 percent of the gap. These parameters will be used in all subsequent suspension analysis in this study.

The object of this investigation is to design a suspension system which will provide maximum effort at the lowest possible power level and be capable of switching between the two operating regions.

Important to these considerations are the output circuits, stabilizing network, sensing circuits, and voltage constraint. These will be discussed in turn.

Output Circuits

The two important parameters for consideration are physical realizability and the capability of being switched from high G to low G operation. Direct output and any directly coupled mixed systems (e.g., sine/square) must have components capable of switching the 2300-volt, high G output. Such switches do not exist. The high G system must operate with a transformer output. Several alternatives can be considered:

- Transformer coupled high and low G square wave system with a "separate sensing" type of bridge
- Parallel output sine systems, separately sensed on high G
- Square wave, high G system with capacitor coupled sine sensing and low G
- Square or sine wave with variable bias level and power supply

The choice between these approaches will be made based on the power required and the ease of switching.

Sensing Circuits

The rotor sensing circuits take one of two forms: a "separate sensing" type, which is a separate capacitor-coupled, high-frequency bridge; or a "self-sensing" type, which consists of a balanced circuit added to the output circuit and operating at the carrier or forcing frequency of a sine wave system.

Since a "separate" sensing bridge measures position by applying a voltage to the electrodes, the bridge voltage can also function as the bias voltage, or be a low G suspension in itself. The self-sensing type of circuit is convenient and simple; however, it is not suitable for the high G suspension because regeneration, which is inherent in such a system, limits loop gain to an unacceptable level.

A self-sensing type of bridge, when used in a low G system, is subject to many potential position drift sources. Each electrode is driven by a current amplifier which accepts inputs from a bias source and the control source's amplifier feedback is from a reference capacitor. A bridge is formed at each electrode which must be nulled. The difference between the two electrode signals is sensed in each axis. Errors in initial null and drift in the reference capacitor (a large value capacitor) and in the differencing operation all produce rotor centering shifts. Furthermore, this whole suspension must operate at a high carrier frequency to give adequate filtering ratios.

Generally, it is undesirable to switch the sensing circuits because of the difficulty in maintaining position reference.

Compensation Networks

It has been shown that the range of frequencies characteristic of the high and low G systems is too large for a single network. Consequently, two networks must be switched to produce break frequencies where they are needed for each system. It is desirable that both networks be active in high G operation so that the switching process does not induce large transients in the suspension loop. The network may be switched by means of diode attenuators or double-emitter transistors from the variable supply.

Voltage Constraints

In the choice of a type of suspension system, one major area of concern has not been considered - that of voltage (or current) constraints. The only presently known worthwhile constraint is on the sum of squares of suspension voltages, or currents (ΣV^2). In this section we will derive the basic conditions necessary to assure that ΣV^2 are equal on all channels. The mechanizations for several systems using sine waves and one for square waves are given.

The ΣV^2 constraint may be applied over all channels simultaneously, keeping the sum in each channel equal to that in the other channels, but not necessarily constant. This type of circuit would be applied to a suspension with automatically variable preload. Such a system is very complex and will not be considered here. The usual constraint is applied in each channel and is used to keep the ΣV^2 a constant in each channel. For this case, consider a channel with voltages applied equalling V_1 and V_2.

The expression $V_1^2 + V_2^2 = C^2$ describes the ΣV^2 condition. The net force produced is proportional to the difference of voltage squares and may be written

$$F = K_o (V_1^2 - V_2^2) \tag{85}$$

where K_o equals the ratio F_o/V_o^2 previously used. The ΣV^2 condition

immediately suggests a geometric interpretation as shown in Figure 28, where the hypotenuse length C of the right triangle and V_1 and V_2 are legs which are varied to satisfy force requirements to support the rotor. The locus of the apex of the right angle is a circle of diameter C.

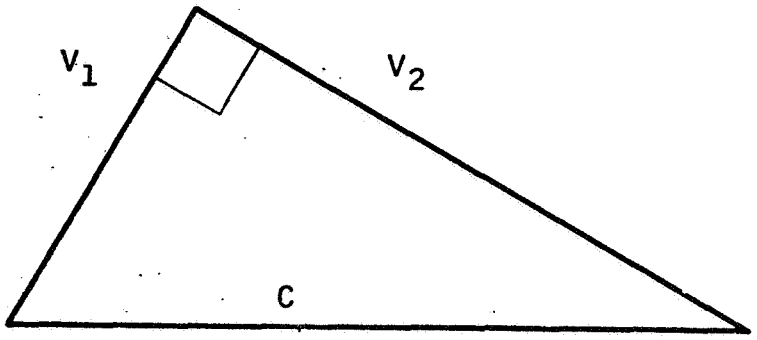

Figure 28. ΣV^2 Relationships

From the conditions that $Vm \geq V_1 \geq 0$, V_2 is maximum at $V_1 = 0$, and V_2 is zero at V_1 maximum (maximum force conditions), it is evident that the constant C represents V_m and, therefore,

$$V_1^2 + V_2^2 = V_m^2$$

It is also evident that at $F = 0$, $V_1^2 = V_2^2 = 1/2\ V_m^2$.

To a linear servo without ΣV^2 control, a bias voltage must be added which will satisfy these conditions. It was shown earlier that for a linear servo the bias voltage is $\frac{V_m}{2}$. Comparing "per electrode" bias force in the two cases gives

$$F_1\ (\Sigma V^2 \text{ control}) = K_o V_1^2 = K_o \cdot 1/2\ V_m^2$$

$$F_1\ (\text{linear}) = K_o V_1^2 = K_o\ 1/4\ V_m^2$$

Thus, the sum of the squares control will multiply the force per electrode by two at zero force input. The advantages of sum of the squares control must be considered with regard to the disadvantages of accepting this higher, necessar bias force.

The geometry of the ΣV^2 problem suggests several methods for control of the voltages. Constraining ΣV^2 to be a constant places the point A of Figure 29 on the circumference of a circle with diameter V_m. In this section we will consider controls based on the quantities V_a and the angle θ defined in Figure 30. Others are possible, but more complex.

For sine systems, the sum of the squares constraint on output voltage or current may be implemented in several ways. These systems are particularly adaptable because of the additional freedom to add quadrature signals which do not upset the current balance requirements. Two methods will be discussed which are based on the concept of producing output quantities which may be plotted as vectors summing to a diameter of a fixed-size circle.

From the phase diagram of Figure 30,

$$V_1 = V_b + V_c + j\,V_a \tag{86a}$$

$$V_2 = V_b - V_c - j\,V_a \tag{86b}$$

where V_a is an added voltage used to make the ΣV^2 condition a reality by means of a servo system. Since V_b is represented by the radius,

$$V_1^2 + V_2^2 = V_m^2 = (2V_b)^2. \tag{87}$$

The sum of the squares of Equations (86) yields

$$V_1^2 + V_2^2 = (V_b + V_c)^2 + V_a^2\,(V_b - V_c)^2 + V_a^2 \tag{88}$$

$$= V_b^2 + 2V_bV_c + V_c^2 + V_a^2 + V_b^2 - 2V_bV_c + V_c^2 + V_c^2$$

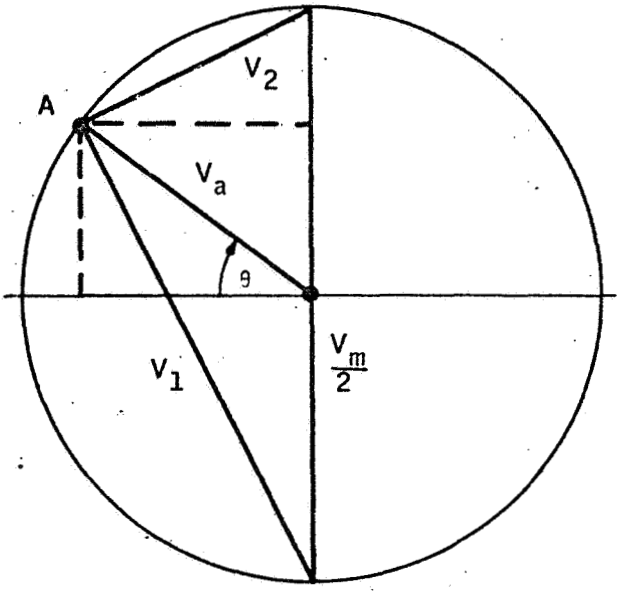

Figure 29. ΣV^2 Control Qualities

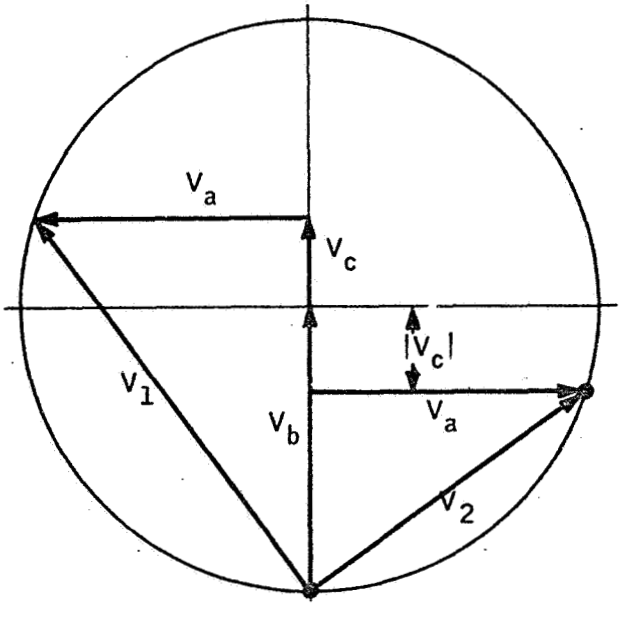

Figure 30. Honeywell ΣV^2 Phase Diagram

Equating the right-hand sides of Equations (87) and (88) gives

$$2V_b^2 + 2V_c^2 + 2V_a^2 = 4V_b^2$$

or

$$V_a^2 + V_c^2 = V_b^2 \tag{89}$$

A voltage, V_a, which satisfies Equation (89) also satisfies ΣV^2 constant condition. Note at the endpoints,

$$V_c = 0, \; |V_a| = |V_b|$$

$$V_c = V_b \; |V_a| = 0$$

The next problem is how to control V_a. The suspension rebalance signal is represented by V_c and is an independent quantity. If V_c changes by a small quantity to V_c', a correction Δ must be made to V_a so that the following equations are satisfied.

$$V_1^2 = (V_b - V'_c)^2 + (V_a + \Delta)^2 \tag{90a}$$

$$V_2^2 = (V_b - V'_c)^2 + (V_a + \Delta)^2 \tag{90b}$$

After the correction, the final value of V_a includes Δ. The correction Δ is, therefore, a voltage that must be reduced to zero by the servo. Expanding Equations (90) and equating the right-hand side of their sum with that of Equation (87) yields an expression that can be factored as follows:

$$2V_a\Delta = V_b^2 - V_c^2 - V_a^2$$

$$= (V_b - \sqrt{V_c^2 + V_a^2})\,(V_b + \sqrt{V_c^2 + V_a^2}) \tag{91}$$

If $\Delta \to 0$ for any nonzero V_a, then the term

$$V_b - \sqrt{V_c^2 + V_a^2} \to 0.$$

If the voltages depicted in Figure 30 are treated as vectors, one deduces that

$$|V_b| = \frac{|V_1 + V_2|}{2}$$

$$\sqrt{V_c^2 + V_a^2} = \frac{|V_1 - V_2|}{2} .$$

The right-hand terms are the two quantities needed to null the servo shown in Figure 31.

Equations (90) can be substituted into the suspension loop force function [Equation (85)] to give

$$F = \{([V_b + V_c]^2 + V_a^2) - ([V_b - V_c]^2 + V_a)\}$$

$$= Ko\ 4V_bV_c . \qquad (92)$$

Note that F does not depend on V_a. The addition of this circuit thus produces no change in the loop transfer function; it merely increases the bias level force by a factor of 2, the gradient by $\sqrt{2}$, the power by $\sqrt{2}$. It may be added or removed at will without changing the rest of the loop. Note that this loop uses the output variables for the control; thus it is not limited in accuracy by further amplification.

A second type of ΣV^2 circuit can be used which controls the phase of V_a as shown in Figure 32. The component $V_a \sin \phi$ is equated to V_c, thus providing the phase angle ϕ. The component $V_a \cos \phi$ is added to $(V_b + V_c)$ and subtracted from $(V_b - V_c)$ to generate V_1 and V_2, respectively. Let Δ now denote a correction to the phase, ϕ, of V_a, when V_c changes by V_e. Again, treating the voltages depicted in Figure 32 as vectors, the correction must be such that

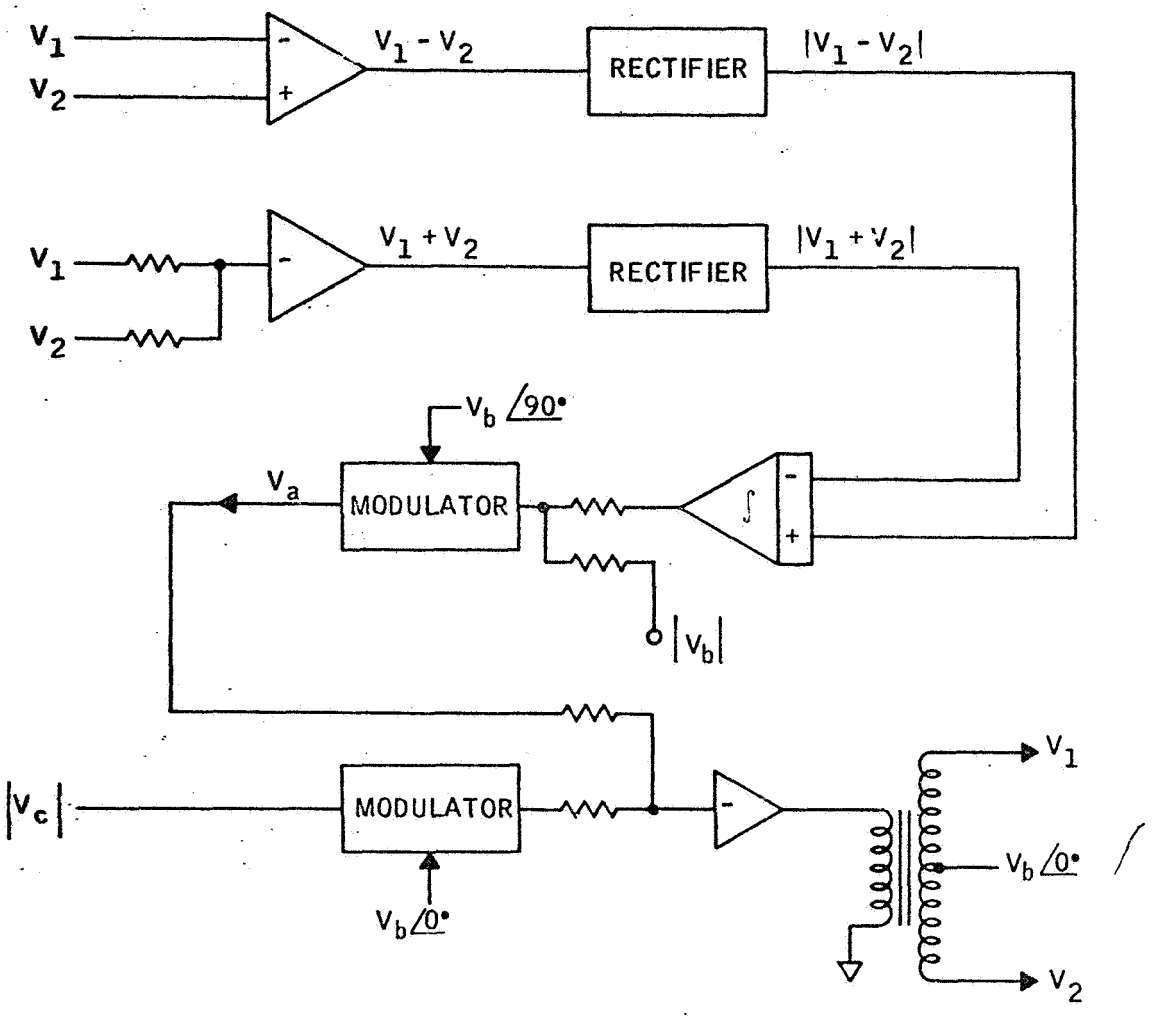

Figure 31. ΣV^2 Servo for Sine Wave Output

$$V_1^2 + V_2^2 = (V_b + V_c + V_e)^2 + V_a^2 \cos^2(\phi + \Delta)$$

$$+ (V_b - V_c - V_e)^2 + V_a^2 \cos^2(\phi + \Delta) = (2V_b)^2$$

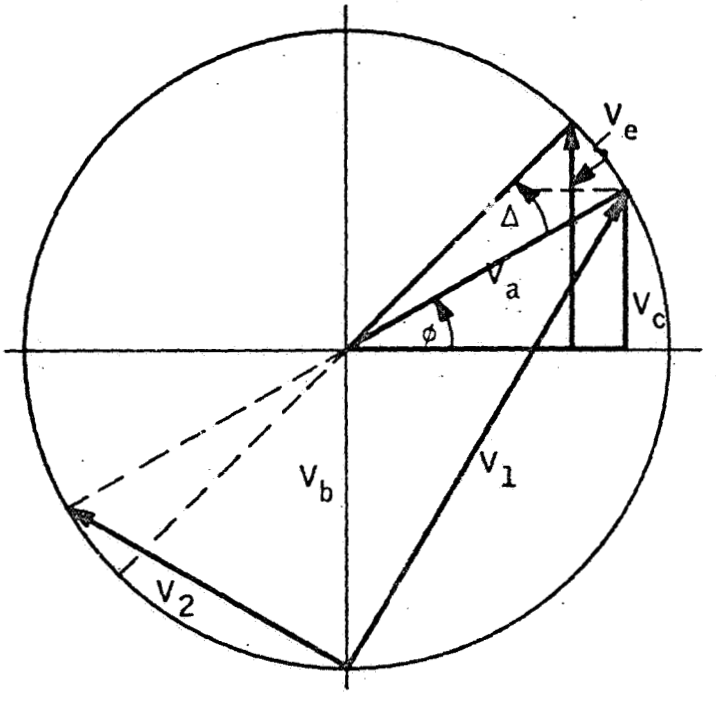

Figure 32. Diagram for Phase Controlled ΣV^2 Control

Expanding this equation yields,

$$4V_b^2 = 2V_b^2 + 2V_c^2 + 2V_e^2 + 4V_eV_c + 2V_a^2 \cos^2(\phi+\Delta) \qquad (93)$$

From Figure 32 it is noted that the magnitude of V_a is constant, and that $|V_a| = |V_b|$. Also, by the control on ϕ $V_c = V_a \sin\phi$, and V_e is an error in the servo producing Δ through a phase modulator.

Thus, $\Delta = K_1 V_e$ and substitution gives

$$2V_b^2 = 2V_b^2 \sin^2\phi + 2V_b^2 \cos^2\phi \cos^2\Delta + \frac{4V_b \sin\phi \cdot \Delta}{K_1}$$
$$+ 2V_b^2 \sin\phi\cos\phi\sin\Delta\cos\Delta + 2V_b^2 \sin^2\phi \sin^2\Delta \qquad (94)$$

The equation is satisfied for all ϕ if $\Delta = > 0$; thus, $V_e > 0$ and since $V_o = V_a \sin(\phi + \Delta) - V_c$, this term must be generated at the servo input.

The block diagram of a phase-control ΣV^2 circuit is shown in Figure 33.

For this case, the suspension loop force equation is given by Equation (92) thus, the loop dynamics are not affected. It also may be added or removed at will without changing the rest of the loop.

If it is desired that the ΣV^2 loop never be removed, the point marked $V_b \angle 90 \pm \phi$ may be used directly to add to and subtract from $V_b \angle 0°$ to give V_1 and V_2 directly. Although the ultimate forcing function is purely $4 V_b V_c$ in this loop as in the others, the dynamics of the ΣV^2 loop enter into the main loop because $V_b \angle \phi$ must be generated.

Note that the loop as shown in Figure 33 is open to the output. Consequently the actual ΣV^2 produced is only as accurate as the output amplifiers. The loop can also be operated closed around the output, however, simply by noting that $V_1 - V_2 = 2V_b \angle 90 \pm \phi$. The difference $V_1 - V_2$ is input to the sine demodulator instead of the $V_b \angle 90 \pm \phi$ from the phase modulator. The loop then takes the form shown in Figure 34.

Again, for this type of control, the suspension loop force function and the sum of the squares function are the same as for the other types.

Another approach may be used which puts the ΣV^2 control directly in the suspension control loop.

If a phase modulator is used (Figure 35) which produces the phase angle as a function of input voltage, the term V_a from Figure 32 may be produced directly.

The equations for V_1 and V_2 are

$$V_1 = V_b + V_a \sin\phi + j V_a \cos\phi$$

$$V_2 = V_b + V_a \sin\phi - j V_a \cos\phi \qquad (95)$$

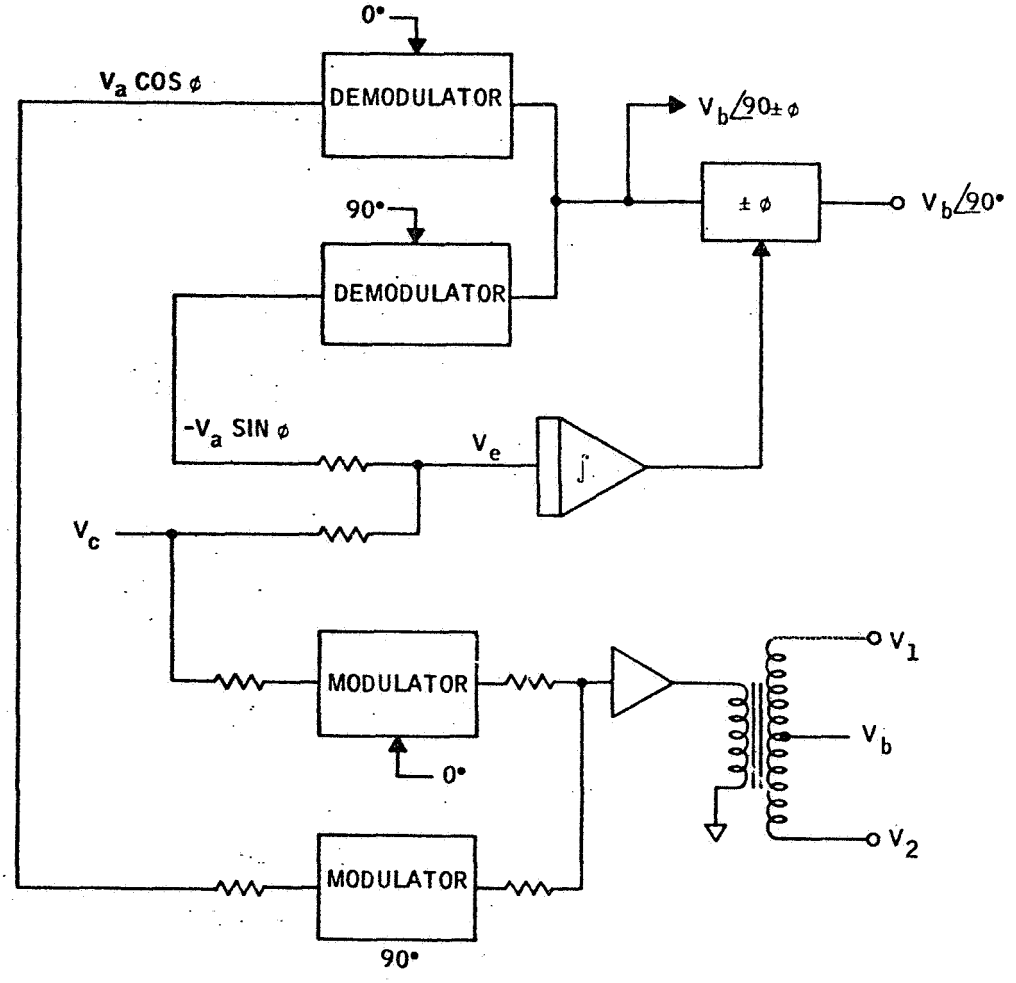

Figure 33. Phase Controlled ΣV^2 Servo (Open Loop)

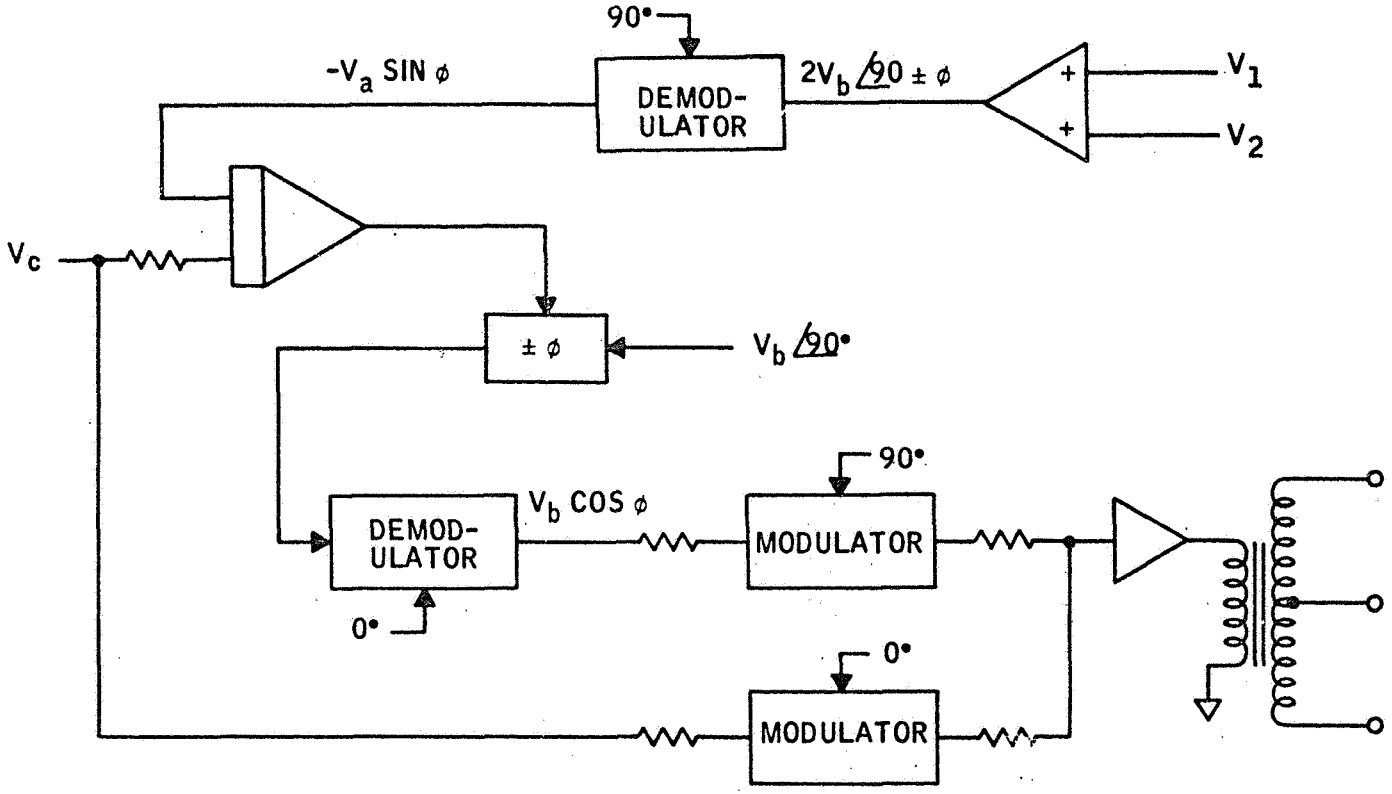

Figure 34. Phase Controlled ΣV^2 Servo (Closed Loop)

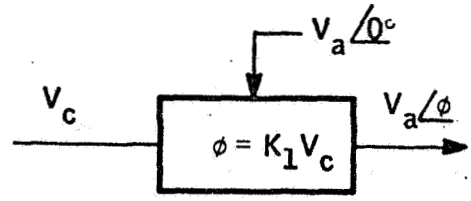

Figure 35. Phase Modulator

The sum of the squares of Equation (95) is

$$V_1^2 + V_2^2 = V_b^2 + V_a^2$$

which satisfies the desired condition. The suspension loop force function is

$$F = K_o (V_1^2 - V_2)^2 = K_o \; 4V_b V_a \sin \phi$$

$$= K_o \; 4V_b \; V_a \sin (K_1 \; V_c) \qquad (96)$$

which differs from the other types of control.

For a displacement-sensing force-output servo, $V_c = K_2 x$, and

$$F = K_o \; 4 \; . \; V_b \; . \; V_a \sin (K_1 \; K_2 x) \qquad (97)$$

The loop gain function is the force/unit distance produced by the loop.

$$\frac{dF}{dX} = K_o \; 4V_b V_a \; K_1 \; K_2 \cos \phi \qquad (98)$$

The gain is $4V_b V_a \; K_1 \; K_2 \; K_o$ at $\phi = 0°$, but decreases to zero as

$\phi \rightarrow \pm 90°$. This is a serious problem in a servo where maximum effort is desired and where conditional stability invariably produces a lower limit on loop gain.

Sum of the squares control in the square wave suspension system is more difficult to implement since there is no way to produce relative phase. Computations must be accomplished using voltage magnitudes only and usually involve multiplying or squaring circuits. The following constraints on the circuit are desirable:

1. A linear function of the control variable
2. Maintain a constant loop gain
3. Loop dynamics remain outside main suspension loop
4. Can be removed if not wanted
5. No multipliers required

Experience with the sine systems leads us to define X from Figure 36 as the control variable. Let R designate the circular radius and a the desired additive voltage which will keep the sum of V_1^2 and V_2^2 a constant.

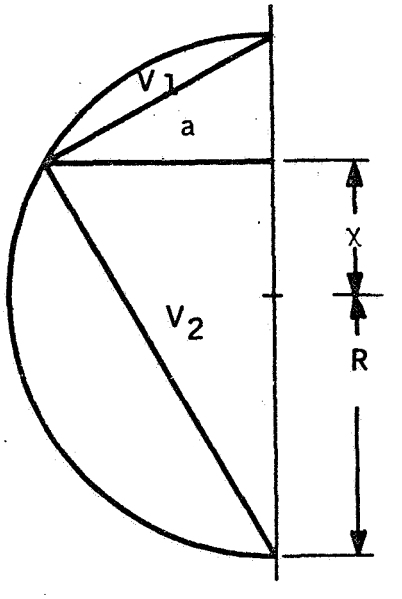

Figure 36. ΣV^2 Geometry for Square Wave Suspension

From Figure 36

$$V_1^2 = a^2 + (R - X)^2$$
$$V_2^2 = a^2 + (R + X)^2 \qquad (99)$$

The constraint on ΣV^2 gives

$$V_1^2 + V_2^2 = 4R^2 = 2a^2 + 2R^2 + 2X^2 \tag{100}$$

The final relation is the sum of (99). Consequently,

$$\begin{aligned} a^2 &= R^2 - X^2 \\ &= (R - X)(R + X) \end{aligned} \tag{101}$$

The suspension loop force function is

$$\begin{aligned} F &= K_o (V_1^2 - V_2^2) \\ &= -4K_o \, X \, R \end{aligned} \tag{102}$$

Thus, this system is also linear with X. Substituting for a from Equation (101) into Equations (99) yields

$$\begin{aligned} V_1^2 &= 2R^2 - 2X\,R \\ V_2^2 &= 2R^2 + 2X\,R \end{aligned} \tag{103}$$

The usual linear system without ΣV^2 is operated by generating output voltages of the form

$$\begin{aligned} V_+ &= R - X \\ V_- &= R + X \end{aligned} \tag{104}$$

which provides the desired loop force function [Equation (102)]. If V+ and V- are generated by the main loop and then corrected to maintain ΣV^2 constant, the dynamics of the ΣV^2 loop will not enter into the main loop equation. Let correction factors D_1 and D_2 be defined such that

$$\begin{aligned} V_1 &= V_+ + D_1 \\ V_2 &= V_- + D_2 \end{aligned}$$

Using Equations (103) and (104), these corrections can be expressed in terms of X and R.

$$D_1 = R\left[\sqrt{2}\ \sqrt{1 - X/R} - (1 - X/R)\right]$$
$$D_2 = R\left[\sqrt{2}\ \sqrt{1 + X/R} - (1 + X/R)\right] \qquad (105)$$

Note that this control automatically maintains constant loop gain . The corrections D_1 and D_2 are functions of X alone and are mirror images of each other with respect to X. To show their form, D_1 is plotted in Figure 37.

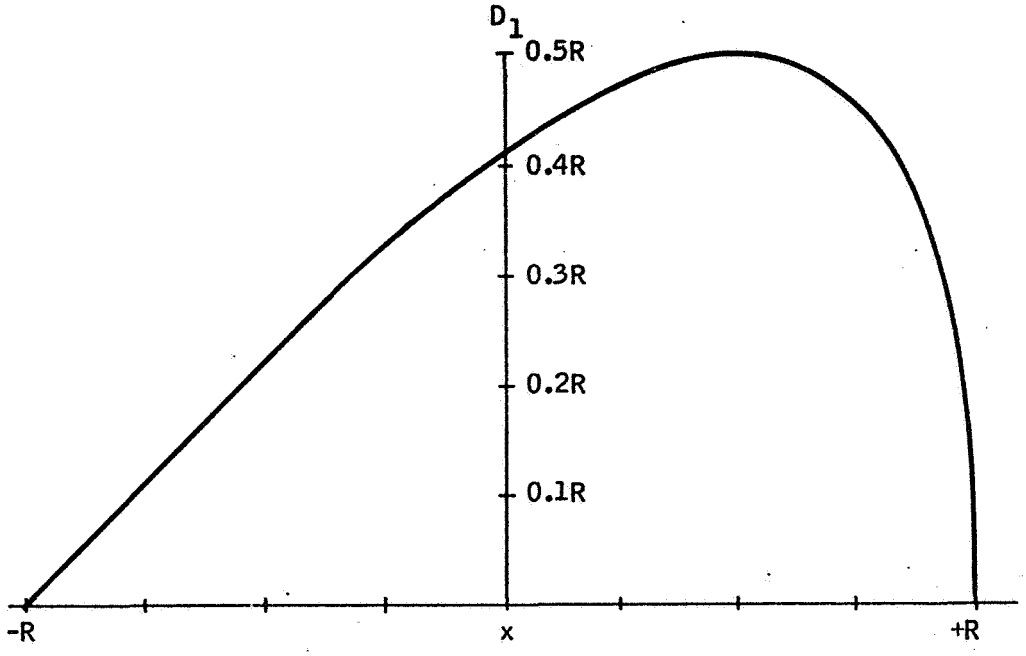

Figure 37. Difference Voltage, D_1

This function may be approximated quite well by simple linear elements in three regions:

$$
\begin{aligned}
D_1^* &= 0.414X + 0.414R \quad && -R<X< 0.15R \\
D_1^* &= 0.475R \quad && 0.15R <X< 0.9R \\
D_1^* &= 4.75X + 4.75R \quad && 0.9R<X<R
\end{aligned}
\tag{106}
$$

The peak error with this approximation is determined by evaluating the deviation of the ΣV^2 from its desired value. In terms of the exact functions (D_1) and their approximations (D_1^*), the fractional error is

$$
E = \frac{2R\,(D_1 - D_1^* + D_2 - D_2^*) + 2x(D_1 - D_1^* - D_2 + D_2^*) + D_1^2 - D_1^{*2} + D_2^2 - D_2^{*2}}{2R^2 + 2x^2 + 2R\,(D_1 + D_2) + 2x\,(D_1 - D_2) + D_1^2 + D_2^2}
$$

The maximum fractional error occurs at $X = 0.98R$ and is equal to 0.076. If such an approximation is used and the maximum tolerable error is specified, the breakpoints and slopes can be determined by using a computer with the values and tolerances based on allowable fractional error. The system diagram for this mathematical formulation could take the form shown in Figure 38.

Error is not determined directly by D_1 and D_1^*; however, these functions turn up in the error assessment and are computed in Table II.

TABLE II.- BREAKPOINT APPROXIMATION

	Interval I	Interval II	Interval III
D_1x	0.2517	0.500	0.163
D_1x^*	0.2264	0.475	0.076
Ex	0.0253	0.025	0.087
x	-0.4534R	+0.500R	+0.984

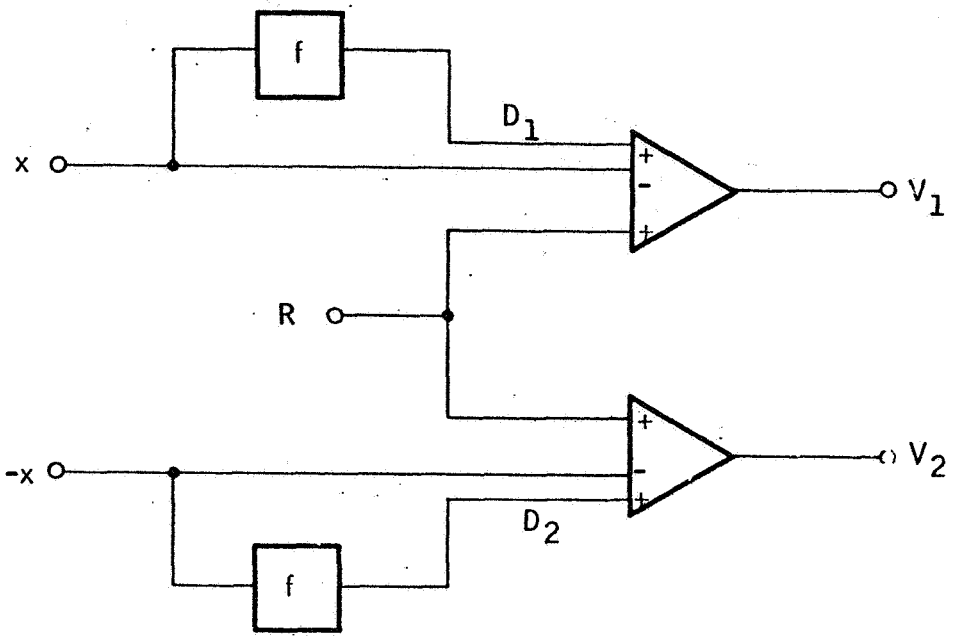

Figure 38. ΣV^2 System Diagram for Square Wave Output

D_1x, D_1x^*, E_x are the desired value, actual value, and error at X, the point of peak deviation ($dE/dX = 0$ for each interval).

The previous paragraphs have shown that sum of the squares control may be implemented for either the sine or square wave systems. Among them, there is no great difference in their complexity. The accuracy of each is sufficient for the application. Adding this voltage constraint need not be a determining factor in deciding which type of suspension to use. It is worthwhile to recall, however, that addition of the constraint in either system raises necessary power output 40 percent and increases force per electrode 100 percent with no acceleration input.

Summary

Since the stabilizing network must be switched and the sensing circuits cannot be switched, decision between the switched or continuously variable bias and output circuitry is reduced to determining which is simplest in terms of hardware. For the continuous system, a point must be chosen where the networks switch modes. The system stability parameters will change continuously. It would be far more desirable to switch everything

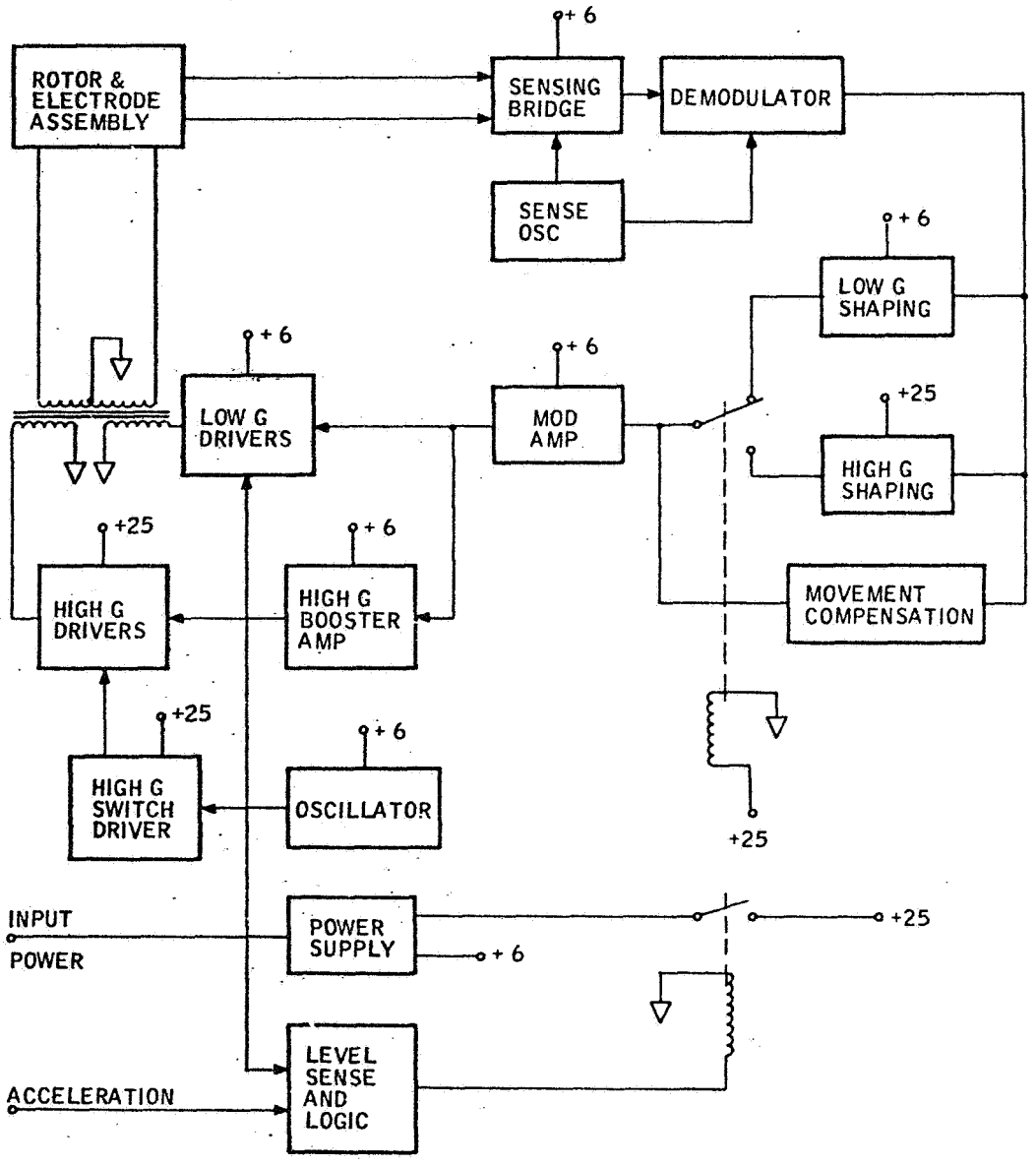

Figure 39. Square Wave Suspension System

simultaneously and optimize performance at each of the two levels. A switch on the power supply level can be made to accomplish this.

A square wave, high G system could have several mechanizations at low G: one such is a low G square wave drive coupled by the high G transformer used. The block diagram of such a system is shown in Figure 39. The high G circuits are controlled by a high-voltage supply (+25V, for example). Assemblies powered by the +25V, such as the high G output circuits and a shaping amplifier, are turned off in the low G region. The sensing bridge is used for bias in the low G region and the drivers nominally operate about zero volts out from the mod amp.

A dual-range sine system is shown in Figure 40. Many of the same approaches are used. A low G current system is the simplest way to maintain balance between the three axes. A second type of dual range system is shown in Figure 41. This uses self-sensing, low G sine wave which is also the sense signal for the high G system. This sensing section may be used with either square or sine high G loops as shown.

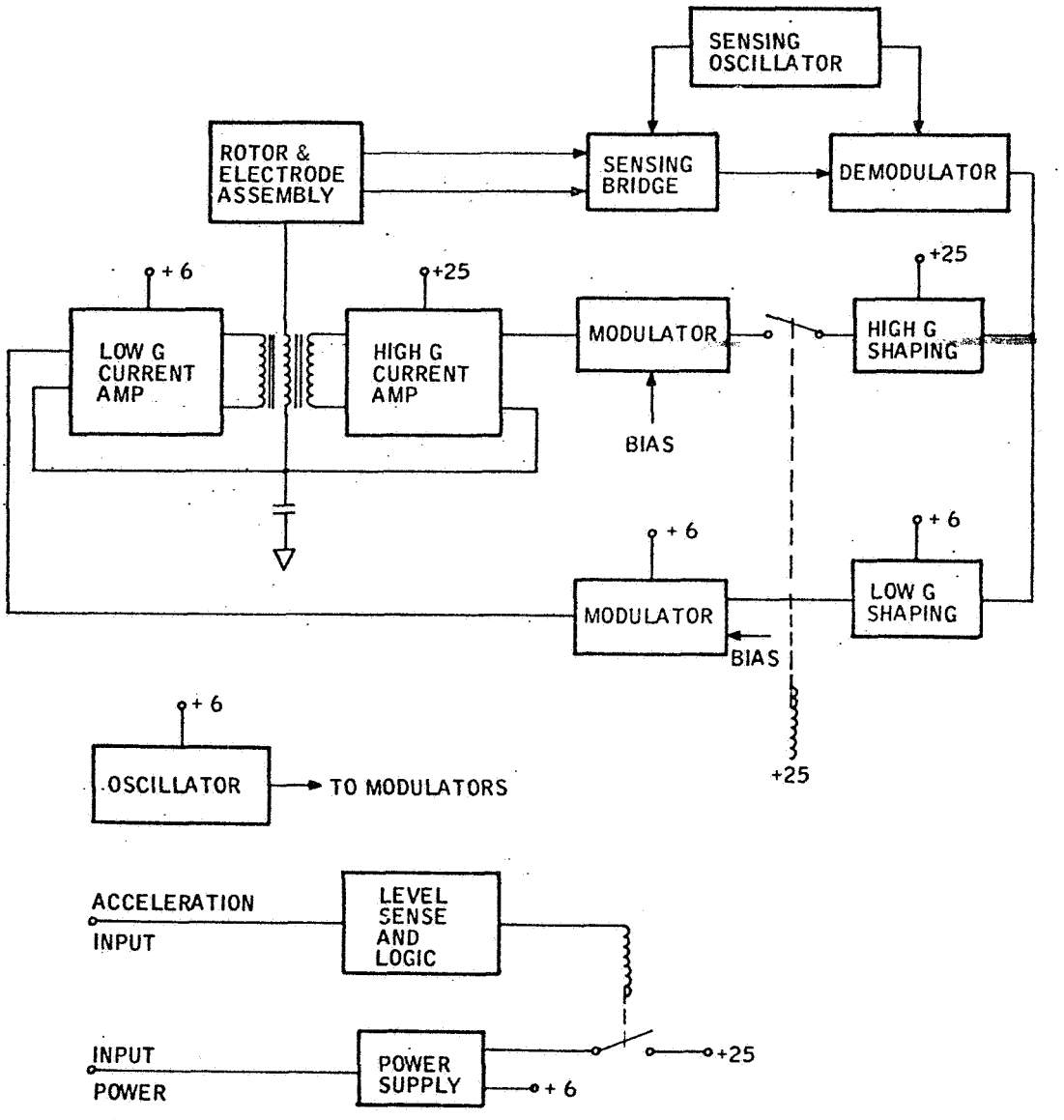

Figure 40. Sine Wave Suspension System

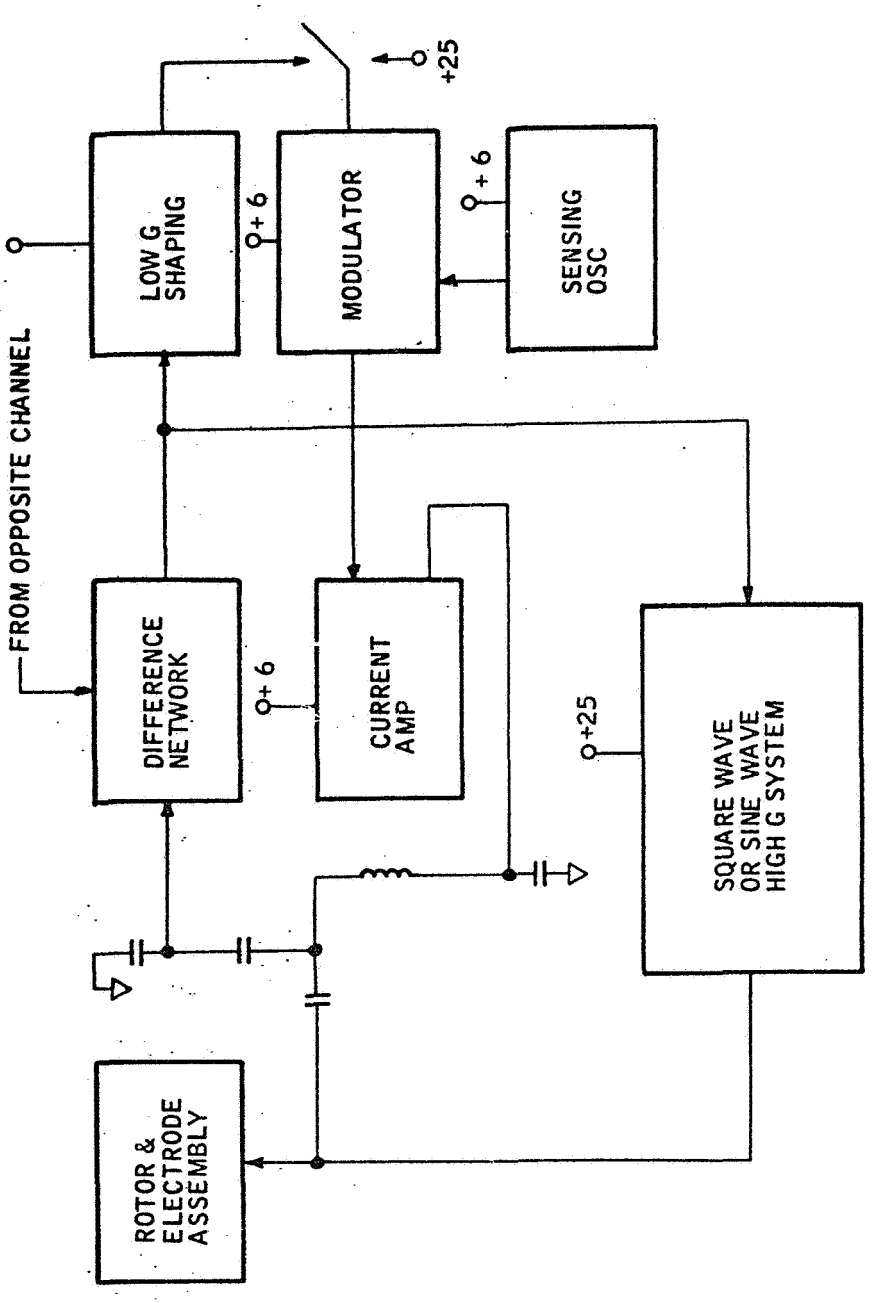

Figure 41. Combination Suspension System

SECTION III
LOW-POWER STUDY

The consumption of power in the gyro suspension system may be divided into two separate areas. The first area is the bias power used by the position-sensing circuits and by the amplifying/compensation circuitry. The second area includes the output circuit power necessary to drive the capacitive load. Power required in each area is considered in the following paragraphs. Choice of a circuit to be breadboarded is made, and the power supply needed is defined.

BIAS LOSSES

The circuit bias losses are most important in the low G operating mode. The discussion of bias losses begins with a definition of low G operation and goes on to consider the impact of supply voltage, signal levels, and network requirements.

Low G Systems

The low G region has been defined as a level of 0.01 G or less. It is most advantageous to reduce bias and maximum force to this level. The reduction of bias (or preload) forces linearly reduces torques produced by electric field anomalies in the gyro, which is desirable for long-term missions. To compare the magnitudes of the values involved with the high G system, force level is scaled by 10^4. Gradients scale by 10^2, power by 10^4, peak current and voltages by 10^2. This means that the necessary voltage output is of the order of 23 volts square wave, that power output is insignificant compared to bias power, that peak currents are in the range of signal transistor capability, and that any one of a great number of circuits could be used to satisfy the requirements.

A list of such systems is given in Table III with a short comment on the usefulness of each.

Since bias power will be a significant factor to consider, some representative circuits were compared with regard to the power consumed. These are listed in Table IV.

TABLE III.- POSSIBLE LOW G SYSTEMS

System	Sensing	Remark
Sine wave	Self or separate	Good
Pulse on demand	Separate	Much added complexity
Pulse width modulated	Separate	Much added complexity
Direct coupled square wave or sine wave	Separate	Needs a switch to couple to electrodes
Transformer coupled square wave	Separate	Good

TABLE IV.- POWER INPUT TO VARIOUS DEVICES FOR A LOW G SYSTEM

Device	Type	Power
μ A 702	Operational Amplifiers	29 mW (low bias)
μ A 709	Operational Amplifiers	30 mW (low bias)
Mc 1533	Operational Amplifiers	20 mW (low bias)
Mc 1433	Operational Amplifiers	20 mW (low bias)
DTμL	Logic	8.5 mW/gate 35 mW/flip-flop 37 mW/one shot 50 mW/clocked flip-flop
LPDTμL	Logic	1 mW/gate 4 mW/flip-flop
Series 54	Logic	10 mW/gate 40 mW/flip-flop
Series 54L	Logic	1 mW/gate 3.8 mW/flip-flop
FET	Transistor	20 mW up for high-frequency gain

The system should use as few parts as possible to keep the power requirements to a minimum.

Some typical usage in sine and square wave suspension systems is given in Table V for the low G loop.

TABLE V - SYSTEM POWER TABULATION

Qty	Description	Function	Power
3	a-c amplifier	Bridge buffer	60 mW
3	d-c amplifier	Amplifier	60 mW
6	d-c/a-c amplifier	Output	180 mW
1	Carrier oscillator		30 mW
3	Sensing oscillator	Position sensing	60 mW

The pulse-on-demand and pulse-width modulated systems need all the functions shown in Table V plus logic circuitry. This is not desirable in a minimum-power configuration. Also, the pulse-width modulated and direct-coupled, Low G circuits need high-voltage blocking switches which do not exist. Thus, the only systems which can be considered have sine or square wave transformer-coupled output. Note that a summation of power listed in Table V is 390 mW. This is a crude estimate; but, it gives some idea of the orders of magnitude involved.

Interaction with Supply Voltage Level

There are three distinct ways in which supply voltage level affects the power requirement of electric devices. They may be described in terms of the type of device:

- Resistive or linear devices
- Regulated devices
- Nonlinear devices

The first group includes all of the resistive biasing networks which are necessary in a system. Examples include base-bias networks, level adjusting networks, and fixed (supply level) devices driving resistive loads such as oscillators. The power in this case is proportional to V^2/R. Great savings can usually be made if the entire system is carefully engineered to operate at the lowest possible voltage level and highest possible

impedance level. Such aims are usually in contradiction with noise rejection requirements; therefore, a compromise must be made.

The second group includes those devices which have fixed or signal level voltage sources outputs. An equivalent circuit appears in Figure 42.

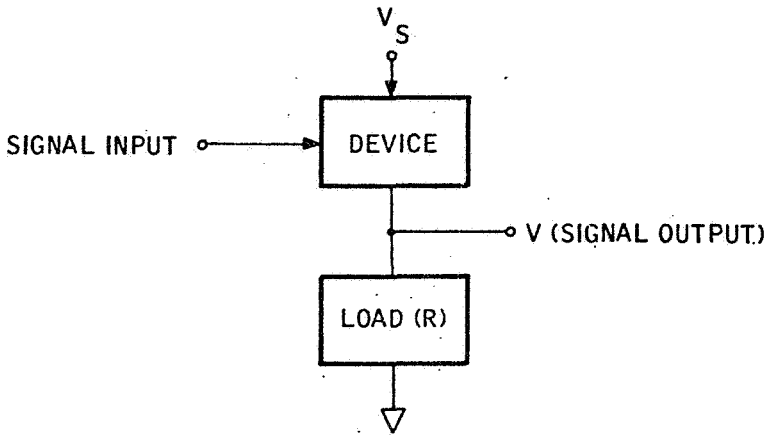

Figure 42. Regulated Device

The power input is determined by the supply voltage, V_S, and the load. The input current is V/R; the total input power is the product of this current and supply voltage:

$$P = \frac{V_S \cdot V}{R} = \frac{V_S}{V} \cdot \frac{V^2}{R} \qquad (108)$$

Thus, at a given level power is linear with supply voltage. The second part of (108) shows that the power supply to output voltage ratio can be thought of as if it were a device efficiency factor. At maximum output (V at its highest value), the highest possible efficiency is desirable; therefore, V_S should be as close to V as possible at that time (minimum drop across the device).

The third group includes amplifiers, shunt voltage regulators, magnetic circuits, and others of which current is not a linear function of voltage. The circuit for a shunt regulator is shown in Figure 43.

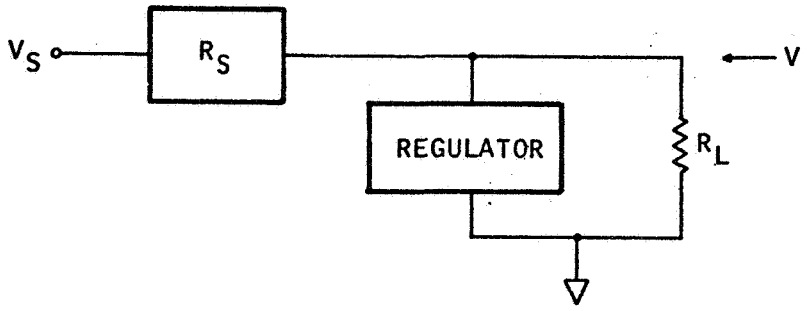

Figure 43. Shunt Regulation Circuit

The current input is determined by V_S, V, and R_S as follows:

$$P = I \cdot V_S = \frac{V_S - V}{R_S} \quad V_S$$

$$= \frac{V_S^2}{R_S} \cdot (1 - V/V_S) \tag{109}$$

Since the two parts of Equation (109) represent the product of a large number (V_S^2/R) and a (usually) small number ($1 - V/V_S$) at design center, a change of V_S changes the power input drastically. For instance, given $V/V_S = 0.9$ and a V_S increase of 10 percent, power input changes from $0.1\ V_S^2/R_S$, to $0.209\ V_S^2/R_S$, an increase of 109 percent. This clearly illustrates that shunt regulators must be designed and handled with the greatest of care. The power input to typical amplifiers increases in some nonlinear fashion with increase in supply voltage. Usually the internal resistive biasing makes this variation nearly square law; for instance, the μA 709 appears to be a nearly constant 12Ω resistor. The nonlinearities inherent in diode and transistor networks usually appear when they are being operated with a supply voltage near the level of the internal diode drops. Magnetic circuits display losses which are nonlinear functions of flux density. Calculations based on these concepts will be made during the design of the proposed suspension system.

Signal Level

Signal levels in the suspension follow the typical values given in Table VI. Note that if design is made for maximum levels (as it obviously must be), then signal level amplifiers must handle about the same voltages for all stages up to the output. This fact can be used to advantage in a dual circuit which is designed so that the signal level amplifiers operate from a low-voltage supply for maximum efficiency, and the output stages operate from a higher-level supply. The output stage then can simply be turned off during reduced power (low G) operation.

TABLE VI. - TYPICAL SIGNAL LEVELS

Device	Normal Output	Maximum Output
Carrier oscillator	1.5 V	1.5 V
Sensing oscillator	10 - 100 V	10 - 100 V
a-c amplifier	1 mV	5 V
d-c amplifier	0.2 V	5 V
Output amplifier	3-8 V	28-50 V

Network Requirements

Amplifiers used for dc and/or compensating amplifiers usually are associated with filter networks of some type or other. These networks typically use large capacitors to form the low-frequency breakpoints necessary for loop stability and static gain adjustment. The amplifiers must have sufficient current capacity to drive such networks without producing a clipped or distorted waveform. This problem may become significant in the (low power) low G loop where breakpoints will occur at 1 cps or lower. A second area of concern is in the power amplifiers used at the suspension output. Their speed of response (slew rate) is very important, and compensation networks cannot be allowed to compromise the risetime of large output voltage level changes which are necessary. Occasionally with amplifiers of this type, extra stages must be added to accomplish the stabilizing function linearly.

OUTPUT CIRCUIT LOSSES

Output losses are dominant in the high G mode of operation, usually amounting to approximately five watts even with bias or 1 G acceleration inputs. These losses may be split into two areas, excitation losses and circuit losses. The excitation losses are those associated with charging electrode capacitance. Circuit losses include the transformer and driver amplifier power input. In the last section of this report, a choice is made of the type circuit to be designed.

Sine Wave Excitation Losses

The sine wave carrier system may take either of two forms, depending on whether the output stage is current driven or voltage driven. Since tuning is necessary at the frequencies used, a direct transformation between the two output circuits can be made. The drive details will be considered separately, but only one output circuit will be analyzed. The parallel and series schematics are shown in Figure 44.

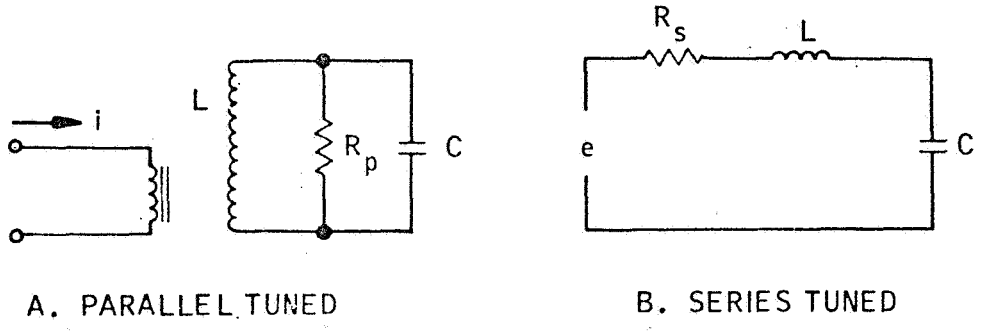

Figure 44. Basic Sine Wave Output Circuits

For the series circuit shown, the current may be related to output voltage through the capacitive impedance, X_c.

$$I = E_o \, j\omega \, C$$

where E_o is the voltage on an electrode.

$$P = |I|^2 R = E_o^2 \omega^2 C^2 \cdot R_s \tag{110}$$

The circuit loss may be computed in terms of its overall Q. The loss will appear in two places, driver circuit and coil. The source resistance is part of R_s, the equivalent series resistance, and need not be taken into account separately. Coil Q is up to 40 for the usual size and frequency range. The circuit Q then will be less than 40. For a series circuit,

$$Q = \frac{\omega L}{R_s} = \frac{1}{R_s \omega C} \tag{111}$$

Thus,

$$P = \frac{E_o^2 \omega C}{Q} \tag{112}$$

For the electrode structure used, C may be calculated as a function of gap, electrode area, and dielectric constant. The electrodes are chosen to best meet requirements for a particular gyro; but, for the usual case, maximum area is the overriding consideration. The maximum usable area is one-sixth the spherical area less the losses due to pickoff and pump ports and electrode insulating splits. The hexahedral (projected cube) electrode configuration will produce about 13 percent less than maximum area, resulting in a capacitance of (see also the expression for C_o in Section II)

$$C = \frac{0.104 \times 10^{-12} D^2}{d_o} \tag{113}$$

where D is nominal diameter and d_o is centered rotor electrode gap.

Substituting (113) into (112) gives power in terms of specified parameters.

$$P = \left(\frac{E_o^2}{d_o^2}\right)\frac{\omega}{Q} D^2 \cdot d\, 0.104 \times 10^{-12} \tag{114}$$

The power dissipated in this output circuit will be compared later with that of other circuits for comparable acceleration levels. It is therefore desirable to express the power in terms of gyro parameters to provide a basis c comparison. To take into account the effective force produced by the sine wave output, E_o^2 must be averaged. At maximum effort,

$$E_o^2 = V_{rms}^2 = V_m^2 \alpha$$

This equation and (45) are successively substituted into (114), yielding the relationship of Equation (115) where

$$P = \frac{G\ T\ \delta\ D^2\ d\ (0.104 \times 10^{-12})}{3.28 \times 10^{-12}} \quad \frac{2\pi f}{Q} \qquad (11$$

$$= 0.0317\ G\ T\ \delta\ D^2\ d\ \frac{2\pi f}{Q}$$

Care must be exercised in the use of this expression so that parameters are not specified which produce gradients above those tolerable. An example may be calculated using values which give a large G force at maximum gradient. The parameters are taken from the graph of Figure 8.

$T = 0.020$ in.
$G = 45$ G's
$\delta = 1.8$ gm/cm^3
$D = 1.5$ in.
$d = 0.002$ in.
$\alpha = 1/2$ (sine wave)
$V/d = 1000$ V/mil (peak)

The result is given in Equation (116) for f = 20 kc and Q = 20.

$$P = 2.31 \times 10^{-4}\ \frac{2\pi f}{Q}$$

$$= 0.231 \times 6.28 \qquad (116$$

$$= 1.45 \text{ (single electrode)}$$

Square Wave Excitation Losses

The square wave suspension/output circuit is comprised of a control voltage applied to a switch and transformer. The transformer steps the voltage level to the proper value and the electrode-rotor capacitance charges to this value. The entire drive system may be considered to be a switch and an equivalent resistor. The circuit is shown in Figure 45.

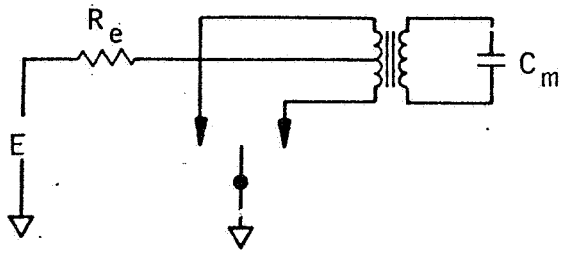

Figure 45. Basic Square Wave Output Circuit

The switch is operated each one-half cycle of the carrier frequency. The transformer driving voltage E may change during one cycle, but here it is assumed to be a constant. Current flows each half cycle charging the capacitor, C_e, to positive and negative maximum voltage. The current has the form of a single time constant exponential with maximum value determined by 2E and R.

$$I = \frac{2E}{R} e^{-t/RC} \tag{117}$$

where R and C are returned to the same transformer side. The power dissipated during each charge cycle is

$$P = I^2R = \left(\frac{2E}{R}\right)^2 R e^{-2t/RC} \tag{118}$$

Total energy is

$$W = \lim \int_0^t I^2 R \, d t \Big]_{t \to \infty}$$

Substituting for current in this expression gives

$$W = \frac{4E^2}{R} \int_0^t e^{-2t/RC}\, dt \Big]_{t \to \infty}$$

$$= \frac{4E^2 C}{2} \left| 1 - e^{-2\,t/RC} \right|_{t \to \infty} \qquad (11$$

$$= 4 \left| \frac{E^2 C}{2} \right| \frac{\text{watt-seconds}}{\text{pulse}}$$

The average power dissipated is the product of this energy per pulse and the number of pulses per second (which is twice the carrier frequency):

$$P = 8 \left| \frac{E^2 C}{2} \right| f \qquad (120$$

This expression is most useful if it is put in terms of gyro parameters. The computations are made for actual hexahedral structure by setting $E = V_m$ and substituting equations for V_m and C from (45) and (113) into (120).

The result is power dissipated as a function of gyro parameters.

$$P_{sq} = \frac{4\, G\, \delta\, T\, D^2\, d\, f\, (104 \times 10^{-12})}{\alpha \qquad 3.28 \times 10^{-12}} \qquad (121$$

$$= 0.0317\, G\, \delta\, T\, D^2\, d \left| \frac{4f}{\alpha} \right|$$

An additional power loss is incurred if the current must flow from a power supply (V_s) that is at a voltage higher than E. For this case, the power used is the product of this (assumed fixed) drop and the current pulses. The power, as a function of time, is

$$P(t) = (V_s - E) \cdot I(t) = (V_s - E) \cdot \frac{2E\, e^{-t/RC}}{R} \qquad (122)$$

from (117). The energy consumed is

$$W = \frac{(V_s - E)\,2E}{R} \int_0^t e^{-t/RC}\,dt \Bigg]_{t \to \infty} \quad \frac{\text{watt-sec}}{\text{pulse}}$$

$$= 2E\,(V_s - E)\,C$$

The power loss is the product of the energy loss per pulse and the number of pulses per second.

$$P = 2\,f\,W = 4\,E\,(V_s - E)\,Cf$$

For clarification, this equation can be written in a different form:

$$P = 8\left[\left(\frac{V_s}{E}\right) \cdot \frac{E^2}{2} - \frac{E^2}{2}\right] C \cdot f$$

Thus, the power already computed is increased by the ratio of V_s to E. Equation (121) is rewritten to reflect this increase.

$$P_{sq} = 0.0317\,G\,\delta\,T\,D^2\,d\,\frac{V_s}{E}\,\frac{4f}{\alpha} \tag{123}$$

This computation is made of power dissipated in the device; however, since all input energy is consumed, this is also the input power. This may be checked by calculating power input to the device using I and V as the input variables.

Using this equation and assuming an efficiency (α) of 0.90, f = 1500 cps with the variables used in (116) results in Equation (124).

$$P = 2.31 \times 10^{-4} \cdot \frac{4f}{\alpha}$$

$$= 1.54 \text{ W direct charging dissipation} \tag{124}$$

Sine Wave Circuit Losses

The sine wave output stage consists of transistors driving a capacitive load nominally tuned by an output transformer or coil. The load is not static, but changes with rotor displacement. These changes mistune the circuit and affect efficiency, necessary input voltage, and overall input power. In this paragraph an expression is derived for circuit efficiency under various conditions for the series and parallel circuits. Also, the size and loss dependencies of the output transformer are explored. The previous example is continued and solved with the new cases presented.

Class A stages need not be considered. Nearly all conceivable systems will have an output transformer that would not tolerate the unbalance or the large dissipation. Class B stages are usually used with the output transistors biased just to cutoff. The power dissipated in the output transistors may be calculated:

$$P_d = 2f \int_0^{\frac{\pi}{\omega}} I_m \sin \omega t \left[V_s - V_m \sin (\omega t + \phi) \right] dt$$

$$= \frac{2f}{\omega} \left(- V_s I_m \cos \omega t \Big]_0^{\frac{\pi}{\omega}} - I_m V_m \left\{ \frac{\cos \phi}{2} \omega t \right] \Big]_0^{\frac{\pi}{\omega}} \right. \tag{125}$$

$$\left. - \frac{\sin \omega t \cos(\omega t + \phi)}{2} \Big]_0^{\frac{\pi}{\omega}} \right\} \Bigg)$$

$$P_d = \frac{1}{\pi} \left(2 V_s I_m - \frac{I_m V_m \pi \cos \phi}{2} \right)$$

Efficiency with a centered rotor ($\phi = 0$) and the collector voltage swing (V_m) just at the supply voltage level (V_s) may be calculated from

$$\eta = \left.\frac{P_o}{P_d + P_o}\right]_{\substack{V_m = V_s \\ \phi = 0}}$$

$$= \frac{\frac{V_m I_m}{2}}{\frac{V_m I_m}{\pi}\left(2 - \frac{\pi}{2}\right) + \frac{V_m I_m}{2}}$$

$= \frac{\pi}{4}$ or 78 percent, the usual ideal Class B output efficiency.

For other values of output voltage with rotor centered, the equation reduces to

$$\eta = \frac{\frac{V_m I_m}{2}}{\frac{2 V_s I_m}{\pi} - \frac{I_m V_m}{2} + \frac{I_m V_m}{2}} \qquad (126)$$

$$= \frac{\pi}{4}\frac{V_m}{V_s}$$

Thus, the efficiency drops linearly as output voltage drops. Rotor miscentering produces phase shift and increases the voltage necessary at the input to a series-tuned circuit. Since the output transistors are current controlled (the collector voltage has little to do with current), driving a reactive load means that the collector voltage shifts phase relative to the current, depending only on load. In Equation (125) ϕ is now nonzero, and the efficiency is reduced. The expected voltage excursion can be calculated from

$$V_o = \frac{V_{in}\left(\frac{1}{sC}\right)}{\frac{1}{sC} + sL + R}$$

for the series case. If we assume that the same output voltage must be produced for either case, then

$$V_o = \frac{V_{ino}}{RS\,C_o} = jQ\,V_{ino}$$

where V_{ino} is the centered, series-circuit input voltage. V_{inx} is the input voltage with rotor displace, related to V_{ino} by

$$\frac{V_{ino}}{RS\,C_o} = \frac{V_{in\chi}}{Rs\,C_x + 1 + s^2\,LC_x}$$

and

$$V_{inx} = \frac{\left(Rs\,C_o\,\frac{C_x}{C_o} + 1 + s^2\,L\,C_o\,\frac{C_x}{C_o}\right)}{RS\,C_o}\,V_{ino}$$

$$= \frac{j\,\frac{C_x}{C_o} + Q\left(1 - \frac{C_x}{C_o}\right)}{j}\,V_{ino} \qquad (127)$$

$$V_{inx} = \left[\frac{C_x}{C_o} - jQ\left(1 - \frac{C_x}{C_o}\right)\right]V_{ino}$$

Now the relationship between C_x and C_o is a function of the distance off center, x.

$$C_x = \frac{C_o}{1 + \frac{K_1 x}{d}} \tag{128}$$

so that

$$V_{inx} = \frac{V_{ino} \left(1 - j Q \frac{K_1 x}{d}\right)}{1 + \frac{K_1 x}{d}} \tag{129}$$

For use in the power expression, the angle ϕ may be evaluated as a function of displacement.

$$\phi = \tan^{-1} \frac{Q K_1 x}{d} \tag{130}$$

The previous example (116) may be recalculated for the case where the rotor suspension has a stiffness of 10-percent gap at full acceleration input. The input voltage centered with maximum output is

$$V_{ino} = \frac{V_{out}}{Q} = \frac{1000 \times 2}{40}$$

$$= 25 \text{ V}$$

This must rise as the output capacitance changes to V_{inx}.

$$V_{inx} = \frac{25\ (1 - j\ 40 \times 0.83 \times 0.1}{1 + (0.83 \times 0.1)}$$

$$= \frac{25\ (1 - j\ 3.32)}{1.083}$$

$$= 80\ V$$

Now if the supply voltage is fixed and must accomodate the 80V level efficier when the rotor is center is decreased. Assuming $V_s = V_m$ at the high level phase angle and then efficiency can be calculated.

The general expression for efficiency may be found from Equation (126).

$$\eta = \frac{\frac{V_m I_m \cos\phi}{2}}{\frac{1}{\pi}\left(2\ V_s\ I_m - \frac{V_m I_m \pi \cos\phi}{2} + \frac{V_m I_m \pi \cos\phi}{2}\right)} \qquad (131$$

$$\eta = \frac{\pi}{4}\frac{V_m}{V_s}\cos\phi$$

The efficiency may be calculated for the following set of parameters:

$$\phi = \tan^{-1} 3.32$$

$$= 73.2°$$

$$\cos\phi = 0.289$$

$\eta = 22.7\%$, full "on" rotor displaced 10 percent.

For the centered rotor, $\cos\phi = 1$; however, output current now is flowing through a large drop which reduces efficiency.

$$V_m/V_s = \frac{1}{3.32}\ ,$$

$\eta = 26\%$

The single electrode power (1.45 watts) given in (116) is multiplied by $\frac{1}{0.227}$ for the off-center case, resulting in 6.37 watts input power.

The parallel-tuned current driver operates similarly to the series-tuned circuit except that feedback is used to ensure that the output current is maintained independent of output voltage. Current is controlled by the suspension system displacement sensor and amplifying system. The schematic of this circuit is shown in Figure 44A. From the diagram, current is

$$I_o(s) = \frac{I_{in} Z}{X_c} = I_{in} Z(s) sC_x \tag{132}$$

where

$$Z(s) = \frac{sL}{\frac{sL}{R} + 1 + s^2 LC_x}$$

For the tuned circuit,

$$s^2 LC_o = -1, \quad \frac{R}{\omega L} = Q$$

Therefore,

$$I_o = \frac{-I_{in} \frac{C_x}{C_o}}{j/Q + 1 - \frac{C_x}{C_o}}$$

$$I_{in} = -j \frac{I_o}{Q} \left[1 - jQ \left(1 - \frac{C_x}{C_o}\right)\right] \frac{C_o}{C_x}$$

As a function of displacement,

$$I_{ino} = -j\frac{I_o}{Q}$$

$$I_{inx} = -j\frac{I_o}{Q}\left(1+\frac{K_1 x}{d}\right)\left(1 - jQ\,\frac{\frac{K_1 x}{d}}{1+\frac{K_1 x}{d}}\right) \tag{132}$$

This is virtually the same phase shift and position sensitivity as was produced for the series resonant circuit. The efficiency and power dissipation calculations are similar also.

Note, however, that if the parallel output circuit is driven by a high-impedance source and high turns ratio tuned transformer, the supply voltage need only be as high as the maximum voltage and turns ratio would indicate. This makes the parallel circuit more desirable since the efficiency is higher for average use. Consequently, actual power used is lower.

At this point, it is useful to consider the components that must be used to mechanize the circuit. The sine wave systems necessarily use an output transformer to step up the usual supply voltage (20 to 50V) to the kilovolt suspension output level.

A series drive would use a low-ratio transformer and tuning inductor or a high-ratio transformer with voltage drive to produce the desired characteristic. Parallel (current feed) outputs use a high-ratio transformer and current drive. Either type must use a magnetically stable core material with fairly high permeability. Molybdenium permalloy temperature-stabilized cores are usually used.

Core loss may be determined from an equation developed by Legg[2]. He showed that the loss could be divided into three components and used the form

$$R/\mu L = aB_m f + cf + ef^2 \tag{133}$$

---

[2] Legg, V. C.: Magnetic Measurements at Low Flux Densities Using the A-C Bridge. Bell System Technical Journal. Vol. 15, Jan. 1936, pp. 39-62.

where

a = hysteresis loss coefficient

B_m = maximum flux density

c = residual loss

e = eddy current loss coefficnet

f = exciting frequency

This may be put into a more familiar form:

$$\frac{2\pi}{Q} = (aB_m + c + ef)\,\mu$$

$$Q = \frac{2\pi}{(a\,B_m + c + e\,f)\mu} \tag{134}$$

B_m is directly proportional to the coil voltage and must not exceed about 3000 gauss with this material. This level is determined by effective inductance changing as the iron saturates, which causes circuit mistuning.

One can use (134) to calculate Q_{core}. It is worth-while to consider an example using values usually encountered to indicate the realizable magnitude of core Q. Assuming a 20 kc exciting frequency, scaling by B_m, and using constants typical of molybdenum permalloy (μ = 125) results in core Q of

$$Q_{core} = 125\left[\frac{2\pi}{1.6 \times 10^{-6} B_m + 30 \times 10^{-6} + 19 \times 10^{-9}(2 \times 10^4)}\right]$$

$$= \frac{2\pi}{2 \times 10^{-4}(B_m + 18.7 + 237)} \tag{135}$$

(Constants used are given in Arnold Engineering Bulletin PC-104C.) For B_m = 0 (typical of "Q Meter" measurements),

$$Q_{core} = 123$$

For an actual coil, the wire used will also produce loss which is not a strong function of frequency in the range of operation generally associated with ESVG output circuits. At 20 kc, a Q of 40 will generally be measured for these coils. This means that, for the coil, there is a fourth additive factor of 530 in the denominator of (134) which results in

$$Q_{coil} = \frac{\pi \times 10^4}{(B_m + 785)} \tag{136}$$

Thus, coil Q is 40 at low values of flux density and decreases to 8.3 at $B_m = 3000$ gauss.

It is instructive to derive equations relating core parameters to gyro mechanical parameters. This allows scaling to be done when a new system is considered and orders the impact of parametric changes. For the condition of initial centered resonance, the necessary core parameters may be found using capacitance and frequency as scaling variables. The core inductance is given by

$$L = L_o N^2 (10^{-6}) \tag{137}$$

L_o is the "inductance constant" which is the inductance in henries of the core with a 1000-turn winding and is usually a specified parameter. The mean core circumference may be denoted by ℓ and area by A_c. Then the inductance constant is described by

$$L_o = \mu A_c / \ell \tag{138}$$

The core inductance must be such that tuning is accomplished. Thus,

$$L = \frac{1}{4 \pi^2 f_o^2 C}$$

where f_o is the operating frequency of the output circuit and C is the capacitance. From this, the relationship between turns and frequency for a given core may be described.

Another important parameter is flux density. As the core approaches saturation, the inductance decreases due to nonlinearities of the core permeability characteristic. This causes the circuit to mistune and become less efficient.

The flux density is computed using the induced voltage of Equation (139).

$$B = \frac{V_p}{N f_o A_c (4.051 \times 10^{-4})} \tag{139}$$

The coil parameters can now be calculated. By substituting the tuning condition and Equation (113) into Equation (137), the number of coil turns is obtained in terms of gyro parameters and $L_o \alpha$

$$N = \frac{10^9}{2\pi f_o D} \sqrt{\frac{d}{0.104\ L_o}} \tag{140}$$

The substitution of Equation (140) into (139) yields

$$B = \sqrt{\frac{0.104\ L_o}{d}} \quad \frac{2\pi D V_p}{A_c (4.051 \times 10^5)} \tag{141}$$

Note that B is a function of neither f_o nor N. Finally, the substitution of Equation (138) into (141) for L_o yields

$$B = 8.57 \times 10^{-7} D \frac{V_p}{d} \sqrt{\frac{\mu d}{A_c \ell}} \tag{142}$$

Generally, the maximum flux density is determined from the curve of flux density versus magnetizing force for the core material. Consequently, it is instructive to compute the core dimensions in terms of gyro parameters:

$$\frac{A\ell}{\mu} = \frac{\pi}{4} \cdot \frac{h}{\mu} \frac{D_2^2 - D_1^2}{} = 7.34 \times 10^{-13} \frac{d}{B^2} D^2 \left(\frac{V_p}{d}\right)^2 \tag{143}$$

where h is core height, and D_2 and D_1 are its outside and inside diameters, respectively. Since the gradient and flux density are material limited, the gyro gap and diameter loosely determine the core dimensions. Small core sizes result in larger flux densities; larger cores may be simply too large for the intended application.

Up to this point there was no necessity for selecting an operating frequency for the output circuit. However, to calculate coil type and charging power, a specific frequency must be chosen. The tuned output circuit produces a lag at $f_1 = \frac{f_o}{2Q}$. To realize sufficient bandwidth, the parallel current driver removes this pole by means of feedback around the output amplifier. In a series tuned circuit, the pole must be cancelled with lead compensation. Both power and output bandwidth depend on this ratio. To produce the assumed bandwidth of 1 kc, 20 kc is selected as the frequency for sine wave operation. From (136) the coil Q at 20 kc is given by

$$Q = \frac{\pi \times 10^4}{B_m + 785}$$

Therefore,

Q_f = Q at full output (B_m = 1250 gauss) is 15.4

Q_b = Q at bias ($V = V_m/2, B_m$ = 625 gauss) is 22.3

The series output circuit example (page) may be expanded to include this variation in Q_o. The effect will be one of less phase shift (better driven efficiency) but greater coil loss. For a maximum effort linear servo (opposite electrode voltage is zero), the bias output voltage is one-half the maximum level. If this maximum core field works out to 2500 gauss, then Q is 9.56 at maximum effort and 15.4 at bias level.

The previous example can be reworked using these values.

Choosing the phase angle at a rotor displacement of 10 percent of the gap,

$$\phi_m = \tan^{-1}(9.56 \times 0.83 \times 0.1)$$

$$= 38.4°$$

$$\frac{V_{in_x}}{V_{in_o}} = \frac{1 - j \cdot 7094}{1 + 0.083} = 1.18$$

$$P_{bias} = \frac{4.61 \times 10^{-4}}{4} \frac{2\pi f}{Q} = 0.94 \text{ watt}$$

$$\eta = \frac{\pi}{4} \frac{1}{1.18} = 66.5\%$$

Power input = 1.41 watts per electrode bias.

At the maximum output level, the gradient on one electrode rises to twice the bias level and goes to zero on the other.

$$P_{max} = \frac{4.61 \times 10^{-4} \times 2\pi \times 2 \times 10^{4}}{9.56}$$

$$= 6.1 \text{ watts per electrode max output}$$

$$\eta = \frac{\pi}{4} \cos 38.4^{\circ}$$

$$= 61.5\%$$

Therefore, power input = 9.9 watts.

Total power consumption in the output stages under this high G condition will be 8.5 watts bias and 15.5 watts at maximum G level input.

Note from Equation (112) that power is linear with output capacitance. The calculations have been made assuming that the rotor-electrode capacitance is the only capacitance on the output circuit. Long, shielded electrode leads, tight transformer shielding, and excessive tuning capacitance all add large amounts of load to the output circuit. This must be taken into account when the power is calculated for a given design.

Square Wave Circuit Losses

Square wave output circuit losses occur in the transformer and in the switching transistors which are used. The transformer loss is quite difficult to assess, since judgments in the selection of material, flux density, and size affect the calculation. In general, there are three calculable areas of loss:

- Core loss
- Copper loss
- Square wave excess loss

The last is actually a function of the first two, but may be separated for clarity. These effects will be estimated and transformer parameters determined.

For laminated iron in the frequency range where eddy current shielding is not significant, the equation for core loss is[3]

$$L = K_h f B^{1.6} + K_e t^2 f^2 B^2 \qquad (144)$$

---

[3] Lawrence and Richards: Principles of AC Machinery. McGraw-Hill Book Co., Inc., 1953, p. 68.

where

B = core flux density

f = frequency

t = lamination thickness

The loss coefficients, K_h and K_e, are computed from magnetic properties curves produced by the manufacturers: "Arnold" curves in this mid-frequency region produce

$$K_h = 2.4 \times 10^{-4}$$

$$K_e = 4.8 \times 10^{-3}$$

for two-mil iron. These values predict fairly accurately (5 percent level) the loss at frequencies in the 1-to 30-kc range for Arnold "C" cores.

However, a form more useful for the prediction of loss with a bandwidth-limited square wave is needed. A desirable form would be a modification of Equation (144) to account for the effect of the harmonic content of the square waveform. A Fourier series may be used to represent the sum of harmonics which will produce the square wave.

For a square wave of amplitude E, the voltage function is given by

$$V(t) = \frac{4E}{\pi} \sum_{n=1}^{\infty} \frac{1}{2n-1} (-1)^{n-1} \cos (2n-1)\, \omega t \qquad (145)$$

For simplicity, substitute

$$V_p = \frac{4E}{\pi}$$

and sum the series in a different manner. Since the loss for each harmonic is additive and does not depend on phase, the simple series

$$V(t) = V_p \sum_n \frac{\cos n\omega t}{n}, \text{ for n an odd integer}$$

will suffice.

For a bandwidth-limited case, the voltage in the n^{th} harmonic is reduced from its normal value by the weighting function

$$V_n = \frac{V_{pn}}{\sqrt{1 + \left(\frac{f_n}{f_o}\right)^2}} \tag{146}$$

where f_o is the (assumed) transformer bandwidth limit and V_{pn} is the normal voltage at that harmonic. Generally, f_o is about 25 times the design frequency f_1. The frequency of the n^{th} harmonic is f_n and can be expressed in terms of f_1:

$$f_n = n f_1$$

Substitution into the series gives

$$V(t) = V_p \sum_{n=1}^{\infty} \frac{1}{\sqrt{1 + \left(\frac{n}{25}\right)^2}} \quad \frac{\cos n \omega t}{n} \quad \text{for n an odd integer}$$

The core loss is proportional to the flux density in the laminations and the frequency by Equation (144). The loss has two components, hysteresis and eddy current. Consider first the hysteresis loss:

$$L_h = K_h B^{1.6} f_n \tag{147}$$

From the equation for induced voltage in a coil,

$$E = -N \frac{d\phi}{dt} \tag{148}$$

the flux density B can be determined.

$$B_n = \frac{V_n}{\sqrt{2}\ N\ f_n\ A_c\ S\ (2.865 \times 10^{-4})} \tag{149}$$

where

N = number of turns on the coil

A_c = cross-section area of the iron core (in.^{2})

S = stacking factor of the core

B_n = peak flux density at frequency f_n (K-gauss)

V_n = peak voltage at frequency f_n

$$L_{hn} = K_h \left(\frac{V_n \, 0.707}{N A_c S (2.865 \cdot 10^{-4})} \right)^{1.6} \frac{f_n}{f_n^{1.6}} \text{ W/lb} \tag{150}$$

Let f_p be the fundamental square wave frequency. Then

$$f_n = n f_p \tag{151}$$

Let

$$V_n = V_p \frac{1}{\sqrt{1 + \left(\frac{n}{25}\right)^2} \cdot n} \quad \text{for n odd integer} \tag{152}$$

Substituting Equation (151) and Equation (152) into Equation (150) yields the equation for total hysteresis loss:

$$L_h = K_h \sum_n \left(\frac{V_p}{N A_c S \, (4.051 \times 10^{-4})} \right)^{1.6} \frac{1}{n^{1.6} \left[\sqrt{1 + (\frac{n}{25})^2} \right]^{1.6}} \frac{n \, f_p}{n^{1.6} f_p^{1.6}}$$

$$L_h = K_h \left(\sum_n \frac{f_p}{n^{2.2} \left[1 + (\frac{n}{25})^2 \right]^{0.8}} \right) \left(\frac{V_p}{N A_c S \, f_p (4.051 \times 10^{-4})} \right)^{1.6}$$

$$= K_h B_p^{1.6} f_p \sum_n \frac{1}{n^{2.2} \left[\left(1 + \frac{n^2}{625} \right) \right]^{0.8}} \tag{152}$$

where B_p is the core flux density associated with V_p and f_p.

$$L_h = K_h \cdot 1.151 \, B_p^{1.6} f_p \tag{153}$$

The eddy current loss is

$$L_e = K_e t^2 B^2 f^2 \tag{154}$$

Substitution of Equation (149) into Equation (154) yields the eddy current loss at each frequency.

$$L_{en} = K_e t^2 \left(\frac{V_n}{N A_c f_n S (4.051 \times 10^{-4})} \right)^2 f_n^2 \qquad (155)$$

Again, a substitution for V_n is made using Equation (152), and the terms are summed over n. This yields the equation for total eddy current loss:

$$L_e = K_e t^2 f_p^2 B_p^2 \sum_n \frac{1}{n^2 \left(1 + \frac{n^2}{625}\right)} \qquad (156)$$

Each term above the twenty-third harmonic is < 0.001; the sum to that point is 1.204, so that

$$L_e = K_e t^2 f_p^2 B_p^2 (1.204) \qquad (157)$$

Thus, total loss from a square wave of frequency f_p is the sum of Equation (153) and Equation (157):

$$L = K_h f_p B_p^{1.6} 1.151 + K_e t^2 f_p^2 B_p^2 1.204 \qquad (158)$$

In some manufacturers' catalogs, the core loss is plotted as a function of frequency and flux density. These equations were compared with the curves for several materials and thicknesses. Results obtained are fairly good when care is taken to avoid regions of incipient core saturation and thicknesses where eddy current shielding becomes a prominent factor. The most important result of the investigation is to show that loss is increased about 20 percent over the loss calculated for the base frequency and flux density when square wave excitation is used. Various types of material may be compared generally by looking at core loss at various flux densities for 0.002-inch iron (Table(VII).

TABLE VII.- COMPARISON OF CORE MATERIAL LOSSES

Material	Max flux (K gauss)	Loss at 1500 cps (watts/lb)	Loss at 1500 cps, 6K gauss (watt/lb)
Silicon steel	10	23.5	10
50-percent nickel	8	4.05	2.5
80-percent nickel	6	1.02	1.02

A second necessary input to the selection process is frequency. The switching frequency is determined by consideration of several factors:

- Charge-induced vibration
- Rotor angular speed
- Bandwidth

The square wave system includes a modulator at its output, and, since the switching frequency is relatively low, interactions occur between the switching inputs and normal rotor motion. Unbalances in applied voltage couple with rotor residual voltage to produce cross-axis motion in phase with the switch drive. This condition necessitates phase control in the suspension loop which is best done outside the servo bandwidth.

Rotor spin speed will be in the 1000- to 1200-cps range, and this too could couple with the switching frequency by means of the radial unbalance. Cross-axis force due to radial unbalance and rotor voltage may reach one- to two-percent of the applied force. The switching frequency must be high enough to make this motion of a negligible magnitude so that net gyro drift is not produced. This limit is in the range of one percent of the gap or 20μ inches. Whatever transformer is used, a bandwidth limit exists which is proportional to its design frequency. For transformers in this class, the factor of proportionality is 20 to 25.

A bandwidth of 1 kc is sufficient for most missions. The circuit inherent lags then must be in the 20-kc range. A switching frequency which will meet all these considerations is about 1500 cps. This is the frequency which will be assumed in the design of the circuit.

This frequency is used in the comparison given in Table VII.

The next consideration is the type of transformer to be used. Since the transformer is driven from an external source, a certain amount of unbalance current must be tolerated. A good figure for the unbalance would be one to five percent of the rms current or in the range of one to five milliamperes in the transformer primary. Maximum permeability would be that amount which allows the offset to become approximately 10 percent of maximum flex density. For a closed-magnetic circuit, the magnetomotive force (H) can be expressed as a function of the turns (N), current (I), and length of the circuit (ℓ). Thus,

$$B = \mu H = \frac{0.4\,\pi\,NI\,\mu}{\ell} \tag{159}$$

assuming that $B_{max} = 600$ gauss; $\ell = 10$ cm, n = 100 turns, and I = 5 mA; the upper bound on effective core permeability μ_{max} is

$$\mu_{max} = \frac{(600)\,(10)}{(5 \times 10^{-3})\,40\pi} = 0.9560 \times 10^{4} \tag{160}$$

These calculations are approximate since we have not designed the transformer; however, they are meant to point out the problem which might exist in this area. Torroidal shapes with 50 or 80 percent nickel-iron display permeabilities ranging from 15 000 to 75 000. This fact prevents us from using a torroid or other closed-core shape.

The other shapes which may be used are "C" core (prestacked) and stacked laminations of the "E-I" variety. The "C" cores can be purchased with silicon iron in thicknesses down to one mil. The stacking process is a manual operation and requires a minimum thickness of six mils. The best usable materials are compared in Table VIII.

TABLE VIII. - COMPARISON OF POWER LOSSES FOR VARIOUS CORE MATERIALS

Flux level (K gauss)	Material	Loss (watts/lb)
10	Silectron 2 mil	24
10	Silectron 4 mil	25
6	Silectron 2 mil	9.2
6	Silectron 4 mil	10
6	48 Alloy 6 mil	4.6

A factor to be considered in designing the transformer is the copper loss and usable wire size for the transformer. For cases where one or the other winding carries very small currents, it is not always possible to use small enough wire, and one winding becomes disproportionately large, thus increasing the overall transformer size. The rms current in the transformer winding may be calculated from Equation (117).

$$I = \frac{2E}{R} e^{-t/RC}$$

$$\left(I_{rms}\right)^2 = \frac{1}{T}\int_0^T \frac{4E^2}{R^2} e^{-2t/RC} dt \qquad (161)$$

$$\frac{1}{T} \frac{2E^2 C}{R^2} \left(1 - e^{-2T/RC}\right)$$

With the assumption of a 93-percent efficient waveform,

$$T = 20\ RC = \frac{1}{2f} \qquad (162)$$

so that

$$R = \frac{1}{40\ Cf} \tag{163}$$

Substituting these relations into Equation (161) yields

$$(I_{rms})^2 = 160\ f^2 E^2 C^2 \tag{164}$$

Equation (113) is substituted into the square root of Equation (164) to give

$$I_{rms} = (1.315 \times 10^{-12}) \frac{E}{d} f\ D^2 \tag{165}$$

For the gyro parameters which have been assumed,

$$I_{rms} = 4.55\ mA \tag{166}$$

for a single winding.

To maintain voltage balance, the winding must be split, but these constants remain valid; therefore, the current in each secondary winding is one-half of the calculated current, or 2.27 mA. A suitable wire current density factor for this class of transformer (air cooled, potted winding, for intermittent use) is 750 circular mils per ampere. The wire area required for 2.27 mA in the secondary would therefore be 1.7 circular mils. This corresponds to approximately No. 48 wire which is virtually impossible to wind in an assembly of this type and size. For a layer winding, No. 40 wire is as small as can be used. Thus, the transformer size will be determined mainly by the window area used by these secondary windings.

From the induction Equation (48) assuming a 93-percent effective square waveform, one finds that

$$E/N = (2.585 \times 10^{-4})\ B_m\ f\ A_c\ S \tag{167}$$

From this equation, an expression for the cross-section area turns product can be derived. The maximum allowable rotor displacement is 15 percent of gap; the maximum output voltage required is

$$E_{max} = 1.15\ (1000\ V/mil \cdot d) = 2300\ V$$

For transformers of this type, the stacking factor S is approximately 0.90. Where B_m = 6 K gauss and f = 1.5 kc, the cross-section area turns product of this winding is

$$N A_c = \frac{E_{max}}{(2.585 \times 10^{-4}) B_m f S} \qquad (168)$$

$$= 1100 \text{ in.}^2 \text{ - Turns}$$

A second important factor is the ratio of window area to equivalent turns. The window area (A_w) is the sum of secondary and primary areas multiplied by an area efficiency factor $1/\gamma$. Let A_1 and A_2 denote the wire areas of the primary and secondary, respectively, and M the turns ratio:

$$A_w = (A_1 \cdot N_p + A_2 N_s)^2 \gamma \qquad (169)$$

where N_s is the number of turns of each secondary winding and N_p is the number of turns of each primary winding. Like the secondary, the primary is also split. Assuming the secondary to be wound with No. 40 wire,

$$A_2 = 12.5 \times 10^{-6} \text{ in.}^2/\text{turn}$$

The turns ratio is determined mainly by capability of the driving circuit. If a low-voltage switch is used, it must carry large peak currents at maximum output. The primary peak current (I_{pp}) may be expressed in terms of the peak secondary current [the upper bound of Equation (161)] and the turns ratio:

$$I_{pp} = \frac{2EM}{R} = 80 \text{ E C f M}$$

Here R has been removed by substituting Equation (163). In the square wave system, the electrodes are split; the split condition is accounted for in the substitution of Equation (113) to yield

$$I_{pp} = (0.416 \times 10^{-11}) \frac{E}{d} f D^2 M$$

For the gyro parameters selected in this study,

$$I_{pp} = 14.1 \text{ M mA}$$

The selection of a switch and the turns ratio may be made by referring to Table IX.

TABLE IX. AVAILABLE SWITCHING TRANSISTORS FOR VARIOUS TURNS RATIOS

M	V_p (volts)	$2V_p$ (volts)	I_{pp} (amp)	Typical Transistors
50	46.0	92.0	0.705	2N5074, 75, 76, 77
55	41.8	83.6	0.775	2N5074, 75, 76, 77
60	38.4	76.8	0.845	2N3057, 2N3020, 2N2891
65	35.4	70.8	0.916	2N4897, 2N3421, 2N3837
70	32.9	65.8	0.986	

It is seen that for M = 55 or less, the choice of switching transistors is limited. A turns ratio of about 65:1 will be assumed in all systems to take advantage of the smaller size transistors available in this range. The primary wire area, A_1, may now be calculated:

$$A_1 = 750 \text{ circular mil/ampere } (I_{rms})_p$$

where $(I_{rms})_p$ is the rms current of the primary winding. This can be related to the rms current in the secondary through the turns ratio:

$$(I_{rms})_p = M \cdot 2.27 \text{ mA} = 146 \text{ mA}$$

The required primary wire area is

$$A_1 = 110 \text{ circular mils} = 86.9 \times 10^{-6} \text{ in.}^2/\text{turn} \qquad (170)$$

The primary can be wound with No. 31 wire which is actually 92×10^{-6} in.^{2}/turn. The window area can now be expressed as a function of $N_s = M N_p$:

$$A_w = \left(N_s (12.5 \times 10^{-6} + \frac{92 \times 10^{-6}}{65} \frac{2}{\gamma} \right)$$

$$= 2.78 \times 10^{-5} \frac{N_s}{\gamma} \text{ in.}^2 \text{ turns}$$

The efficiency factor for this type of transformer is about 35 percent. Thus,

$$A_w = 7.95 \times 10^{-5} N_s \text{ in.}^2 \text{ turns} \quad (171)$$

The core area-window area product of the transformer can now be calculated from Equations (169) and (171):

$$A_c A_w = 0.0874 \text{ in.}^4$$

Table X lists the characteristics of some transformer cores which could be used. Two AH-126 or AH-123 "C" cores, or E-I 625 laminations can be used to produce the core geometry shown in Figure 46. If a single "C" core is considered (Figure 47), an AH-140 or AL-13 core is suitable. Note that this shape is inefficient in utilizing available space. The use of less iron produces less core loss, but results in higher leakage reactance which limits the risetime of the output voltage. It is also more difficult to wind, since 60 percent more turns are necessary than with the two-core or E-I designs. This design, therefore, is one which should be avoided.

The characteristics of an example transformer built on the E-I 625 or (2) AL-123 cores are summarized in Table XI.

TABLE X.- TRANSFORMER CORE CHARACTERISTICS

Type	Two AL-123, E-I625	Two AH-126	AH-140 or AL-13
Geometry	(Figure 46)	(Figure 46)	"C" core (Figure 47)
Length (L)	1.75 in.	2.00 in.	1.875 in.
Width (W)	1.25 in.	1.125 in.	1.875 in.
Height (H)	1.50 in.	1.625 in.	1.50 in.
Volume	3.29 in.^3	3.65 in.^3	3.97 in.^3
Core weight	0.220 lb	0.220 lb	0.150 lb
Core area	0.250 in.^2	0.234 in.^2	0.156 in.^2
Window area	0.375 in.^2	0.375 in.^2	0.563 in.^2

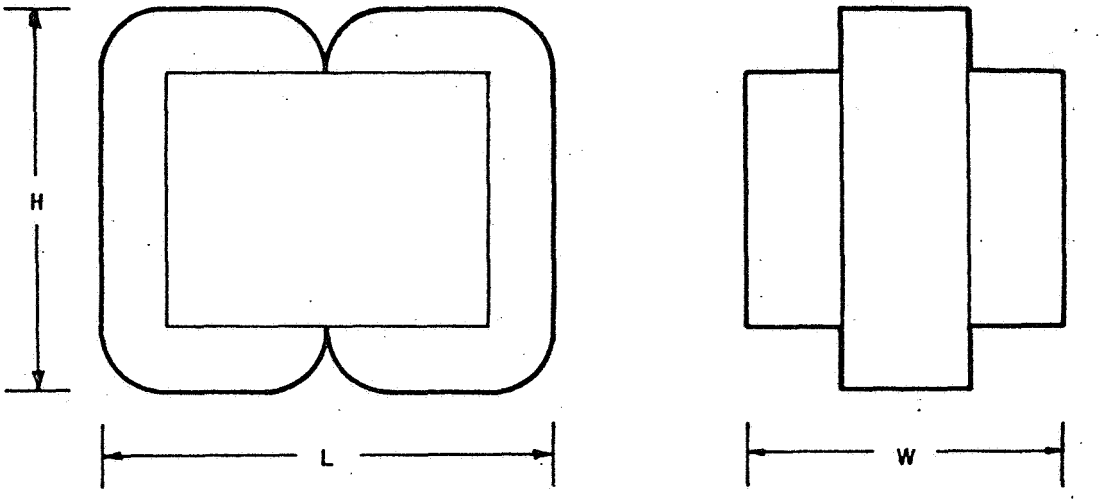

Figure 46. Geometry of Transformer Built from Two "C" Cores

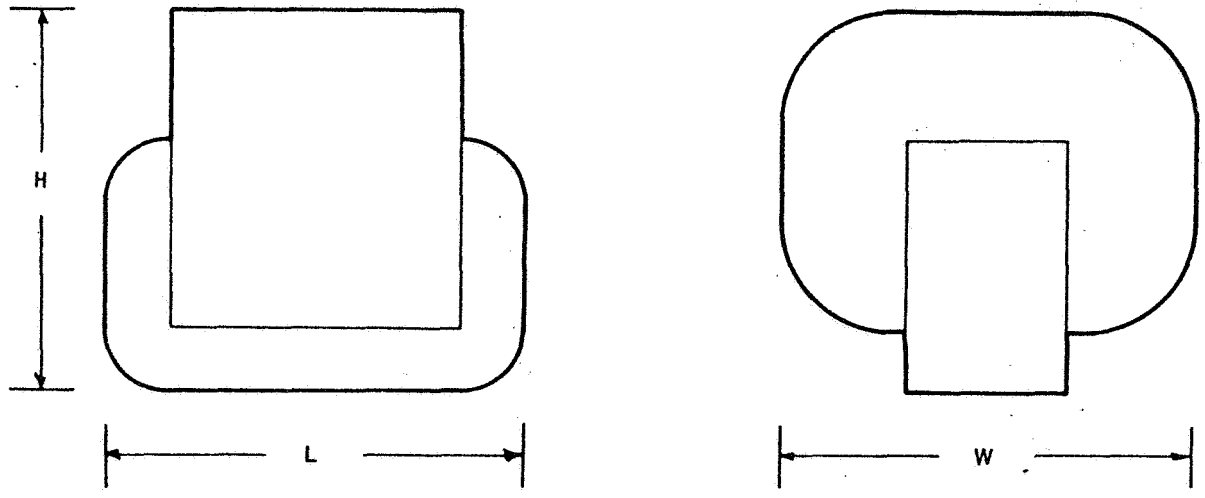

Figure 47. Geometry of Single "C" Core Transformer

TABLE XI. - CHARACTERISTICS OF A TRANSFORMER SUITABLE FOR SQUARE WAVE OUTPUT CIRCUIT

External volume	3.3 in.^{3}
Weight (estimate)	0.35 lb
Core loss (full output)	1.64 W (silicon 2 mil)
	0.85 W (48 alloy 6 mil)
Core loss (1/2 maximum bias level)	0.137 W (silicon 2 mil)
	0.095 W (48 alloy 6 mil)
Turns ratio	65:1
Output voltage	2300 V maximum
Input voltage	35.2 V maximum
Peak current	0.916 amp

The switching transistors at the system output dissipate power during the switching interval through their effective collector resistance. This power is part of the output capacitor-charge power and will be considered a part of that power dissipation. Transformer resistance, modulator effective resistance, and voltage drop are also included. The power required to drive the transistors is not included.

The drive circuit for a half-channel output is shown in Figure 48.

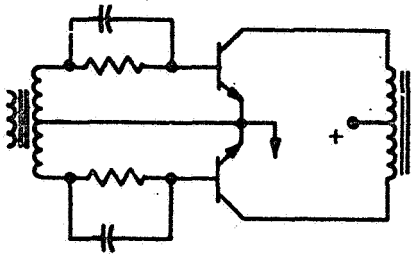

Figure 48. Square Wave Output Circuit

For saturated operation, the transistor is linear enough to treat as a resistor. For transistors of the types given in Table IX, the equivalent resistance is typically 0.1 ohm and at the most 0.2 ohm. The power dissipated is determined by the rms current in the primary given by Equation (170). The estimated power dissipated by the transistor at saturation is

$$P = (I_{rms})^2 R = (0.146)^2 (0.2) = 4.4 \text{ mW}$$

Power is needed to drive the transistors. Since each transistor is "on" one-half the time, the base driving power is one-half the product of "turn-on" base current and saturated base voltage. A current of 50 mA will keep the transistor saturated for any contemplated operation. This current must be supplied from a source with sufficient voltage to allow for any differences among the transistors. A 1.5-V source is sufficient; therefore,

$$P = \frac{0.05 \times 1.5}{2} = 0.0375 \text{ W}$$

Choice of Circuit to be Tested

The final choice of suspension system can be made on the basis of comparisons between parameters which have been derived in the preceding sections. The desired characteristics are outlined below.

- High G: Need large bandwidth, separate sensing good static stiffness, maximum G capability. Output circuit power dominates.
- Low G: Simple system, need low power and low bias force. Bias power predominates.
- Switching: Sensing circuits cannot be switched, desirability of using the same output circuits is obvious. Level change must be done in a comparatively short time.

The high G systems are best compared on the basis of power level and maximum G capability. Other parameters have been already chosen to make the loops similar in terms of response characteristics.

The power input to each system may be found and compared by using the equations derived in the previous section. The power dissipated by the sine wave system is given in Equation (115) and the efficiency of the Class B drivers is given by Equation (131). Input power may be computed from the ratio of these factors:

$$P_{in} = \frac{P_d}{\eta} = \frac{0.0317 \, G \, T \, \delta \, D^2 \, d \, V_g}{\pi \, V_m \cos \phi} \quad \frac{8 \pi f}{Q} \tag{172}$$

For the square wave system, total power input is given by Equation (123); with some changes in the nomenclature, these quantities can be compared. Primes are added to all the letters that represent parameters associated with the square wave system.

$$\frac{P}{P'} = \frac{\dfrac{0.0317\, G\, T\, \delta\, D^2\, V_g}{\pi\, V_m \cos\phi} \quad \dfrac{8\pi f}{Q}}{\dfrac{0.0317\, G'\, T'\, \delta'\, D'^2\, d'\, V}{E} \quad \dfrac{4 f'}{d'}} \tag{173}$$

A fair comparison would be to connect each type of system to the same mechanical assembly and compute input power at the same G level. For this case the mechanical parameters drop out and the power ratio becomes

$$\frac{P}{P'} = \frac{2\, V_o\, f\, E\, \alpha'}{V_m \cos\phi\, Q\, V\, f'} \tag{174}$$

Equation (174) may be investigated for the particular cases of interest, bias output and full G output.

At this point, care must be taken in the evaluation. For the same voltage gradient, the square wave system will provide nearly twice the force, hence twice the G level of the sine system. Thus, to provide this comparison, the output level of the two systems must be different. It is assumed that each system is designed to be full on ($V_o = V_m$ and $V = E$) at specified G input (assume $\alpha = 0.93$).

$$\frac{P}{P'} = \frac{2 f\, (0.93)}{Q f' \cos\phi}$$

$$= \frac{1.86\, f}{Q \cos\phi\, f'}$$

For the previous example, Q was 9.56 at maximum output. Using this value and the same 10 percent excursion results in

$$\frac{P}{P'} = \frac{1.86}{9.56\, (0.794)} \frac{f}{f'} = 0.245 \frac{f}{f'}$$

For the case of bias input, $V = 2E$ but $V_b = 2\,(1.18)\, V_m$ by Equation (129) using $Q = 9.56$ at maximum output.

For the bias G case,

$$\frac{P}{P'} = \frac{2(1.18)\ f(0.93)}{Q\ f'} = \frac{(4)\ f}{f'}$$

This comparison is made to show the power output dependence on Q and switching frequency. If a sine wave carrier in the range of 20 kc is assumed, then an equivalent power square wave system would switch in the 2 to 5 kc range. If the square wave system were switched at 1500 cps, a system could be realized which would have nearly twice the force capability of the equivalent power sine system.

Basic Equations (112) and (120) are of the same form and show that power is dependent on output energy stored and frequency of the charge - discharge cycle. The other, more complex equations, (115) and (121), only represent the fact that the stored energy converts directly to a form dependent on gyro physical parameters and force input. Note the direct dependence on gap and diameter at a given G level. Rotor thickness is inversely proportional to maximum G, and from Equation (114) it can be seen that there is an upper bound on power dissipated for a given configuration.

Efficiency of the driving source depends linearly on voltage of the supply. This means that for a given type of operation, the supply level could be minimized for maximum efficiency. Trying to maximize efficiency of the Class B driver in the face of changing tuning parameters is a far more fundamental problem. One method would be to servo the tuning to keep always at or near zero phase. This would be complex and probably use more power than it would save. A second technique is to change drive frequency to keep the circuit in resonance. This would mean that a three-axis gyro would have six separate oscillating frequencies. This is not immediately impossible, but would enormously complicate the problem of sensing rotor position and making a stable electronic loop.

Various examples have been made in the text to illustrate the applications of the equations which have been derived. These have not all used the same set of parameters. The parameters selected under general considerations will be used to recompute power for each of the types of systems. These parameters are repeated in Table XII.

TABLE XII. - GYRO MECHANICAL PARAMETERS

Mean rotor thickness	$T = 0.017$ in.
Rotor-electrode gap	$d = 0.002$ in.
Rotor diameter	$D = 1.5$ in.
Maximum displacement	$X = 0.15\ d$
Maximum gradient	$(V/d)_{max} = 1000$ V/mil

The power levels found in the following calculations are compared in Table XIII.

The series sine system power input is calculated in detail below using the parameters of Table XII.

Peak off-center output voltage:	E_{max} = 2300 V
Peak centered output voltage:	2000 V
Permissible rotor translation:	15 percent of gap
Transformer turns ratio	65:1

The required power supply voltage (V_m) is calculated from Equation (129) for the maximum displacement:

$$V_{inx} = \frac{V_{ino}\left(1 - j\,Q_f \frac{K_1 x}{d}\right)}{1 + \frac{K_1 x}{d}}$$

where

$$V_{ino} = \frac{E_{max}}{65} = 35.4 \text{ V}$$

$$\frac{K_1 x}{d} = (0.83)(0.15) = 0.125$$

Therefore,

$$V_o = \left| V_{inx} \right|_{max} = 68 \text{ V}$$

To calculate bias level and full output power, the equations for driving power, rotor-electrode capacitance, the current-voltage phase angle, and efficiency [Equations (112), (128), (130), and (131)] are employed:

$$P_o = \frac{E_o^2 \omega C_x}{Q}$$

$$C_x = \frac{C_o}{1 + \frac{K_1 x}{d}}$$

$$\phi = \tan^{-1} \frac{Q K_1 x}{d}$$

$$\eta = \frac{\pi}{4} \frac{V_m}{V_o} \cos \phi$$

From the definition of efficiency, the power dissipated in the transistors is

$$P_d = P_o \left(\frac{1}{\eta} - 1\right)$$

so that the input power required to drive the circuit is

$$P_{in} = P_o + P_d = P_o/\eta$$

At bias level,

$$E_o = \frac{E_{max}}{2} = 1150 \text{ V peak, or } 814 \text{ V rms}$$

$$V_m = \frac{V_{ino}}{2} = 17.7 \text{ V}$$

$$P_o = \frac{E_o^2 \omega C_o}{Q_b} = 0.435 \text{ W} \qquad (175)$$

where C_o is calculated from Equation (113). The efficiency is

$$\eta = \frac{\pi}{4} \frac{17.7 \text{ V}}{68 \text{ V}} = 0.205$$

since $\phi = 0$ when the rotor is centered.

Therefore, the input power is

$$P_{in} = \frac{P_o}{\eta} = 2.13 \text{ W} \tag{176}$$

At full output,

$$E_o = 2300 \text{ V peak, or } 1630 \text{ V rms} \tag{177}$$

$$V_m = V_o = 68 \text{ V}$$

$$\phi = \tan^{-1} (15.4)(0.125) = 62.5° \tag{178}$$

The driving power is

$$P_o = \frac{E_o^2 \omega C_o}{Q_f(1 + \frac{Kx}{d})} = 2.254 \tag{179}$$

Since $V_m = V_o$, the efficiency of the circuit is

$$\eta = \frac{\pi}{4} \cos 62.5° = 0.362 \tag{180}$$

The input power at full output is

$$P_{in} = \frac{P_o}{\eta} = \frac{2.254}{0.362} = 6.23 \text{ W} \tag{181}$$

The total power of all the output circuits is calculated by adding together the power required to drive each electrode. At zero acceleration, the power level is six times P_{in} given in Equation (176), or 12.78 watts. When one channel is driven at full output and the other two channels are at bias level, the power level is

$$P_t = 6.23 + 4(2.13) = 14.75 \text{ W}$$

It is interesting to compare the power dissipated in the output transistors at the output levels. At bias level, where the efficiency = 0.205, the transistors dissipate 1.69 watts per electrode. At maximum output, the efficiency improves somewhat to 0.362, but the power dissipated increases to 3.69 watts.

The parallel drive system produces a current controlled by the suspension loop. The voltage required to drive the system is merely the ratio of output voltage to the turns ratio. The output current, however, increases as mistuning occurs. Except for the supply voltage, these factors produce nearly the same maximum conditions as for the series tuned system.

The supply voltage is that required to generate the maximum electrode voltage, which is V_{ino}. Therefore, $V_\delta = 35.4$ volts. At bias level conditions, the output voltage requirements are the same as those given in the series example; hence, the driving power is that given in Equation (175). The efficiency, however, is different:

$$\eta = \frac{\pi}{4}\frac{17.7}{35.4} = 0.342$$

The bias level power input is

$$P_{in} = \frac{0.435}{0.340} = 1.28 \text{ W}$$

At zero acceleration the system power level is 7.68 watts.

At full output, the electrode voltage requirement is that of Equation (177). The rotor is at maximum displacement; thus, the driving power is given by Equation (179) and the phase is given by Equation (178). The output voltage V_m is equal to supply voltage V_s; therefore, the efficiency and input power is the same as the series tuned system [Equations (180) and (181), respectively]. With the other two channels driven at bias level, the power level is

$$P_t = 6.23 + 4(1.28) = 11.35 \text{ W}$$

The square wave system power input is a sum of charging power and driver losses. These losses have been calculated for the proper parameters in that section. The charging losses are calculated below and a summary given in Table XIII. The basic equation for power (120) can be put in a form using the specified gyro parameters:

$$P = 0.416 \times 10^{-12}\left(\frac{E^2}{d^2}\right) D^2 \, d \, f \qquad (182)$$

$$P = 0.416\,(2.25)\,(2 \times 10^{-3})\,(1.5 \times 10^{3}) \qquad (183)$$

$$= 2.81 \text{ watts direct "charging" dissipation at full output}$$

The total power dissipated by the square wave system is summarized in Table XIII.

TABLE XIII. SQUARE WAVE SYSTEM POWER

Power at	V_m	$V_m/2$	$V_m/4$
Charging power [Equation (183)]	2.810 W	1.405 W	0.703 W
Transformer loss (49 alloy) [Equation (158)]	0.850	0.095	0.011
Transistor driving power	0.450	0.450	0.450
Total	4.110	1.950	1.164

Several possible operating conditions exist, since the square wave system is inherently single phased and bias may be run lower than the three-phase balanced sine systems. Four conditions are given here:

One channel full on + 1/2 bias on four electrodes = 11.91 watts

1/2 bias on six electrodes = 11.70 watts

One channel full on + 1/4 bias on four electrodes = 8.766 watts

1/4 bias on all six electrodes = 6.984 watts

The transformer magnetizing current flows in such a direction that during the switching interval it adds directly to the discharge current. Thus, the energy stored in the core becomes part of that needed for capacitor charging and was previously added to the power requirement in Equation (181).

Table XIV summarizes the capability and power level for each system. Two items appear in the square wave power columns because the square wave system, being single phased, can be operated at a lower bias level than 1/2 maximum voltage.

The square wave system has the following advantages at high G.

- Readily adapted to separate sensing
- Maximum G capability at a given gradient
- Relatively simple electronics
- Relatively simple setup
- Variable bias level

TABLE XIV. - COMPARISON OF MAXIMUM ACCELERATION AND POWER OF HIGH G SUSPENSION SYSTEMS

System	Output Frequency (kc)	Capability (G)		Bias Power (watts)	Maximum Power (watts)
Square Wave	1.5	100	$V_b = \frac{V_{max}}{2}$	11.70	11.91
			$V_b = \frac{V_{max}}{4}$	6.98	8.76
Series Sine	20	54		12.78	14.75
Parallel Sine	20	54		7.68	11.35

It has average power input, but larger output transformers. Power is dissipated in the transformer and added resistor which is an easily controlled area (power is mostly dissipated in the output transistors in the sine system).

The simplest low G mechanization is a series-resonant, self-sensing sine system. However, this could not be used during high G operation, even for sensing, because the sensing frequency is not compatible with low-power operation and the sensing circuits cannot be switched. The next level of simplicity is the square wave system. It also has the advantages of direct coupling capability. The sensing voltages applies at high G will be useful as bias input at low G.

The system which will be designed is that shown on Figure 49. This circuit requires a two-level power supply. This will be discussed in the next part of this section.

VARIABLE VOLTAGE POWER SUPPLY

It became obvious through the development of the dual-range suspension system that the operation would be greatly facilitated by use of a dual-level power supply. This approach has the following advantages:

- Zero bias power in high G circuits during low G operation
- No interaction between circuits
- Definite two-level "preset" loop stability
- High G supply level design not compromised

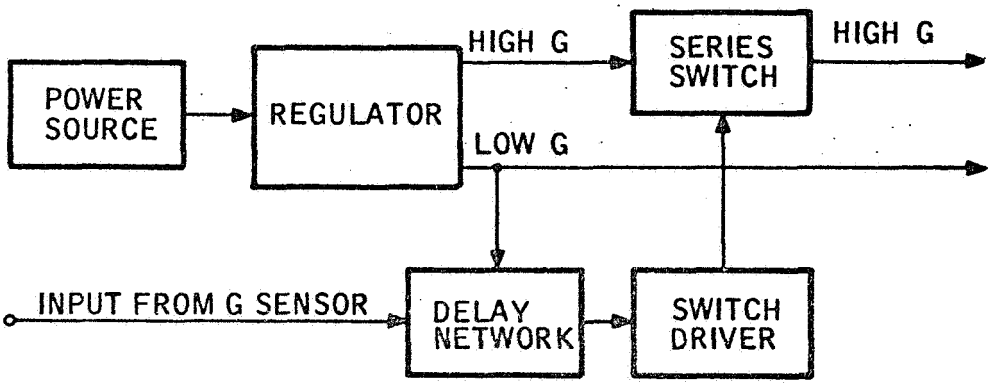

Figure 49. Dual Level Power Supply

Study of Parameters Necessary

The operation of the power supply can best be understood in light of what the suspension is required to do while switching modes. The steps required during mode switching may be summarized as follows:

- Normal high G operation
- Input level drops to 10^{-2} G
- G sensor output switches
- Bias and networks switch to low level
- High G power supply turns off

The time allowed for the switch may be deduced from the conditions at that instant. Assume a one-fourth biased 100 G suspension. The input acceleration is less than 10^{-2} G and may be neglected. The worst case would be the condition where one side bias shut off before the other. Bias force level under the assumption, is 100/16 G. Assuming that the rotor can move 200 μ in. (10 percent gap), the total time is found from

$$T^2 = \frac{2d}{A} = \frac{2 \cdot x\ 200 \times 10^{-6}}{\frac{100}{16} \cdot 386} = 16.58 \times 10^{-8}\ (ms)^2 \tag{184}$$

$$T = 0.407\ ms$$

It is necessary to switch the bias and networks with power "ON" so that normal feedback will be available to damp the inevitable transients which will occur in the amplifiers.

Summary and Block Diagram

The power supply must have the basic parts shown in the block diagram of Figure 49.

The circuit which will be designed will not include the power source and regulator. Current will be furnished by laboratory regulated supplies.

SECTION IV
OUTPUT CIRCUIT DESIGN AND TEST

A block diagram of the circuitry which was designed, built, and tested is shown in Figure 50. It may be separated (arbitrarily) into the output circuit proper and the power switch; however the major part of the work was devoted to the output circuits.

Generally, the basic suspension requirements described in Sections II and III can be satisfied. During the test phase, the design factors which were treated in the earlier sections (and some factors which were not considered) were checked out. Difficulties which were encountered led to circuit modifications. A discussion of these difficulties and of the changes made in the circuitry is included in this section. The final schematics and piece parts prints were released at Honeywell under device number EG1006AA01 for future reference.

DESIGN OF CIRCUITS

Output Circuits

In this section the design of the output circuit subassemblies is considered. Particular emphasis is placed on the aspect of output transformer design since this is a critical component in the circuit. The oscillator, power amplifier, and switching output are all designed to operate at 1500 cps. The amplifiers which provide the "modulator" function are designed to provide a slew rate and output current capability such that the output risetime would be one-twentieth the cycle time or less than 33 microseconds.

The output circuit provides force with a square wave, audio-frequency output voltage and operates over a range of voltage corresponding to force levels over a range of 10^4. The circuits which were conceived accomplish this as follows:

- The amplifiers which provide the modulating function are split at a point of 10:1 gain down from the high G output
- The high G output drives a 67:1 turns ratio at a maximum of 35 volts, producing the necessary 2300 volts output
- The low G output drives a 10:1 turns ratio at maximum of 4 volts; this winding is actually a tap on the secondary winding of the output transformer
- The secondary (low G) circuit is switched directly by the oscillator and is always "on"

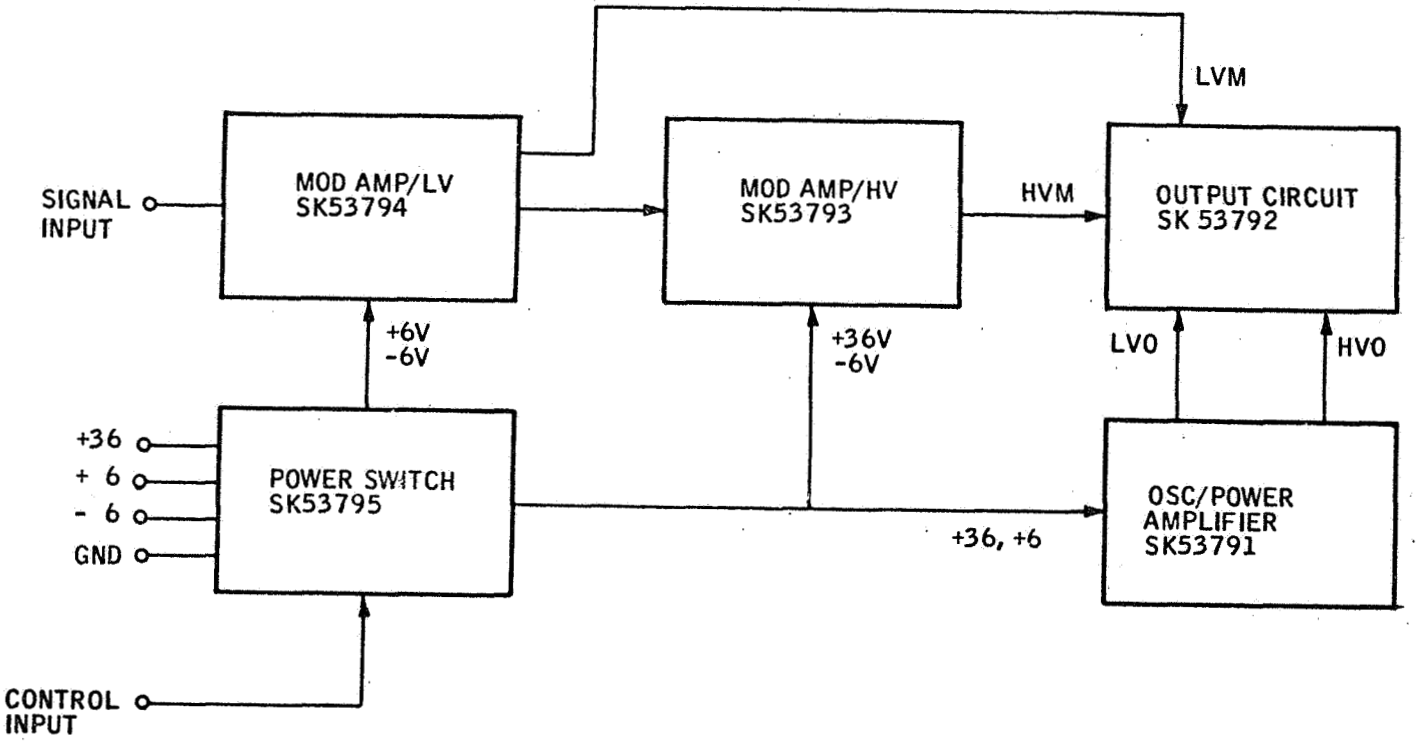

Figure 50. Diagram of Breadboard Suspension Output Circuit

- The primary (high G) circuit is switched by the power amplifier which is turned off during low G operation

- Since -4 volts is needed at the secondary switch, a ±6 volt supply is used. The input modulating amplifier is a μA 709 run at ±6 volts (3 volts below rating)

Oscillator. -- The 1500-cps square wave oscillator circuit produces drive voltage for the secondary switching circuit transistors and the power amplifier input. Since these output functions must be separated, a transformer-coupled, magnetic multivibrator design was used. The oscillator was designed to drive the following loads:

- Six secondary transistors each half cycle at 2 mA, 1.5 volts, 18 mW

- Feedback at 0.7 mA, 1.5 volts, 0.91 mW

- Power amp drive voltage

  1 transistor each half cycle

  1.0 volt, 1.3 mA, 1.3 mW

The total power is 20.21mW which is furnished by the +6-volt line. The object, of course, is to develop this power at maximum efficiency. Losses appear in a circuit of this type in five areas:

- V_{CE} drop in switching

- Resistance loss in transformer

- Core loss in transformer

- Magnetizing loss in transformer

- Starting and bias circuits

Two types of bias and starting circuits were considered:

- Back-biased diode

- Resistance biasing

The diode bias circuit is shown in Figure 51. The necessary feedback voltage (V_1) is calculated from the variations of diode and transistor input voltages. Writing the loop equation results in

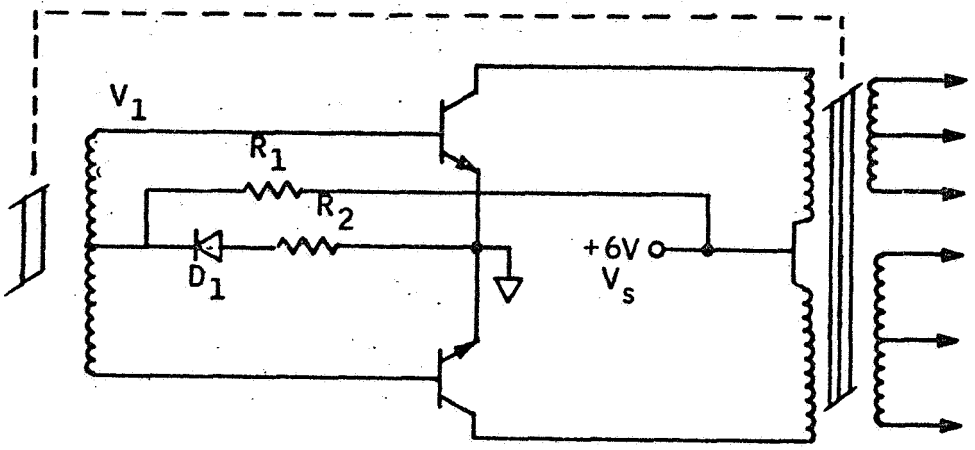

Figure 51. Diode Bias Circuit

$$I_{bo}\left(1+\frac{\Delta I_b}{I_{bo}}\right)=\frac{V_1-V_{be}-V_d}{R_2}\left(1-\frac{\Delta V_{be}+\Delta V_d}{V_1-V_{be}-V_d}\right)$$

where

I_{bo} = Nominal base current

V_1 = Feedback voltage

V_{be} = Transistor base-emitter drop

V_d = Diode forward drop

Δ = Changes in the quantities

V_s = Supply voltage

For an allowable $\Delta I_b/I_{bo} = 0.4$ and specifications $V_{be} = 0.67 \pm 0.05$ V, $V_d = 0.59 \pm 0.03$ V, the feedback voltage must be 1.46 volts or greater. Power lost is $1.46 \times I_{bo}$, or 1.02 mW.

The value R_1 in Figure 51 is determined by whatever resistance is needed to produce sufficient I_{bo} to start the oscillation. For the transistors selected, I_{bo} is 25 μA; therefore, a 240 KΩ resistor was used.

The circuit may be altered by producing feedback voltage with a nontapped transformer winding. At the expense of a second diode, a lead and some winding space is saved. A desirable result of this alteration is a slight unbalance in the starting circuit.

The resistance bias circuit differs from the diode bias type only in that the diode (D_1 in Figure 51) is absent. Different values of R_1 and R_2 are used to start and bias the circuit. The circuit is characterized by two loop equations relating supply voltage, divider current, base current, and feedback voltage: a "turn-on" condition and a "turn-off" condition. A simultaneous solution of these conditions results in an equation for R_2. Let A represent the "turn-off" voltage. Then

$$R_2 = \frac{V_s (V_{be} + 3\Delta V_{be} - A)}{2 I_{bo} (V_s - V_{be} + \Delta V_{be})}$$

$$= 1240\,\Omega \text{ for } A = 0.5 \text{ V}$$

Then

$$R_1 = R_2\left[\frac{V_s}{V_{be} + \Delta V_{be}} - 1\right]$$

$$= 9100\,\Omega$$

$$I_1 = \frac{V_s + I_{bo} R_2}{R_1 + R_2} = 0.665 \text{ mA}$$

Total power used is

$$P = P_1 + P_2$$

$$= V_1 I_{bo} + V_s I_1 = 4.387 \text{ mW}$$

Although the circuit is simpler, it expends 3.4 mW more than the diode circuit to meet all of the requirements. Since the oscillator is in the low G system where power conservation is important, the diode circuit was used. Components for the circuit were selected from those which were specified for this operating regime, giving numbers on which to base an accurate comparison. They are:

- Diode - 1N4610 fast, specified forward drop, relatively inexpensive
- Transistor - 2N4960 series specified V_{ce} and V_{bo} limits for this current range.

These transistors produce negligible (0.07 V) forward drop; thus, the power loss is also negligible.

The transformer is best wound on a toroid using low-loss 80-percent alloy core material. Calculations indicated that the smallest "standard" tape core size or a "miniature" core of over 450 maxwells capacity is suitable. The core used is Honeywell part number 947110 with nominal capacity of 471 maxwells, tape thickness of 0.5 mil, and core material 4-79 mo-permalloy

The familiar voltage equation must be modified to use the "flux capacity" concept. The flux capacity, ϕ is given by

$$\phi = 2 B \times A_c \times S \tag{185}$$

where A_c is core area in square centimeters, S is the stacking factor and B is the peak flux density in k gauss. The induced voltage per turn is

$$e/N = B \times A_c \times S \times f \times 2.585 \times 10^{-4} \tag{186}$$

with A_c given in square inches, and f in cps. Substituting (185) into (186) gives

$$e/N = 2.00 \times 10^{-5} \phi f$$

For our core, $e/N = 1.416 \times 10^{-2}$. The turns for the various windings with e = 6 V are given in Table XV.

TABLE XV. - OSCILLATOR WINDINGS

Primary	=	424 turns per side (6 V)
Driver output	=	71 turns per side (1 V)
Feedback	=	106 turns (total) (1.5 V)
Secondary Output	=	106 turns per side (1.5 V)

Since primary current is 2.125 mA per side (assuming 80-percent efficiency), the transformer wire will be larger than necessary for the first three windings. The secondary output current is 12 mA. Using the same current density for this winding results in the data of Table XVI for window area calculations.

TABLE XVI - WINDOW AREA CALCULATION

Winding	Turns	Wire Size	Window Area
1	848	No. 38	13,300 circular mils
2	142	No. 38	2,230 circular mils
3	106	No. 38	1,660 circular mils
4	212	No. 36	5,300 circular mils
Total area used			22,490 circular mils
Shuttle area			42,000 circular mils
Core area needed			64,490 circular mils
Core area available			72,900 circular mils

The design was used and the part drawing is SK 53640 (Figure 69).

Losses in the transformer are the major contributors to power loss in the oscillator. Three categories were considered: magnetizing current loss, core loss, and copper loss. The magnetizing loss may be estimated from a knowledge of the average magnetizing force (H_{avg}) needed to drive the core to saturation. This value may be found by integrating the constant current flux reset curves given in the manufacturers' literature. This technique is discussed in greater detail later on when output transformer losses are considered.

The power loss is the product of average current and input voltage, V_s.

$$P = V_s I$$

$$= \frac{V_s \times H_{avg} \times \ell \times 2.02}{N}$$

where ℓ is the core length for our set of parameters and $H_{avg} = 0.0452$ oersteds (from Figure 53) resulting in a power loss of 1.422 mW.

Core loss is found in the manufacturer literature in terms of watts per pound at a specified frequency. For 80-percent nickle-iron at 7000 gauss, 1500 cps, the loss is 1.5 watts per lb. The estimated core weight (calculated) is 0.00169 lb, producing a core loss of 2.54 mW.

Copper loss is calculated by estimating the winding resistance and multiplying by current squared. These calculations are outlined in Table XVII.

TABLE XVII. - COPPER LOSS

Winding	Resistance	Current (mA)	Copper Loss (mW)
1	23.3 Ω	$\ell_1 = 4.25$	$P_1 = 0.418$
2	5.83Ω	$\ell_2 = 0.7$	$P_2 = 0.003$
3	3.90Ω	$\ell_3 = 1.3$	$P_3 = 0.007$
4	3.65Ω	$\ell_4 = 12.0$	$P_4 = 0.526$
Total copper loss = 0.954 mW			

From these calculations, the total power loss may be estimated and checked with test results with no load, the power input as the sum of magnetizing power, core loss, and feedback power:

$$P_{NL} = 1.422 + 2.54 + 1.05 = 5.01 \text{ mW}$$

Loaded, the power input is the no-load power plus copper loss and output power:

$$P_L = 5.01 + 0.954 + 19.3 = 25.264 \text{ mW}$$

The efficiency is the ratio of output power to input power:

$$\text{Efficiency} = \frac{19.3}{25.26} = 0.76 \text{ or } 76\%$$

The final oscillator design is shown with the power amplifier in Figure 52.

Power Amplifier. -- The power amplifier is a simple push-pull switching assembly. It uses +35 volts for input supply and is turned off during low G operation. Since a slight switching unbalance probably will exist, a lower-permeability, 50-percent, nickle-iron core material will be used. The load is the primary power switching transistors in the output circuit; six are to be driven at a time with a 1.5 V source delivering a maximum 68 mA per switch. The total load is therefore 612 mW. With the high-voltage supply (+35 volts) and assuming 80-percent efficiency, the input current is

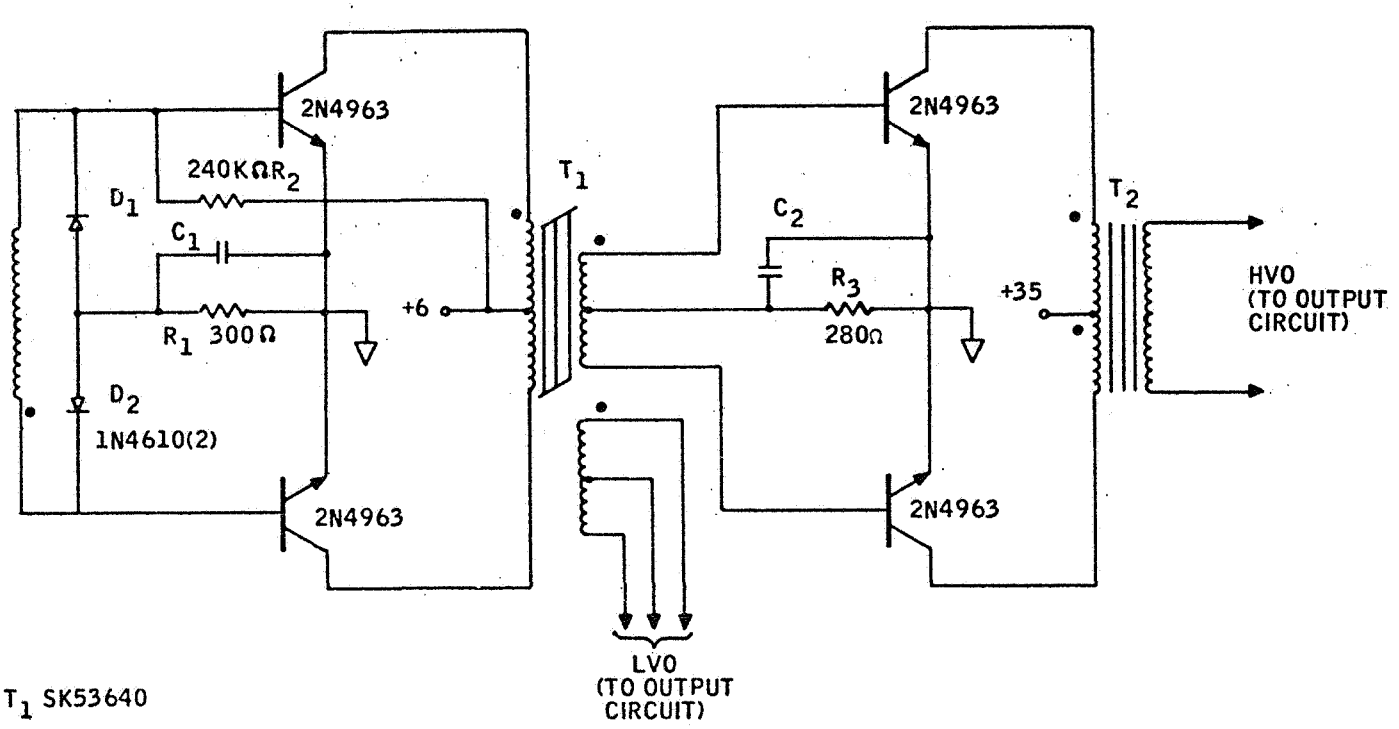

1. T_1 SK53640
2. T_2 SK53641
3. C_1, C_2 TO BE SELECTED IN TEST

Figure 52. Oscillator/Power Amplifier

$$I_p = \frac{0.612}{(0.8)(35)} = 22 \text{ mA}$$

From this calculation, the turns ratio, and assuming a reasonable current density (1500 CM/amp) the required window area can be determined.

$$A_w = 117 \times 10^{-6} N$$

From the voltage Equation (167), the required core area is

$$A_c = 14.7/N$$

The core size needed, therefore, has a core area-window area product of 0.00172. A core meeting this requirement is the standard 52000 - 2H.

Power loss in the amplifier is produced primarily by the transformer. These factors are summarized in Table XVIII.

TABLE XVIII. - POWER AMPLIFIER LOSS

Loss	Factors	Value (mW)
Core	7.5×10^{-3} lb at 3.4 W/lb	25.5
Magnetizing	$H_{avg} = 0.105$	13.6
Copper	$R_s = 0.142$ Ω/side	23.7
	$R_p = 87$ Ω/side	25.0
Transistor	0.07 V, 16 mA	1.1

The no-load power input is 39.1 mW.

The loaded power input is no-load power plus copper loss and output, which is 699.8 mW.

The amplifier efficiency is 87 percent.

The final design is shown with the oscillator in Figure 52.

Output Circuit

The output circuit encompasses the output transformer, the high G (primary) switching circuit, and the low G (secondary) switching circuit. The switches and transformer make up an assembly which is functionally very similar to the square wave power amplifier. The high G output operates through a 67:1 step-up ratio to provide 2300 volts from the 35-volt supply. The low G circuit has a 10:1 step-up ratio to produce approximately 30 volts maximum from an amplifier capable of about 4 volts, but with one diode drop interposed.

The transistor switches are specified by the following parameters.

Primary: 2-amp peak current (calculated)

70-volt V_{ce}

120-mA avg current (calculated)

< 1-microsecond switching times

Secondary: 230-volt V_{ce}

< 1-microsecond switching time

The output transformer is the heart of this circuit (indeed, of the whose system). It occupies more volume than any other part, and a suspension system uses six transformers. The transformer design requirements are

- Produce 2300 volts with negligible corona
- Be as efficient as possible
- Be as small as possible
- Use available core material and shape

The dependence of core shape on transformer properties was considered carefully to provide these features. The following paragraphs show the derivations for the relationships between parameters which will result in the greatest efficiency with least volume.

The expression for efficiency is first divided into two types of factors, design and geometric. The design factors are: flux density, current density, winding efficiency, material lamination thickness, etc. The geometric factors are functions only of the linear dimensions of the core.

The efficiency of the transformer is given by

$$\eta = \frac{100\ P_{out}}{P_{in}} = 100\left(\frac{P_{in} - \text{Loss}}{P_{in}}\right) = 100\left(1 - \frac{\text{Loss}}{Pin}\right) \tag{187}$$

where η is the efficiency in percent, P_{out} and P_{in} are the output and input power respectively at rated load, and loss is the power consumed by the transformer internally. Obviously, for highest efficiency the ratio of loss to P_{in} must be minimized.

Loss is made up of three components:

1) Core loss
2) Copper loss
3) Magnetizing current

The third component is included because current which must be supplied from a direct source is lost when dissipated, unless it is stored and reused each cycle (by turning or capacitance loading).

The core loss is the sum of a component produced by eddy currents in the laminations and a component produced by hysteresis in the iron. An equation for these losses was developed in Section II [Equation (144)] and is repeated below:

$$\text{Loss} = (K_e t^2 f^2 B^2 + K_h f B^{1.6})\ \delta\ \text{Volume} \tag{188}$$

Loss = Eddy current loss coefficient
K_h = Hysteresis loss coefficient
f = Frequency of operation
B = Core flux density in k gauss
t = Lamination thickness
δ = Density, lb per cubic inch

The volume factor is the product of core area and effective length for cores designed to have reasonably uniform flux density:

$$\text{Volume} = A_c \cdot \ell_e \cdot S$$

where A_c is the gross core area, ℓ_e is the length of the core, and S is the stacking factor for the particular iron chosen.

The magnetizing current is nonlinear and displays a waveform which depends on the shape of the core hysteresis loop. For the switched voltage to be applied (square wave), the waveform of flux is linear. Using this fact with the constant current reset curves for the material allows us to calculate magnetomotive force (H) as a function of time. The average H for a given material and flux density can then be graphically determined. Figures 53 and 54 show H versus time for two materials used extensively in signal transformers. The loss is calculated from the product of average current and supply voltage.

$$\text{Loss} = I_{avg} \cdot V_s \tag{189}$$

Now

H = Magnetomotive force $\frac{0.4\ NI}{\ell_e\ 2.54}$

N = Number of turns

I = Current in wire

where ℓ_e is the magnetic path length in inches.

Rearranging gives

$$I = \frac{2.54}{0.4\pi} \cdot \frac{H\ \ell_e}{N} \tag{190}$$

This equation is solved for the current and substituted into Equation (189). Using (167) for the induced voltage in (189) gives

$$\text{Loss} = \frac{2.54}{0.4\ \pi}\ B\ f\ S\ (2.585)\ 10^{-4}\ H_{avg}\ \ell_e\ A_c \tag{191}$$

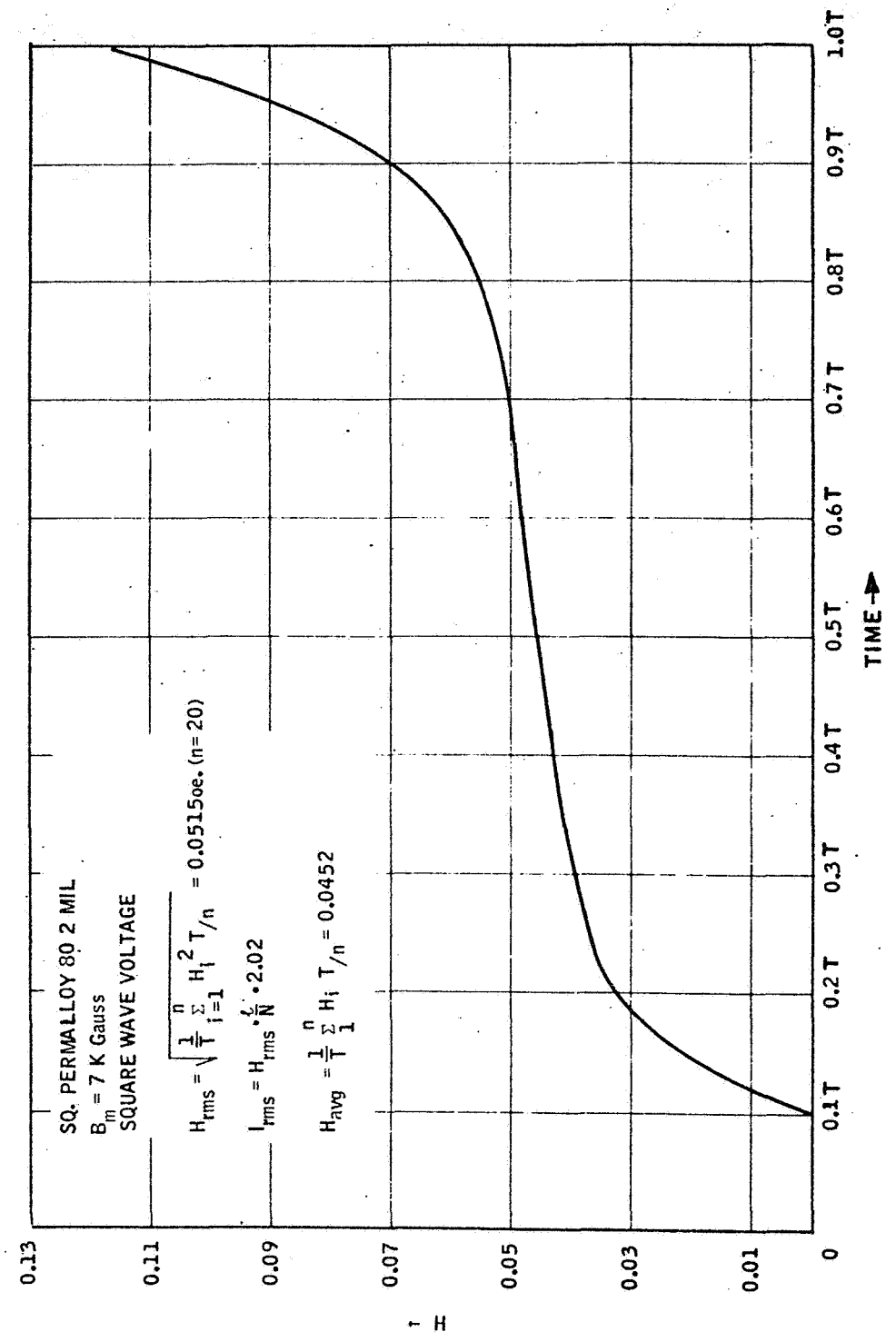

Figure 53. Magnetomotive Force Function for Square Permalloy 80 2-mil Material

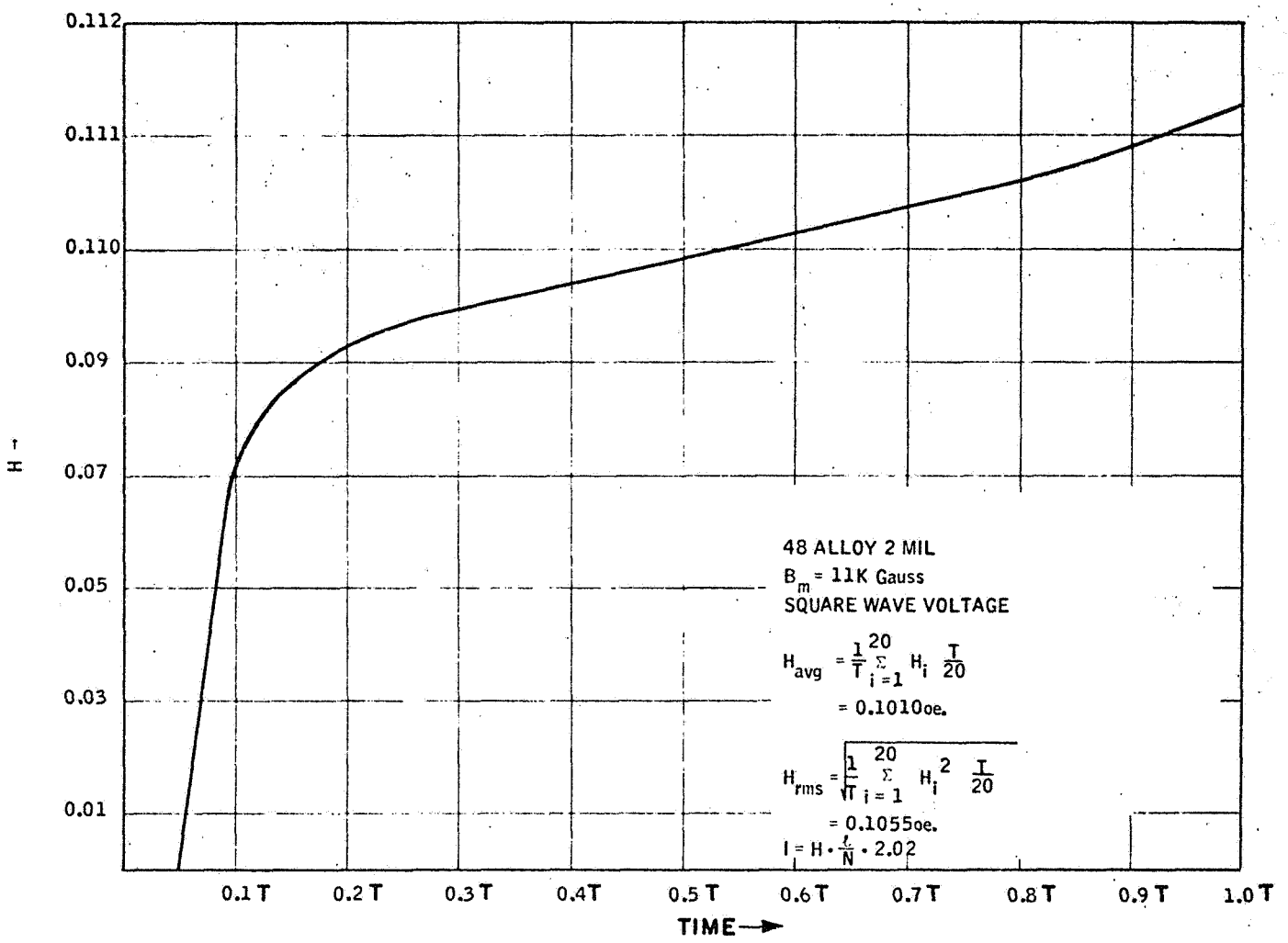

Figure 54. Magnetomotive Force Function for 48-Alloy 2-mil Material

where the H_{avg} is determined graphically.

The total copper loss may be simply represented as the sum of the ohmic (I^2R) losses in the primary and secondary windings. If more windings are present, their loss (and volume) must be accounted for, but the same principles are applied. These equations are used to solve for the loss in terms of design parameters.

$$\text{Loss} = \sum_{i=1}^{n} I_i^2 \, R_i \tag{192}$$

where

$$R_i = \frac{\rho \, L_i}{A_i}$$

$$A_i = \frac{I_i \, J_i \, \pi}{4} \tag{193}$$

$$L_i = N_i \, L_{mi}$$

I_i = Winding current

R_i = Winding resistance

ρ = Resistivity of winding material

L_i = Length of wire in winding

A_i = Area of wire

J_i = Current density in wire CM/amp

N_i = Turns in winding

$L_{n.i}$ = Mean length of turn in winding

The total area used is the window area:

$$A_w = \sum_{i=1}^{n} A_i \cdot N_i \cdot \frac{1}{\gamma} \tag{194}$$

where γ is a winding efficiency factor which varies for the style of winding and insulation used, but is usually 30 to 50 percent for small transformers with round wire. Substitution of Equations (193) into (194) and (192) results in the following loss and area equations:

$$\text{Loss} = \sum_{i=1}^{n} \frac{I_i \times N_i \times \rho \times L_{mi} \times 4}{J_i \times \pi} \tag{195}$$

$$\gamma A_w = \sum_{i=1}^{n} \frac{I_i \times J_i \times \pi \times N_i}{4} \tag{196}$$

The desired form of the equation for loss is a product of two terms, one containing the coil design factors and the second containing geometric (core shape) relationships. The ideal situation is that in which the power density is uniform in the fully loaded winding and core.

This implies the equality of the loss per unit volume in the separating windings. The following equations may thus be written:

$$\frac{\text{Loss}}{\text{Vol}} = \frac{I_1^2 R_1}{L_{m1} A_1 N_1 \gamma} = \frac{I_2^2 R_2}{L_{m_2} A_2 N_2 \gamma} = \cdots \frac{I_n^2 R_n}{L_{m_n} A_n N_n \gamma}$$

or

$$\frac{I_1^2 \rho}{\gamma A_1^2} = \frac{I_2^2 \rho}{\gamma A_2^2} \cdots \frac{I_n^2 \rho}{\gamma A_n^2}$$

Substitution of (193) for A_i gives

$$\frac{\text{Loss}}{\text{Vol}} = \frac{16\rho}{\gamma\pi^2} \frac{1}{J_1^2} = \frac{16\rho}{\gamma\pi^2 J_2^2} = \cdots \frac{16\rho}{\gamma\pi^2 J_n^2}$$

Thus, for constant power density, the wire current densities must be equal in all windings. The currents in the windings are related by the equation

$$I_1 = \frac{N_2}{N_1} I_2 + \frac{N_3}{N_1} I_3 \cdots$$

$$I_1 N_1 = \sum_{i=2}^{n} N_i I_i \tag{197}$$

This assumes that winding one is the current input (primary) winding and expresses the fact that primary current is the sum of secondary currents reflected to the primary. This result may be used in the window area expression (196) to give

$$\gamma A_w = \frac{\pi J}{4} \sum_{i=1}^{n} I_i N_i$$

$$= \frac{\pi J}{4} \left[I_1 N_1 + \sum_{i=2}^{n} I_i N_i \right] \tag{198}$$

$$= \frac{\pi J}{2} I_1 N_1$$

Thus, for equal current density, the primary winding will occupy one-half the available window area.

The loss equation (195) may be similarly separated into two parts:

$$\text{Loss} = \frac{4\rho}{\pi J}\left[I_1 N_1 L_{m1} + \sum_{2}^{n} I_i N_i L_{mi}\right] \tag{199a}$$

The secondary loss may be found in terms of the primary loss by resorting to the equal-power density equation. Let us define L_{ms} so that the product of L_{ms} and half the window area yields secondary winding volume. Then,

$$\frac{\text{Loss}}{\text{Vol}} = \frac{I_1^2 R_1}{\frac{\gamma A_w}{2} L_{m1}} = \frac{\sum_{2}^{n} I_i^2 R_i}{\frac{\gamma A_w}{2} L_{ms}} \tag{199b}$$

Substitution of the relationships for R_i, A_i, and L_i (193) into (199) yields

$$\frac{4\rho I_1 N_1}{\pi_o} = \frac{4\rho}{\pi J} \frac{\sum_{2}^{n} I_i N_i L_{mi}}{L_{ms}} \tag{200}$$

or

$$\sum_{2}^{n} I_i N_i L_{mi} = I_1 N_1 L_{ms}$$

Thus, the total loss equation reduces to

$$\begin{aligned} \text{Loss} &= \frac{4\rho}{\pi J}[I_1 N_1 [L_{m1} + L_{ms}] \\ &= \frac{8\rho\gamma}{\pi^2 J^2} [L_{m1} + L_{ms}] A_w \end{aligned} \tag{201}$$

which is the desired equation.

In summary, three areas where loss occurs have been identified, and equations have been derived relating the loss to design parameters and core parameters. The sum of Equations (188), (191), and (201) gives the total loss in the transformer:

$$\text{Loss} = (K_e t^2 f^2 B^2 + K_h f B^{1.6}) \delta \cdot A_c \cdot L_e \cdot S$$

$$+ \frac{2.54}{0.4\pi} B \cdot f \cdot S \cdot 2.585 \cdot 10^{-4} H_{avg} L_e \cdot A_c \qquad (202)$$

$$+ \frac{8 \rho \gamma}{\pi^2 J^2} [L_{m_1} + L_{ms}] A_w$$

The factor $\frac{8 \rho \gamma}{\pi^2 J^2}$ is the winding power density; its value is 0.374 watts per cubic inch for γ = 35 percent and J = 700 CM per amp. Iron loss may be determined directly from the manufacturers' curves. Twelve-mil "c" cores have a guaranteed maximum loss of 0.9 watts per lb or 0.24 watts per cubic inch at 15 K gauss, 60 fps. The numbers used are for line-type transformers which are optimized for all-day efficiency and thus turn out very reasonably in terms of our assumption of ideal conditions for power density.

To minimize the loss to input power ratio, the input must be expressed in terms of design and mechanical parameters. The total transformer capacity may be expressed in terms of its input voltage and current V_1 and I_1. Their product is

$$P_{in} = V_1 I_1 = N_1 B_f A_c S \cdot 2.585 \cdot 10^{-4} \frac{2\lambda A_w}{N J \pi} \qquad (203)$$

$$= \frac{5.170 \times 10^{-4} f \cdot S}{J \pi} \cdot B \cdot A_c \cdot A_w$$

Note that capacity scales as the product of core area and window area. For transformers driven from a direct source, $V_1 I_1$ represents power (as opposed to tuned or alternating-source transformers where power factor of the magnetizing current is important). The combination of (202) and (203) gives

$$\frac{\text{Loss}}{P_{in}} = \frac{(K_e t^2 f B + K_h B^{0.6}) J \delta \pi}{5.170 \times 10^{-4}} \frac{L_e}{A_w}$$

$$+ \frac{2.54}{0.4\pi} \frac{H_{avg} \cdot J\pi}{2} \frac{L_e}{A_w}$$

$$+ \frac{8 \rho \gamma}{5.170 \times 10^{-4} \cdot f \cdot S \cdot B} \frac{L_m + L_{ms}}{A_c}$$

or in more manageable form

$$\frac{\text{Loss}}{P_{in}} = K_i \frac{L_e}{A_w} + K_c \frac{(L_{m1} + L_s)}{A_c} \tag{204}$$

where K_i and K_c are factors which are dependent on the design choices made, based on desired operation, regulation, environment, etc. Since the ratio is a linear sum, minimum values of the core parameter ratios give greatest efficiency.

It is instructive to consider finding minimum values for a given core type and to see how they scale with core size.

Figure 55 depicts a core with dimension shown, which could be built up from E-I laminations or two "C" shapes side by side. For this core,

$$A_c = WT$$

$$L_e = 2L + 2E + 8 \cdot 1/4\ T$$

$$= 2L + 2E + 2T \qquad (205)$$

$$A_w = L \cdot E$$

$$L_{m1} + L_{ms} = 4W + 4T + \frac{4\pi E}{2}$$

The general problem is to minimize loss for a given power level; i.e., L/P a minimum for $(A_w) \cdot (A_c)$ = a constant.

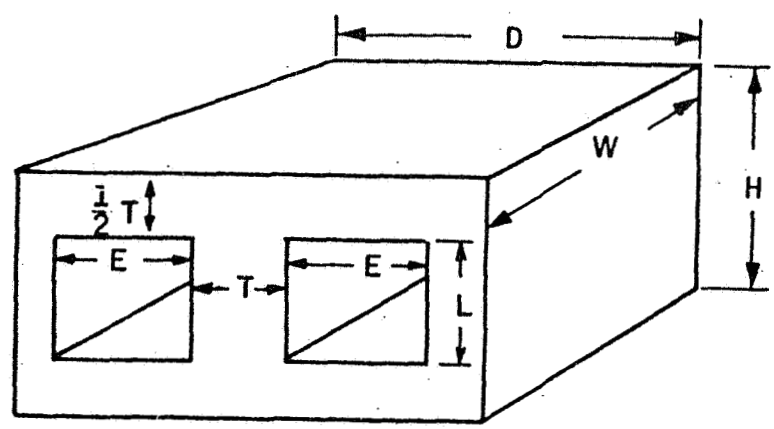

Figure 55. Core Parameters

In reality, we can only choose among core types which do exist. Since there is little reason to making a better (more efficient, higher power) unit than is needed, the smallest core which will do the job is usually selected. When the lamination is chosen, T and E are known; therefore, W is the only parameter we can control.

Let $E = \alpha T$, where $1/4 < \alpha < 4$ for most available cores.

We have two ratios to minimize:

$$\frac{L}{A_w} \text{ and } \frac{L_s + L_p}{A_c}$$

Using the relations (205) gives

$$\frac{L_e}{A_w} = \frac{2\,(L + E + T)}{L \cdot E} = \frac{2\,[L + T\,(1 + \alpha)]}{\alpha\, LT} \tag{211}$$

$$\frac{L_s + L_p}{A_c} = \frac{4\,(W + T + \frac{\pi E}{2})}{WT} = \frac{4\,[W + T(1 + \frac{\pi\alpha}{2})]}{WT}$$

Since we have assumed that power capacity remains constant,

$$WTLE = \text{constant}$$

or

$$WT^2\, L\alpha = \text{constant}$$

Since L and T are set by the lamination shape, we will derive ratios which will help to identify those cores best suited for the application. Since any length stack can be used within reason, W is not "preset." Note that core and copper loss coefficient depend on L and W, respectively, and are, therefore, somewhat decoupled. Normalizing the L_e/A_w ratio, calling it R, and then removing W from the constraint gives

$$R = \frac{L + T\,(1 + \alpha)}{\alpha\, LT} = \left[\frac{1}{\alpha T} + \frac{1 + \alpha}{\alpha}\ \frac{1}{L}\right]$$

$$T^2\, L\, \alpha = K_o/W$$

The ratio R is maximized by setting its differential to zero

$$\partial R = -\frac{1}{\alpha T^2}\,\partial T - \frac{(1+\alpha)}{\alpha}\,\frac{1}{L^2}\,\partial L = 0$$

$$= -L^2\,\partial T - (1+\alpha)\,T^2\,\partial L = 0$$

From the constraint,

$$2T\,L\,\partial T + T^2\,\partial L = 0$$

$$T^2\,\partial L = -2TL\partial T$$

Substitution gives

$$L^2\,\partial T = (1+\alpha)\,2T\,L\partial T$$

and (207)

$$L/T = 2\,(1+\alpha)$$

Note that a common condition is $\alpha = 1$.

For this case $L/T = 4$. It is interesting also to note the outside core dimensions as α varies. Expressions for the core height and width are: $H = L + T = 2T\,(1+\alpha) + T$ and $D = 2E + 2T = 2\alpha T + 2T$. Their ratio is

$$\frac{T\,(3+2\alpha)}{T\cdot 2\,(1+\alpha)} = H/D = \frac{3+2\alpha}{2\,(1+\alpha)}$$

Again, for $\alpha = 1$, $H/D = 1.25$.

One of the most useful small cores (EE186-187) has $\alpha = 1$, $L/T = 3.66$, $H/D = 1.17$. A plot of L/T ratios for various α is given in Figure 56. It is shown in Figure 58 and in Figure 59 that cores do not become outlandishly shaped for extreme α, but retain a good degree of squareness ($H \cong D$). Also note that $L/D = 1$ for all α.

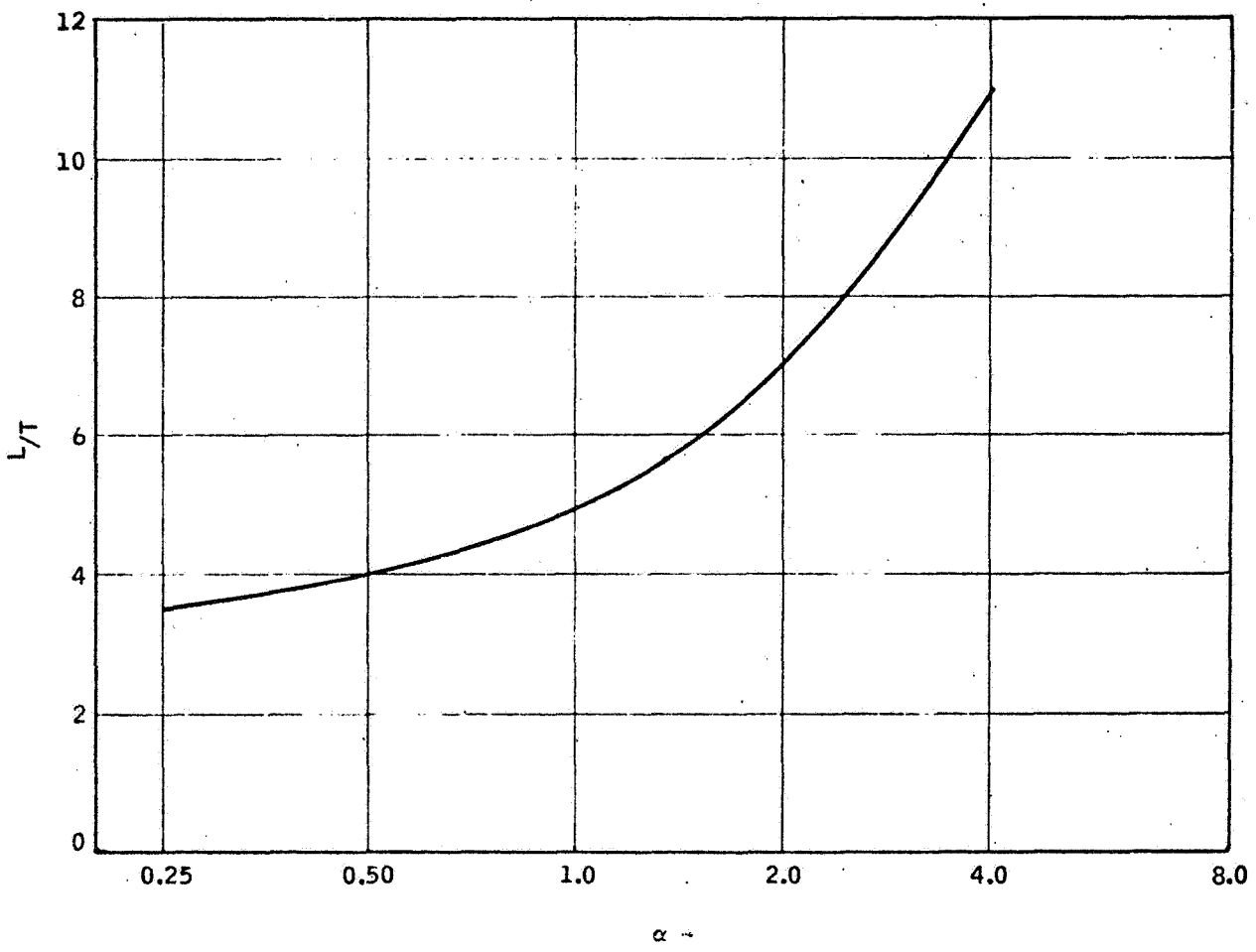

Figure 56. Optimum L/T Ratio versus α for E-I Cores

The same operations can be performed on the copper loss ratio:

$$\frac{L_s + L_p}{A_c}$$

Again, letting $E = \alpha T$ and normalizing,

$$R = \frac{W + T\,(1 + \frac{\pi\alpha}{2})}{WT} = \frac{1}{T} + \frac{(1 + \frac{\pi\alpha}{2})}{W}$$

For this constraint, L is not a variable; therefore, we can remove it.

$$WT^2\,\alpha = \frac{K_o}{L}$$

Again, optimizing R,

$$\partial R = -\frac{1}{T^2}\,\partial T - \frac{(1 + \frac{\pi\alpha}{2})}{W^2}\,\partial W = 0$$

$$W^2 \partial T + (1 + \tfrac{\pi\alpha}{2})\,T^2\,\partial W = 0$$

From the constraint

$$T^2 \partial W + 2TW\partial T = 0$$

and substitution gives

$$W^2 \partial T = (1 + \tfrac{\pi\alpha}{2})\,2T\,W\partial T$$

$$W/T = (2 + \pi\alpha) \qquad (208)$$

The graph of W/T versus α is given in Figure 57. A plot of W/D versus α is shown with H/D in Figure 58. Note that the ratios stay close to 1, indicating that cores with lowest loss coefficients are nearly cubic as shown in Figures 59a, 59b, and 59c.

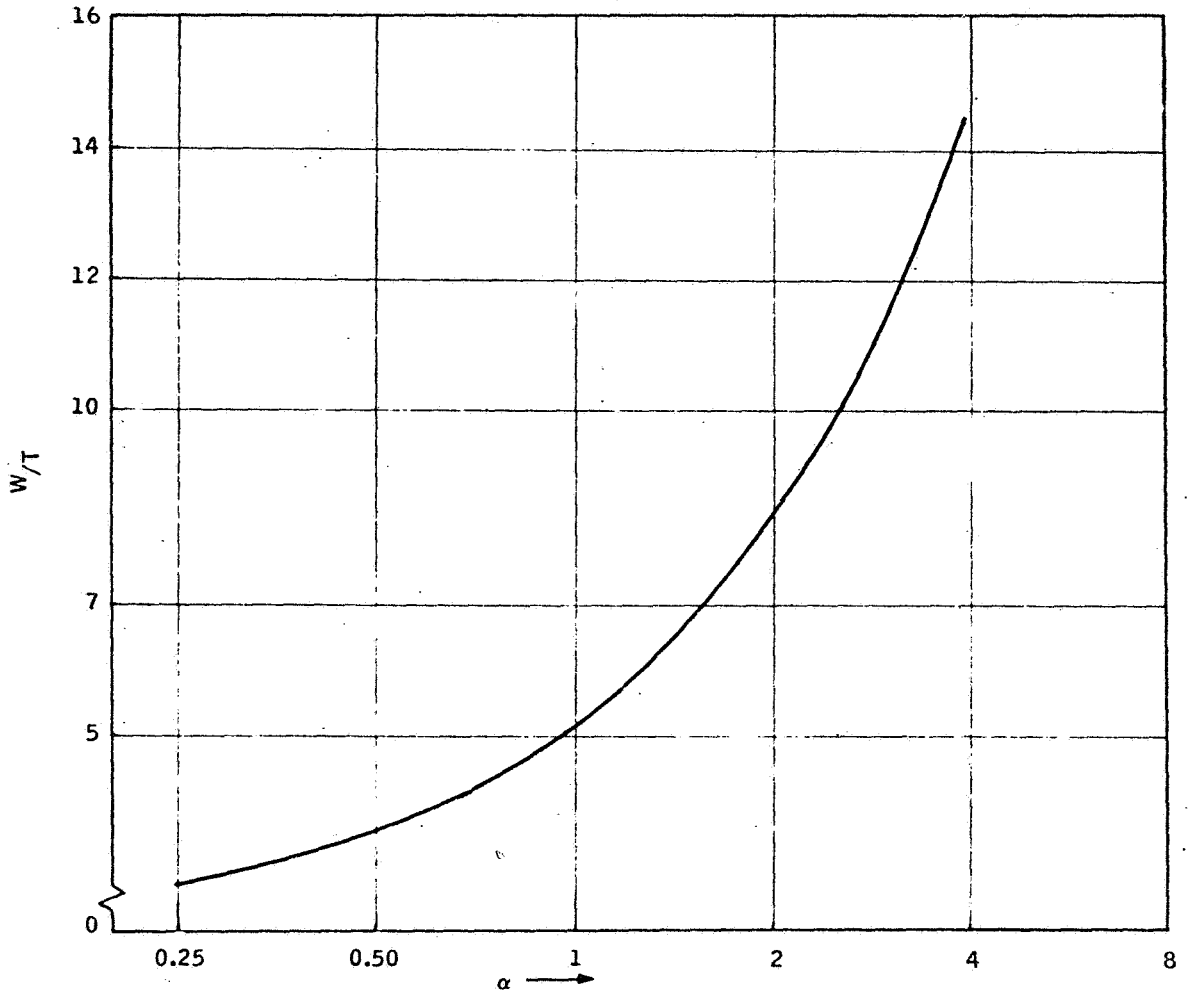

Figure 57. Optimum W/T Ratio versus α for E Cores

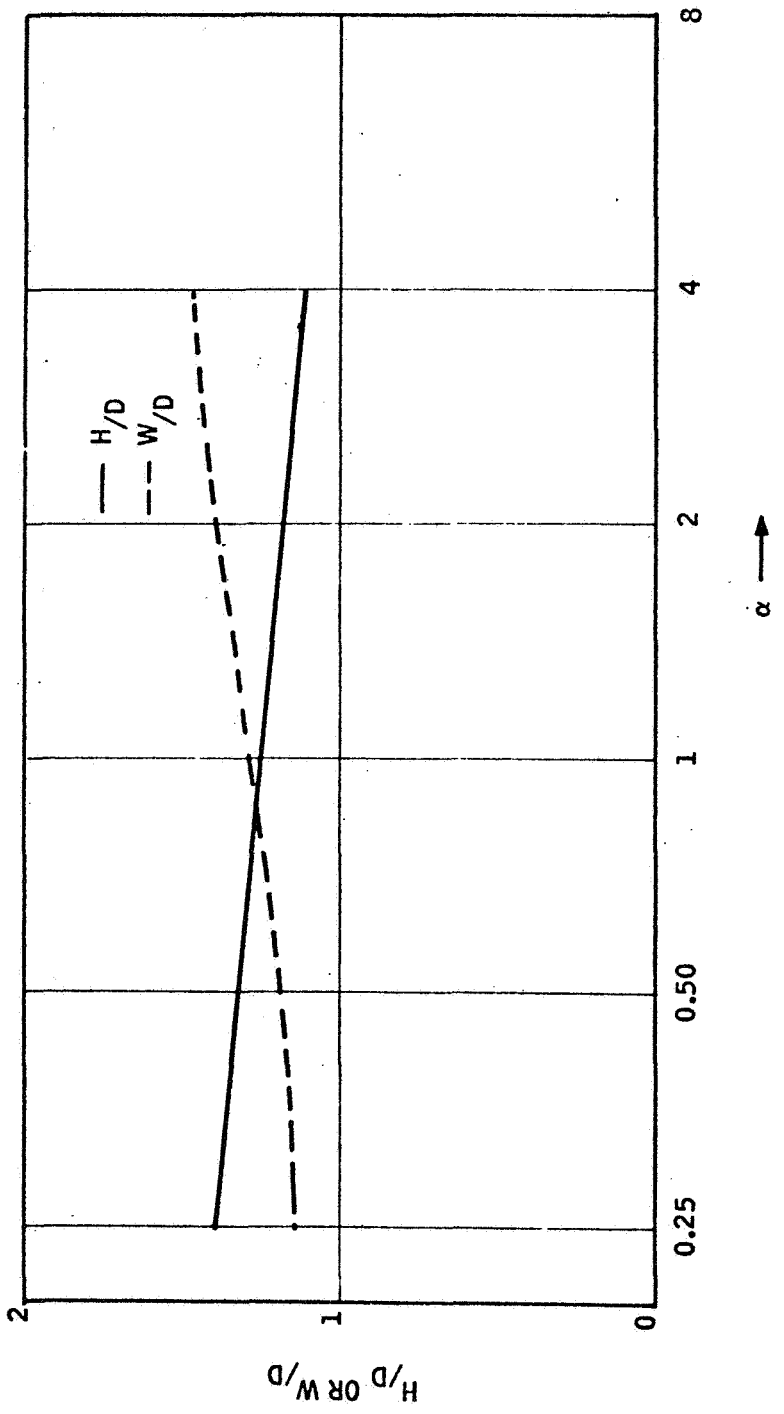

Figure 58. Optimum W/D Ratio versus α for E Cores

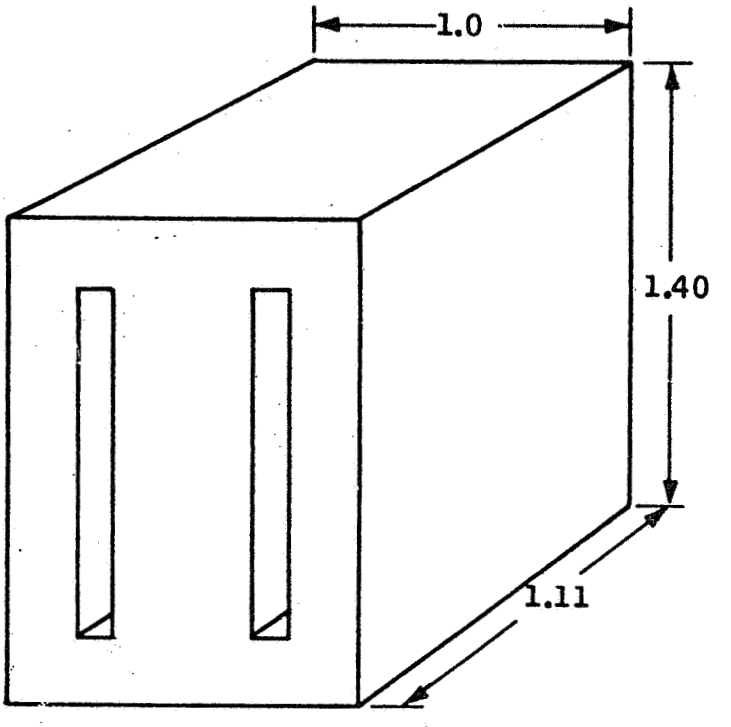

Figure 59a. Optimum Core Shape; α = 1/4

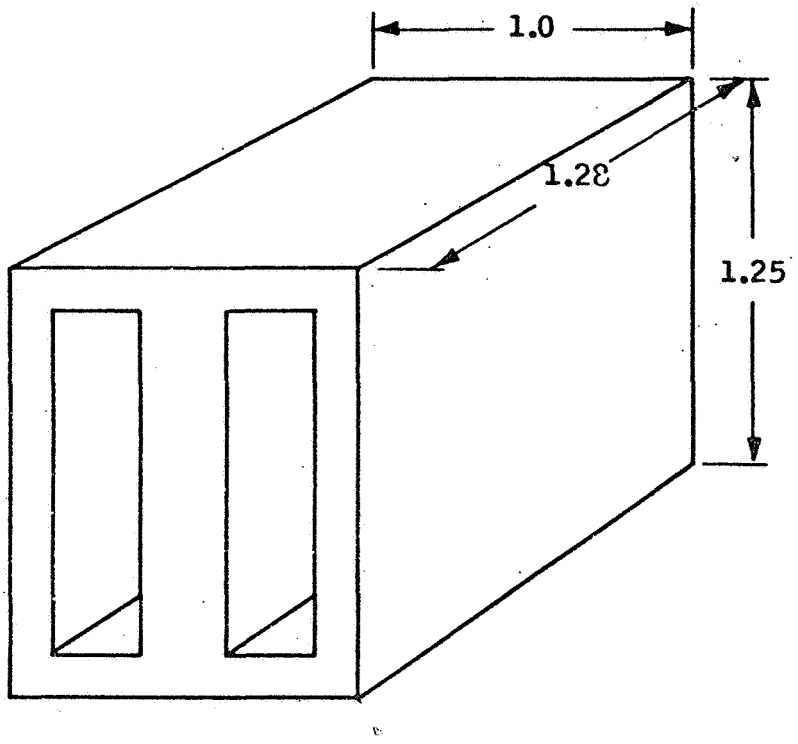

Figure 59b. Optimum Core Shape; $\alpha = 1$

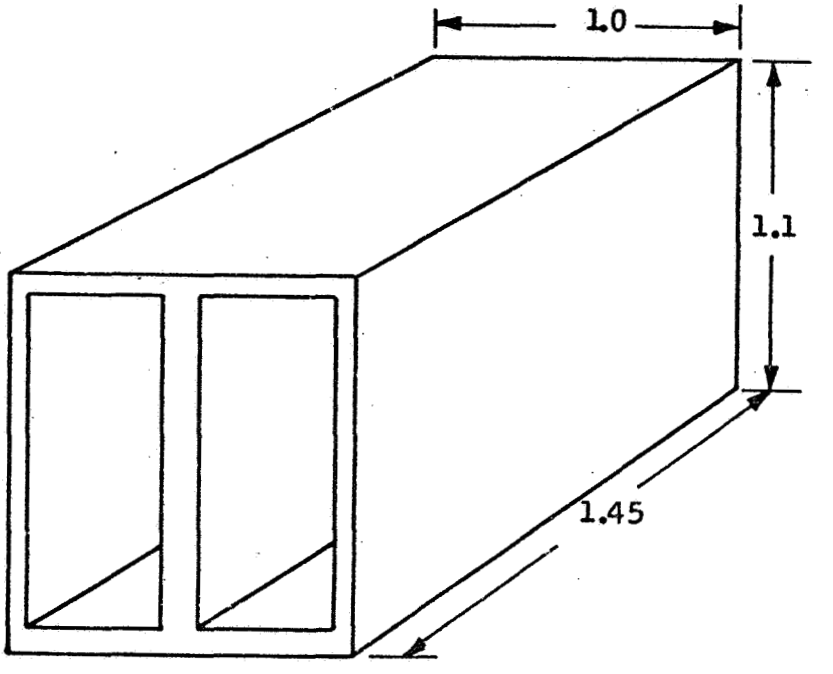

Figure 59c. Optimum Core Shape; $\alpha = 4$

Another important transformer parameter is the overall volume as expressed by the product of the linear dimensions. It is usually desirable to produce signal level and small power transformers in the minimum volume since they must be packaged in other equipment.

The dependence of volume on chosen lamination shape may be derived for the core shown in Figure 55.

$$V = (2T + 2\alpha T)(L+T)(W + 2\alpha T)$$
$$= 2(\alpha T^2 LW)\frac{(1+\alpha)}{\alpha T}\left[1 + \frac{2\alpha T}{W} + \frac{T}{L} + \frac{2\alpha T^2}{LW}\right] \quad (209)$$

Now

$$\alpha T^2 LW = A_c A_w \quad (210)$$

This is a quantity calculated as the first step in the design; therefore, it is a known quantity. Substitution of (210) into (209) gives

$$V = 2A_c \cdot A_w \left(\frac{1+\alpha}{\alpha T}\right)\left(1 + \frac{2\alpha T}{W} + \frac{T}{L} + \frac{2\alpha^2 T^4}{K}\right) \quad (211)$$

Note the uniqueness of this equation.

The product $(A_c A_w)$ is known and α is a design parameter; W/T and L/T are each functions of α alone for the best efficiency. Thus, the volume varies as a function of (αT) for a given power level $(A_c A_w)$.

The derivative of volume with respect to T, set to zero, may be used to determine the minimum volume as a function of T:

$$\frac{dv}{dT} = \frac{2 A_c A_w (1+\alpha)}{\alpha T}\left(\frac{8\alpha^2 T^3}{A_c A_w} + \frac{2\alpha}{W} + \frac{1}{L}\right) = 0$$

Simplifying, the result is

$$\alpha T^2 = \sqrt{\frac{A_c A_w}{6}} \tag{212}$$

Thus, for the condition where W and L are fixed by efficiency considerations, (αT^2) for minimum volume may be found. This is not, by any means, a general result. We actually want to compare transformer volume for different core geometries. This must be basically a trial and error process since none of the parameters are fixed until a core type is chosen. When the core type is selected, all of the parameters are then determined. Thus these equations can only be used as a guideline. Core families (L/T a fixed ratio, W/T = 1, for example) may be compared, however, by expanding the derivative to include variation of α.

The size of the suspension output transformer was approximately determined in Section II to estimate losses. The detailed design follows much the same procedures but is modified by the equations derived in the previous paragraphs. Other efficient core shapes are considered and three transformer designs are compared. Two of them are then considered for the breadboard work.

In Section II study, the equation relating current, voltage, and frequency was derived. Symbols used and design parameters are

C_T	=	Capacitance of electrode	117 pf
I_{pp}	=	Peak primary current	1.83 amp
I_{prms}	=	rms primary current	0.145 amp
M	=	Turns ratio	65
V_s	=	Source voltage	35.2 volts
γ	=	Winding efficiency	0.32
A_p	=	Primary wire area (No. 28)	172.3×10^{-6} in.^{2}
A_s	=	Secondary wire area (No. 40)	12.56×10^{6} in.^{2}

It was noted that the minimum secondary area is limited by the minimum wire size recommended for transformer windings, and not by current density. More space for this winding is required; this places a premium on a (small) choice of ℓ_c/A_w (core loss coefficient) for the most efficient design.

Other parameters are:

$$A_w/N_s = 95.2 \times 10^{-6} \text{ in.}^2/\text{secondary turn}$$

$$A_c \cdot N_s = 1100 \text{ in.}^2 - \text{secondary turn}$$

Therefore,

$$A_w A_c = 0.1045 \text{ in.}^4$$

This product is the basic determinant of core type and size. Many shapes can produce this product; the final selection must be made on the basis of relative core loss, number of turns, and volume. An indicator of which core is most volume-efficient is the comparison of (αT^2) for each core with the optimum value obtained by substituting the value of $(A_c A_w)$ given above into Equation (212).

$$\alpha T^2 = \sqrt{\frac{A_c A_w}{6}} = 0.131$$

The characteristics of cores in this range are listed in Table XIX.

Copper loss in this transformer is part of R_1, the charging resistance. This is determined by bandwidth (risetime) and requires padding; it is not a factor in core selection. The cores producing the least volume with lowest ℓ_e/A_w ratios are the EI-375 and the EI-21.

Transformers based on each of these cores were designed. The first unit built to test the feasibility of this core was the EI-375. It was intended that if difficulties were encountered because of the long stack (bobbin tolerance, etc.) the EI-21 would be tested. The EI-375 transformer outline is shown in Figure 60. A picture of the finished EI-375 is shown in Figure 61. The prints used to build the transformer are Figures 62 and 63. Note how well the αT^2 product predicted the range of minimum volume cores.

Bobbins were designed for each of the transformers. The outlines are shown in Figures 64 and 65 [SK53642-(HV-375) and SK53653-(HV-21)]. These were built into two transformers, HV-375 (SK53643) and HV-21 (SK53652). The calculated values for core loss are

HV-375 = 1.40 W

HV-21 = 1.41 W

The output circuit into which these transformers were built is shown in Figure 66.

TABLE XIX. - CORE CHARACTERISTICS

Parameters \ Core Types	EI-27	EI-375	EI-50	EI-21	EI-625	EI-75
$A_c A_w$	0.0176	0.03276	0.047	0.0635	0.114	0.237
α	0.667	0.832	0.50	0.624	0.5	0.5
αT^2	0.0936	0.117	0.125	0.156	0.195	0.281
$\ell_e/\alpha W$	18.00	12.31	15.96	12.79	12.80	10.66
$\frac{\ell_s + L_p}{A_c}$	14.3	18.4	14.4	17.25	18.9	27.0
W/T	5.96	3.19	2.23	1.65	0.92	0.44
W(in.)	2.24	1.2	1.11	0.825	0.575	0.33
A_c	0.84	0.45	0.55	0.412	0.359	0.247
N_s	1310	2450	1980	2690	3060	4450
Vol ($in.^3$)	3.00	2.82	3.02	3.10	3.52	5.0
W/T_{opt}	4.0	4.5	3.5	3.9	3.5	3.5

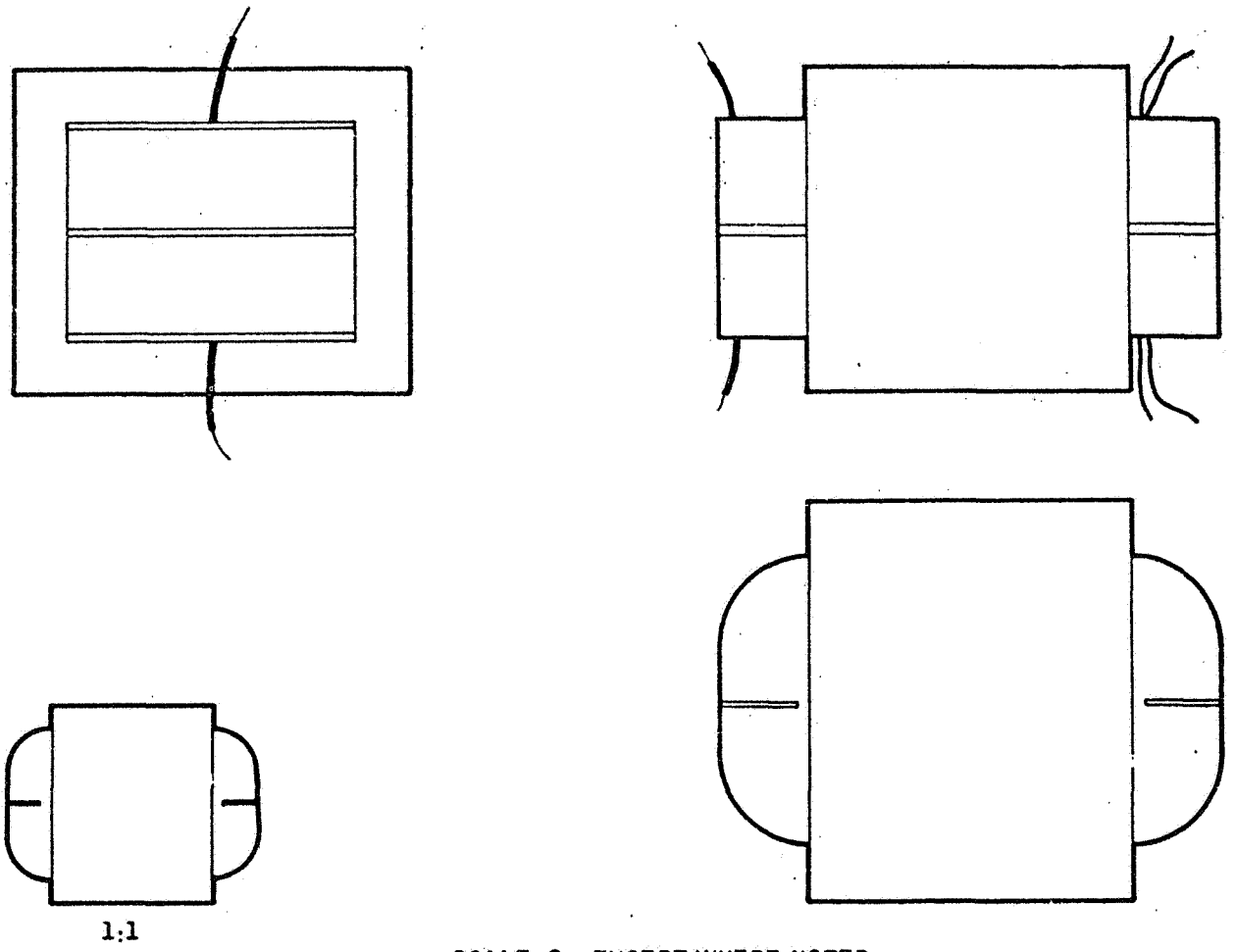

Figure 30. EI-375 Output Transformer Outline

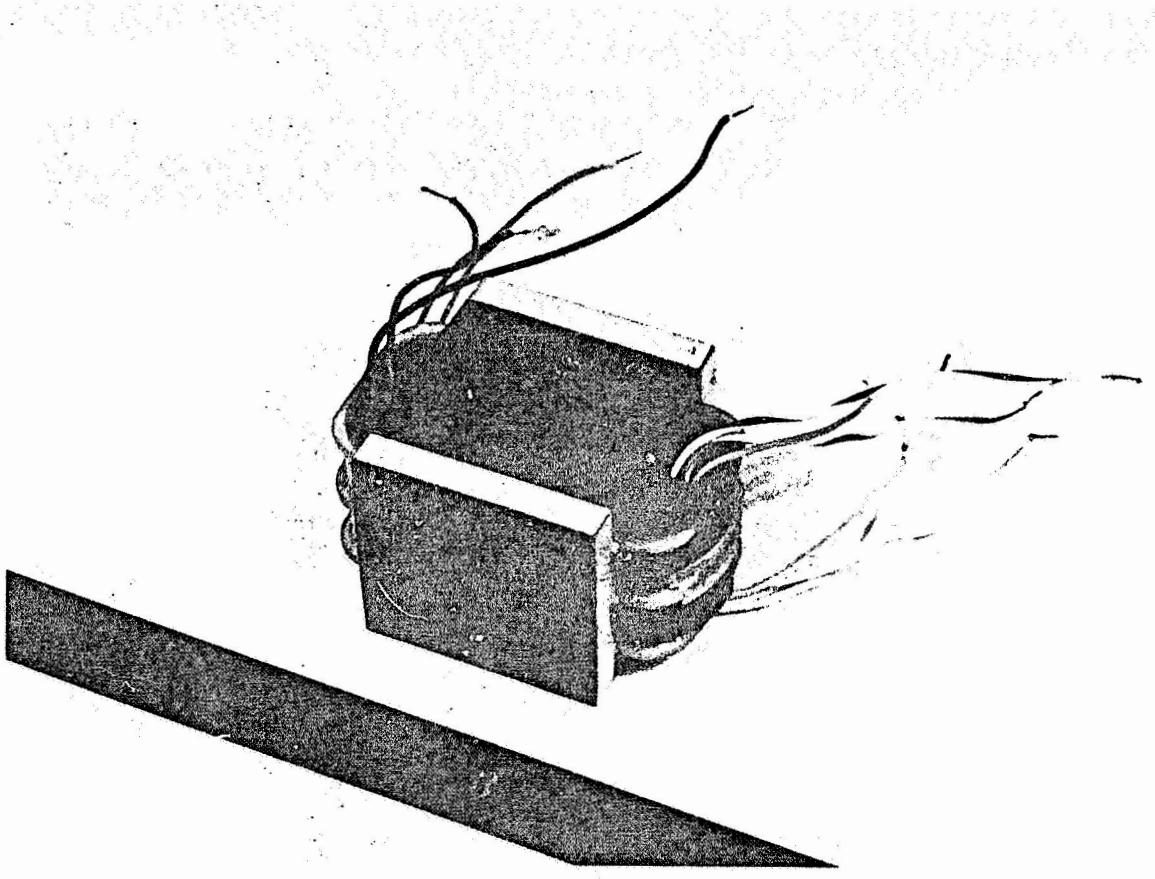

Figure 61. Finished EI-375 Transformer

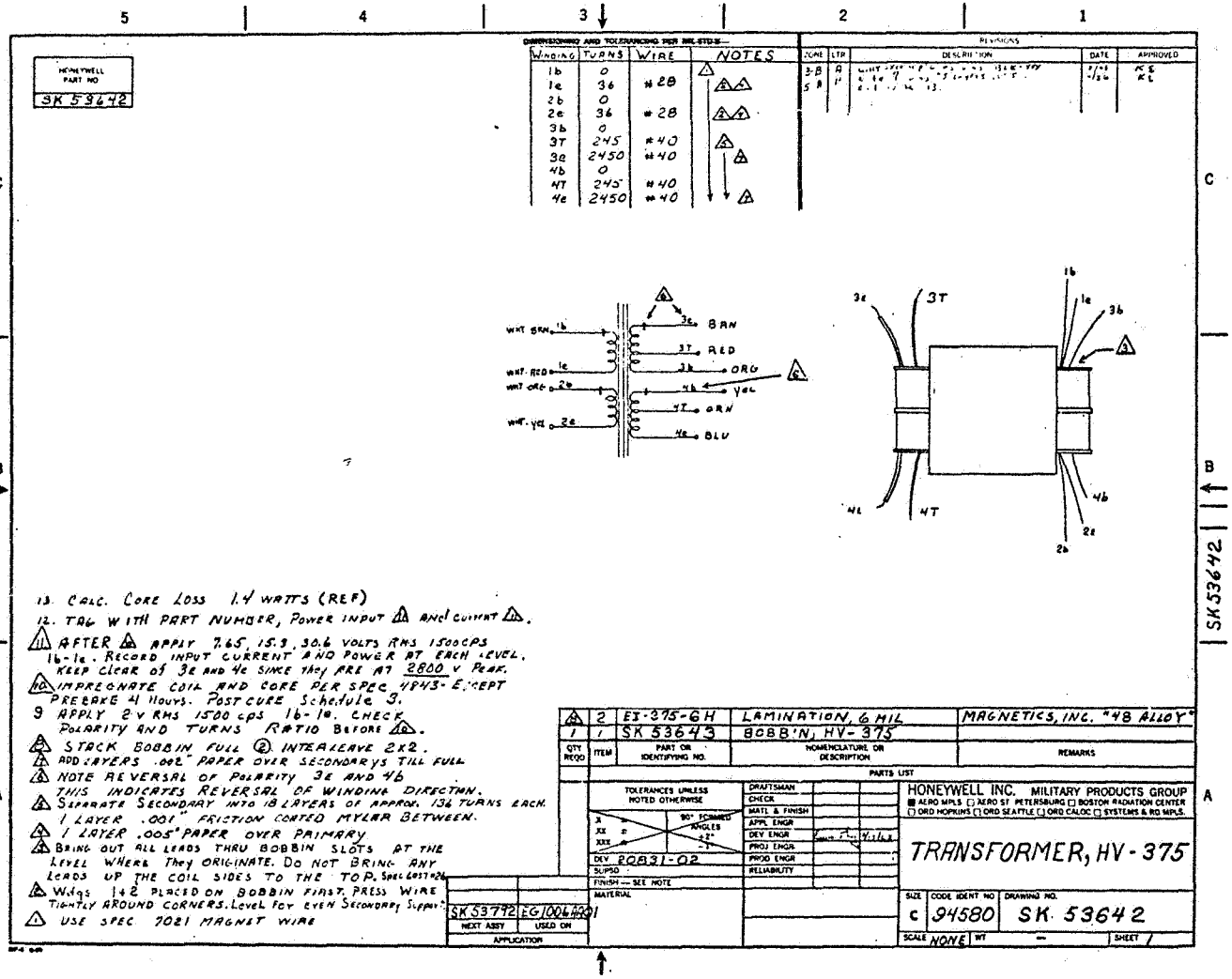

Figure 62. HV-375 Transformer Drawing

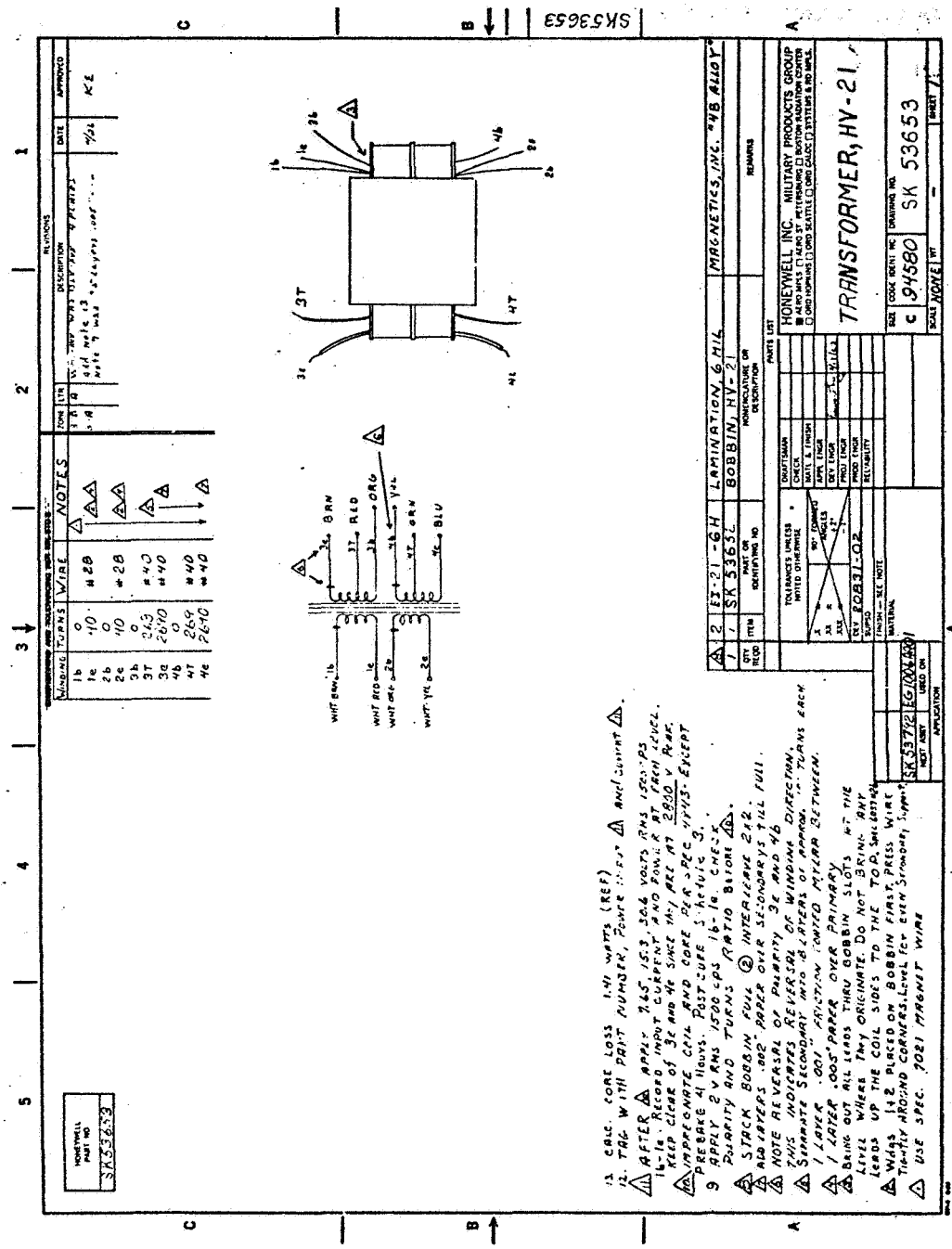

Figure 63. HV-21 Transformer Drawing

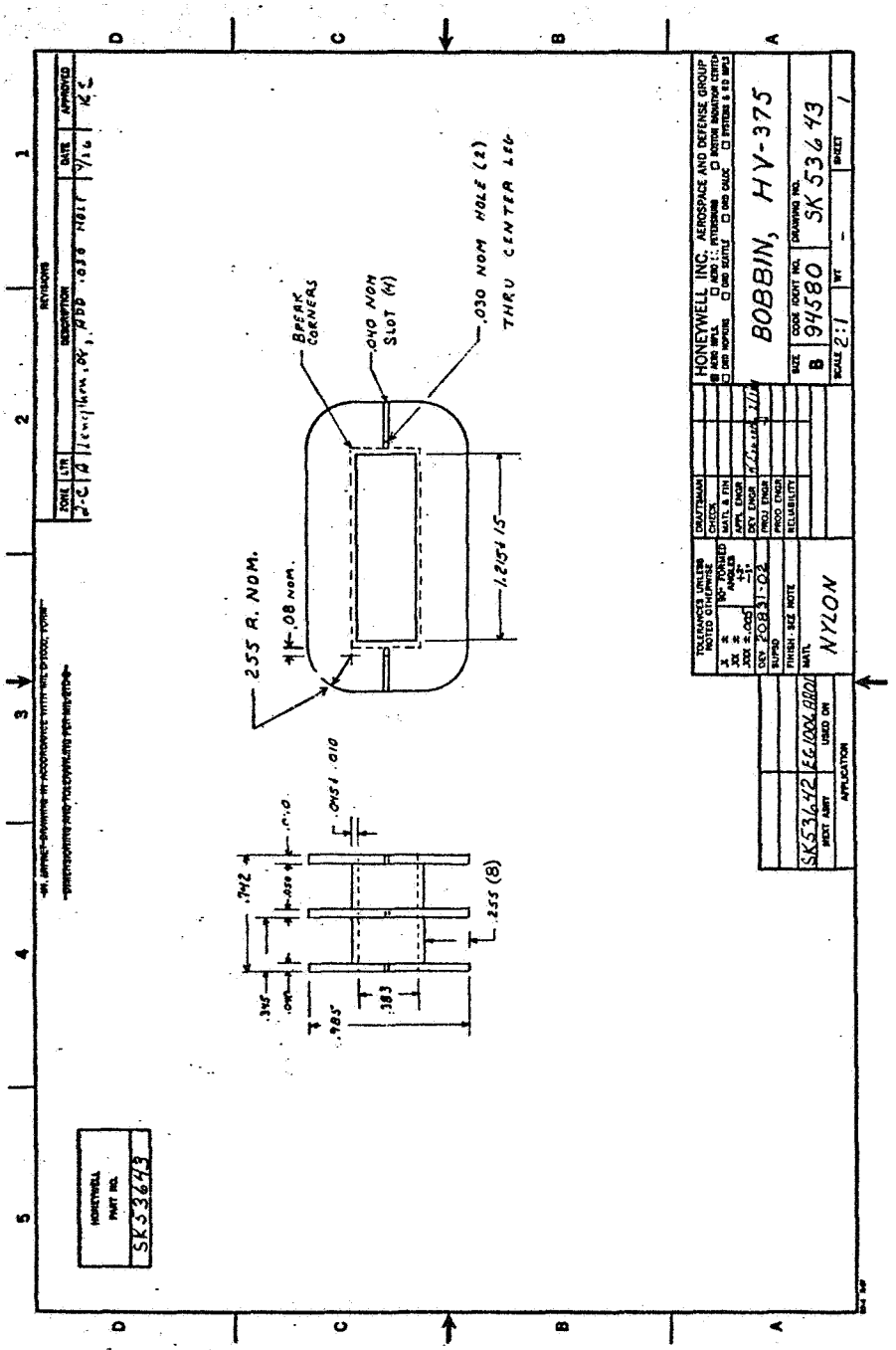

Figure 64. HV-375 Bobbin Drawing

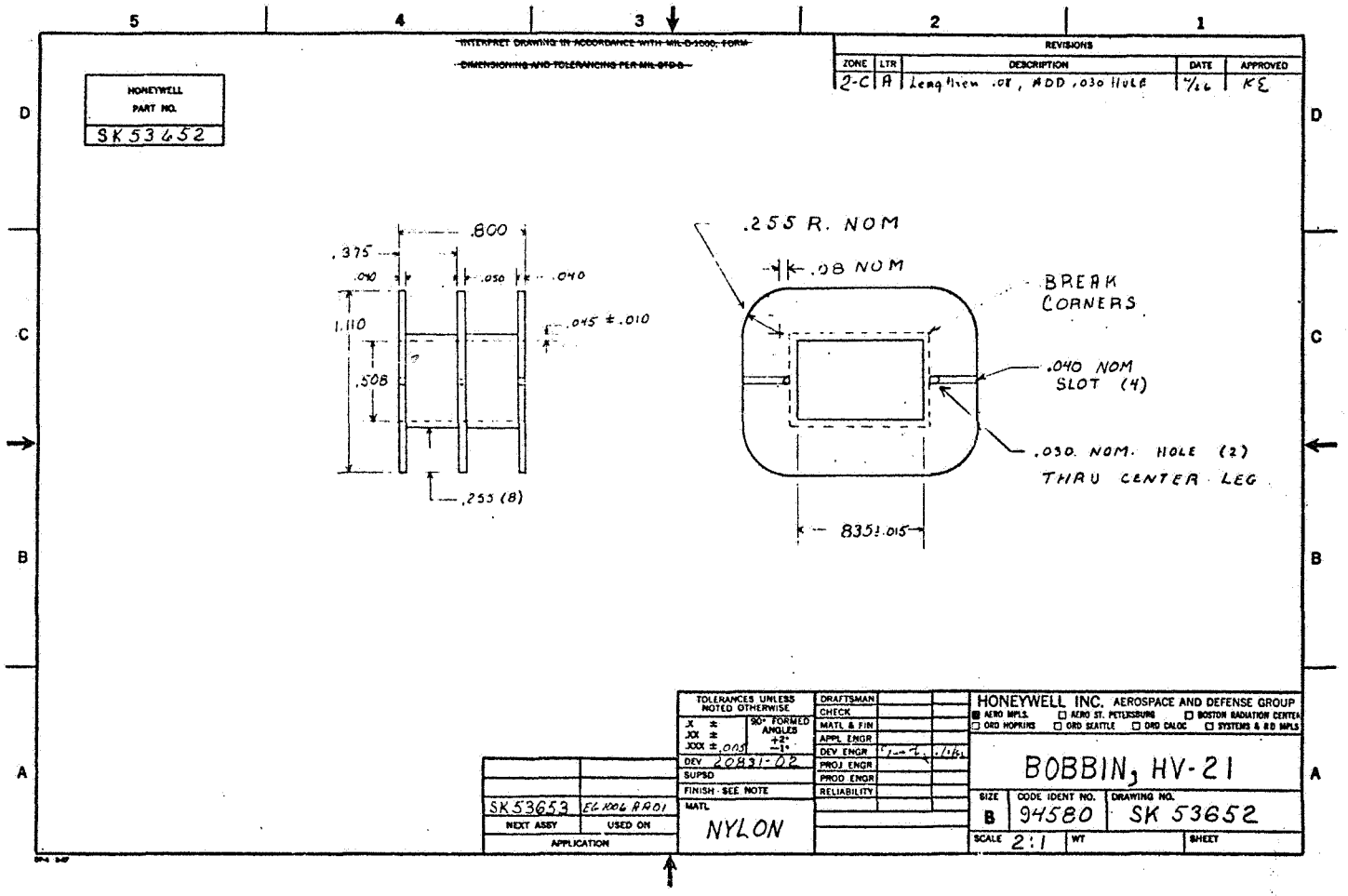

Figure 65. HV-21 Bobbin Drawing

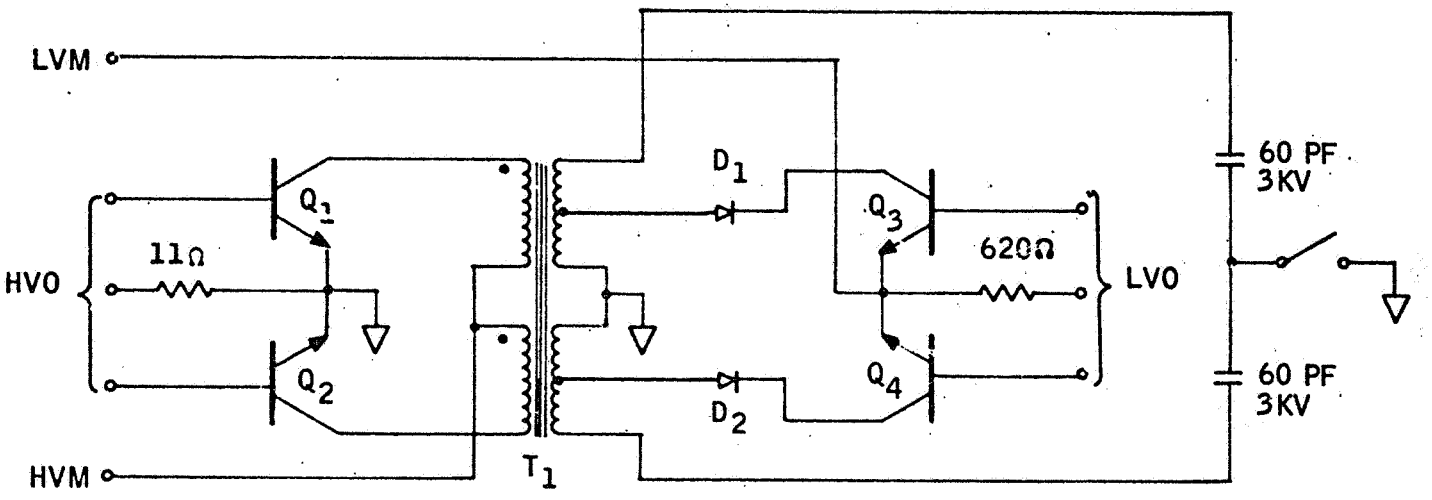

D_1, D_2 1N5006 OR MR1337-5

Q_1, Q_2 2N4897

Q_3, Q_4 SE7030

Figure 66. Output Circuit Diagram

Low G mod amp. -- The low G mod amp must have the following capabilities:

- Provide a summing point at its input
- Produce a negative going 0 to -4 volt output
- Drive 1k Ω resistor
- Low power consumption

It was decided to use an integrated amplifier, μ a 709 operated at ±6 volt. This device was selected because of its apparent ability to drive close to the negative supply, retain reasonable voltage gain at reduced supply voltage, and drive the 1k Ω load. The power input is expected to be approximately 12 mW since the amplifier looks like a 12k Ω resistor for other supply voltages. A diode clamp is used so that the output cannot be driven positive during transients. The usual compensation networks are added and the final design is shown in Figure 67.

High G mod amp. -- The high G mod amp must have the following characteristics:

- Maximum "full on" efficiency
- Handle two-amp pulse currents
- Have low-bias power
- Small crossover distortion
- Zero output at zero input
- Internal impedance less than 10 percent of effective load resistance
- Handle reverse currents

The last item is necessary to ensure discharge of the equivalent output capacitance during falling transients. The design is divided into four sections: the input stage, a current source to reduce crossover distortion, a PNP-NPN output stage, and the stabilization networks.

The transfer function of the amplifier may be calculated from Figure 68. Its gain is

$$\frac{e_o}{e_{in}} = \frac{R_f}{R_i} \quad \frac{\beta}{1+\beta}$$

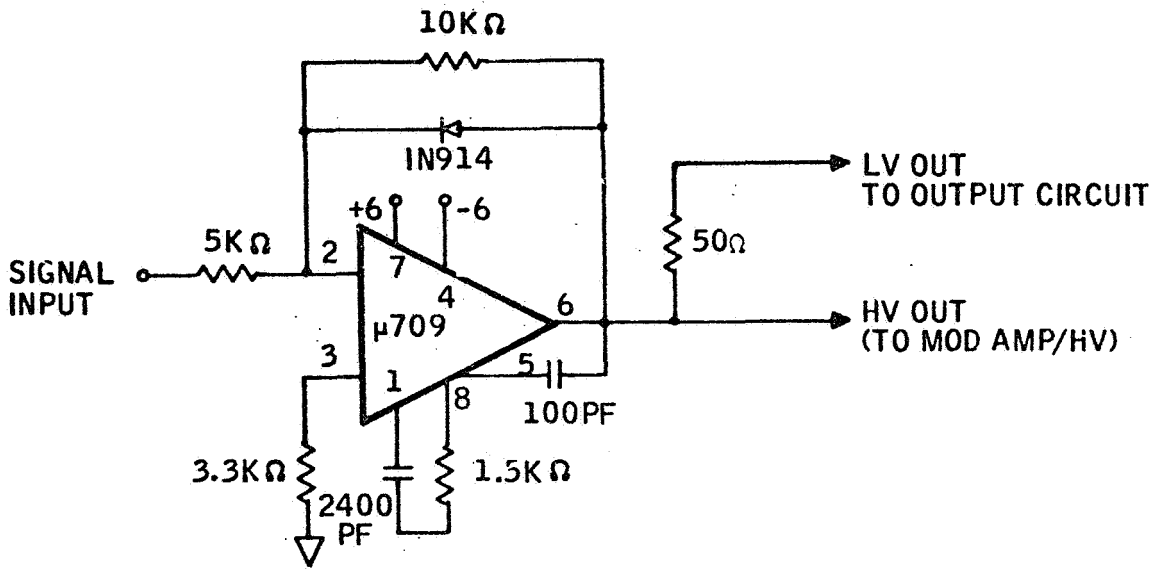

1. A BIAS CIRCUIT WILL BE ADDED
2. MUST BE TESTED FOR NEGATIVE INPUT STABILITY
3. TESTED FOR OPERATION ABOUT ± 6V
4. PIN 4 (-6V) CONNECTED TO CASE - BE CAREFUL

Figure 67. Low-Voltage Mod Amp Circuit Diagram

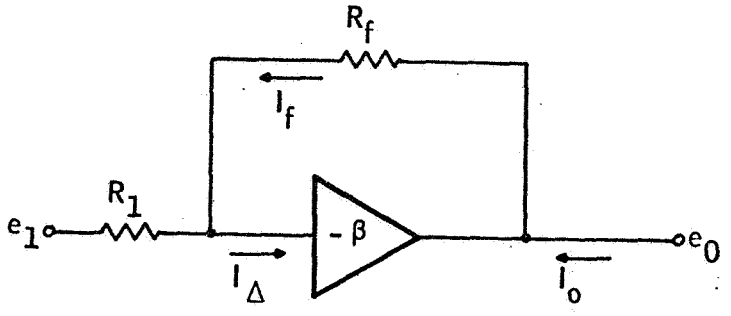

Figure 68. Operational Amplifier Circuit Diagram

The output current and voltage are related by the effective output impedance R_o:

$$R_o = \frac{e_o}{I_o} = \frac{I_f R_f}{\beta I_\Delta} = \frac{R_f}{\beta}$$

Thus, the usual feedback resistance of the order of 10^4 ohms must be around an amplifier with current gain of the order of 10^4 amps per amp. The input resisistance is included as part of β for these calculations.

The input stage controls amplifier drift and bias levels. To keep drift low and bias at zero with zero input, a differential stage is used. The balance requirements are not stringent since this is an output amplifier, and a pair of unmatched high-gain transistors are used. A current source from emitters to the negative supply completes this stage.

The output stage requirements conflict seriously. For example, the amplifier must be capable of handling two amps, 35 volts, but must be biased at a level of half watt or less to be compatible with the real power use of the suspension. Consequently, two stages must precede the output in order to bring the bias current level within acceptable bounds. These stages also provide the necessary current gain, but produce zero-crossing offset. The output drive stages are PNP-NPN and NPN-PNP, which produces a symmetric, high-gain circuit easily biased at near the 18-volt level with low-power dissipation.

To reduce the effect of zero-crossing offset, a current source must be used. This stage is interposed between the differential input and the output driver.

It is a grounded-base, emitter-input stage and also serves as the amplifier initial adjustment point. The amplifier is shown in Figure 69.

The amplifier as conceived in the preceding paragraphs has the following gain phase characteristics (approximately).

	Static Gain	Gain at Frequency of
Input stage	G = 60	hfe = 1 at 6 mc
Current source/1st driver	G = 2	hfe = 1 at 100 mc
Second driver stage	G = 50	hfe = 2 at 100 mc
Output stage	G = 50	hfe = 2 at 60 mc
Bias networks	G = 1/4	------

The input stage rolloff also takes into account the capacitive effects (estimated). Total amplifier gain equals 75,000 nominal (98 dB) with phase crossover nominally at 3 mc. These stages produce a characteristic as shown in Figure 70. The output resistance determines the required loop gain. The effective resistance as seen by the output switching transistors is in the 10 ohm range; therefore, a 1-ohm output resistance at 1500 cps is desired. Thus, a loop gain of 80 dB is needed at this frequency with a 10k Ω feedback resistor. This point is plotted in Figure 71; the two networks needed are shown also. Since nominal values for the gains and stage rolloff frequencies have been used, the analysis is only approximate. Networks shown will be finalized during the testing phase when the necessary impedance is known.

Crossover of the compensation shown is at about 2 mc. Estimated phase margin is 40°.

VARIABLE-VOLTAGE POWER SUPPLY

A variable-voltage supply is necessary to achieve the dual purpose of providing a large-output capability for high G inputs and low-power consumption under less rigorous conditions. The principle may be illustrated very simply (see Figure 72). For applications of this type, a constant value load is usually driven from a constant voltage supply, but the maximum voltage to which the load must be driven is lower for the less rigorous conditions.

From Figures 72a and 72b, we see that for constant V_1, the output power drops as the square of e_o, but the input only drops linearly. Thus, for wide disparity between e_o and V_1, a very inefficient system results; power can

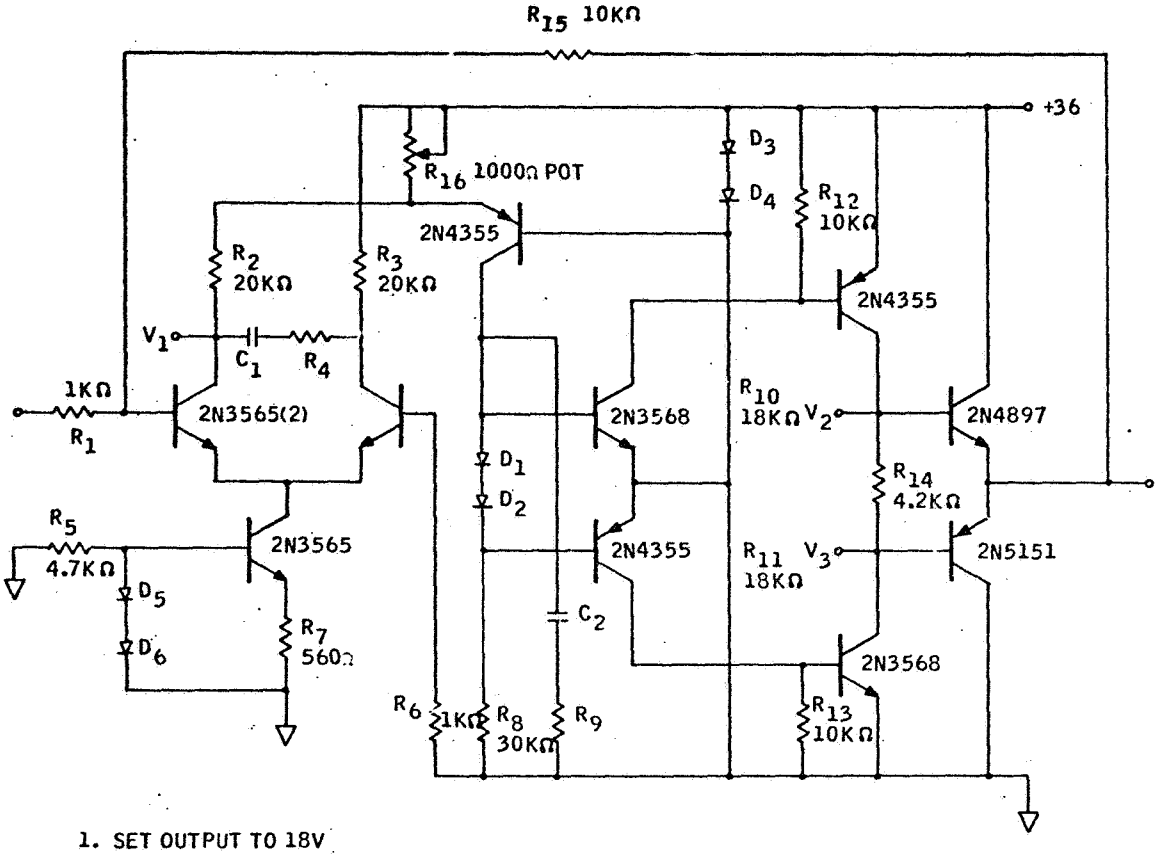

1. SET OUTPUT TO 18V
2. SET R_{16} TO V_1 = 23.5V
3. SELECT R_8 SO $V_2 - V_3 = 0.7V$
4. C_1, C_2, R_4, R_9 TO BE SELECTED DURING TEST
5. $D_1 - D_6$ 1N4610

Figure 69. Mod Amp Output Section, High-Voltage Mod Amp Circuit Diagram

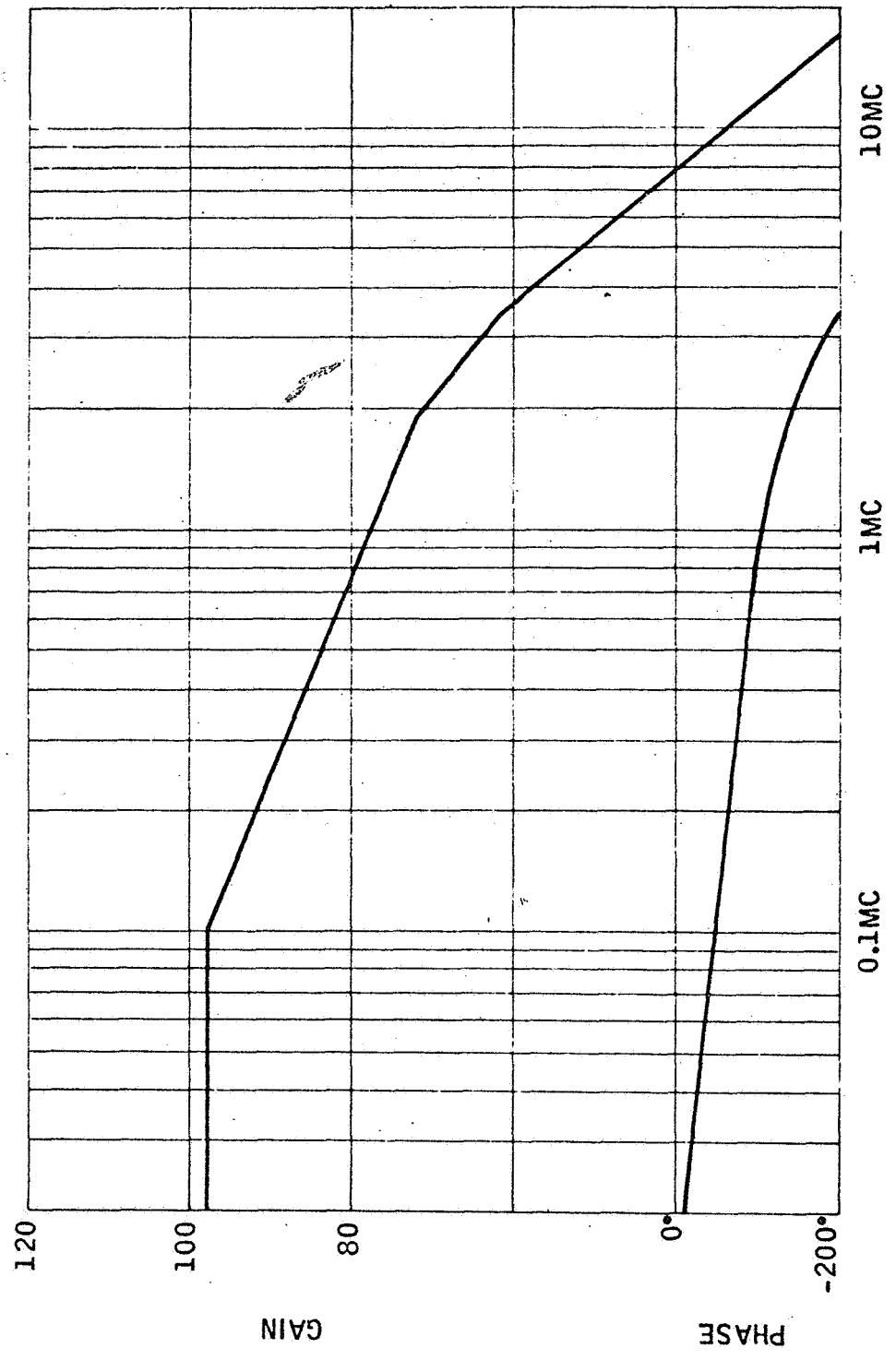

Figure 70. 20 Log Gain versus Frequency - Uncompensated Mod Amp

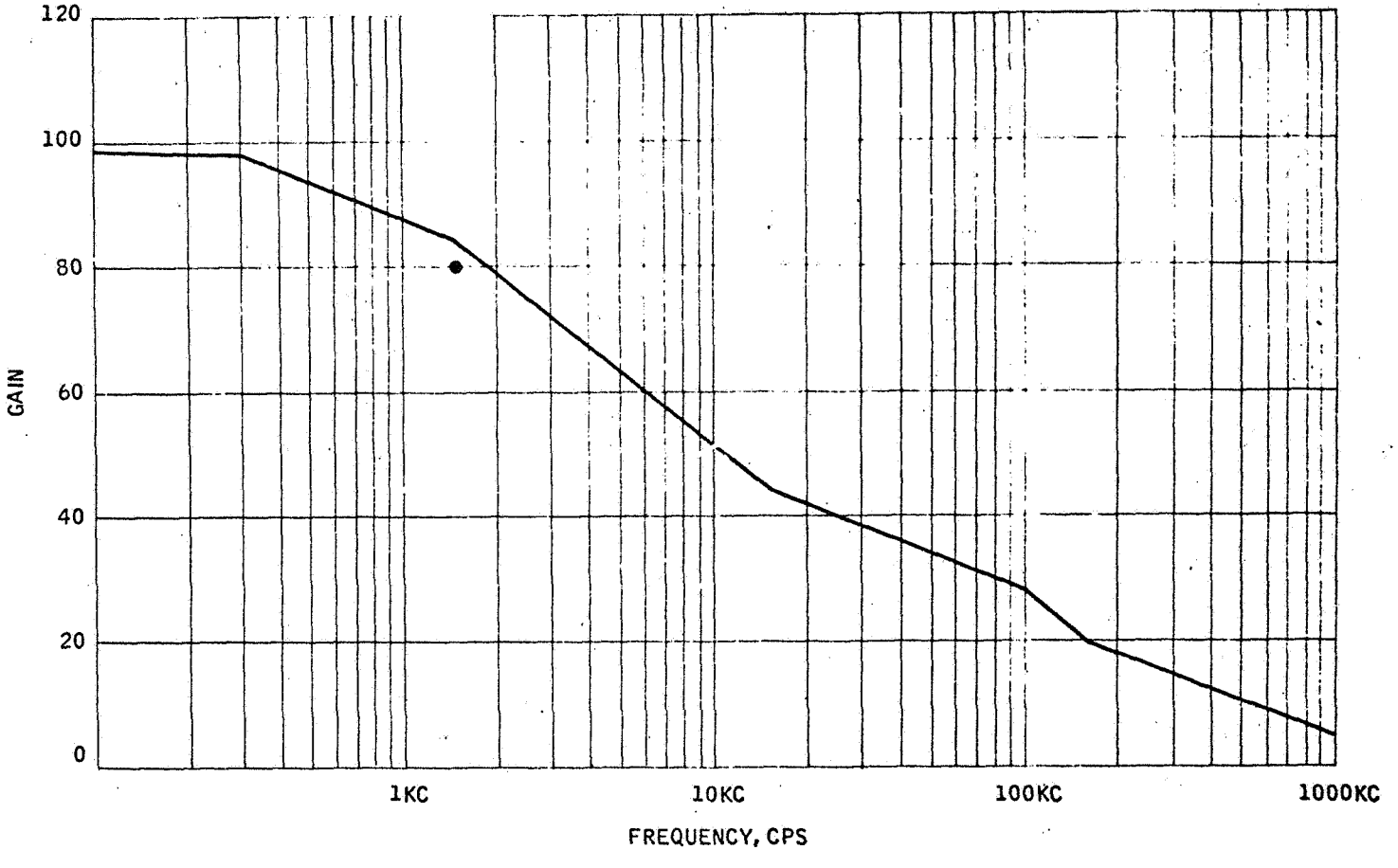

Figure 71. 20 Log Gain versus Frequency - Compensated Mod Amp

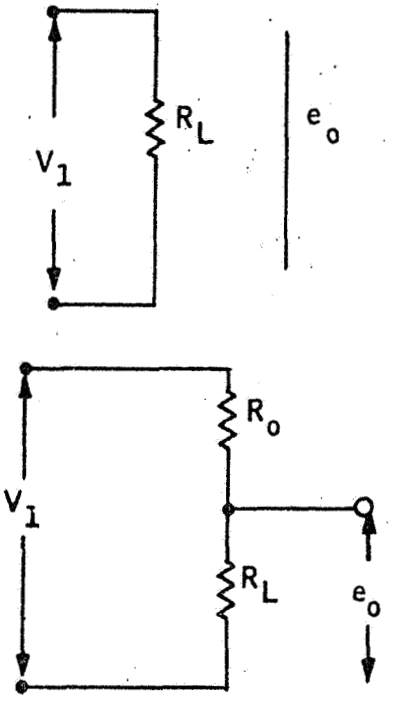

$e_o = V_1$

$P_{in} = V_1 \times \frac{e_o}{R_L}$

$P_o = \frac{e_o^2}{R_L}$

$\eta = \frac{P_o \times 100}{P_{in}} = 100\%$

FOR $V_1 = 35V$, $R_L = 350\Omega$, $P_o = P_{in} = 3.5W$

$P_o = e_o^2 / R_L$

$P_{in} = V_1 \frac{e_o}{R_L}$

$\eta = \frac{P_o \times 100}{P_{in}} = \frac{e_o}{V_1} \times 100\%$

FOR $V_1 = 35V$, $R_L = 350\Omega$, $\eta = 50\%$

$P_o = 0.875\ W$, $P_{in} = 1.750W$

Figure 72. Variable-Voltage Power Supply Circuits

be saved by reducing V_1. An example can be made of the suspension which is being designed. At maximum output, 100 G's is produced; the orbit or low-power condition is defined as a region of 0.01 G or less. The voltage ratio necessary to produce this output force ratio is 100:1. This voltage must be produced by a transformer. With semiconductor output devices (0.3 to 0.5 volt drop), a 100:1 range can only be accommodated efficiently by a 300 to 500 volt supply. This is impractically high; therefore, the turns ratio must also be changed when the range is changed. The high-range maximum voltage for our example is 35 volts from a 36-volt supply. Low-range maximum is 4 volts from a 6-volt supply. Load resistance is constant at about 350 Ω. Table XX lists the various valves of power required.

TABLE XX. - POWER CONSUMPTION

Range	High	High	High	Low	Low
Output Voltage	35V	17.5V	3V	3V	1.5V
P_o	3.5W	0.875W	0.026W	0.026W	0.0065W
P_{in}	3.6W	1.80W	0.308W	0.052W	0.026W
η	97%	48.6%	8.5%	50%	25%

Thus, the change from the 35-volt supply to the 6-volt supply makes a difference of 256 mW in just one output circuit. To this must be added the cost (in power) of biasing a 35-volt modulator and the 36-volt power supply. For our design, this bias power is of the order of 350 mW and 500 mW respectively.

The bias must be switched off and networks reset for the maintenance of stability in the suspension loop. This must be accomplished in a very short time. The switching will be done in a 0.01 G or lower ambient. To keep the rotor centered to within 200 micro inches means a "dead" time of less than 0.4 microseconds. This problem was discussed in Section III.

An important problem is the unavoidable transient which occurs when the bias is switched to zero. This transient can only be controlled by the active low-output impedance-modulation amplifier. The high-range supply must be "on" until this transient is reduced to negligible value. Finally, the supply must go to zero volts. These operations can be accomplished by a switch and supply with the following characteristics.

1. "Low G" control switches bias, networks, and timing circuit simultaneously

2. Bias goes to zero

3. Networks switch to new value

4. Timing circuit runs high-range supply to zero

The timing circuit can be a simple R-C discha· ge into a (nonlinear) transistor switch circuit. The circuit design is shown in Figure 73.

TEST OF CIRCUITS

The circuit test results are reported in the same order as the design of the circuits are presented. Any design changes resulting from these tests are noted. The power consumption, efficiency, and dynamic capability are discussed for each circuit.

Oscillator - Power Amplifier

The final schematic for the oscillator-power amplifier is shown in Figure 74 (SK 53791). Transformers T_1 and T_2 are shown in Figures 75 and 76 (SK 53640 and SK53641), respectively. The oscillator was tested no-load and with a 51 Ω resistor in series with a diode as an equivalent load. The power amplifier was also tested under loaded and no-load conditions; the load consisting of a diode and 1 Ω resistor in series. Output current was 344 mA compared to a (calculated) maximum of 408 mA (nominal 300 mA) when the circuit is operated. Results of the tests are tabulated in Table XXI.

No changes were made in either design. The oscillator peaking capacitor (C_1) had the effect of reducing overshoot if a large (10,000 pF) value was used; it was omitted during subsequent testing. Peak currents are high enough that a capacitor is needed across the device terminals to reduce power-line cross coupling. No-load power is the sum of feedback, case, and magnetizing losses. Earlier calculations predicted the power to be 4.98 mW; thus, agreement is quite close in this area. Load losses were estimaged to be 1.25 mW; copper loss was estimated to be 0.95 mW. The actual load loss is 25.8 - 19.3, or 6.5 mW. Removing the 5.2 mW no-load losses yields 1.3 mW for actual copper loss.

Power amplifier no-load power input of 45.5 mW compares to the calculated value of 39.1 mW; however, load loss (42.5 mW) is less than the 49.8 mW calculated. A check of the calculation shows that full-power output was assumed (408 mA versus 344 mA). When the test conditions are assumed, good correlation with test results occur.

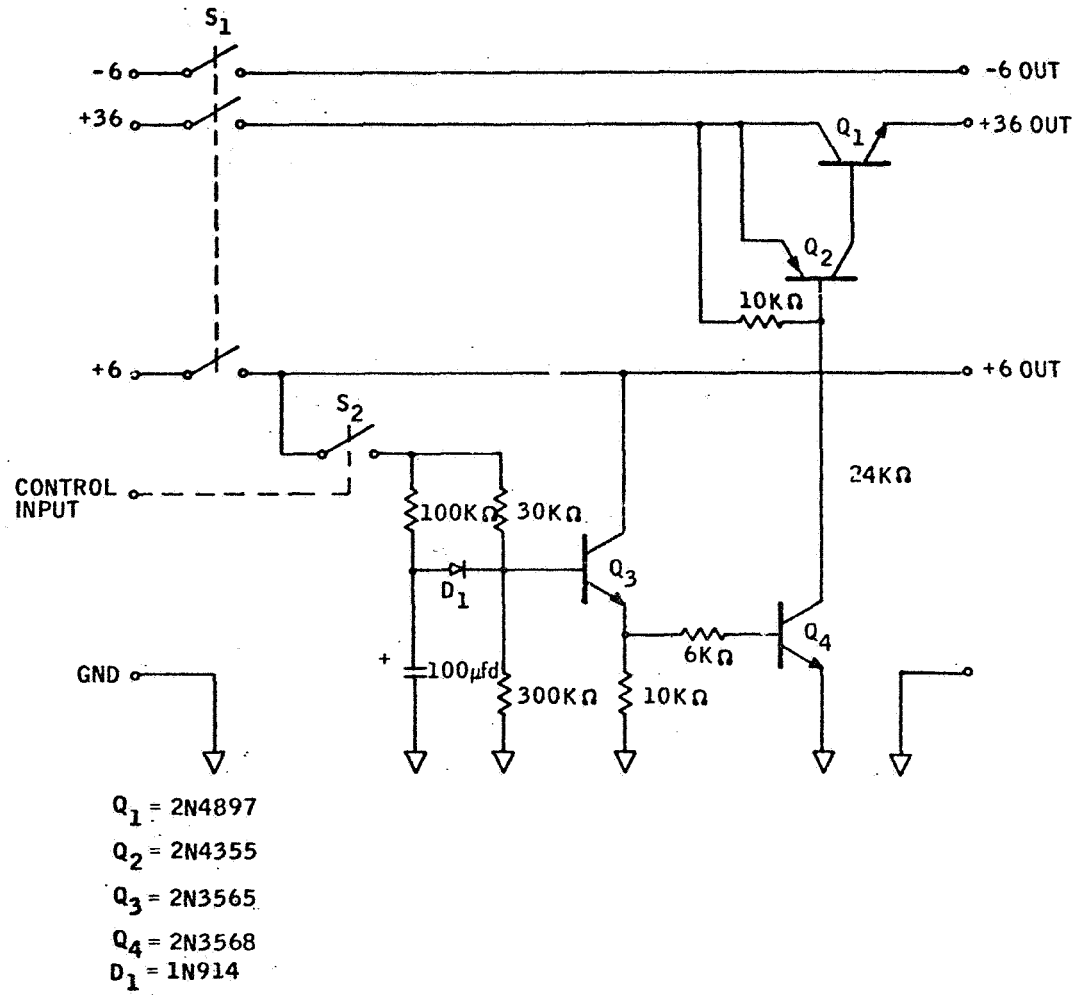

Figure 73. Power Switch Circuit Diagram

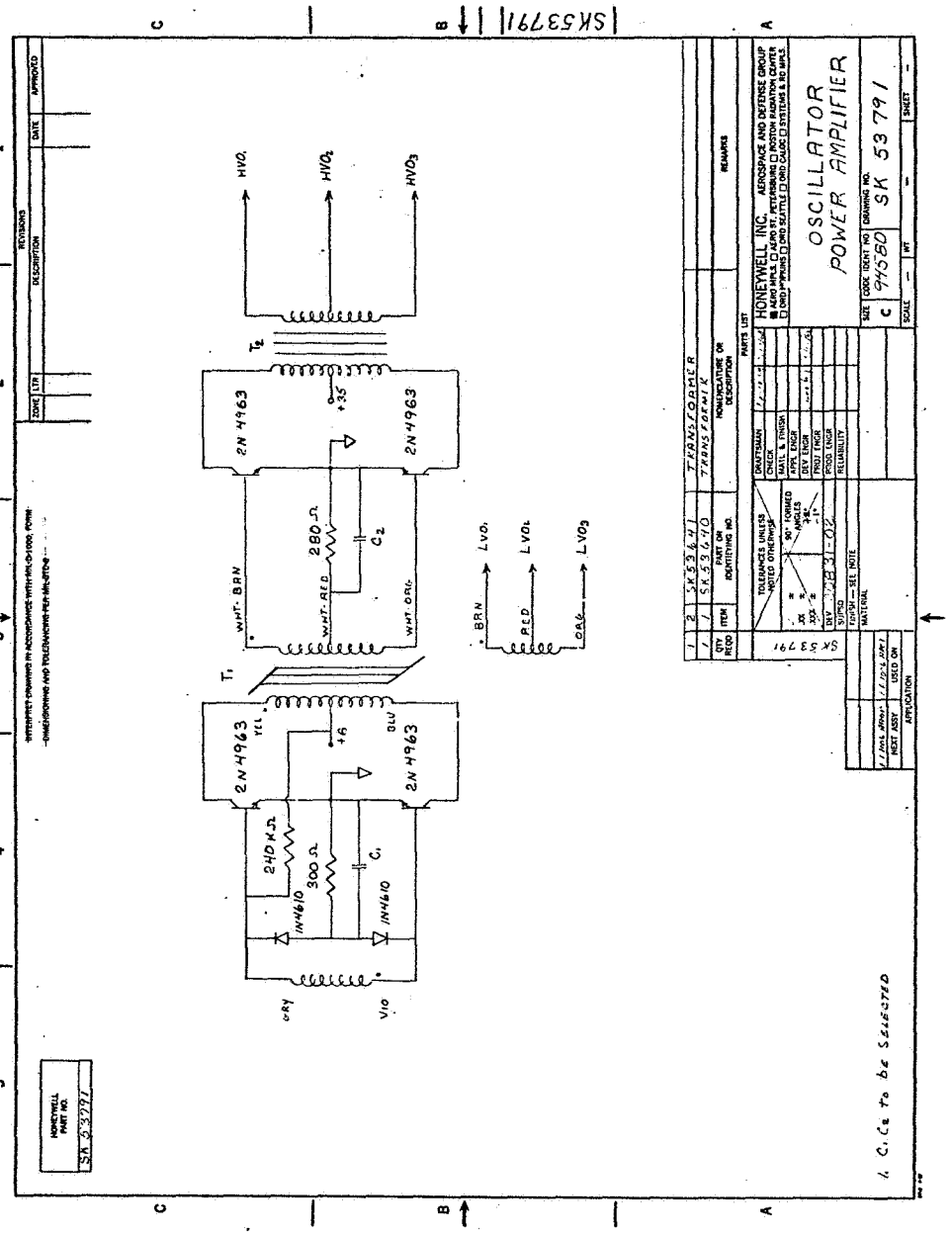

Figure 74. Oscillator Power Amplifier Drawing

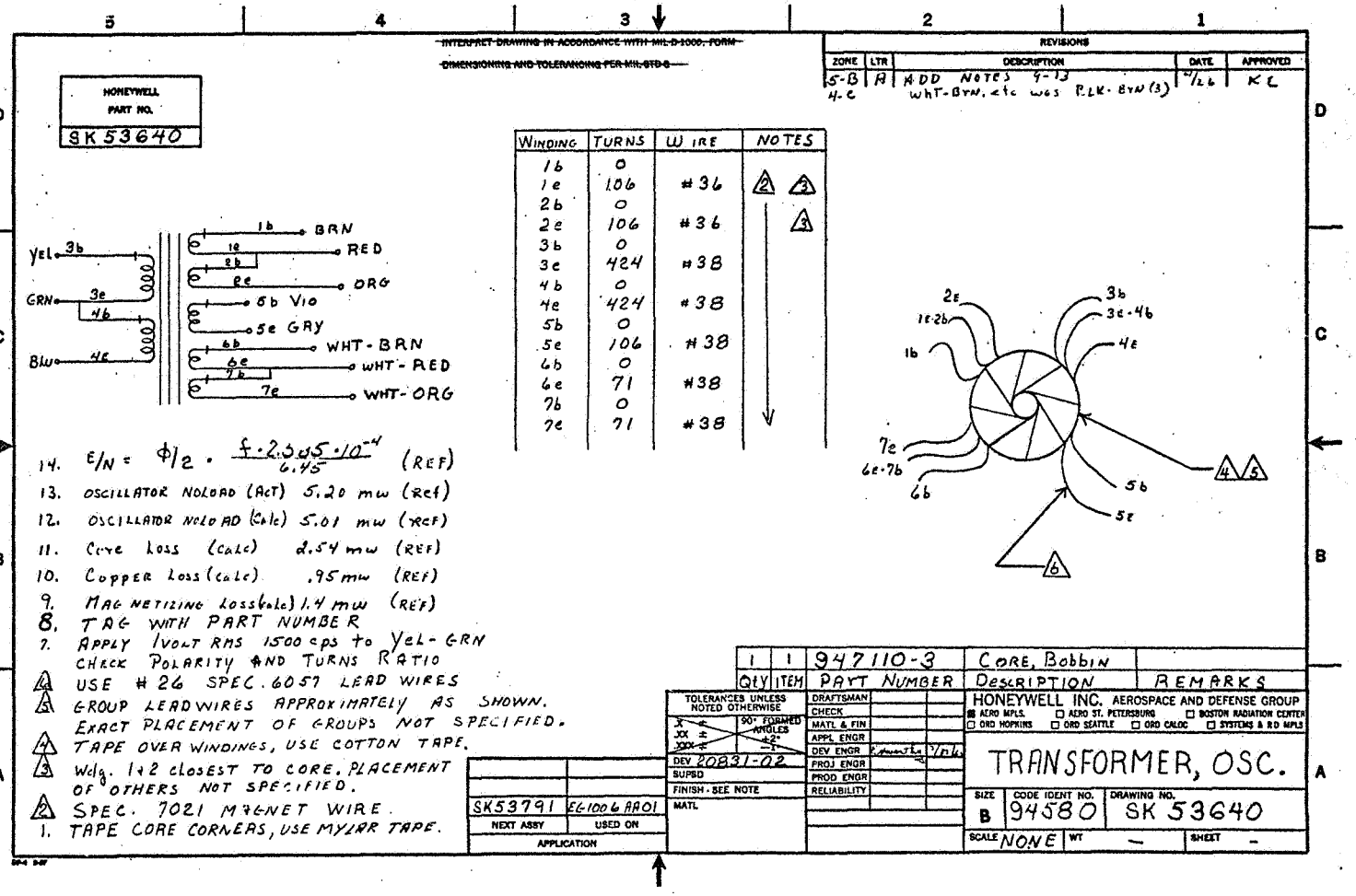

Figure 75. Oscillator Transformer Drawing

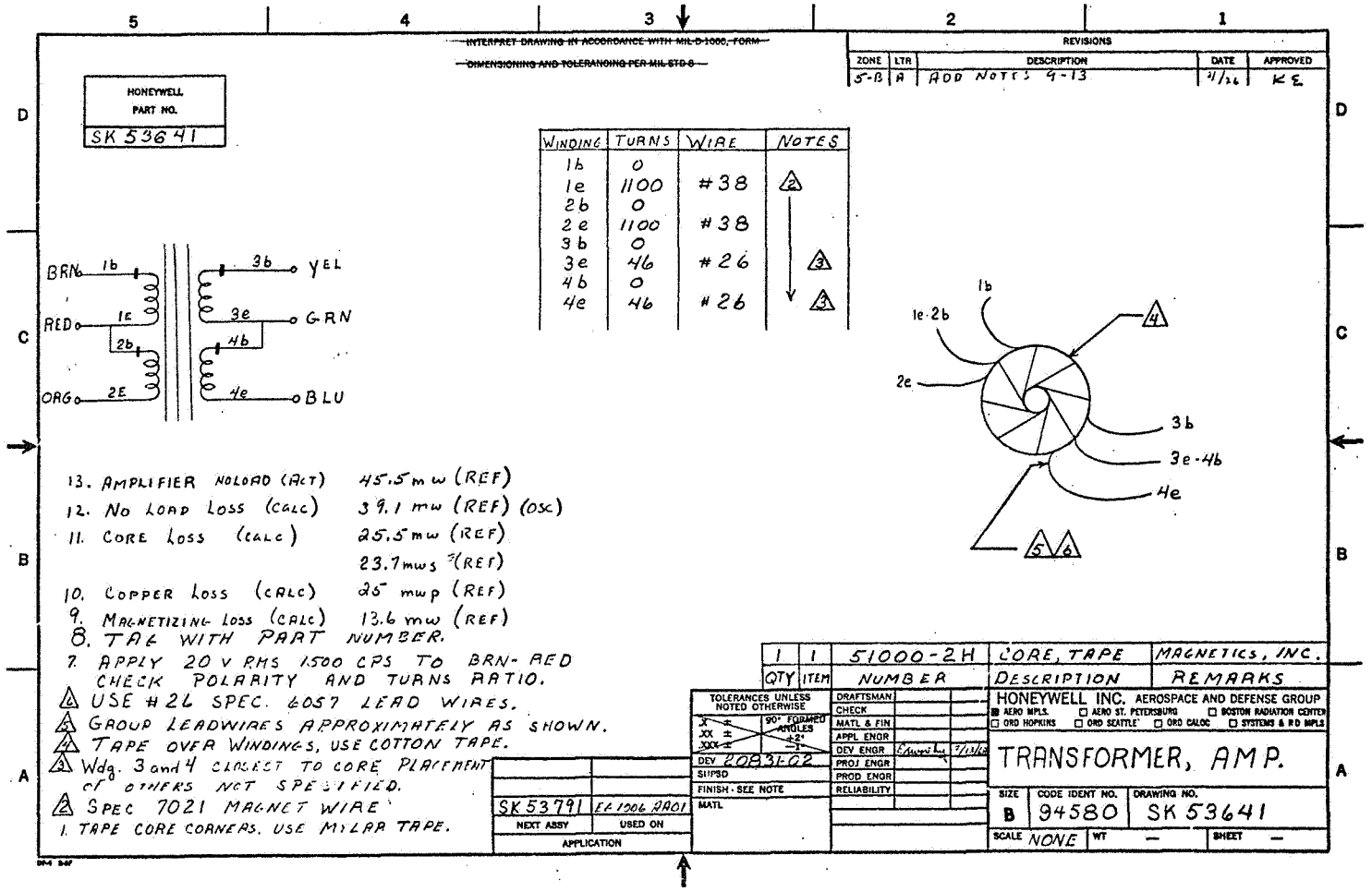

Figure 76. Amplifier Transformer Drawing

TABLE XXI. - POWER-AMP-OSCILLATOR TEST TABULATION

	No Load	Loaded
Oscillator		
Power input	5.2 mW	25.8 mW
Power output	---	19.3 mW
Efficiency	---	75%
Rise time (100%)	0.75 μsec	0.6 μsec
Peak current	55 mA	55 mA
Magnetizing current	0.4 mA peak	0.4 mA peak
Overshoot	25% (single peak)	16%
Power amplifier		
Power input	45.5 mW	560 mW
Power output	---	472 mW
Efficiency	---	84%
Load loss	---	42.5 mW
Rise time (100%)	1.1 μsec	1.1 μsec
Overshoot	0	0

Output Circuit

No difficulties were encountered while building the output transformers. The bobbins are of nonstandard size and were machined using block nylon. The exposed ends were not made deep enough to accommodate the leadwire splices. A change has been made on the print to deepen the bobbin in this area. The transformers were impregnated using an epoxy compound and then tested. Corona appeared between the outer coil and the inside of the core of HV-375 at about 2170 volts. This condition was cured by filling the

void with silicone rubber RTV compound. It would probably be advantageous to encapsulate the transformers after they are impregnated.

The first problem encountered was in the area of transformer internal capacitance and leakage reactance. A coupling unbalance between coils on the same side of the bobbin and coils on opposite sides caused waveform unbalance. The leakages measured between various coils in the transformer are summarized in Table XXII.

TABLE XXII.- LEAKAGE INDUCTANCE MEASUREMENT

Leakage	HV-375	HV-21
Primary to primary	0.156 mH	0.160 mH
Primary to secondary (same)	0.035 mH	0.044 mH
Primary to secondary (opposite)	0.142 mH	0.155 mH

These measurements mean that when the same side of the primary is "on," the 0.035-mH leakage and the self capacitance determine the wavefront. When the opposite primary is "on," the wavefront is determined by 0.156 mH. This 4.5:1 change affects damping factor and ringing. An oscillograph of output waveform looks like Figure 77.

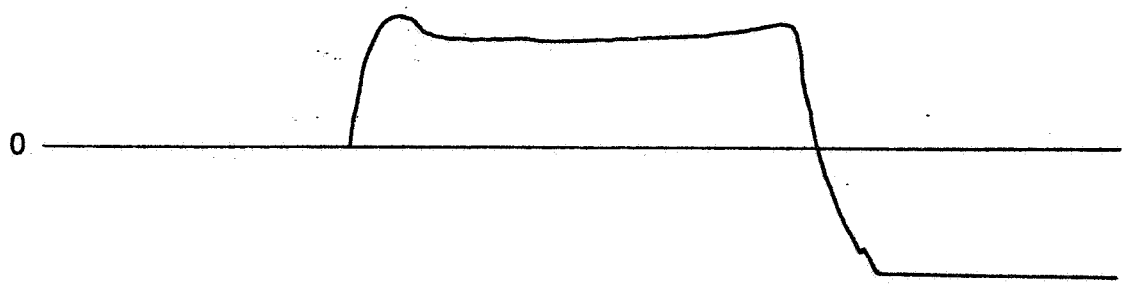

Figure 77. Typical Output Waveform

Transformer capacitance was calculated assuming that the (series) sum of layer-to-layer capacitance was negligible. The edge and "outside" layer calculations result in 10.7 pF across each secondary half and 4 pF coupling between them. Effectively, this amounts to 18.7 pF per half, or a total of 37.4 pF stray capacitance. This effective capacitance was determined by measuring the wavefront ringing frequency with and without load. These measurements indicated 41.5 pF actual capacitance. Bridge measurements gave readings about three times this value. The difficulty with bridge measurements is that the whole (parallel plate) side capacitance is effective, where, in the actual transformer, the energy stored in the electric field depends on voltage distribution. Since equivalent capacitance is that which stores an equal amount of energy at the device terminals, the equivalent capacitance is usually lower than the bridge measured values. Referred to each coil, the output capacitive load is increased from 60 to 80.7 pF. This will increase the power input to the circuit 13.5 percent.

It is recommended in future designs that the primary coils be wound with double wire (Twineze) or bifilar led through the bobbin center lag to equalize leakage inductance to the two secondary coils and to reduce leakage between the two primary coils.

In the primary circuit, the input current, peak current, and waveform were the items of interest. According to the theory, the peak current is limited by transformer resistance and an external padding resistor. It was not realized that the current charging the transformer internal capacitance would create a peak not associated with the output circuit. To alleviate this condition, a resistor was added in series with the transistor collector. A reasonable compromise was made between peak current and rise time with 11 ohms in each collector and 80 k ohms in each output lead. The total input resistance is 20 Ω (which affects mod-amp design). Note that this resistance is higher than that thought necessary to produce the risetime which was measured. This is due to the peaking effect of the leakage reactance. This combination of parameters produces a peak current of approximately 3.4 amps, a risetime (10 percent to 90 percent) of 10 μsec up to 1/4 full output and 18 μsec at full output, and a fall time of 21 μsec up to 1/4 full output and 28 μsec at full output.

Adding these two resistors produced an apparent change in the form of reduced power loss. Data taken with a single output resistor was compared to that taken with two resistors. This is shown in Table XXII. Note however, that the single-resistor data were taken with the HV-375 transformer and the two-resistor data with the HV-21 transformer. Differences between these transformers were great enough to invalidate exact comparison.

A second problem affecting power input to the circuit is due to magnetizing current. It was found that part of this current flows through the power supply as opposed to the previous assumption that it all flowed into the capacitance. Although the current flow is difficult to separate experimentally, several tests were conducted to determine the percentage flow into the power source. The magnetizing current flow may be calculated with a knowledge of

the magnetizing inductance. The HV-375 measured 11.9 mH; the HV-21 measured 16.2 mH. Since most of the data has been taken using the HV-21, one example is calculated here using this transformer. The magnetizing current is related to applied voltage by the equation:

$$E = L \frac{di}{dT}$$

when E is a constant value, the change of current is a ramp of peak value.

$$\Delta i = \frac{E}{L} \Delta T$$

The experimental comparison was made at 8.7 volts using the values given for the HV-21:

$$\Delta i = \frac{8.7}{0.0162} \cdot \frac{1}{3000} = 181 \text{ mA}$$

Average current is 90.5 mA. The experimental measurement can be expected to produce a waveform with the following parts:

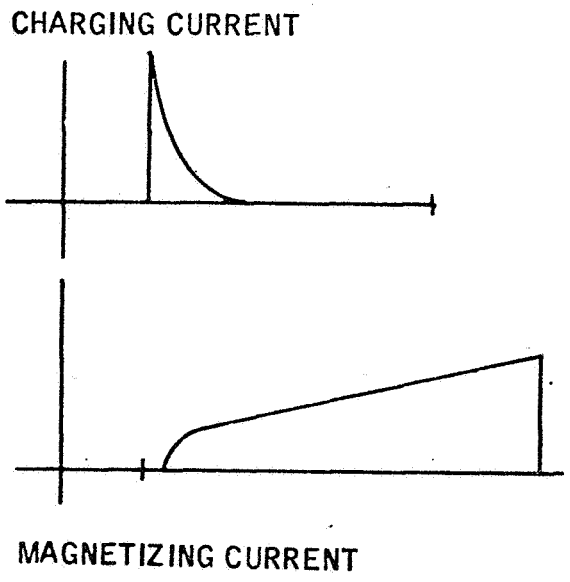

Figure 78. Output Current Functions

Thus, the magnetizing current may be estimated by ignoring the initial spike and measuring only the slope which follows. At 8.7 volts input, this results in a peak current of 34 mA and an average of about 21 mA. It is quite linear with input. It is apparent, therefore, that at this level, 23 percent of the magnetizing current flows through the power supply. Table XXIII compares power level data with the calculations.

To duplicate the conditions as closely as possible, the following operations were performed:

- Magnetizing current is removed
- Total capacitance is scaled to that previously used (117 pF)

The system power requirements are compared in TableXXIV.

The secondary output circuit was tested to check the same characteristics. The risetime measured at 8 μsec, fall time 13 μsec, and, with input at 4 volts, output of 36 volts was produced. At this point, the average current was 0.9 mA. In the system, this current flows from a 6-volt supply; thus, the power level is 5.4 mW at "full on." The circuit is shown in Figure 79 (SK 53792).

Low G Mod Amp

When tested alone, the low G mod amp met the conditions outlined in the design section. It had the following measured characteristics:

Input power	1k load, 0 volts	10.3 mW
Input power	1k load, -4 volts	42.5 mW
d-c gain		1.92
Maximum output	1k load	-5.11 volts
Frequency response	±0.7 volts about 0	28 kc
Frequency response	±1 volt about -2 volts	52 kc
Slew rate		4.4 volts in 17 μsec

A problem appeared when the secondary circuit was driven due to reverse current spikes. This necessitated adding the buffer stage shown on SK53794, Figure 80. This buffer increases full power output dissipation by 24 mW.

TABLE XXIII. - CIRCUIT POWER TABULATION

Single resistor (HV-375)					
E_{in} (V)	I_{in} (mA)	I_m (mA)	$(I_{in}-I_m)$ (mA)	Scaled (mA)	36V Power (W)
8.7	64	21	43	31.2	1.12
17.5	128	42	86	62.2	2.24
35	(peak current too high - scales to 5.0 W)				
Two resistors (HV-21)					
8.7	70	21	49	35.5	1.28
17.5	120	42	78	56.5	2.03
25	170	60.4	109.6	79.4	2.85
30	200	72.5	127.5	92.6	3.34
35	230	85.0	145	105	3.78

TABLE XXIV. - SYSTEM POWER

System 1	Condition	1/4 Biased (W)	1/2 Biased (W)
Calculated	Scaled	7.68	11.02
Single resistor		9.48	13.96
Two resistor		9.90	11.90
Single resistor	Actual	18.41	27.7
Two resistor		18.40	25.6

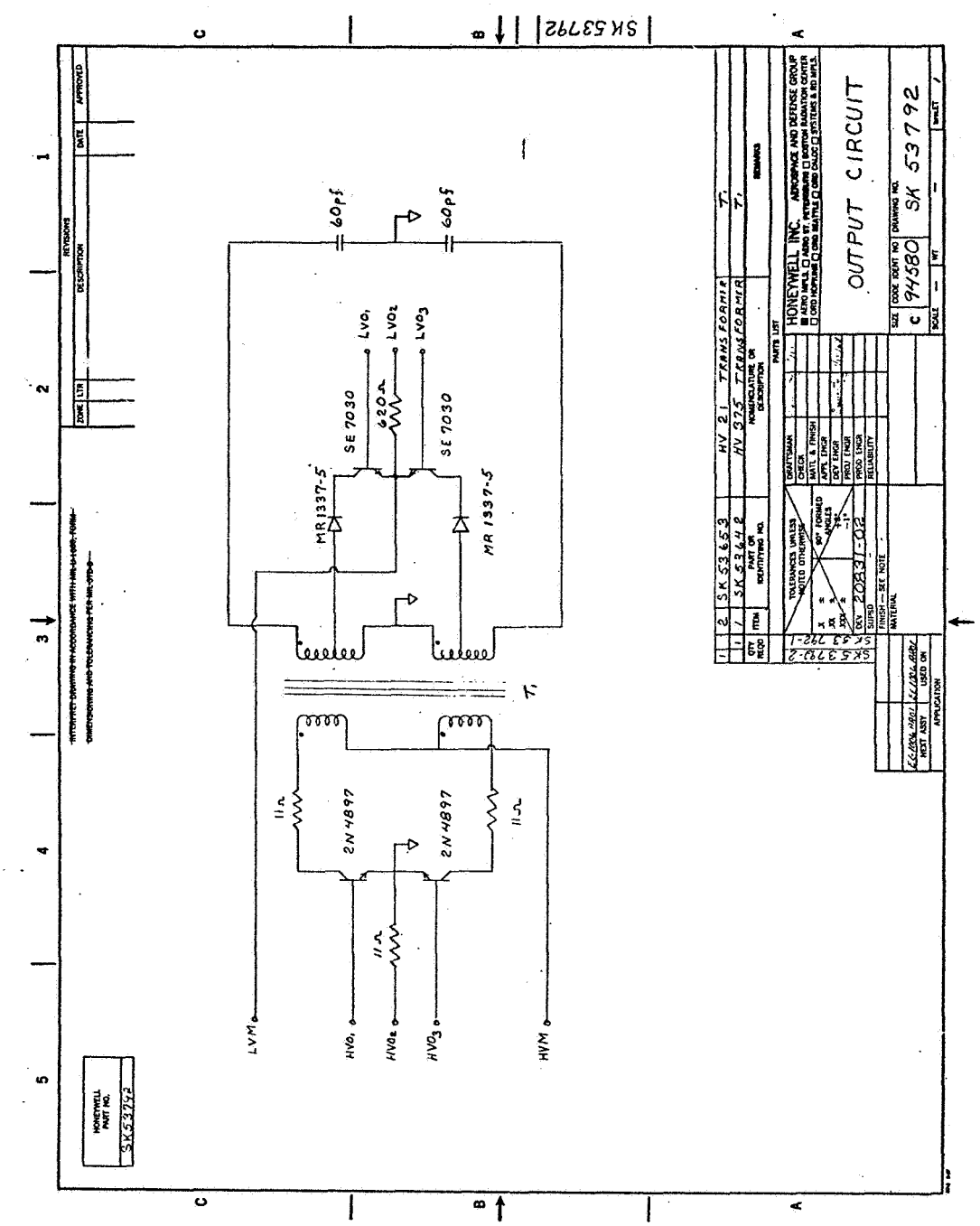

Figure 79. Output Circuit Drawing

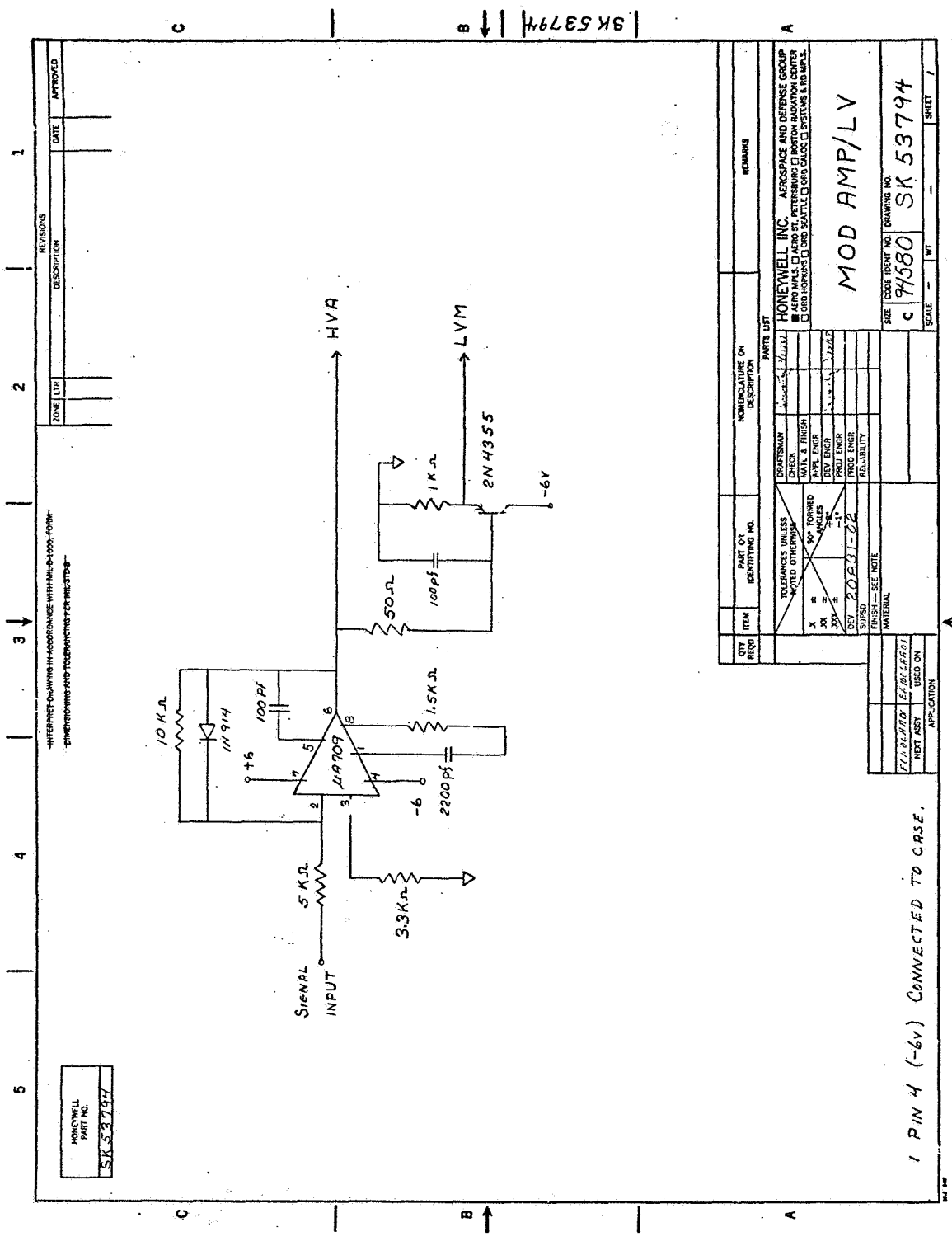

Figure 80. Low-Voltage Mod Amp Drawing

High G Mod Amp

The mod amp was built as shown in Figure 69. Two problems appeared immediately:

- Compensation networks caused distortion at large signal medium frequency (±10 volts/17 volts, 5 kc)
- Base resistors are too large to allow proper bias

The base resistors were simply changed to the lower values shown in Figure 81. The compensation networks present a more complex problem since the number of points available in the amplifier capable of driving the network is limited. Since the ringing frequency with marginal compensation turned out to be higher than expected (8-10 mc range) and since the output impedance did not have to be as low as originally assumed, it was decided to add a buffer stage to drive a single network.

A bias pot was added and the amplifier tested. The results are shown in Tables XXV and XXVI and the circuit in Figure 81 (SK53793).

The amplifier slew rate at 35 to 0 volts (fall time) is 7 μsec; from 0 to 35 volts (risetime), 20 μsec. The output impedance versus frequency was measured and is tabulated below.

TABLE XXV. - OUTPUT IMPEDANCE

Frequency (kc)	Input Voltage	Output /100 Ω (mV)	Impedance (ohms)
0.5	1.3	3	2.4
1	1.8	6	3.3
2	2.0	12	6.0
5	2.0	26	13.1
10	2.2	56	26.1
20	2.2	112	53.5

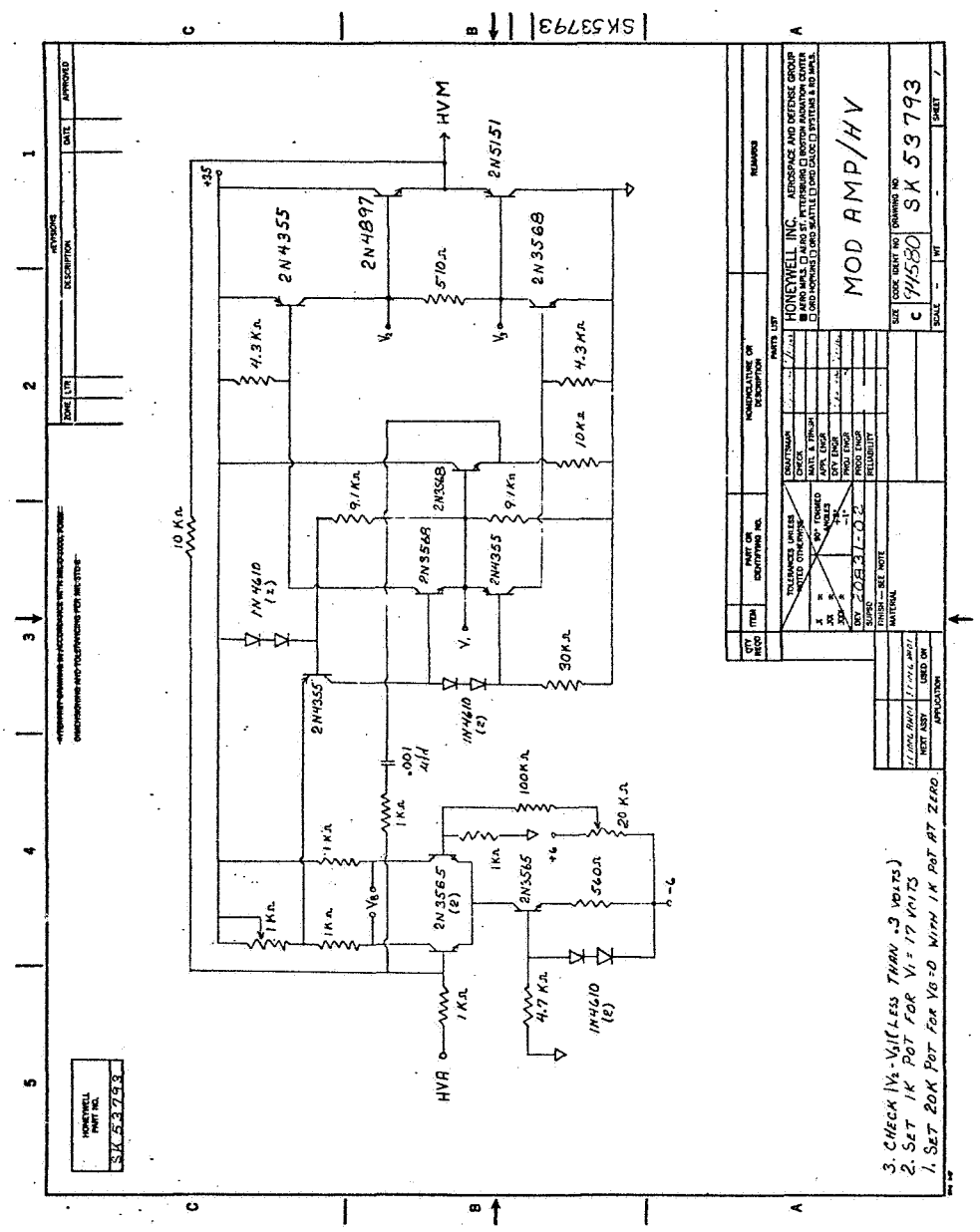

Figure 81. High-Voltage Mod Amp Drawing

The bias power and that delivered to the load is tabulated in Table XXV. The supply voltage is a constant 35 volts.

TABLE XXVI. - HIGH G MOD AMP POWER

Voltage Output	Load	Current Input	Total Power (mW)	Load Power	Bias Power (mW)
0.6	1k Ω	6.7	234	0	234
8.78	1k Ω	16.0	560	77.1 mW	252
17.50	1k Ω	25.0	875	306 mW	262
34.40	1k Ω	43.0	1510	1182 mW	310
0.6	350 Ω	7.7	269	0	269
8.78	350 Ω	32.0	1120	220 mW	242
17.50	350 Ω	58.0	2030	875 mW	280
34.4	350 Ω	111.0	3880	3385 mW	440

Variable Voltage Power Supply

The circuit was built as shown in Figure 73. The only problem noted was that the delay time was awkwardly long. The 100-μ F timing capacitor was replaced with a 1-μ F capacitor. Switch-off time occurred in less than one second. All transients were damped in that time. Bias turn-off was measured to be the same as the mod amp slew rate (fall time; approximately 4 μsec from 17 volts to zero).

The power switch circuit diagram is shown in Figure 82 (SK53795).

System Test

The circuits were connected as shown in Figure 83 (EG1006AA01). The oscillator, power amplifier operated and switched off as designed. The mod amp circuits also operated correctly at low-output voltage, but when output reached 6 volts, the entire circuit locked up. The problem was traced to a current pulse in the secondary switching circuit. The secondary transistors switch "on" while the secondary voltage (due to the primary bias) is still dropping. The difference in time is 7 μsec. No actual problems are produced by this action, but the mod amp must handle the current pulse. To facilitate proper operation, the buffer stage shown in Figure 80 was added. A photograph of the circuits connected together is given in Figure 84.

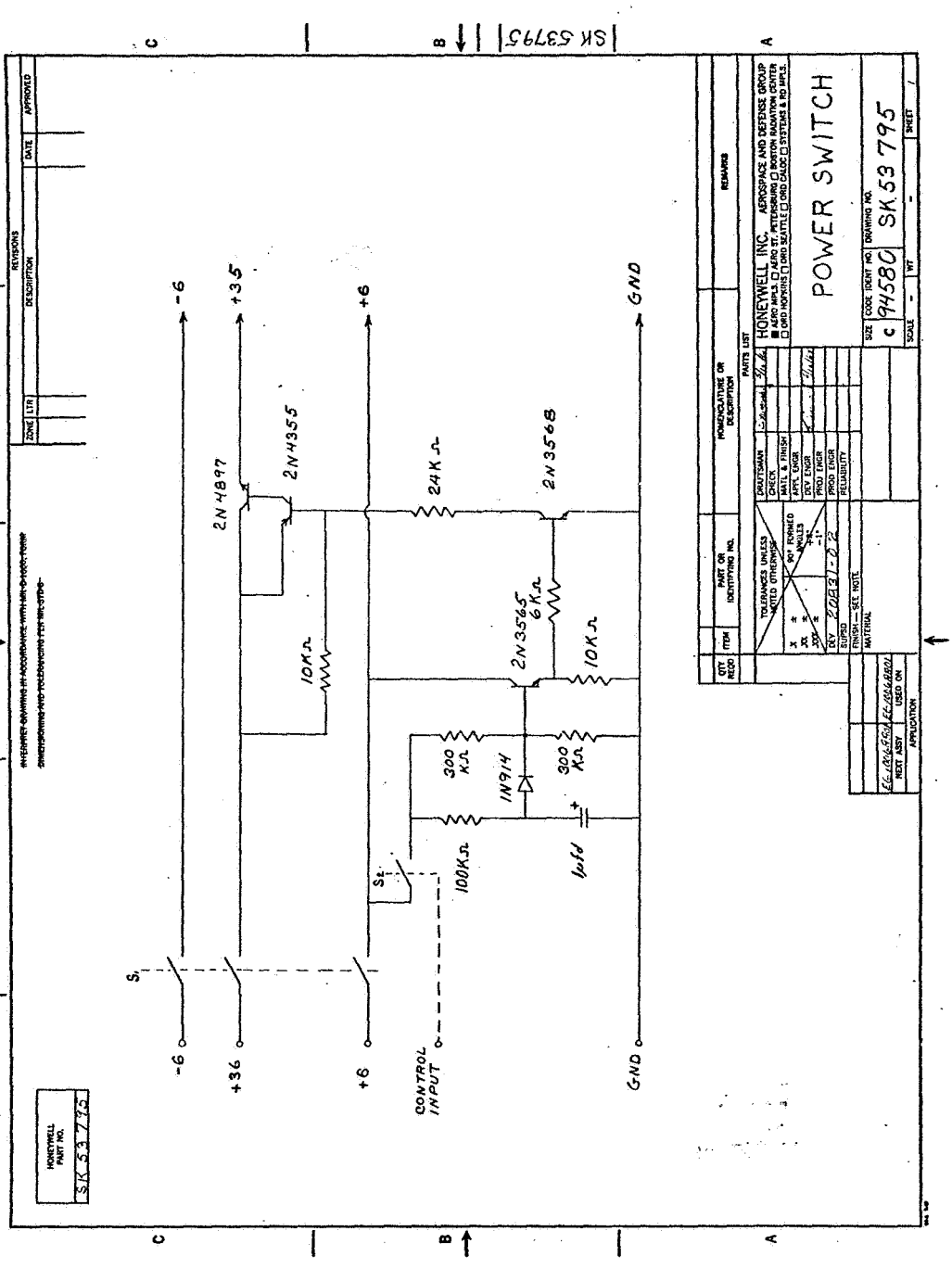

Figure 82. Pow r Switch Drawing

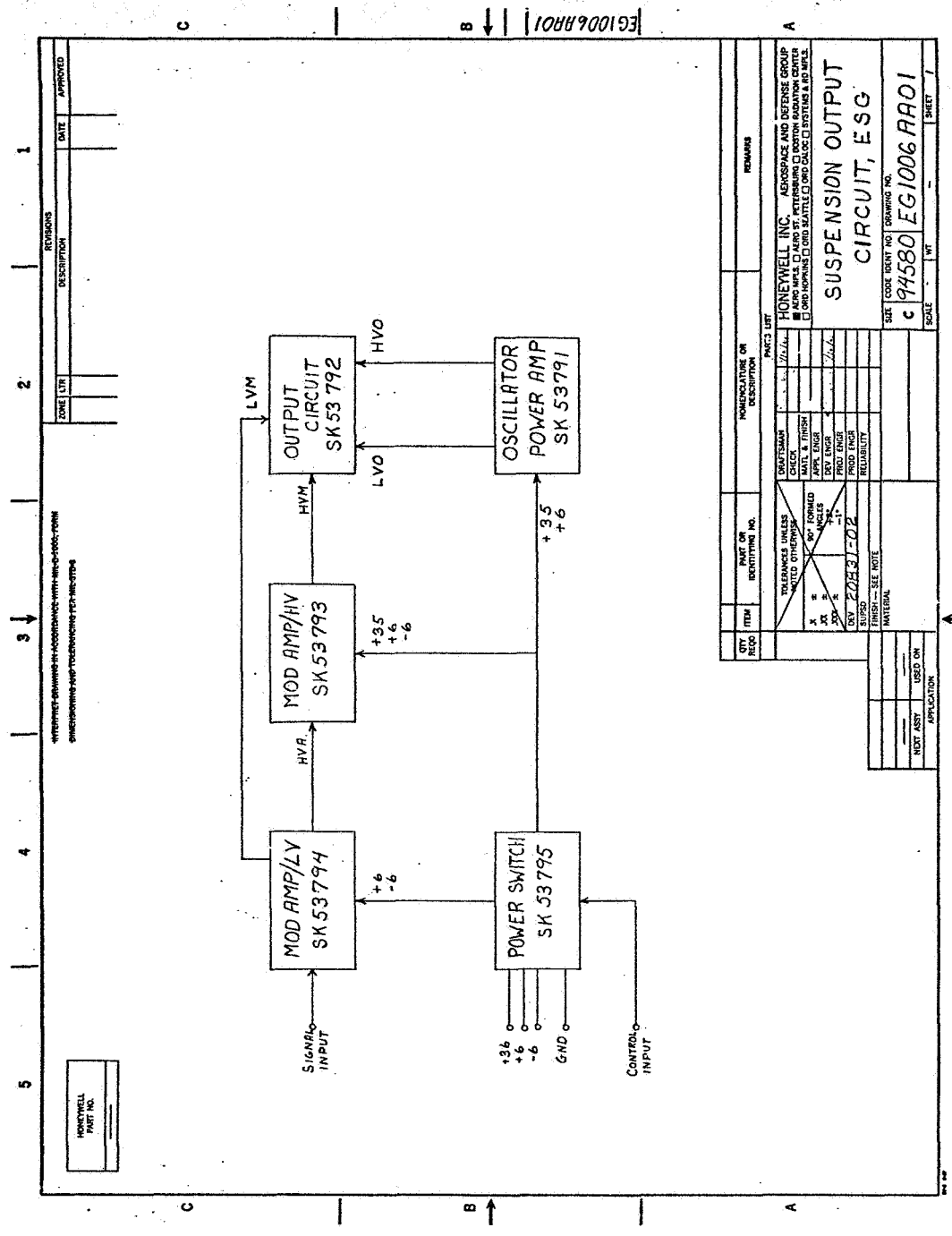

Figure 83. Output Circuit Block Diagram

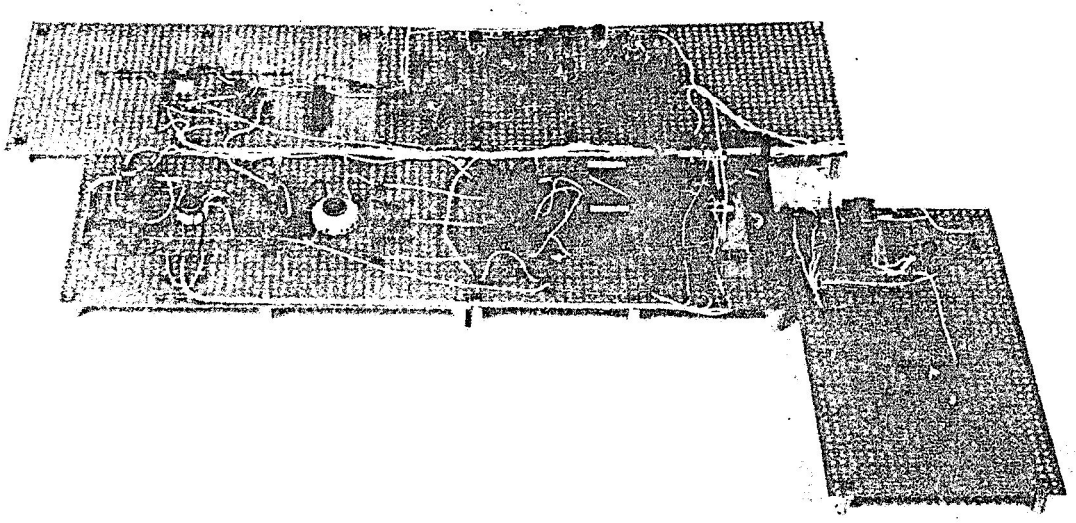

Figure 84. Photo of Tested Circuits